frontiers | Research Topics

Ehlers-Danlos syndrome: From bedside to bench

Edited by
Tomoki Kosho, Ken-ichi Matsumoto, Delfien Syx and Shujiro Hayashi

Coordinated by
Anupriya Kaur

Published in
Frontiers in Genetics

ISSN 1664-8714
ISBN 978-2-8325-4557-7
DOI 10.3389/978-2-8325-4557-7

About Frontiers

Frontiers is more than just an open access publisher of scholarly articles: it is a pioneering approach to the world of academia, radically improving the way scholarly research is managed. The grand vision of Frontiers is a world where all people have an equal opportunity to seek, share and generate knowledge. Frontiers provides immediate and permanent online open access to all its publications, but this alone is not enough to realize our grand goals.

Frontiers journal series

The Frontiers journal series is a multi-tier and interdisciplinary set of open-access, online journals, promising a paradigm shift from the current review, selection and dissemination processes in academic publishing. All Frontiers journals are driven by researchers for researchers; therefore, they constitute a service to the scholarly community. At the same time, the *Frontiers journal series* operates on a revolutionary invention, the tiered publishing system, initially addressing specific communities of scholars, and gradually climbing up to broader public understanding, thus serving the interests of the lay society, too.

Dedication to quality

Each Frontiers article is a landmark of the highest quality, thanks to genuinely collaborative interactions between authors and review editors, who include some of the world's best academicians. Research must be certified by peers before entering a stream of knowledge that may eventually reach the public - and shape society; therefore, Frontiers only applies the most rigorous and unbiased reviews. Frontiers revolutionizes research publishing by freely delivering the most outstanding research, evaluated with no bias from both the academic and social point of view. By applying the most advanced information technologies, Frontiers is catapulting scholarly publishing into a new generation.

What are Frontiers Research Topics?

Frontiers Research Topics are very popular trademarks of the *Frontiers journals series*: they are collections of at least ten articles, all centered on a particular subject. With their unique mix of varied contributions from Original Research to Review Articles, Frontiers Research Topics unify the most influential researchers, the latest key findings and historical advances in a hot research area.

Find out more on how to host your own Frontiers Research Topic or contribute to one as an author by contacting the Frontiers editorial office: frontiersin.org/about/contact

Ehlers-Danlos syndrome: From bedside to bench

Topic editors
Tomoki Kosho — Shinshu University, Japan
Ken-ichi Matsumoto — Shimane University, Japan
Delfien Syx — Ghent University, Belgium
Shujiro Hayashi — Dokkyo Medical University, Japan

Topic coordinator
Anupriya Kaur — Post Graduate Institute of Medical Education and Research (PGIMER), India

Citation
Kosho, T., Matsumoto, K.-i., Syx, D., Hayashi, S., Kaur, A., eds. (2024). *Ehlers-Danlos syndrome: From bedside to bench*. Lausanne: Frontiers Media SA.
doi: 10.3389/978-2-8325-4557-7

Table of contents

frontiers | Frontiers in Genetics

TYPE Editorial
PUBLISHED 26 April 2024
DOI 10.3389/fgene.2024.1399386

OPEN ACCESS

EDITED AND REVIEWED BY
Jordi Pérez-Tur,
Spanish National Research Council (CSIC), Spain

*CORRESPONDENCE
Tomoki Kosho,
ktomoki@shinshu-u.ac.jp

RECEIVED 11 March 2024
ACCEPTED 09 April 2024
PUBLISHED 26 April 2024

CITATION
Kosho T, Hayashi S, Matsumoto K-i, Syx D and Kaur A (2024), Editorial: Ehlers-Danlos syndrome: from bedside to bench. *Front. Genet.* 15:1399386. doi: 10.3389/fgene.2024.1399386

Editorial: Ehlers-Danlos syndrome: from bedside to bench

Tomoki Kosho[1]*, Shujiro Hayashi[2], Ken-ichi Matsumoto[3], Delfien Syx[4] and Anupriya Kaur[5]

[1]Department of Medical Genetics, Shinshu University School of Medicine, Matsumoto, Japan, [2]Department of Dermatology, Dokkyo Medical University, Mibu, Japan, [3]Department of Biosignaling and Radioisotope Experiment, Interdiscipnary Center for Science Research, Organization for Research and Academic Information, Shimane University, Matsue, Japan, [4]Department of Biomolecular Medicine, Center for Medical Genetics Ghent (CMGG), Ghent University Hospital, Ghent, Belgium, [5]Medical Genetics, Advanced Pediatric Center, PGIMER, Chandigarh, India

KEYWORDS

Ehlers-Danlos syndrome, heritable connective tissue disorders (HCTD), clinical, pathophysiological, collagen, delineation

Editorial on the Research Topic
Ehlers-Danlos syndrome: from bedside to bench

The Ehlers-Danlos syndromes (EDS) comprise a genetically heterogeneous group of heritable connective tissue disorders, clinically characterized by skin hyperextensibility, joint hypermobility, and tissue fragility. The currently used nomenclature and classification, published in 2017, recognizes 13 types (Malfait et al., 2017), and several additional types have also been described (Malfait et al., 2020). The pathomechanisms of EDS include abnormalities in the genes for fibrillar collagen types I, III, and V; enzymes modifying or processing these collagens; enzymes involved in the biosynthesis of the glycosaminoglycan chains of proteoglycan; and proteins playing more complex roles in the maintenance of extracellular matrices. Furthermore, clinical overlaps among cases with different types as well as discoveries of EDS-like phenotypes with novel pathomechanisms have been described. The spectrum of EDS is considered to be much wider than expected, and it would help delineate this clinical and pathophysiological spectrum to describe and share clinical and pathophysiological findings of variable and valuable cases.

The scope of this Research Topic (https://www.frontiersin.org/research-topics/31359/ehlers-danlos-syndrome-from-bedside-to-bench/magazine) is to make clinical and pathophysiological delineation of the wide and complex spectrum of EDS. In total, 10 reports are published including four original research articles, five case reports, and one mini review.

Four reports attempted clinical and pathophysiological delineation of vascular EDS (vEDS), the most severe subtype of EDS. Ishikawa et al. described detailed ultrastructural findings as well as clinical features in patients with vascular EDS. Irregularity in the size of collagen fibrils was suggested in 27 patients with vEDS, and the variation tended to be lower in those with less serious vascular complications (Ishikawa et al.). Wei et al. described an association between digestion tract events and non-glycine missense variants from a Chinese family (Wei et al.). Hayashi et al. described a mildly affected Japanese patient found to be caused by a unique in-frame duplication variant in *COL3A1* without alteration in the [Gly-X-Y] triplet repeat sequence of type III collagen (Hayashi et al.). Angwin et al. introduced the first experience of pre-implantation genetic diagnosis with surrogacy in vEDS, which could provide a choice for women with vEDS wishing to have unaffected

biological children without pregnancy/delivery-related critical events but also provide necessity of careful discussion considering hypothetical and potential risks of all relevant procedures based on ethical, legal, and social backgrounds of each community (Angwin et al.).

Two reports were about classical-like EDS caused by variants in the tenascin-X (TNX) gene (*TNXB*) (clEDS type 1). Yamaguchi et al. established a custom next-generation sequencing-based screening system for this subtype, and provided comprehensive clinical and molecular delineation of this subtype from a cohort comprising nine patients (Yamaguchi et al.). *TNXA*-derived variations were found in >75% and all patients had gastrointestinal complications including perforation, diverticulitis, gastrointestinal bleeding, intestinal obstruction, rectal/anal prolapse, and gallstones (Yamaguchi et al.). Okuda-Ashitaka and Matsumoto made a comprehensive review of experimental studies about TNX using TNX-deficient ($Tnxb^{-/-}$) mice; they introduced mechanical allodynia in *Tnxb*−/− mice, inhibited by the anticonvulsant drug gabapentin and a mu-opioid agonist but not by a NSAID indomethacin, and also introduced studies suggesting various roles of TNX (e.g., tumor suppression, epithelial wound healing, liver fibrosis) (Okuda-Ashitaka and Matsumoto).

Two reports are about *AEBP1*-related EDS (classical-like EDS [clEDS] type 2), which represents the 14th subtype following the 13 subtypes according to the 2017 international classification of EDS (Malfait et al., 2017). Angwin et al. (Angwin et al.) and Yamaguchi et al. (Yamaguchi et al.) described additional patients with clEDS type 2; hair loss was recognized as a characteristic feature of this subtype, and importance of a few but critical complications such as vascular or bowel events was also stressed.

The other two reports were about periodontal EDS (pEDS). Angwin et al. described non-oral manifestations in 21 adult patients with periodontal EDS from two United Kingdom cohorts. Easy bruising, pretibial plaques, and brain white matter abnormalities were observed in more than 80% (Angwin et al.). Liao et al. reported the first transcriptomic analysis of patient-derived cells of periodontal EDS. Differential gene expression was found only in monocytes but not in gingival fibroblasts; genes in such biological processes as neutrophil-mediated immunity, response to bacterium, and TNF-α and IL-17 pathway were enriched; and disease ontology enrichment analysis suggested enrichment of genes related to periodontal host defense, inflammatory response, skin disease, and vascular development (Liao et al.).

All these reports are expected to make a substantial contribution in understanding complex clinical and pathophysiological characteristics of various subtypes of EDS. Hopefully, based on these evidences, international collaborative clinical and pathophysiological investigations will be conducted to make a further delineation of each subtype, to provide evidences in establishing better management of patients as well as to develop etiology-based therapies.

Author contributions

TK: Writing–original draft, Writing–review and editing. SH: Writing–review and editing. K-iM: Writing–review and editing. DS: Writing–review and editing. AK: Writing–review and editing.

Funding

The author(s) declare that no financial support was received for the research, authorship, and/or publication of this article.

Conflict of interest

TK is a member of the endowed chair named “Division of Clinical Sequencing, Shinshu University School of Medicine”, which is sponsored by BML, Inc. and Life Technologies Japan Ltd., a subsidiary of Thermo Fisher Scientific Inc.

The remaining authors declare that the research was conducted in the absence of any commercial or financial relationships that could be construed as a potential conflict of interest.

Publisher’s note

References

Malfait, F., Castori, M., Francomano, C. A., Giunta, C., Kosho, T., and Byers, P. H. (2020). The Ehlers-Danlos syndromes. *Nat. Rev. Dis. Prim.* 6 (1), 64. doi:10.1038/s41572-020-0194-9

Malfait, F., Francomano, C., Byers, P., Belmont, J., Berglund, B., Black, J., et al. (2017). The 2017 international classification of the Ehlers-Danlos syndromes. *Am. J. Med. Genet. Part C, Seminars Med. Genet.* 175 (1), 8–26. doi:10.1002/ajmg.c.31552

frontiers | Frontiers in Genetics

ORIGINAL RESEARCH
published: 28 April 2022
doi: 10.3389/fgene.2022.834928

Transcriptome Analysis of Monocytes and Fibroblasts Provides Insights Into the Molecular Features of Periodontal Ehlers-Danlos Syndrome

Zhuoyi Liao [1,2†], Tian Zhao [1,2†], Ningxiang Wang [1,3], Jiaqi Chen [1,2], Weibin Sun [1] and Juan Wu [1]**

[1]Department of Periodontology, Nanjing Stomatological Hospital, Medical School of Nanjing University, Nanjing, China, [2]Central Laboratory of Stomatology, Nanjing Stomatological Hospital, Medical School of Nanjing University, Nanjing, China, [3]Department of Stomatology, Nanjing Hospital of Chinese Medicine, Nanjing University of Traditional Chinese Medicine, Nanjing, China

Periodontal Ehlers–Danlos syndrome (pEDS) is a rare hereditary disorder characterized by severe early-onset periodontitis with premature tooth loss, pretibial hyperpigmentation, and skin fragility. It is caused by mutant variants in the *C1R* and *C1S* genes that result in C4 cleavage and local complement cascade activation, as well as other possible consequences. However, the exact functional consequences of this activation remain unclear. To shed light on molecular mechanisms underlying pEDS and to identify novel molecular targets that may expand treatment strategies, we performed transcriptome profiling by RNA sequencing of monocytes and gingival fibroblasts from two patients with pEDS. Compared to normal controls, differential expression of genes was found only in monocytes but not gingival fibroblasts. Most of the significant genes were enriched in biological processes such as neutrophil-mediated immunity, response to bacterium, TNF-α and IL-17 pathway which are related to inflammation response and immune response. In disease ontology enrichment analysis, genes related to periodontal host defense, inflammatory response, skin disease, and vascular development, including *MMP9*, *VEGFA*, *IL10*, *IL1A*, *IL1B*, *IL2RA,* and *IL6*, were significantly enriched and also validated by qPCR and ELISA. Overall, the present study provides the transcriptomic data of pEDS for the first time and the distinct molecular features in monocytes of pEDS might serve as a tool to better understand the disease.

Keywords: Ehlers-Danlos syndrome, periodontitis, transcriptomics, monocytes, RNA-sequencing

OPEN ACCESS

Edited by:
Loredana Bury,
University of Perugia, Italy

Reviewed by:
Ines Kapferer-Seebacher,
Innsbruck Medical University, Austria
Chengsong Zhu,
University of Texas Southwestern Medical Center, United States

***Correspondence:**
Weibin Sun
wbsun@nju.edu.cn
Juan Wu
juanwu@smail.nju.edu.cn

†These authors have contributed equally to this work

Specialty section:
This article was submitted to Genetics of Common and Rare Diseases, a section of the journal Frontiers in Genetics

Received: *14 December 2021*
Accepted: *30 March 2022*
Published: *28 April 2022*

Citation:
Liao Z, Zhao T, Wang N, Chen J, Sun W and Wu J (2022) Transcriptome Analysis of Monocytes and Fibroblasts Provides Insights Into the Molecular Features of Periodontal Ehlers-Danlos Syndrome. Front. Genet. 13:834928. doi: 10.3389/fgene.2022.834928

INTRODUCTION

The Ehlers–Danlos syndromes (EDS) are a clinically and genetically heterogeneous group of heritable connective tissue disorders characterized by joint hypermobility, skin hyperextensibility, and tissue fragility (Malfait et al., 2017). In 2017, The International EDS Consortium proposed a revised EDS classification (Malfait et al., 2017), and currently, 14 subtypes of EDS are recognized (Blackburn et al., 2018). Among all subtypes of EDS, periodontal Ehlers–Danlos syndrome (pEDS) (also known as EDS type VIII, OMIM#130080) is a specific EDS subtype caused by autosomal dominant pathogenic variants in complement 1 subunit genes *C1R* and *C1S*, with early severe periodontitis as the predominant clinical feature (Kapferer-Seebacher et al., 2016). The other clinical manifestations of pEDS include lack of attached gingiva, pretibial hyperpigmentation, skin fragility with abnormal scars,

and easy bruising (Malfait et al., 2017). Treatment of pEDS remains a huge challenge. Most of the current studies published have focused on describing the clinical features of the pEDS and/or identifying genetic variants (Wu et al., 2018; Kapferer-Seebacher et al., 2021). The pathogenesis of pEDS is only partly understood. From previous research (Kapferer-Seebacher et al., 2016), it is confirmed that pEDS is caused by pathogenic variants *C1R* (type 1, MIM 613785) and *C1S* (type 2, MIM 120580) genes, which encode the C1r and C1s subunits of the first step of the classical complement cascade, a major antimicrobial pathway of the innate immune system (G'al et al., 2009). Experimental evidence suggests that the *C1R* and/or *C1S* variants may cause extracellular presence of activated C1s without microbial triggers (Bally et al., 2019; Gröbner et al., 2019), which would lead to gingival hyperinflammation in response to mild biofilm accumulation, and subsequently rapidly progressing periodontal destruction. However, there are other pEDS clinical features unrelated to biofilm pathogens and apparently could not be explained by the above hypothesis and the detailed mechanisms remain largely unknown. To gain insights into altered gene expression patterns and dysregulated biological processes underlying molecular pathology of pEDS, we carried out transcriptome profiling by RNA sequencing of monocytes and gingival fibroblasts from two patients with pEDS compared with normal controls.

METHODS

Study Approval

This study was conducted according to the Declaration of Helsinki for Human Rights and all procedures were reviewed and approved by the Ethics Committee of Nanjing Stomatological Hospital, Medical School of Nanjing University (2018NL-037). All participants provided written informed consent before their enrollment in the present study. Samples were de-identified before analysis.

Participant Recruitment

Monocytes were obtained from two patients with pEDS from our previous study (Wu et al., 2018). Patients' information was as follows: the proband IV-1 (male, 25 years old, referred as pEDS1 in this study) was found with both a missense mutation in *C1R* (c.265T > C) and a frameshift mutation in *COL3A1* (c.1322delG); the proband's mother III-2 (female, 48 years old), referred as pEDS2 in the present study, only had the same mutation in *C1R*. Normal controls were periodontal healthy adults who showed no BOP, PD ≤ 3 mm, and no CAL, who underwent crown lengthening surgery for the restorative purpose in the Department of Periodontology, Nanjing Stomatological Hospital, Medical School of Nanjing University and exclusions included acute illness, pregnancy, and other systemic diseases.

Gingival tissues were obtained from two pEDS patients during their tooth extraction surgery, while control gingival tissues were obtained from three periodontal healthy adults during the crown lengthening surgery. All participants in the present study underwent clinical examination, and the detailed clinical data of all individuals involved in this study were recorded.

Isolation and Culture of Monocytes Extracted from Human Blood Samples

Blood samples collected from two pEDS patients and three normal controls were used to extract peripheral blood mononuclear cells (PBMCs) using density gradient centrifugation. PBMCs of each group were added with RPMI1640 medium (Gibco) containing 2%FBS (Gibco) and incubated at 37°C with 5% CO2 for 2 h. Then the supernatant was harvested and stored for the later experiment of enzyme-linked immunosorbent assay (ELISA). The remained cells were isolated monocytes and washed twice by sterile PBS (Servicebio) gently. RPMI1640 medium supplemented with 10% FBS, 100 U/ml penicillin, and 100 μg/ml streptomycin (HyClone) for further culture for 12 h.

Isolation and Culture of Human Gingival Fibroblasts

Gingival connective tissues were obtained from 2 pEDS patients during tooth extraction surgery and three normal controls during crown lengthening surgery. The collected gingival tissue was immersed in DMEM (Gibco) supplemented with 100 U/ml penicillin, and 100 μg/ml streptomycin (HyClone); and the tissue was cut into pieces, approximately 1 × 1 mm in size and placed in DMEM supplemented with 10% FBS, 100 U/ml penicillin, and 100 μg/ml streptomycin; tissue was then incubated at 37°C with 5% CO_2, HGF at the 2^{nd} passage was harvested for future experiments.

Gene Expression Profiling

Total RNA was isolated from monocytes and gingival fibroblasts by TRIzol reagent (Invitrogen) according to the manufacturer's instructions. The RNA samples were quality assessed and the mRNA is enriched using magnetic beads with Oligo (dT). The mRNA was then broken into short fragments by adding fragmentation buffer, and one-stranded cDNA was synthesized using random hexamers as templates, followed by the addition of buffer, dNTPs, and DNA polymerase I and RNase H. The double-stranded cDNA was purified with AMPure XP beads and was end-repaired, added with polyA tails and adapters sequences. After size selection, PCR amplification, and purification, the library was finally obtained. After the quality assessment of the library, RNA sequencing was performed on an Illumina HiSeq X Ten instrument. The raw reads were cleaned by removing adapter sequences, trimming low-quality ends, and filtering low-quality reads (Phred quality <20) using TrimGalore (version 0.6.5). Transcriptome quantification of transcript expression was carried out by using the mapping-based mode of Salmon (version 1.5.2) with the pre-built version of the full-decoy salmon index provided by Salmon.

RNA-Seq Data Analysis

Normalisation and differential expression between patients and normal controls were evaluated using DESeq2 (version 1.32.0) (Love et al., 2014), implemented in R (version 4.1.2). DESeq2 uses

a count-based negative binomial model to detect differentially expressed genes (DEGs). DEGs were defined as genes with the adjusted *p*.value < 0.05 and the absolute value of fold change >1.5 ($|log_2FC| > 1.5$).

Principal component analysis (PCA), dendrogram and hierarchical clustering heatmap were performed with the variance stabilization transformation values obtained by DESeq2 R package from the gene expression values: PCA was calculated for the whole dataset by using princomp function of R (Anders and Huber, 2010); The dendrogram was created by hclust function and ggplot2 package (version 3.3.5) (Wickham, 2016, p. 2); The hierarchical clustering heatmap was generated by ComplexHeatmap (version 2.10.0) package (Gu et al., 2016) using the top 100 DEGs.

Since there are only two pEDS samples and one of them was a rare case with both pEDS and vEDS, three-dimensional volcano plots were created with scatterplot3d (version 0.3–41) (Ligges & Mächler, 2003): the logarithm of fold change between pEDS1 and normal controls ($\log_2 FC_{pEDS1-normal}$) was represented on the x axis, the logarithm of fold change between pEDS2 and normal controls ($\log_2 FC_{pEDS2-normal}$) was represented on the y axis and the overall adjusted p.value was represented on the z axis. The filtering criteria included:1) The overall adjusted p.value <0.05; 2) $|\log_2 FC_{pEDS1-normal}|$>1.5 and 3) $|\log_2 FC_{pEDS2-normal}|$>1.5. The differential analysis in this step was performed with edgeR (version 3.36.0) (Robinson et al., 2010) and limma (version 3.50.0) (Ritchie et al., 2015).

For Over-Representation Analysis (ORA) and Gene Set Enrichment Analysis (GSEA), GO and KEGG enrichment analysis using detected DEGs and gene set enrichment analysis (GSEA) using ranked gene lists were performed with the software package clusterProfiler (Yu et al., 2012; Wu et al., 2021) (R-version 4.1.2, clusterProfiler_4.0.5) to identify enriched biological processes and molecular functions; The filtering standard for ORA and GSEA geneList is $|\log_2 FC|$>1.5. The query was carried out on all filtered DEGs by selecting a threshold of FDR-adjusted *p*-value less than 0.05. Similarly, the filtering adjusted *p*-value for GSEA should also be less than 0.05.

All the R packages we used in the analysis are listed in **Supplementary Table S1**.

STRING Network Analysis

STRING networks can provide information on the molecular mechanism underlying clinical features. A STRING network of DEGs involved in periodontitis and genes involved in the classical complement activation pathway was constructed using the STRING protein query (Szklarczyk et al., 2021) (STRING Version 11.5) and Cytoscape software (Shannon et al., 2003; Doncheva et al., 2019) (Cytoscape Version 3.8.2). The lines represent interaction associations between nodes and line thickness indicates the strength of data support. Selected DEGs were mapped to STRING to identify the interactive relationships among those genes. A confidence score of 0.4 was set as the cut-off criterion, and the node size in periodontitis-related genes is mapped to the logFC values of gene expression value in monocytes. Additionally, an extended STRING network showing the interaction between classical complement pathway and all DEGs in this study was also created, which could be found in **Supplementary Figure S2A**. We also identified the top 10 hub genes and sub-networks by using a Cytoscape plugin cytoHubba (**Supplementary Figure S2B**) (Chin et al., 2014).

Quantitative Reverse Transcription PCR for Validation

Relative expression levels of a series of selected DEGs (*MMP9*, *VEGFA*, *IL10*, *IL1A*, *IL1B*, *IL2RA*, and *IL6*) identified by RNA sequencing were confirmed by RT-qPCR using different RNA extractions obtained from monocytes cultures of corresponding pEDS and normal controls. 3 μg of total RNA were reverse-transcribed with random primers by standard procedure. RT-qPCR was performed with SYBR Green qPCR Master Mix (Life Technologies), 10 ng of Cdna, and with 10 μM of each primer set. The experiment was performed using the ABI PRISM 7500 Real-Time PCR System by standard thermal cycling conditions: Preincubation for 30 s at 95°C, followed by 40 cycles of 95°C for 10 s and 60°C for 30 s. GAPDH and CYC1 reference genes were amplified for normalization of Cdna loading. All specific primers used in the present study were summarized in **Supplementary Table S2**.

Enzyme-Linked Immunosorbent Assay

Enzyme-linked Immunosorbent Assay (ELISA) based quantification of IL-1β (Neobioscience Technology) concentration was measured using concentrated supernatants that we collected in monocytes isolation steps, following the supplier's instructions.

Statistics

For RT-qPCR, relative mRNA expression levels were normalized to the geometric mean of these reference genes and analyzed using the $2^{-\Delta\Delta Ct}$ method. Results were expressed as the mean value of relative quantification [mean (SD)]. Statistical significance between groups was determined using unpaired Student's t-test (ns = not significant, * = $p < 0.05$, ** $p < 0.01$, *** $p < 0.001$, **** $p < 0.0001$) with the R package ggpubr (Kassambara, 2020) (R-version 4.1.2, ggpubr_0.4.0). For ELISA, statistical significance between groups was determined with the R package ggpubr (Kassambara, 2020) (R-version 4.1.2, ggpubr_0.4.0). Results were tested for normality with Shapiro-Wilk's test. Since not all sample groups passed the normality test, we applied the unpaired, non-parametric Wilcoxon test (ns = not significant, * = $p < 0.05$, ** $p < 0.01$, *** $p < 0.001$, **** $p < 0.0001$).

RESULTS

Participant Enrollment

Two pEDS patients and three periodontal healthy adults (two males at 25 and 28 years old as normal1 and normal2 respectively; one female at 25 years old as normal3) were recruited in this study. The detailed clinical data of all individuals involved in this study were summarized in **Table 1**, oral photographs of all individuals were available in **Supplementary Figure S1**. As

TABLE 1 | The clinical findings of all individuals including age, gender, gingiva specimen sampling position, and periodontal examination results.

ID	Age (y)	Sex	Sampling Site	BOP	PD (mm)			CAL (mm)		
pEDS1	25	Male	13	+	15	11	10	15	13	13
					13			13		
					5	6	14	5	6	14
pEDS2	48	Female	13	+	7	3	5	13	6	5
					13			13		
					6	2	4	9	4	5
Normal1	25	Male	11	-	3	3	2	0	0	0
					11			11		
					2	1	2	0	0	0
Normal2	28	Male	21	-	2	3	1	0	0	0
					21			21		
					2	2	2	0	0	0
Normal3	25	Female	11	-	2	2	2	0	0	
					11			11		
					2	1	2	0	0	0

described in our previous work (Wu et al., 2018), it is worth noting that pEDS1 also carried a frameshift variant in *COL3A1* and thus might be affected by vascular EDS (vEDS).

Quality Assessment of Transcriptome Profiling

The correlation between pEDS and control group was evaluated by quality assessment methods including principal component analysis (PCA) and dendrogram. For the monocytes, PCA shows two principal components that could account for 73.8% of the variability between the samples (**Figure 1A**). The dendrogram of hierarchical clustering (**Figure 1B**) show a clear clustering of the controls and the pEDS patients based on gene expression values. However, for the HGF, no significant pattern can be found in the clustering of gene expression values between different samples (**Figures 1C,D**). The normalized count matrix files of monocyte and fibroblast can be found in **Supplementary Tables S3, S4**.

Differential Expression Analysis

Differentially expressed genes (DEGs) were identified by DESeq2 R package according to the filtering criteria. Approximately 3% of the detected transcriptome showed differential expression in monocytes and there were 338 DEGs in pEDS patient-derived monocytes, of which 246 genes were up-regulated and 92 genes were down-regulated. The complete list of DEGs could be found in **Supplementary Table S5**. Hierarchical heatmaps of the top 100 differential expressed genes within the monocyte and gingival fibroblast samples were shown in **Figures 2A,B**, which implied that a significant pattern can only be observed in monocytes but not in gingival fibroblasts. In addition, it should be noted that C1R and C1S were not differentially expressed in both monocytes and gingival fibroblasts from pEDS group.

Since one of two pEDS patients was a rare case with both pEDS and vEDS, three-dimensional volcano plots were created to present the DEGs (**Figures 2C,D**): A total of 92 DEGs were identified in monocytes but no DEGs could be found in HGF. It should also be noted that 45 DEGs could be identified between sample pEDS1 and pEDS2 but no significant result was identified in the subsequent ORA and GSEA analysis (data not shown).

Over-Representation Analysis and Gene Set Enrichment Analysis of Differentially Expressed Genes in Monocytes.

With the identified 338 DEGs, GO and KEGG enrichment analysis, as well as GSEA, were performed using the software package clusterProfiler (Version 4.0.5) (Yu et al., 2012; Wu et al., 2021). Most of the significant results are enriched in up-regulated genes (**Figure 3B**), especially in the pathway of biological processes, which are mainly related to inflammation response and immune response (**Figure 3A**). This finding is consistent with GSEA results (shown in **Figure 3C**), which are also highly enriched in pathways with positive enrichment scores (NES). Combined with differential expression analysis, it could be identified that some DEGs, i. e, RETN, DEFA1, ANXA3, LTF, and LCN2, are specifically involved in neutrophil, myeloid cell activation, and mediated immunity events. The complete list of GO-GSEA results were summarized in **Supplementary Table S6**. For the KEGG enrichment analysis, the most significant results were focused on the IL-17 signaling pathway and TNF signaling pathway. The complete enriched results of GO and KEGG analysis are summarized in **Supplementary Table S7**.

The Disease Ontology Enrichment Analysis of DEGs in Monocytes and Validation by Reverse Transcription-qPCR and Enzyme-Linked Immunosorbent Assay

The detailed mechanism behind complement pathway disruption and related pEDS clinical manifestations is not yet explained. Disease Ontology (DO) was developed to create a consistent description of gene products with disease perspectives, and accurate disease descriptions can discover new relationships between genes and disease (Schriml et al., 2012). Thus, we performed DO analysis with upregulated DEGs to help us to better understand the relationship between the mutant variants and pEDS. As shown in **Figure 4A**, the DO enriched results can be divided into several categories, which is separately related to different aspects of clinical features of pEDS: periodontal destruction, skin fragility, vascular complication, and joint hypermobility [Colors represent different clinical features of pEDS; Horizontal axis represent Fold Enrichment of each DO category, which is defined as GeneRatio/BgRatio in clusterProfiler (Yu et al., 2015)]. Besides, to identify genes related to the pathogenesis of pEDS, the overlapping between DO categories of periodontal destruction, vascular complications, and skin disease were selected (**Figure 4B**). The complete list of DO terms of upregulated DEGs is shown in **Supplementary Table S8**. The selected DEGs including *MMP9*, *VEGFA*, *IL10*, *IL1A*,

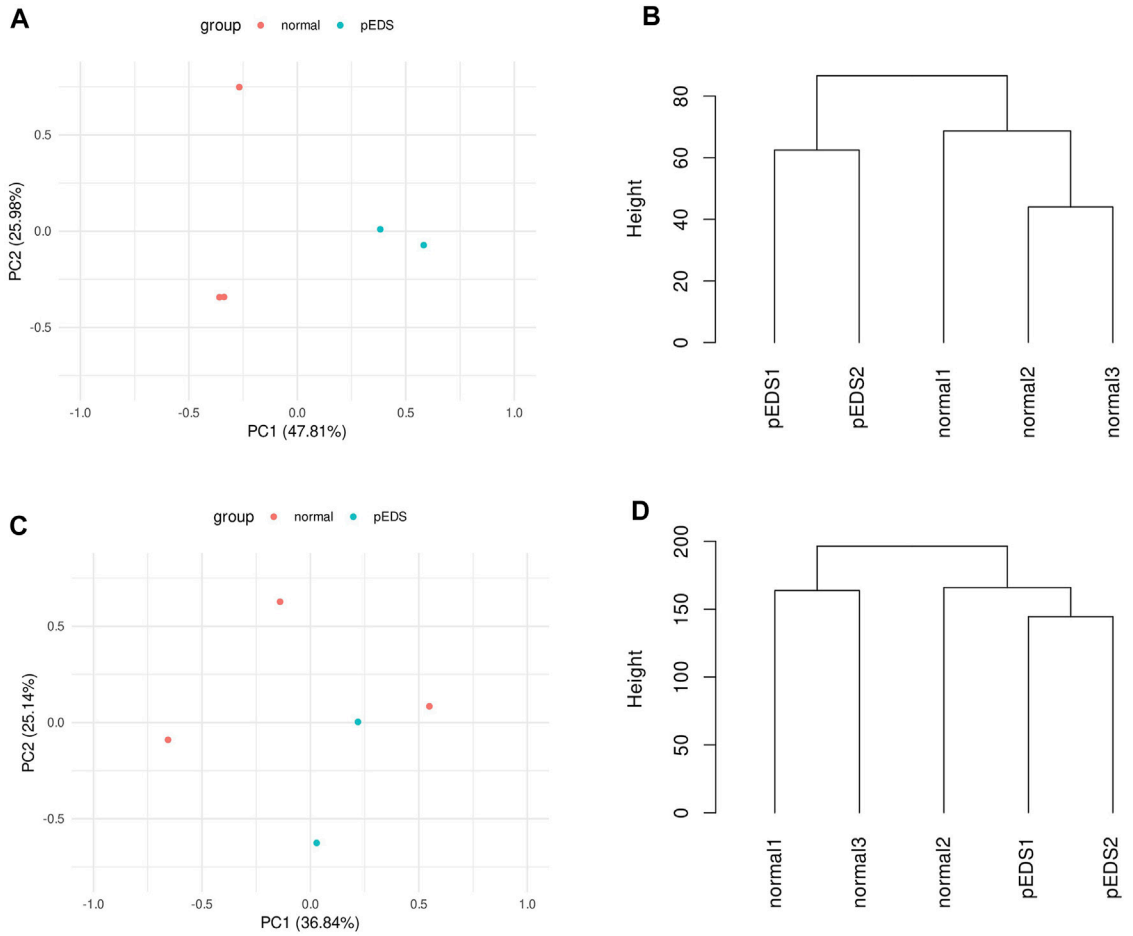

FIGURE 1 | The correlation between pEDS and control group was evaluated by quality assessment methods including principal component analysis (PCA) and dendrogram. **(A)** PCA shows 73.8% of the variability within the monocyte samples is accounted by two principal components. Note the clustering of pEDS (green) vs. normal controls (red); **(B)** For monocytes, dendrogram shows a clear clustering of the controls and the pEDS subjects based on gene expression values; **(C,D)** As for HGF samples, the first two principal components can not separate pEDS (green) from normal controls (red); and samples from same group do not cluster. Dendrogram, consistent with PCA result, does not show a significant clustering pattern.

IL1B, *IL2RA,* and *IL6* were identified and validated by RT-qPCR. All 7 genes are significantly expressed in the pEDS group compared to controls (**Figure 5A**). MMP9, IL10, IL1A, IL1B, IL6 were also measured as the top 10 hub genes (**Supplementary Figure S2B**) by cytoHubba (Chin et al., 2014), confirming their important roles in pathomechanism of pEDS. ELISA was also performed to measure the IL-1 β concentration of supernatants collected in monocytes isolation steps (**Figure 5B**). Similar to the qPCR result, the IL-1β concentration was also significantly higher in the monocytes of pEDS patients.

STRING Network

As shown in **Figure 6**, the STRING network shows the relationship between genes involved in the classical complement activation pathway and the DEGs related to periodontitis. The overlapped genes from DO analysis including *MMP9*, *VEGFA*, *IL10*, *IL1A*, *IL1B*, *IL2RA*, *IL6* are also in the STRING networks and showed closer interaction among the nodes. The pathogenic mutant variant, *C1R/C1S* were located the upstream of STRING network and not directly connected to the periodontitis-related genes. Additionally, in the extended STRING network consisted of classical complement pathway and DEGs in this study (**Supplementary Figure S2A**), the nodes of C1R/C1S only connected to other complement components but not any DEG, which implied that the extracellularly active C1s protein might have other potential targets that has yet been found (Bally et al., 2019).

DISCUSSION

Transcriptomics have been utilized to disclose the key alterations of biological processes triggering human diseases, thus offering novel instruments useful not only for the comprehension of their underlying mechanisms but also for their molecular diagnosis and clinical therapy (Casamassimi et al., 2017). Previous studies (Chiarelli et al., 2016, 2018, 2019; Lim et al., 2019) performed transcriptome analysis on other EDS subtypes, which succeeded

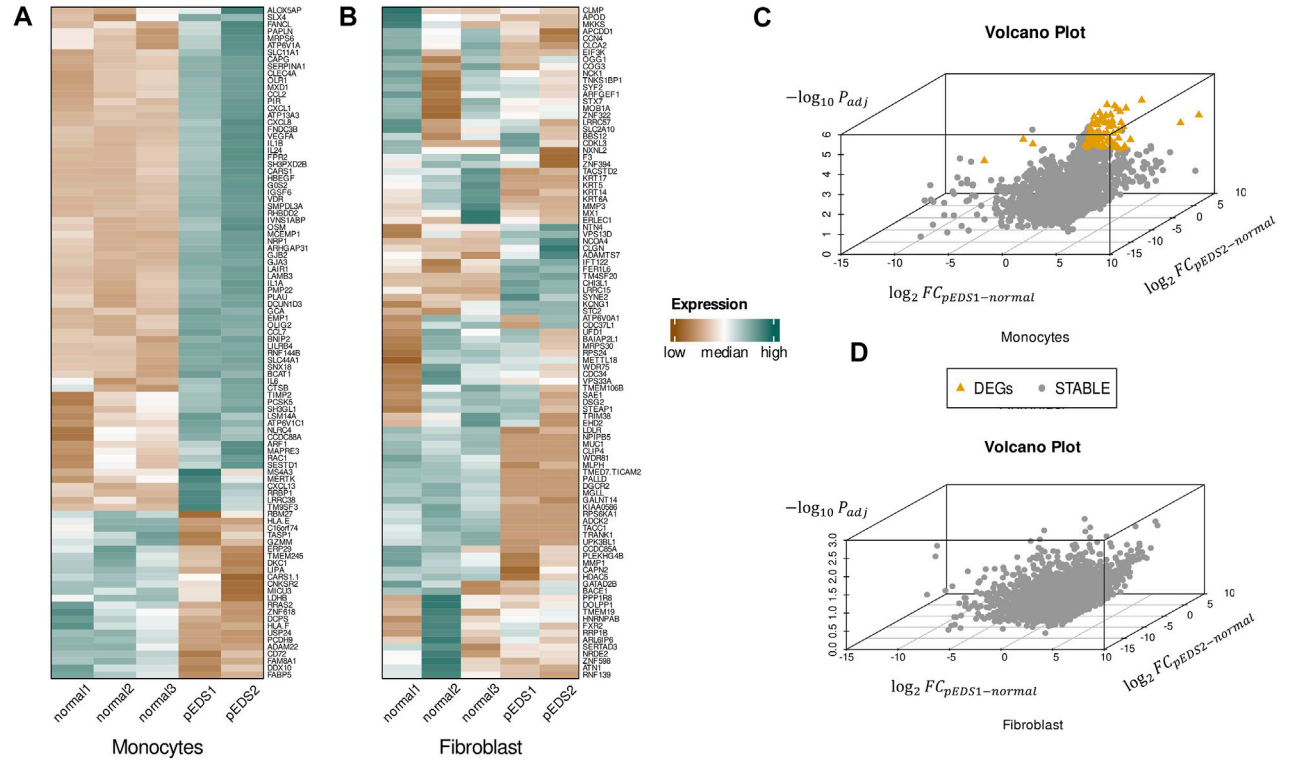

FIGURE 2 | Three dimensional volcano plot and hierarchical heatmap of the DEGs found within the monocyte and gingival fibroblast samples. **(A,B)** Hierarchical heatmap of the top 100 differential expressed genes within the monocyte and gingival fibroblast samples. Red denotes increased expression, and green denotes decreased expression. A significant pattern can only be observed in monocytes but not in gingival fibroblasts. **(C,D)** Three-dimensional volcano plots for monocytes and fibroblasts: $\log_2 FC_{pEDS1-normal}$ was represented on the x axis, $\log_2 FC_{pEDS2-normal}$ was represented on the y axis and the overall adjusted *p*.value was represented on the z axis. The filtering criteria included:1) The overall adjusted *p*.value <0.05; 2) | $\log_2 FC_{pEDS1-normal}$ |>1.5 and 3) | $\log_2 FC_{pEDS2-normal}$ |>1.5. Orange triangle denotes DEGs, gray point denotes not differentially expressed genes. DEGs were only found in monocytes.

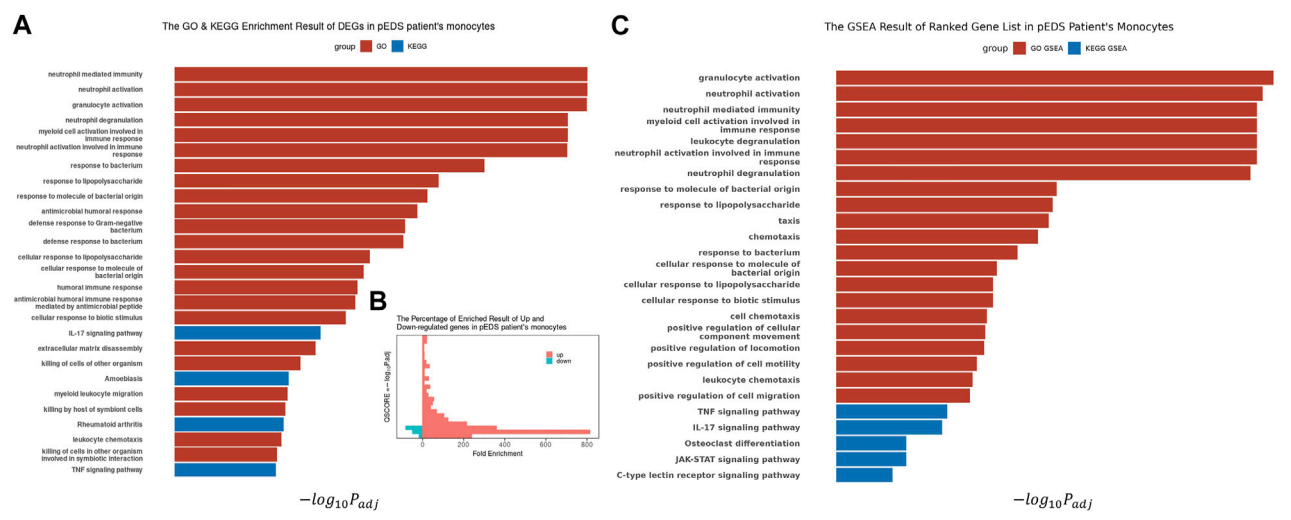

FIGURE 3 | The Biological Processes GO Enrichment Result and GSEA result of DEGs in pEDS patients' monocytes. **(A)** Biological processes related to inflammation response and immune response are significantly enriched; **(B)** Most of the significant results are contributed by upregulated genes, which also have higher Fold Enrichment (defined as GeneRatio/BgRatio in clusterProfiler) compared to downregulated genes; **(C)** The GSEA analysis result also showed similar enriched result in pathways related to immunity, inflammation, IL-17 pathway and TNF-α pathway.

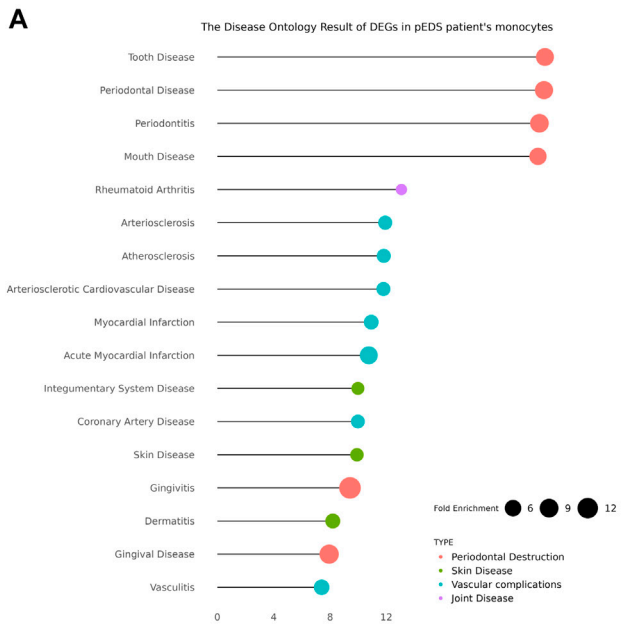

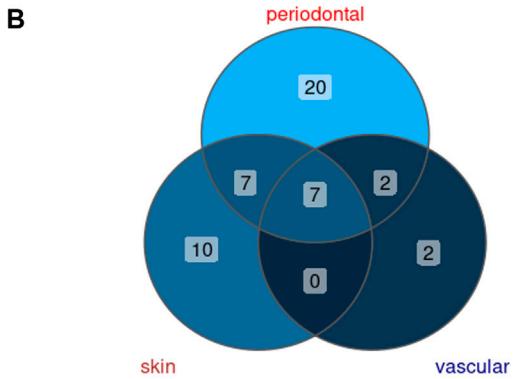

	SYMBOL	GENENAME	padj	logFC	status
1	MMP9	matrix metallopeptidase 9	3.55e-08	2.53	UP
2	VEGFA	vascular endothelial growth factor A	1.01e-15	3.03	UP
3	IL1A	interleukin 1 alpha	8.59e-24	3.09	UP
4	IL1B	interleukin 1 beta	3.41e-17	2.26	UP
5	IL2RA	interleukin 2 receptor subunit alpha	7.16e-04	1.69	UP
6	IL6	interleukin 6	4.92e-02	2.97	UP
7	IL10	interleukin 10	1.93e-02	1.76	UP

FIGURE 4 | The Disease Ontology Enrichment Analysis Result of DEGs in pEDS patients' monocytes and the overlapped enriched genes between DO categories of periodontal destruction, vascular complication, and skin disease in pEDS patients' monocytes. **(A)** The DO results can be divided into four categories which are separately related to different clinical features of pEDS: periodontal destruction, skin fragility, vascular complication, and joint hypermobility (Colors represent different clinical features of pEDS; Horizontal axis represent Fold Enrichment of each DO category, which is defined as GeneRatio/BgRatio in clusterProfiler); **(B)** seven genes including *MMP9, VEGFA, IL10, IL1A, IL1B, IL2RA*, and *IL6* have been found as the overlapped genes in three different DO categories and all of them were significantly upregulated in monocytes of pEDS.

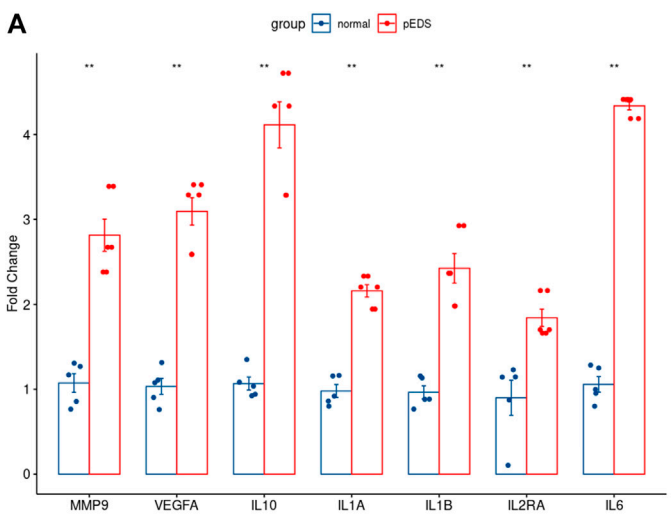

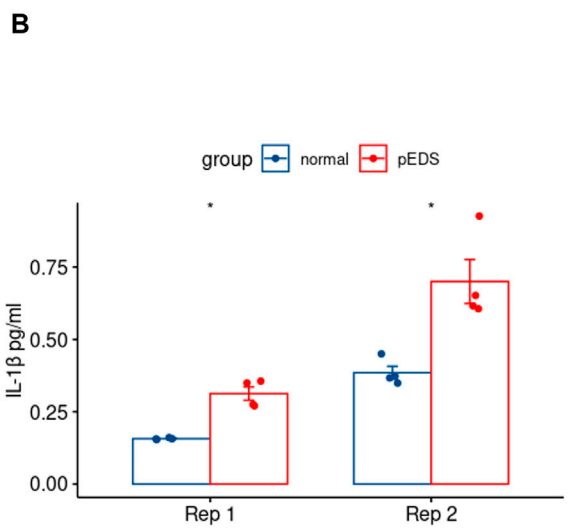

FIGURE 5 | RT-qPCR of the overlapped genes and the ELISA result of IL-1β expression in pEDS patients' monocytes were performed to validate the RNA sequencing results of pEDS patients. **(A)** In RT-qPCR analysis, gene expression levels were measured in four independent replicates per subject, and t-tests were performed (ns = not significant, *$p < 0.05$, **$p < 0.01$, ***$p < 0.001$, ****$p < 0.0001$). All seven genes including *MMP9, VEGFA, IL10, IL1A, IL1B, IL2RA*, and *IL6* are significantly expressed in pEDS group ($p < 0.01$); **(B)** For ELISA experiment, data are expressed as mean (SD). (ns = not significant, *$p < 0.05$, **$p < 0.01$, ***$p < 0.001$, ****$p < 0.0001$). IL-1β concentration was also significantly higher in the monocytes of pEDS patients ($p < 0.05$).

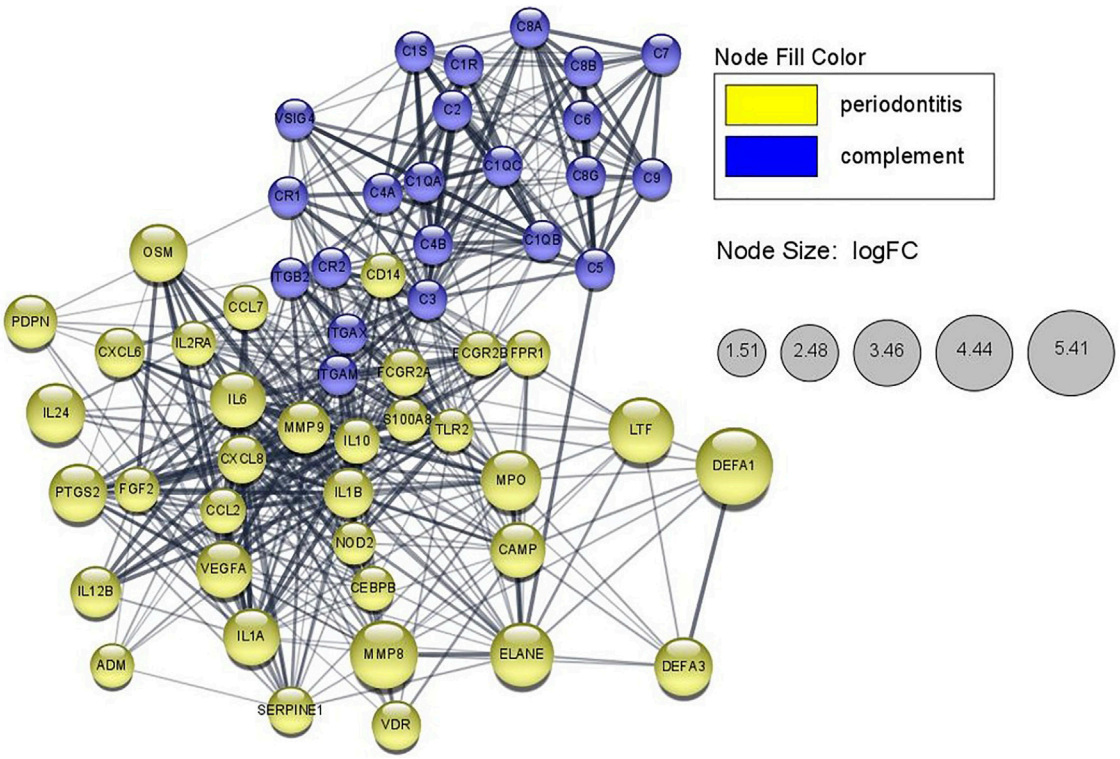

FIGURE 6 | STRING network showing periodontitis-related proteins that possibly interacted with the classical complement pathway in monocytes of pEDS patients. The lines represent interaction associations between nodes and line thickness indicates the strength of data support. The node size in periodontitis-related genes is mapped to the logFC values of gene expression value in monocytes of pEDS patients.

in revealing some of the mechanisms underlying these rare diseases. Up until now, the pathophysiology of pEDS is not well understood, and the current study described the first molecular evidence of significant gene expression changes in pEDS cells (monocytes and gingival fibroblasts) that could provide insights into the pathogenesis of the disease. Although the sample size is small and the findings will therefore need to be confirmed in other patients, our results provide a step forward towards understanding of the complex pathogenetic basis of pEDS. Multiple DEGs were identified only in monocytes but not in gingival fibroblasts. Approximately 3% of the detected transcriptome showing differential expression in monocytes and a total of 338 DEGs were identified in monocytes compared to normal control. ORA and GSEA analysis observed changes in neutrophil-mediated immunity, response to bacterium, humoral immune response, IL-17 pathway, and TNF-α pathway, of which are related to immune response and inflammatory response; DO analysis also identified potential target genes including *MMP9*, *VEGFA*, *IL10*, *IL1A*, *IL1B*, *IL2RA*, and *IL6*, which may be related to periodontal destruction, vascular complication, and skin disease of pEDS; In addition, STRING network analysis showed the relationship between genes involved in the classical complement activation pathway and the DEGs related to periodontitis. The overlapped genes from DO analysis are also in the STRING networks and some of them are considered as hub genes which highly interacted with other DEGs. This finding implied that these genes might play important roles in the pathophysiology of pEDS.

IL-17 Pathway and Periodontal Destruction

In ORA and GSEA, genes related to the IL-17 pathway were enriched in pEDS monocytes. Previous studies has reported that, IL-17, IL-17–producing lymphocytes and innate immune cells are potentially important players in the pathogenesis of periodontitis (Hajishengallis, 2014). Besides, elevated expression level of IL-17 has been closely related to periodontitis (Ohyama et al., 2009; Darveau, 2010). Overall, IL-17 is a double-edged sword when it comes to inflammatory illnesses like periodontitis (Zenobia & Hajishengallis, 2015).

On the one hand, IL-17 has been demonstrated to protect against extracellular pathogens (Khader et al., 2009; Hernandez-Santos and Gaffen, 2012) and can trigger the generation of antimicrobial peptides (Liang et al., 2010), which are assumed to be protective in periodontitis (Diamond et al., 2008; Gorr, 2009). On the other hand, through upregulating matrix metalloproteases and RANKL, IL-17 can also facilitate connective tissue degradation and bone resorption (Lubberts, 2008). IL-17 could also facilitate neutrophil recruitment and increase inflammation by downregulating the endogenous anti-inflammatory molecule Del-1 (Eskan et al., 2012).

IL17 can also be involved in periodontitis development through the complement pathway. Complement and IL-17 are both involved in the regulation of neutrophil recruitment, which is an important mechanism in maintaining periodontal homeostasis (Eskan et al., 2012; Hajishengallis and Hajishengallis, 2014). It is also reported that single nucleotide polymorphisms in the components C5 and IL-17 have been linked to a higher risk of periodontal disease (Chai et al., 2010a; Corrêa et al., 2012; Kadkhodazadeh et al., 2013), implying that both molecules may play a role in the illness's development. Although complement has a complex effect on IL-17 expression, it has been observed that complement, in collaboration with Toll-like receptors, can increase IL-17 synthesis in murine periodontal tissue (Abe et al., 2012). Mice lacking either C5Ar or Toll-like receptor-2, on the other hand, are protected from experimental periodontitis (Hajishengallis et al., 2011; Liang et al., 2011). In pEDS, the extracellularly activated C1s can activate the classical complement cascade and cleave more C4 and C2, which are components of the C3 convertase complex in the classical pathway (Bally et al., 2019). This disruption might ultimately induce the production of C5a (Ricklin and Lambris, 2013). With the support of Toll-like receptor-2 (TLR2 is also one of the upregulated DEGs and top 10 hub genes found in monocytes), abundant C5a may activate C5aR and upregulate IL-17, IL-1, IL-6, and TNF (Abe et al., 2012). Ultimately, IL-17 could facilitate neutrophil recruitment and result in periodontal destruction in synergy of other cytokines (Abe et al., 2012).

Selected DEGs and Periodontal Destruction

Apart from IL-17, other upregulated genes we identified in DO analysis also can be potential players in the periodontal destruction of pEDS. For upregulated MMP9, it has been suggested that matrix metalloproteinases (MMPs) are key proteases involved in destructive periodontal diseases (Buduneli and Kinane, 2011; Sorsa et al., 2011). The most prevalent MMPs in periodontal tissues are MMP-8 and MMP-9, which reflect the severity, development, and treatment response of periodontal disease (Mäntylä et al., 2006). MMP-9 has been linked to periodontal soft tissue degradation and has been found to work with MMP-13 in alveolar bone resorption and periodontal tissue distruction (Hernández et al., 2006; Hernández et al., 2011).

IL-1α, IL-1β and IL-6 are proinflammatory cytokines that are thought to play a role in periodontitis development. Nonsurgical periodontal therapy has been shown to result in a statistically significant reduction in overall levels of these cytokines in gingival crevicular fluid (GCF) (Reis et al., 2014). Nonetheless, IL-6 and IL-10 polymorphisms are found to be potential risk factors for periodontitis (Scapoli et al., 2012). In addition, Afacan et al. reported that the concentrations of VEGF and TNF-α in GCF were significantly higher in the periodontitis group than in the gingivitis and healthy groups (Afacan et al., 2018). Total amounts of VEGF and TNF-α in GCF were positively correlated with the site-specific clinical periodontal parameters and with each other. Increased GCF VEGF and TNF-α levels in both chronic and aggressive forms of periodontitis might suggest the role of the TNF-α/VEGF pathway in the pathogenesis of periodontal diseases (Afacan et al., 2018). In conclusion, the up-regulation of these selected DEGs is strongly connected to the pathogenesis of periodontitis and has the potential to be the possible pharmacological target.

Classical Complement Pathway and Periodontitis

The gain-of-function *C1R* and/or *C1S* variants are now recognized to be the essential element in the pathogenesis of pEDS. The extracellular presence of activated C1s can activate the conventional complement cascade without the presence of other signals (Gröbner et al., 2019). *In vitro* studies suggests that the production or release of active C1r serine protease may promote gingival hyperinflammation in response to mild biofilm, leading to severe periodontal damage (Bally et al., 2019; Gröbner et al., 2019).

The potential role of complement in human periodontitis was first recognized in the 1970s and 1980s when researchers looked into the GCF under different periodontal statuses (Attstroum et al., 1975; Courts et al., 1977; Schenkein and Genco, 1977). GCF samples from periodontitis patients were found to have complement-dependent hemolytic activity, indicating that GCF contains a functional complement system (Courts et al., 1977; Boackle, 1991). Recent studies also suggest an association between complement and periodontitis. A rare case of aggressive periodontitis with gingival angioedema was linked to deficiency of the C1INH (Roberts et al., 2003). People with periodontitis had a significantly higher occurrence of a single nucleotide polymorphism affecting C5 (rs17611), compared to healthy controls (Chai et al., 2010b). Another study identified C3 as one of the top 21 most promising candidate genes involved in periodontal disease using microarray experiments (Zhan et al., 2014). As for C5, it was reported that C5a can induce the activation of C5Ar in a murine periodontal disease and cause significant bone loss with the help of cytokines like IL-17, IL-1β, IL-6, and TNF (Abe et al., 2012). Conversely, C4 might have a protective effect against periodontitis since partial C4 gene deficiencies are significantly more common in periodontitis patients than in healthy individuals (Seppänen et al., 2007).

In this study, STRING network analysis showed a close relationship between genes involved in the classical complement pathway and DEGs in this study. C3, as previously reported, was located as the central element in the complement pathway (Ricklin and Lambris, 2013) and also showed closer links to other nodes in the STRING network. Meanwhile, *C1R* and *C1S* were upstream of the classical complement pathway and not directly connected to DEGs according to the evidences provided by STRING. Several DEGs such as MMP9, VEGFA, IL10, IL1A, IL1B, and IL6 that validated by RT-qPCR were also included in the STRING network and showed close connections to the complement pathway, which implied that they may play as important regulators between *C1R*/*C1S* mutation and downstream periodontal phenotypes. However, further research is necessary to confirm the relationship between genes

involved in the classical complement pathway and our selected DEGs.

Limitations

Firstly, we acknowledged that our study has a small sample size (due to patient cohort size), which may affect the power of some observations. In addition, only two pEDS patients were enrolled and one of them was affcted by both pEDS and vEDS, which means our result need to be confirmed in other patients in further research. Besides, compared to previous transcriptomic profiling of other EDS subtypes (Chiarelli et al., 2016, 2018, 2019), we used gingival fibroblasts rather than skin fibroblasts. It is not certain that other ECM producing cells, i.e., vascular smooth muscle cells, and skin fibroblasts, would show the same results in terms of gene expression profile. Finally, in the present study, we only validated the RNA-sequencing result by RT-qPCR and ELISA. Further research must be designed and performed to validate the results we found in this study.

CONCLUSION

In conclusion, our approach illustrates global Mrna profiling changes of several genes and related biological processes that could offer novel insights into the pEDS pathophysiology. Approximately 3% of the detected transcriptome showed differential expression and were identified only in monocytes but not in gingival fibroblasts, multiple DEGs were enriched in neutrophil-mediated immunity, response to bacterium, humoral immune response, IL-17 pathway, and TNF-α pathway. Potential target genes including *MMP9*, *VEGFA*, *IL10*, *IL1A*, *IL1B*, *IL2RA*, and *IL6* were significantly upregulated in monocytes which related to periodontal destruction, vascular complication, and skin disease. However, additional functional work is required to verify whether these up-regulated factors are essential in the pEDS mechanism.

DATA AVAILABILITY STATEMENT

The datasets presented in this study can be found in online repositories. The names of the repository/repositories and accession number(s) can be found below: https://www.ncbi.nlm.nih.gov/geo/query/acc.cgi?acc=GSE190786.

ETHICS STATEMENT

The studies involving human participants were reviewed and approved by the Ethics Committee of Nanjing Stomatological Hospital, Medical School of Nanjing University. The patients/participants provided their written informed consent to participate in this study. Written informed consent was obtained from the individual(s) for the publication of any potentially identifiable images or data included in this article.

AUTHOR CONTRIBUTIONS

Contribution: TZ and NW performed RNA sequencing experiments; ZL analyzed results; JC made the figures; TZ recruited patients, performed consent, and recorded clinical data; ZL, WS, and JW designed the research and wrote the paper.

FUNDING

This work was supported by grants from the Natural Science Foundation of Jiangsu Province (BK20200149), Medical Science and technology development Foundation, Nanjing Department of Health (YKK20152), and National Natural Science Foundation of China (82001111). The sponsors of this study are public or nonprofit organizations that support science in general.

ACKNOWLEDGMENTS

The authors thank the patients for their kind availability for this study.

SUPPLEMENTARY MATERIAL

The Supplementary Material for this article can be found online at: https://www.frontiersin.org/articles/10.3389/fgene.2022.834928/full#supplementary-material

Supplementary Figure S1 | Oral photographs of all individuals enrolled in this study.

Supplementary Figure S2 | The extended STRING network as well as the top 10 hub genes calculated by cytoHubba. A: The STRING network constructed by the classical complement pathway and all DEGs. C1R/C1S nodes only showed direct connections to other complement component. B: Top 10 hub genes included *CCL2, CXCL1 ,CXCL2, CXCL8, IL1A, IL1B, IL6, IL10, MMP9* and *TLR2*. the color from yellow to red denotes the degree of hub genes interacted with other DEGs.

Supplementary Table S1 | All the R packages and software used for RNA sequencing data analysis in this study.

Supplementary Table S2 | Specific gene primers used for RT-qPCR in the study.

Supplementary Table S3 | The normalized read counts of monocytes.

Supplementary Table S4 | The normalized read counts of fibroblasts.

Supplementary Table S5 | List of DEGs that are up-regulated and down-regulated in pEDS patients' monocytes over controls.

Supplementary Table S6 | The complete list of GO-GSEA results in pEDS patients' monocytes over controls.

Supplementary Table S7 | The complete list of enriched GO and KEGG terms of DEGs in pEDS patients' monocytes over controls.

Supplementary Table S8 | The complete list of enriched DO terms of upregulated DEGs in pEDS patients' monocytes over controls.

REFERENCES

Abe, T., Hosur, K. B., Hajishengallis, E., Reis, E. S., Ricklin, D., Lambris, J. D., et al. (2012). Local Complement-Targeted Intervention in Periodontitis: Proof-Of-Concept Using a C5a Receptor (CD88) Antagonist. *J.I.* 189, 5442–5448. doi:10.4049/jimmunol.1202339

Afacan, B., Öztürk, V. Ö., Paşalı, Ç., Bozkurt, E., Köse, T., and Emingil, G. (2018). Gingival Crevicular Fluid and Salivary HIF-1α, VEGF, and TNF-α Levels in Periodontal Health and Disease. *J. Periodontol.* 18, 0412. doi:10.1002/jper.18-0412

Anders, S., and Huber, W. (2010). Differential Expression Analysis for Sequence Count Data. *Genome Biol.* 11 (10), R106. doi:10.1186/gb-2010-11-10-r106

Attstroum, R., Laurel, A.-B., Lahsson, U., and Sjouholm, A. (1975). Complement Factors in Gingival Crevice Material from Healthy and Inflamed Gingiva in Humans. *J. Periodontal Res.* 10, 19–27. doi:10.1111/j.1600-0765.1975.tb00003.x

Bally, I., Dalonneau, F., Chouquet, A., Gröbner, R., Amberger, A., Kapferer-Seebacher, I., et al. (2019). Two Different Missense C1S Mutations, Associated to Periodontal Ehlers-Danlos Syndrome, Lead to Identical Molecular Outcomes. *Front. Immunol.* 10, 2962. doi:10.3389/fimmu.2019.02962

Bally, I., Dalonneau, F., Chouquet, A., Gröbner, R., Amberger, A., Kapferer-Seebacher, I., et al. (2019). Two Different Missense C1S Mutations, Associated to Periodontal Ehlers-Danlos Syndrome, lead to Identical Molecular Outcomes. *Front. Immunol.* 10, 2962. doi:10.3389/fimmu.2019.02962

Beikler, T., Peters, U., Prior, K., Eisenacher, M., and Flemmig, T. F. (2008). Gene Expression in Periodontal Tissues Following Treatment. *BMC Med. Genomics* 1, 30. doi:10.1186/1755-8794-1-30

Blackburn, P. R., Xu, Z., Tumelty, K. E., Zhao, R. W., Monis, W. J., Harris, K. G., et al. (2018). Bi-allelic Alterations in AEBP1 Lead to Defective Collagen Assembly and Connective Tissue Structure Resulting in a Variant of Ehlers-Danlos Syndrome. *Am. J. Hum. Genet.* 102, 696–705. doi:10.1016/j.ajhg.2018.02.018

Blighe, K., Rana, S., and Lewis, M. (2021). EnhancedVolcano: Publication-Ready Volcano Plots with Enhanced Colouring and Labeling. .

Boackle, R. J. (1991). The Interaction of Salivary Secretions with the Human Complement System - A Model for the Study of Host Defense Systems on Inflamed Mucosal Surfaces. *Crit. Rev. Oral Biol. Med.* 2, 355–367. doi:10.1177/10454411910020030401

Buduneli, N., and Kinane, D. F. (2011). Host-derived Diagnostic Markers Related to Soft Tissue Destruction and Bone Degradation in Periodontitis. *J. Clin. Periodontol.* 38, 85–105. doi:10.1111/j.1600-051x.2010.01670.x

Casamassimi, A., Federico, A., Rienzo, M., Esposito, S., and Ciccodicola, A. (2017). Transcriptome Profiling in Human Diseases: New Advances and Perspectives. *Ijms* 18 (8), 1652. doi:10.3390/ijms18081652

Chai, L., Song, Y.-Q., Zee, K.-Y., and Leung, W. K. (2010a). Single Nucleotide Polymorphisms of Complement Component 5 and Periodontitis. *J. Periodontal Res.* 45, 301–308. doi:10.1111/j.1600-0765.2009.01234.x

Chai, L., Song, Y.-Q., Zee, K.-Y., and Leung, W. K. (2010b). Single Nucleotide Polymorphisms of Complement Component 5 and Periodontitis. *J. Periodontal Res.* 45, 301–308. doi:10.1111/j.1600-0765.2009.01234.x

Chiarelli, N., Carini, G., Zoppi, N., Dordoni, C., Ritelli, M., Venturini, M., et al. (2016). Transcriptome-Wide Expression Profiling in Skin Fibroblasts of Patients with Joint Hypermobility Syndrome/Ehlers-Danlos Syndrome Hypermobility Type. *PLoS ONE* 11, e0161347. doi:10.1371/journal.pone.0161347

Chiarelli, N., Carini, G., Zoppi, N., Dordoni, C., Ritelli, M., Venturini, M., et al. (2016). Transcriptome-wide Expression Profiling in Skin Fibroblasts of Patients with Joint Hypermobility Syndrome/Ehlers-Danlos Syndrome Hypermobility Type. *PLoS ONE* 11 (8), e0161347. doi:10.1371/journal.pone.0161347

Chiarelli, N., Carini, G., Zoppi, N., Ritelli, M., and Colombi, M. (2019). Molecular Insights in the Pathogenesis of Classical Ehlers-Danlos Syndrome from Transcriptome-wide Expression Profiling of Patients' Skin Fibroblasts. *PLoS ONE* 14, e0211647. doi:10.1371/journal.pone.0211647

Chiarelli, N., Carini, G., Zoppi, N., Ritelli, M., and Colombi, M. (2018). Transcriptome Analysis of Skin Fibroblasts with Dominant Negative COL3A1 Mutations Provides Molecular Insights into the Etiopathology of Vascular Ehlers-Danlos Syndrome. *PLoS ONE* 13, e0191220. doi:10.1371/journal.pone.0191220

Chiarelli, N., Carini, G., Zoppi, N., Ritelli, M., and Colombi, M. (2018). Transcriptome Analysis of Skin Fibroblasts with Dominant Negative COL3A1 Mutations Provides Molecular Insights into the Etiopathology of Vascular Ehlers-Danlos Syndrome. *PLoS ONE* 13 (1), e0191220. doi:10.1371/journal.pone.0191220

Chiarelli, N., Ritelli, M., Zoppi, N., and Colombi, M. (2019). Cellular and Molecular Mechanisms in the Pathogenesis of Classical, Vascular, and Hypermobile Ehlers–Danlos Syndromes. *Genes* 10, 609. doi:10.3390/genes10080609

Chin, C.-H., Chen, S.-H., Wu, H.-H., Ho, C.-W., Ko, M.-T., and Lin, C.-Y. (2014). cytoHubba: Identifying Hub Objects and Sub-networks from Complex Interactome. *BMC Syst. Biol.* 8. doi:10.1186/1752-0509-8-S4-S11

Corrêa, J. D., Madeira, M. F., Resende, R. G., Correia-Silva, Jde. F., Gomez, R. S., de Souza, Dda. G., et al. (20122012). Association between Polymorphisms in interleukin-17A and -17F Genes and Chronic Periodontal Disease. *Mediators Inflamm.* 2012, 846052. doi:10.1155/2012/846052

Courts, F. J., Boackle, R. J., Fudenberg, H. H., and Silverman, M. S. (1977). Detection of Functional Complement Components in Gingival Crevicular Fluid from Humans with Periodontal Disease. *J. Dent Res.* 56, 327–331. doi:10.1177/00220345770560032001

Darveau, R. P. (2010). Periodontitis: A Polymicrobial Disruption of Host Homeostasis. *Nat. Rev. Microbiol.* 8, 481–490. doi:10.1038/nrmicro2337

Diamond, G., Beckloff, N., and Ryan, L. K. (2008). Host Defense Peptides in the Oral Cavity and the Lung: Similarities and Differences. *J. Dent Res.* 87, 915–927. doi:10.1177/154405910808701011

Doncheva, N. T., Morris, J. H., Gorodkin, J., and Jensen, L. J. (2019). Cytoscape StringApp: Network Analysis and Visualization of Proteomics Data. *J. Proteome Res.* 18, 623–632. doi:10.1021/acs.jproteome.8b00702

Dutzan, N., Konkel, J. E., Greenwell-Wild, T., and Moutsopoulos, N. M. (2016). Characterization of the Human Immune Cell Network at the Gingival Barrier. *Mucosal Immunol.* 9, 1163–1172. doi:10.1038/mi.2015.136

Eskan, M. A., Jotwani, R., Abe, T., Chmelar, J., Lim, J.-H., Liang, S., et al. (2012). The Leukocyte Integrin Antagonist Del-1 Inhibits IL-17-mediated Inflammatory Bone Loss. *Nat. Immunol.* 13, 465–473. doi:10.1038/ni.2260

G'al, P., Dob'o, J., Z'avodszky, P., and Sim, R. B. M. (2009). Early Complement Proteases: C1r, C1s and MASPs. A Structural Insight into Activation and Functions. *Mol. Immunol.* 46, 2745–2752.

Gorr, S.-U. (20092000). Antimicrobial Peptides of the Oral Cavity. *Periodontol* 51, 152–180. doi:10.1111/j.1600-0757.2009.00310.x

Gröbner, R., Kapferer-Seebacher, I., Amberger, A., Redolfi, R., Dalonneau, F., Björck, E., et al. (2019). C1R Mutations Trigger Constitutive Complement 1 Activation in Periodontal Ehlers-Danlos Syndrome. *Front. Immunol.* 10, 2537. doi:10.3389/fimmu.2019.02537

Gu, Z., Eils, R., and Schlesner, M. (2016). Complex Heatmaps Reveal Patterns and Correlations in Multidimensional Genomic Data. *Bioinformatics* 32 (18), 2847–2849. doi:10.1093/bioinformatics/btw313

Hajishengallis, E., and Hajishengallis, G. (2014). Neutrophil Homeostasis and Periodontal Health in Children and Adults. *J. Dent Res.* 93, 231–237. doi:10.1177/0022034513507956

Hajishengallis, G. (2014). Immunomicrobial Pathogenesis of Periodontitis: Keystones, Pathobionts, and Host Response. *Trends Immunol.* 35, 3–11. doi:10.1016/j.it.2013.09.001

Hajishengallis, G., Liang, S., Payne, M. A., Hashim, A., Jotwani, R., Eskan, M. A., et al. (2011). Low-abundance Biofilm Species Orchestrates Inflammatory Periodontal Disease through the Commensal Microbiota and Complement. *Cell Host & Microbe* 10, 497–506. doi:10.1016/j.chom.2011.10.006

Hernández, M., Dutzan, N., García-Sesnich, J., Abusleme, L., Dezerega, A., Silva, N., et al. (2011). Host-Pathogen Interactions in Progressive Chronic Periodontitis. *J. Dent Res.* 90, 1164–1170. doi:10.1177/0022034511401405

Hernandez, M., Valenzuela, M. A., Lopez-Otin, C., Alvarez, J., Lopez, J. M., Vernal, R., et al. (2006). Matrix Metalloproteinase-13 Is Highly Expressed in Destructive Periodontal Disease Activity. *J. Periodontol.* 77, 1863–1870. doi:10.1902/jop.2006.050461

Hern'andez-Santos, N., and Gaffen, S. L. (2012). Th17 Cells in Immunity to Candida Albicans. *Cell Host Microbe* 11, 425–435.

Kadkhodazadeh, M., Baghani, Z., Ebadian, A. R., Youssefi, N., Mehdizadeh, A. R., and Azimi, N. (2013). IL-17 Gene Polymorphism Is Associated with Chronic Periodontitis and Peri-Implantitis in Iranian Patients: A Cross-Sectional Study. *Immunological Invest.* 42, 156–163. doi:10.3109/08820139.2012.746697

Kapferer-Seebacher, I., Oakley-Hannibal, E., Lepperdinger, U., Johnson, D., Ghali, N., Brady, A. F., et al. (2021). Prospective Clinical Investigations of Children with Periodontal Ehlers-Danlos Syndrome Identify Generalized Lack of Attached Gingiva as a Pathognomonic Feature. *Genet. Med.* 23, 316–322. doi:10.1038/s41436-020-00985-y

Kapferer-Seebacher, I., Pepin, M., Werner, R., Aitman, T. J., Nordgren, A., Stoiber, H., et al. (2016). Periodontal Ehlers-Danlos Syndrome Is Caused by Mutations in C1R and C1S , Which Encode Subcomponents C1r and C1s of Complement. *Am. J. Hum. Genet.* 99, 1005–1014. doi:10.1016/j.ajhg.2016.08.019

Kassambara, A. (2020). Ggpubr: 'ggplot2' Based Publication Ready Plots. Available at: https://CRAN.R-project.org/package=ggpubr.

Khader, S. A., Gaffen, S. L., and Kolls, J. K. (2009). Th17 Cells at the Crossroads of Innate and Adaptive Immunity against Infectious Diseases at the Mucosa. *Mucosal Immunol.* 2, 403–411. doi:10.1038/mi.2009.100

Liang, S. C., Nickerson-Nutter, C., Pittman, D. D., Carrier, Y., Goodwin, D. G., Shields, K. M., et al. (2010). IL-22 Induces an Acute-phase Response. *J.I.* 185, 5531–5538. doi:10.4049/jimmunol.0904091

Liang, S., Krauss, J. L., Domon, H., McIntosh, M. L., Hosur, K. B., Qu, H., et al. (2011). The C5a Receptor Impairs IL-12-Dependent Clearance ofPorphyromonas Gingivalisand Is Required for Induction of Periodontal Bone Loss. *J.I.* 186, 869–877. doi:10.4049/jimmunol.1003252

Ligges, U., and Mächler, M. (2003). Scatterplot3d—An R Package for Visualizing Multivariate Data. *J. Stat. Softw.* 8 (11), 1–20. doi:10.18637/jss.v008.i11

Lim, L., Opitz, L., Opitz, H., and Rohrbach, G. (2019). Transcriptome Profiling of Primary Skin Fibroblasts Reveal Distinct Molecular Features between PLOD1- and FKBP14-Kyphoscoliotic Ehlers-Danlos Syndrome. *Genes* 10 (7), 517. doi:10.3390/genes10070517

Love, M. I., Huber, W., and Anders, S. (2014). Moderated Estimation of Fold Change and Dispersion for RNA-Seq Data with DESeq2. *Genome Biol.* 15, 550. doi:10.1186/s13059-014-0550-8

Lubberts, E. (2008). IL-17/Th17 Targeting: On the Road to Prevent Chronic Destructive Arthritis? *Cytokine* 41, 84–91. doi:10.1016/j.cyto.2007.09.014

Malfait, F., Francomano, C., Byers, P., Belmont, J., Berglund, B., Black, J., et al. (2017). The 2017 International Classification of the Ehlers-Danlos Syndromes. *Am. J. Med. Genet. C Semin. Med. Genet.* 175, 8–26. doi:10.1002/ajmg.c.31552

Mäntylä, P., Stenman, M., Kinane, D., Salo, T., Suomalainen, K., Tikanoja, S., et al. (2006). Monitoring Periodontal Disease Status in Smokers and Nonsmokers Using a Gingival Crevicular Fluid Matrix Metalloproteinase-8-specific Chair-Side Test. *J. Periodontal Res.* 41, 503–512. doi:10.1111/j.1600-0765.2006.00897.x

Ohyama, H., Kato-Kogoe, N., Kuhara, A., Nishimura, F., Nakasho, K., Yamanegi, K., et al. (2009). The Involvement of IL-23 and the Th17 Pathway in Periodontitis. *J. Dent Res.* 88, 633–638. doi:10.1177/0022034509339889

Reis, C., Da Costa, A. V., Guimarães, J. T., Tuna, D., Braga, A. C., Pacheco, J. J., et al. (2014). Clinical Improvement Following Therapy for Periodontitis: Association with a Decrease in IL-1 and IL-6. *Exp. Ther. Med.* 8, 323–327. doi:10.3892/etm.2014.1724

Ricklin, D., and Lambris, J. D. (2013). Complement in Immune and Inflammatory Disorders: Pathophysiological Mechanisms. *J.I.* 190, 3831–3838. doi:10.4049/jimmunol.1203487

Ritchie, M. E., Phipson, B., Wu, D., Hu, Y., Law, C. W., Shi, W., et al. (2015). Limma powers Differential Expression Analyses for RNA-Sequencing and Microarray Studies. *Nucleic Acids Res.* 43 (7), e47. doi:10.1093/nar/gkv007

Roberts, A., Shah, M., and Chapple, I. L. C. (2003). C-1 Esterase Inhibitor Dysfunction Localised to the Periodontal Tissues: Clues to the Role of Stress in the Pathogenesis of Chronic Periodontitis? *J. Clin. Periodontol.* 30, 271–277. doi:10.1034/j.1600-051x.2003.01266.x

Robinson, M. D., McCarthy, D. J., and Smyth, G. K. (2010). EdgeR: a Bioconductor Package for Differential Expression Analysis of Digital Gene Expression Data. *Bioinformatics* 26 (1), 139–140. doi:10.1093/bioinformatics/btp616

Scapoli, L., Girardi, A., Palmieri, A., Carinci, F., Testori, T., Zuffetti, F., et al. (2012). IL6 and IL10 Are Genetic Susceptibility Factors of Periodontal Disease. *Dent Res. J. (Isfahan)* 9, S197–S201. doi:10.4103/1735-3327.109754

Schenkein, H. A., and Genco, R. J. (1977). Gingival Fluid and Serum in Periodontal Diseases: II. Evidence for Cleavage of Complement Components C3, C3 Proactivator (Factor B) and C4 in Gingival Fluid. *J. Periodontol.* 48, 778–784. doi:10.1902/jop.1977.48.12.778

Schriml, L. M., Arze, C., Nadendla, S., Chang, Y.-W. W., Mazaitis, M., Felix, V., et al. (2012). Disease Ontology: A Backbone for Disease Semantic Integration. *Nucleic Acids Res.* 40, D940–D946. doi:10.1093/nar/gkr972

Seppänen, M., Lokki, M.-L., Notkola, I.-L., Mattila, K., Valtonen, V., Nieminen, A., et al. (2007). Complement and C4 Null Alleles in Severe Chronic Adult Periodontitis. *Scand. J. Immunol.* 65, 176–181. doi:10.1111/j.1365-3083.2006.01886.x

Shannon, P., Markiel, A., Ozier, O., Baliga, N. S., Wang, J. T., Ramage, D., et al. (2003). Cytoscape: A Software Environment for Integrated Models of Biomolecular Interaction Networks. *Genome Res.* 13, 2498–2504. doi:10.1101/gr.1239303

Sorsa, T., Mäntylä, P., Tervahartiala, T., Pussinen, P. J., Gamonal, J., and Hernandez, M. (2011). MMP Activation in Diagnostics of Periodontitis and Systemic Inflammation. *J. Clin. Periodontol.* 38, 817–819. doi:10.1111/j.1600-051x.2011.01753.x

Szklarczyk, D., Gable, A. L., Nastou, K. C., Lyon, D., Kirsch, R., Pyysalo, S., et al. (2021). The STRING Database in 2021: Customizable Protein-Protein Networks, and Functional Characterization of User-Uploaded Gene/measurement Sets. *Nucleic Acids Res.* 49, D605–D612. doi:10.1093/nar/gkaa1074

Wickham, H. (2016). *ggplot2: Elegant Graphics for Data Analysis*. Springer-Verlag New York. Available at: https://ggplot2.tidyverse.org.

Wu, J., Yang, J., Zhao, J., Wu, J., Zhang, X., Leung, W. K., et al. (2018). A Chinese Family with Periodontal Ehlers-Danlos Syndrome Associated with Missense Mutation in the *C1R Gene*. *J. Clin. Periodontol.* 45, 1311–1318. doi:10.1111/jcpe.12988

Wu, T., Hu, E., Xu, S., Chen, M., Guo, P., Dai, Z., et al. (2021). clusterProfiler 4.0: A Universal Enrichment Tool for Interpreting Omics Data. *The Innovation* 2, 100141. doi:10.1016/j.xinn.2021.100141

Yu, G., Wang, L.-G., Han, Y., and He, Q.-Y. (2012). clusterProfiler: An R Package for Comparing Biological Themes Among Gene Clusters. *OMICS: A J. Integr. Biol.* 16, 284–287. doi:10.1089/omi.2011.0118

Yu, G., Wang, L.-G., Yan, G.-R., and He, Q.-Y. (2015). DOSE: An R/Bioconductor Package for Disease Ontology Semantic and Enrichment Analysis. *Bioinformatics* 31, 608–609. doi:10.1093/bioinformatics/btu684

Zenobia, C., and Hajishengallis, G. (20152000). Basic Biology and Role of Interleukin-17 in Immunity and Inflammation. *Periodontol. 2000* 69 (1), 142–159. doi:10.1111/prd.12083

Zhan, Y., Zhang, R., Lv, H., Song, X., Xu, X., Chai, L., et al. (2014). Prioritization of Candidate Genes for Periodontitis Using Multiple Computational Tools. *J. Periodontol.* 85, 1059–1069. doi:10.1902/jop.2014.130523

Conflict of Interest: The authors declare that the research was conducted in the absence of any commercial or financial relationships that could be construed as a potential conflict of interest.

Publisher's Note: All claims expressed in this article are solely those of the authors and do not necessarily represent those of their affiliated organizations, or those of the publisher, the editors and the reviewers. Any product that may be evaluated in this article, or claim that may be made by its manufacturer, is not guaranteed or endorsed by the publisher.

frontiers | Frontiers in Genetics

TYPE Case Report
PUBLISHED 18 November 2022
DOI 10.3389/fgene.2022.1017446

OPEN ACCESS

EDITED BY
Kenji Kurosawa,
Kanagawa Children's Medical Center, Japan

REVIEWED BY
Nadia Akawi,
United Arab Emirates University, United Arab Emirates
Joshi Stephen,
Baylor College of Medicine, United States

*CORRESPONDENCE
Shujiro Hayashi,
shayashi@dokkyomed.ac.jp

SPECIALTY SECTION
This article was submitted to Genetics of Common and Rare Diseases, a section of the journal Frontiers in Genetics

RECEIVED 12 August 2022
ACCEPTED 02 November 2022
PUBLISHED 18 November 2022

CITATION
Hayashi S, Yamaguchi T, Kosho T and Igawa K (2022), Case report: Mild phenotype of a patient with vascular Ehlers–Danlos syndrome and *COL3A1* duplication mutation without alteration in the [Gly-X-Y] repeat sequence. *Front. Genet.* 13:1017446. doi: 10.3389/fgene.2022.1017446

Case report: Mild phenotype of a patient with vascular Ehlers–Danlos syndrome and *COL3A1* duplication mutation without alteration in the [Gly-X-Y] repeat sequence

Shujiro Hayashi[1]*, Tomomi Yamaguchi[2,3,4], Tomoki Kosho[2,3,4,5] and Ken Igawa[1]

[1]Department of Dermatology, Dokkyo Medical University School of Medicine, Mibu, Japan, [2]Department of Medical Genetics, Shinshu University School of Medicine, Matsumoto, Japan, [3]Center for Medical Genetics, Shinshu University Hospital, Matsumoto, Japan, [4]Division of Clinical Sequencing, Shinshu University School of Medicine, Matsumoto, Japan, [5]Research Center for Supports to Advanced Science, Shinshu University, Matsumoto, Japan

Background: Vascular-type Ehlers–Danlos syndrome (vEDS) is an autosomal dominant inherited disorder caused by a deficit in collagen III as a result of heterogeneous mutations in the α1 type III collagen gene (*COL3A1*). Patients with vEDS often experience the first major complications in their early 20s and >80% have at least one complication by their 40s, reducing their average life expectancy to 48 years. Most commonly, vEDS variants are heterozygous missense substitutions of a base-pair encoding a glycine (Gly) residue of the [Gly-X-Y] repeat of the *COL3A1* protein. When a peptide chain derived from a mutant allele is present in the procollagen triple helical structure, the helical structure cannot be maintained. Therefore, typically, the mutated collagen peptide induces a dominant negative effect on procollagen production. We reported the case of a patient with vEDS and a unique novel duplication mutation without alteration in the [Gly-X-Y] triplet repeat sequence.

Case presentation: A 58-year-old man developed a sudden disorder of consciousness and abdominal pain and was consequently taken to a nearby hospital, where an intra-abdominal aneurysm was found, in addition to mild small joint hypermobility and acrogeria. There has been no history of spontaneous pneumothorax, dislocation, or subcutaneous hematoma. The analysis of genomic DNA from a blood sample identified a likely pathogenic in-frame duplication mutation in the *COL3A1* gene coding region. Interestingly, this mutation is not expected to alter the [Gly-X-Y] triplet repeat sequence. We verified the mutation's pathogenicity by performing an analysis of synthetic procollagen from cultured skin fibroblasts, electron microscopy, and mRNA expression analysis of unfolded protein response sensors for endoplasmic reticulum (ER) stress.

Conclusion: Although the clinical findings of the case were mild, when compared to typical vEDS, decreased α1 collagen III levels and

morphological abnormalities of the collagenous bundles were observed in the patient samples when compared with the normal control samples. Our evidence supports the conclusion that this variant is pathogenic. However, unlike the common vEDS, ER stress was not observed, and the mild phenotype presentation was suggested to be due to the unique mutation, allowing the triple helical structure to be maintained to a certain extent.

KEYWORDS

Vascular Ehlers–Danlos syndrome, COL3A1, triplet repeat sequence, endoplasmic reticulum stress, unfolded protein response, in-frame mutation

Introduction

Vascular-type Ehlers–Danlos syndrome (vEDS) is an autosomal dominant inherited disorder with a frequency of 1: 100,000–250,000 (Byers et al., 2017). vEDS is caused by a deficit in collagen III that results from heterogeneous mutations in the α1 type III collagen gene (*COL3A1*). The reduction in collagen III can affect the hollow organ walls, such as those of the uterus, intestines, and medium- and large-sized arteries, and the fragility of the connective tissues. In addition to various characteristic manifestations, such as translucent skin, easy bruising, characteristic facial appearance, small joint hypermobility, acrogeria, and others, vEDS patients occasionally also experience fatal complications, such as macrovascular rupture, intestinal perforation, and uterine rupture during pregnancy (Shimaoka et al., 2010; Malfait et al., 2017). Patients with vEDS often experience their first major complication in their early 20s and >80% of them have at least one complication by their 40s, reducing their average life expectancy to 48 years (Pepin et al., 2000).

Collagen proteins comprise a triple helical structure from three peptide chains, and this distinctive structure provides strong stability to the protein. To achieve a triple helical structure, three rich amino acids, namely, glycine (Gly), proline, and modified proline called hydroxyproline, are required. Gly should be one of the three consecutive amino acids to maintain the triple helical structure (Kramer et al., 1999). Most commonly, vEDS variants are heterozygous missense substitutions at a Gly-coding residue in the context of [Gly-X-Y] repeats, and secondly, vEDS are splice-site mutations in *COL3A1* (Frank et al., 2015). The mutant collagen peptide induces a dominant negative effect on procollagen production. Procollagen is organized as a triple helical structure formed by three peptide chains (Frank et al., 2015). When a peptide chain derived from the mutant allele is present in the procollagen triple helical

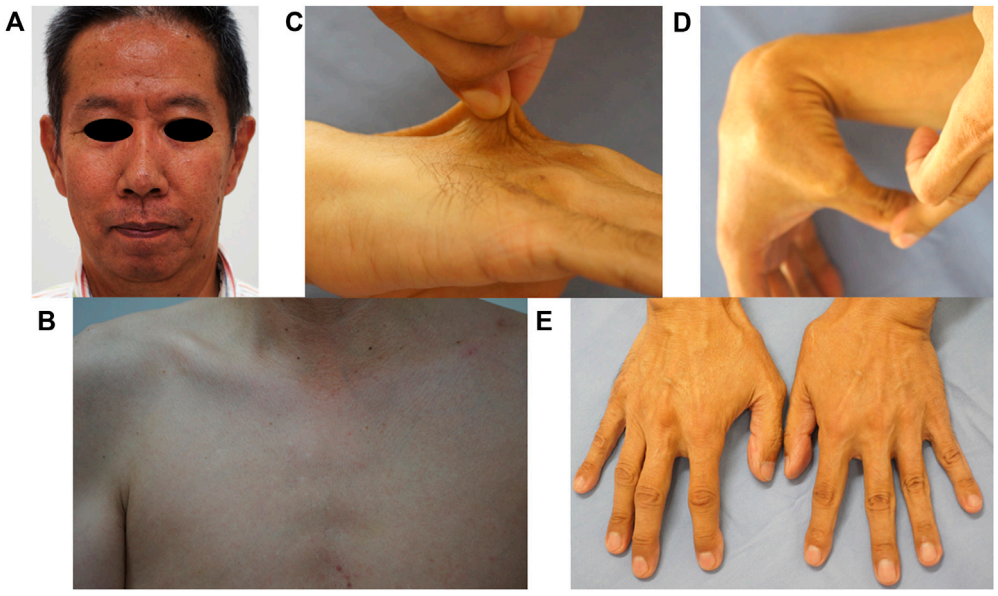

FIGURE 1
Clinical findings. No remarkable findings in terms of vEDS facial features **(A)**, no permeability of subcutaneous blood vessels **(B)**, and no skin hyperextension **(C)** were observed. Mild small joint hypermobility **(D)** and acrogeria were observed **(E)**.

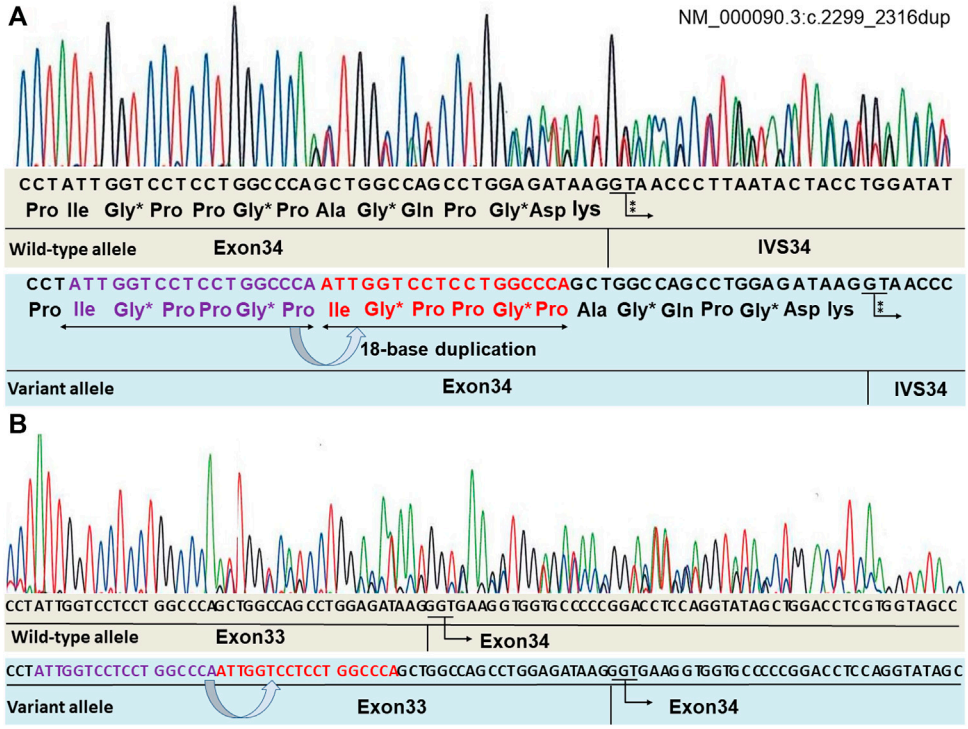

FIGURE 2
Mutation analysis of the *COL3A1* genomic DNA identified a variant (NM_000090.3:c.2299_2316dup). The repeating sequence of [Gly-X-Y] is retained in the variant allele. "*" indicates Gly positioned in a triplet repeat sequence. "□" indicates GT, indicating the beginning of the intron **(A)**. RNA sequencing is shown in **(B)**. mRNA obtained from the fibroblasts of the patient was converted to cDNA using reverse transcriptase, and Sanger sequencing analysis of the cDNA was performed. There are no abnormal nucleotides in the border of exons 33–34. Both alleles have the normal subsequently transcribed exon 34 without an exon skip.

structure, the helical structure cannot be maintained (Malfait et al., 2017). The expression level of collagen III produced by fibroblasts of the patients is extremely low, approximately 10%–20% when compared to normal healthy individuals (Shimaoka et al., 2010).

Here, we report the case of a patient with vEDS and a unique novel duplication mutation without alteration in the [Gly-X-Y] triplet repeat sequence. This case shows a mild phenotype, suggesting that the triple helical structure of collagen III chains may have been maintained with this particular mutation to some extent.

Case presentation

At presentation, a 58-year-old man developed a sudden disorder of consciousness and abdominal pain and was taken to a nearby hospital, where multiple intra-abdominal aneurysms were found. The aneurysm was under control owing to the administration of antihypertensive drugs, but the patient was referred to our facility because of suspected hereditary connective tissue disease due to the presence of joint hypermobility. The patient's parents are deceased and had not undergone genetic testing prior to death. Upon patient interview, it was revealed that neither parent had any symptoms attributed to vEDS. Furthermore, informed consent was obtained from the patient for the publication of clinical photographs. No remarkable vEDS facial feature, subcutaneous blood vessel permeability, or skin hyperextension was observed (Figures 1A–C). Contrarily, mild small joint hypermobility and acrogeria were observed (Figures 1D,E). The patient had no history of spontaneous pneumothorax, dislocation, or subcutaneous hematoma. Additionally, no known relatives, including his two daughters, had symptoms of suspected vEDS. The in-frame duplication mutation in the *COL3A1* gene was identified through the sequencing analysis of genomic DNA from the blood sample (see below).

The patient was suspected of having vEDS; however, the onset at old age and good clinical course presentation are atypical for vEDS. Thus, we proceeded with the verification of the pathogenicity of the gene mutation identified in this case after obtaining an informed consent from the patient.

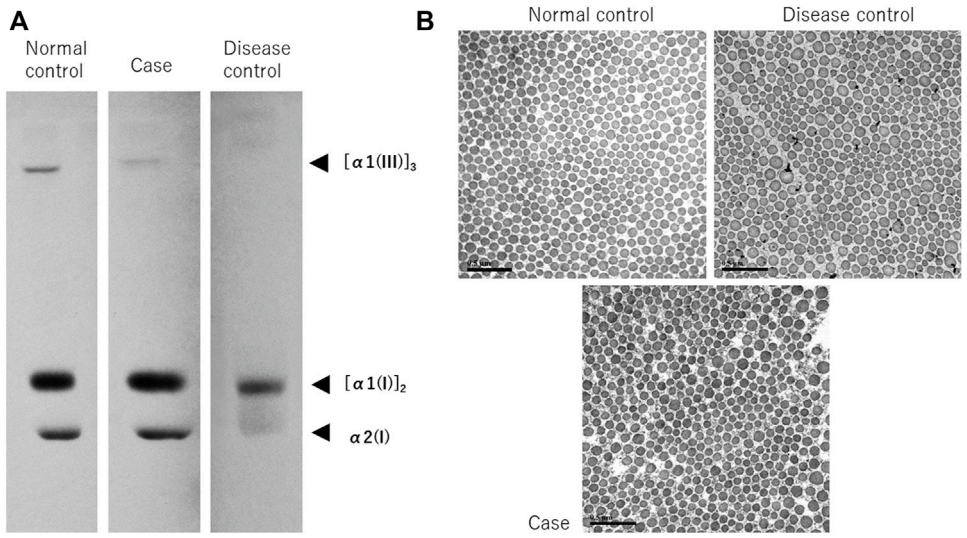

FIGURE 3
Synthetic analysis of procollagen and electron microscopy of collagenous bundles. Procollagen from cultured skin fibroblasts was electrophoresed and analyzed **(A)**. In the disease control, α1 collagen III is barely visible, but in the normal control, it is apparent. Contrarily, the expression in this case's sample is at an intermediate level between the normal and disease control samples, suggesting a deficiency in expression. Observation of collagenous bundles under TEM **(B)**, bar; 0.5 μm). Numerous small collagenous bundles were found in the disease control, and as a result, the size difference was conspicuous. However, the size was similar to that of the normal control. In the present case, the size difference was milder than it was in the disease control, owing to the structural abnormalities observed when compared with the normal control.

After the analysis, the patient understood that the symptoms were probably due to vEDS. The patient had two asymptomatic daughters in their 20s. It is a given that the identified mutation could lead to a mild phenotype if inherited and symptoms could develop in his daughters in the future even if they have been currently asymptomatic. The patient was informed regarding the importance of genetic testing for his daughters, but they declined to undergo the recommended evaluation. During the clinical course, the prescribed antihypertensive drug was switched to celiprolol, and no serious complications occurred during the 8 years after the diagnosis.

Methods

Determination of the base sequence on the genomic DNA extracted from the blood samples was performed using the Sanger sequencing method as previously reported (Shimaoka et al., 2010). Observation of the tissues obtained by skin biopsy with transmission electron microscopy (TEM) and real-time reverse-transcription polymerase chain reaction (RT-PCR) was performed according to a previously reported protocol (Ishikawa et al., 2021). The analysis of synthetic procollagen from cultured skin fibroblasts was conducted according to a protocol described elsewhere (Shimaoka et al., 2010). Briefly, dermal fibroblasts were cultured to confluence in 100 × 20-mm dishes in DMEM containing 10% FBS. Furthermore, the fibroblasts were incubated with DMEM containing 1% FBS and 5 μCi·ml^{-1} of 2,3-[3 H] proline in the presence of 50 μg·ml^{-1} of L-ascorbic acid 2-phosphate for 24 h. The labeled proteins secreted into the culture medium were precipitated by the addition of 5% trichloroacetic acid, and the precipitate was dissolved in 0.05 mol·L^{-1} acetic acid and digested with pepsin. Moreover, the labeled proteins were separated using sodium dodecyl sulfate–polyacrylamide gel electrophoresis in the presence or absence of 2-mercaptoethanol. The radioactive bands were detected by fluorography. We compared these samples with the samples of a single normal control (a 65-year-old man) and a vEDS disease control (a 53-year-old man having c.3365 + 1G>A in *COL3A1* in genome DNA), who were matched by age and sex. The following sequences reported in the past were used as the primers used in real-time RT-PCR (Li et al., 2016). *ATF6B*: forward 5′-GAGTCATCGCGTCTCTCCAC, reverse 5′-GGC CTCAGAGTTGACGGAAG, *CHOP*: forward 5′-AAGGCA CTGAGCGTATCATGT, reverse 5′-TGAAGATACACTTCC TTCTTGAACA, and *GAPDH*: forward 5′-GGCCTCCAAGGA GTAAGACC-3′, reverse 5′-CTGTGAGGAGGGGAGATT CA-3′.

Tukey's test was implemented for the statistical analysis of the real-time RT-PCR data. *p*-values of ≤0.05 were considered significant. The data are presented as the mean ± standard error of the mean. Statistical comparisons were performed using the

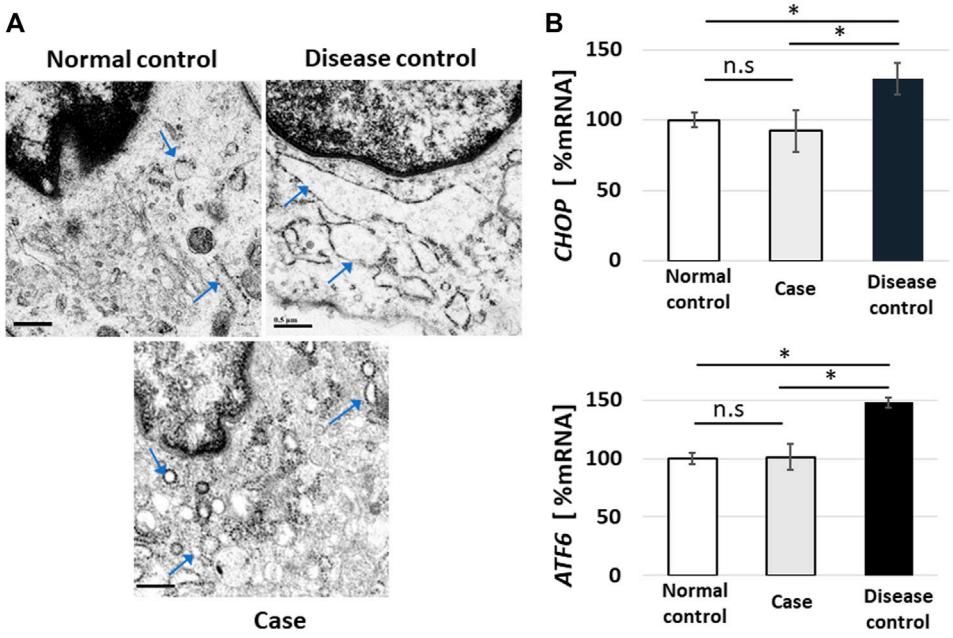

FIGURE 4
Endoplasmic reticulum (ER) stress and real-time reverse-transcription polymerase chain reaction (RT-PCR) for unfolded protein response sensors. Fibroblasts showed no dilation of the ER in the normal control, but images showing dilated fibroblasts of the ER were obtained in the disease control. In the present case, the expansion of the ER was not noticeable (arrowheads indicate ER **(A)**; bar, 0.5 μm). In real-time RT-PCR using mRNA extracted from cultured fibroblasts, PCR was performed on four technical replicates of each mRNA sample, and the results were averaged. *ATF6* and *CHOP* were highly expressed in the disease control when compared to the normal control; however, their expression levels in the present case were almost the same as those of the normal control **(B)**, error bar: standard error, ns: not significant, $*p < 0.05$).

Statistical Package for the Social Sciences version 18 (SPSS, Inc., Chicago).

Results

Results of the genetic analysis point to an in-frame duplication in the α1 type III collagen gene as the source of vascular-type Ehlers–Danlos syndrome pathology

By performing Sanger sequencing on the patient's genome DNA, the [heterozygous] mutation (NM_000090.3: c.2299_2316dup (p.Ile767_Pro772dup) was detected in the *COL3A1* gene, encoding α1 type III collagen. This 18-bp in-frame variant maintained the common collagen motif of the [Gly-X-Y] triplet repeat sequence (Figure 2A). This mutation was not registered in the dbSNP of the National Center for Biotechnology Information and the gnomAD. The mutation was predicted as "deleterious" on the basis of the *in silico* pathogenic prediction using MutationTaster. However, the pathogenicity of this in-frame variant could not be assessed by annotation with the others in multiple *in silico* programs. Therefore, it was difficult to determine the pathogenicity based only on the genetic analysis.

To address the possibility of this duplication mutation leading to a splicing anomaly, the mRNA obtained from the fibroblasts of the patient was converted to cDNA using reverse transcriptase, and Sanger sequencing analysis of the cDNA was performed. Evidence for the presence of a splicing variant was not found (Figure 2B).

Results of the collagen analysis suggest that the mutation affects α1 type III collagen gene protein expression

Procollagens from the cultured skin fibroblasts were electrophoresed and analyzed using our previously reported methods (Shimaoka et al., 2010). vEDS is caused by the inhibition of the synthesis of functional proteins due to a dominant negative effect. The synthesis of collagen III is predicted to be extremely low in patients with vEDS. As expected, in the disease control, α1 collagen III was barely visible, although it was apparent in the normal control. Contrarily, the expression of α1 collagen III in the patient's

sample was at an intermediate level between those of the normal and disease control samples, demonstrating a deficiency in expression (Figure 3A).

Collagenous bundles show intermediate morphology between typical vascular-type Ehlers–Danlos syndrome and healthy samples

TEM showed numerous small collagenous bundles in the disease control, and as a result, the size difference was conspicuous. However, the size was similar to that of the normal control. This finding is in line with the characteristic findings in vEDS (Smith et al., 1997; Ishikawa et al., 2021). Contrarily, in the present case, the degree of size difference in the collagenous bundles was lesser than it was in the disease control, but the collagenous bundles were observed to exhibit structural abnormalities when compared with those of the normal control (Figure 3B).

Endoplasmic reticulum stress is not apparent in the case

Endoplasmic reticulum (ER) stress is a state in which abnormal proteins of a higher-order structure or proteins that are not normally modified accumulate in the ER lumen, and this can be observed as an expansion of the ER under TEM (Ishikawa et al., 2021). Since ER stress damage cells, cells are equipped with a system to avoid this, which is referred to as the unfolded protein response, wherein *CHOP* and *ATF6* expressions increase (Wu et al., 2007; Li et al., 2016). ER stress is observed in vEDS (Muller et al., 2012; Ishikawa et al., 2021). In this study, TEM showed no dilation of the ER in the normal control, but dilations of the ER were confirmed in the images of the disease control. Contrarily, in the present case, the expansion of the ER was not noticeable (Figure 4A). In real-time RT-PCR using mRNA extracted from the cultured fibroblasts, PCR was performed on four technical replicates of each mRNA sample, and the averages of the results were determined. *ATF6* and *CHOP* were highly expressed in the disease control when compared to the normal control; however, their expression levels in the present case were almost the same as those of the normal control (Figure 4B).

Discussion and conclusion

According to the American College of Medical Genetics and Genomics (ACMG) guidelines (Richards et al., 2015), PM2 (not registered in the database) and PM4 (in-frame variant) corresponded to the patient's variant. *In silico* analysis with multiple programs has been difficult to assess in in-frame variants. Since neither parent had symptoms of vEDS, this variant was presumably the *de novo* variant; however, the parent's genes could not be confirmed. Therefore, the evaluation of the ACMG guidelines remains at "Variant of Unknown Significance (VUS)." However, the clinical findings were mild in the present case and were consistent with the symptoms caused by abnormalities in *COL3A1*, and a decreased collagen III was also confirmed *in vitro*. In the TEM analysis, morphological abnormalities of collagenous bundles were apparent when compared with those of the normal control. We attributed these findings to abnormalities in *COL3A1*, although VUS was assessed at the ACMG. Contrarily, this case interestingly showed no evidence of ER stress.

In vEDS cases with the commonly reported Gly mutations in the [Gly-X-Y] repeats or splice-site mutations, the aberrant peptide chains produced by the mutant alleles inhibit the formation of normal peptide triple helices. Practically, the expression level of collagen III is reduced to nearly 10% that of healthy people, which is known as a dominant negative effect (Mao and Bristow, 2001; Shimaoka et al., 2010; Malfait et al., 2017). In collagen fibers, the repeating sequence of [Gly-X-Y] is critically important for maintaining the triple helical structure; if even one of the three peptide chains has an abnormality in the repeating sequence, the triple helical structure cannot be maintained (Mao and Bristow, 2001). Adverse effects of pathogenic gene mutations do not manifest themselves only in protein synthesis processes. Moreover, aberrant peptide chains those fail to construct a triple helical structure due to protein folding in the ER accumulate in the ER (Malfait et al., 2017; Ishikawa et al., 2021), causing ER stress and consequent cell damage (Schroder and Kaufman, 2005).

Conversely, epidemiological studies have already shown that vEDS patients with nonsense mutation display a mild phenotype (Pepin et al., 2014). In nonsense mutations, the abnormal alleles stop producing the peptide chains, which is called haploinsufficiency. Therefore, the peptide chain produced is only from the normal allele, and the dominant negative effect is avoided. Theoretically, collagen III levels were reduced to 50% when compared to the normal control with less major detrimental effects. Furthermore, it is expected that the nonsense variant also has a reduced ER stress response because there is no accumulation of any aberrant peptide chains in the ER (Muller et al., 2012).

In patients with vEDS, although collagen III must be theoretically extremely low from birth, serious complications occur more frequently in adulthood and later, which are rarely seen during infancy (Malfait et al., 2017). Although the pathophysiology of vEDS is still not fully explained, it is considered that the various symptoms in vEDS are caused by a hybrid of two factors: the direct effect of the decrease in collagen III and damaged fibroblasts caused by ER stress (Ishikawa et al., 2021). However, hypothetically, if an in-frame mutation that does not affect the order of [Gly-X-Y] occurs, as in this case, the folding phenomenon in the ER would be mostly normal. Then,

the triple helical structure can be maintained in the ER. The absence of an ER expansion might be an indication of avoidance of the dominant negative effects. On the other hand, the mutation in the present case involves the incorporation of two more [Gly-X-Y] residues into the helix. In the collagenous bundles, collagen III would be composed of peptide chains of different lengths (normal length and two [Gly-X-Y] residues as long length) in this case. Presumably, such collagenous bundles are unstable in the extracellular matrix and fragile outside the cell. In this case, the mildly reduced collagen expression, minor morphological abnormalities of the collagenous bundles, and near-normal ER stress support this hypothesis. The lack of ER stress would be associated with a mild phenotype. We have previously reported a case of a gene mutation that does not affect the [Gly-X-Y] repeats, which was a 9-bp deletion. That case was also confirmed to show a mild phenotype (Hayashi et al., 2020). Although there are a few reports of such gene mutations, which are in-frame duplications/deletions in multiples of nine, there is a possibility that such mild phenotypes may not cause serious symptoms. Moreover, patients with such cases may have not gone through genetic examinations at a medical institution due to overlooked vEDS. Thus, there may be undiagnosed patients.

Unfortunately, it is not easy to clearly determine whether the triple helical structures are composed of different lengths of peptide chains in combinations of wild-type and mutant alleles (not affecting the [Gly-X-Y] repetitions) in the extracellular matrix. Furthermore, there are many individual differences in ER stress responses due to the influence of epigenetics (Ramos-Lopez et al., 2018); thus, there is no conclusive evidence to conclude that just the absence of ER stress is associated with dominant negative avoidances. Therefore, this study has its limitations and cannot go beyond the hypothesis.

In conclusion, in the present study, our analyses has indicated that the identified mutations, which are in-frame duplications/deletions in multiples of nine, might underlie the pathogenesis observed in vEDS with a mild phenotype. Identifying the pathogenicity of this unique variant, which has morphological abnormalities in the collagenous bundles despite lower ER stress, is very important for elucidating the pathophysiology of vEDS in the future. The age at onset and severity of vEDS greatly vary regardless of the variant present among the patients, and it is important to investigate the role of ER stress in this clinical difference.

Data availability statement

The data sets for this article are not publicly available due to concerns regarding participant/patient anonymity. Requests o access the data sets should be directed to the corresponding author.

Ethics statement

The studies involving human participants were reviewed and approved by the Dokkyo Medical University Clinical Research Review Board. The patients/participants provided their written informed consent to participate in this study. Written informed consent was obtained from the individual(s) for the publication of any potentially identifiable images or data included in this article.

Author contributions

Conceptualization: SH and KI; data curation: SH; funding acquisition: SH; investigation: SH, TK, and TY; project administration: SH; supervision: TK and KI; writing–original draft preparation: SH.

Funding

This research was supported by the Research Grant Award 2022 of Dokkyo International Medical Education and Research Foundation.

Acknowledgments

We thank Miki Kanno, Takashi Namatame, Kinichi Matsuyama, and Kazumi Akimoto for their technical assistance.

Conflict of interest

The authors declare that the research was conducted in the absence of any commercial or financial relationships that could be construed as a potential conflict of interest.

The handling editor KK declared a past co-authorship with the author TY.

Publisher's note

References

Byers, P. H., Belmont, J., Black, J., De Backer, J., Frank, M., Jeunemaitre, X., et al. (2017). Diagnosis, natural history, and management in vascular Ehlers–Danlos syndrome. *Am. J. Med. Genet. C Semin. Med. Genet.* 175, 40–47. doi:10.1002/ajmg.c.31553

Frank, M., Albuisson, J., Ranque, B., Golmard, L., Mazzella, J. M., Bal-Theoleyre, L., et al. (2015). The type of variants at the COL3A1 gene associates with the phenotype and severity of vascular Ehlers–Danlos syndrome. *Eur. J. Hum. Genet.* 23, 1657–1664. doi:10.1038/ejhg.2015.32

Hayashi, S., Lin, W., Hamasaki, Y., and Igawa, K. (2020). Vascular Ehlers-Danlos syndrome patient with a novel COL3A1 gene deletion mutation without alteration in the triple sequence of (Gly-X-Y) repeat. *J. Dermatol.* 47, e390–e391. doi:10.1111/1346-8138.15558

Ishikawa, S., Kosho, T., Kaminaga, T., Miyamoto, M., Hamasaki, Y., Yoshihara, S., et al. (2021). Endoplasmic reticulum stress and collagenous formation anomalies in vascular-type Ehlers–Danlos syndrome via electron microscopy. *J. Dermatol.* 48, 481–485. doi:10.1111/1346-8138.15766

Kramer, R. Z., Bella, J., Mayville, P., Brodsky, B., and Berman, H. M. (1999). Sequence dependent conformational variations of collagen triple-helical structure. *Nat. Struct. Biol.* 6, 454–457. doi:10.1038/8259

Li, Y. H., Tardif, G., Hum, D., Kapoor, M., Fahmi, H., Pelletier, J. P., et al. (2016). The unfolded protein response genes in human osteoarthritic chondrocytes: PERK emerges as a potential therapeutic target. *Arthritis Res. Ther.* 18, 172. doi:10.1186/s13075-016-1070-6

Malfait, F., Francomano, C., Byers, P., Belmont, J., Berglund, B., Black, J., et al. (2017). The 2017 international classification of the Ehlers–Danlos syndromes. *Am. J. Med. Genet. C Semin. Med. Genet.* 175, 8–26. doi:10.1002/ajmg.c.31552

Mao, J. R., and Bristow, J. (2001). The ehlers–danlos syndrome: On beyond collagens. *J. Clin. .* 107, 1063–1069. doi:10.1172/JCI12881

Müller, G. A., Hansen, U., Xu, Z., Griswold, B., Talan, M. I., McDonnell, N. B., et al. (2012). Allele-specific siRNA knockdown as a personalized treatment strategy for vascular Ehlers–Danlos syndrome in human fibroblasts. *FASEB J.* 26, 668–677. doi:10.1096/fj.11-182162

Pepin, M. G., Schwarze, U., Rice, K. M., Liu, M., Leistritz, D., and Byers, P. H. (2014). Survival is affected by mutation type and molecular mechanism in vascular Ehlers-Danlos syndrome (EDS type IV). *Genet. Med.* 16, 881–888. doi:10.1038/gim.2014.72

Pepin, M., Schwarze, U., Superti-Furga, A., Byers, P. H., and Superti-FurgA, A. (2000). Clinical and genetic features of Ehlers–Danlos syndrome type IV, the vascular type. *N. Engl. J. Med.* 342, 673–680. doi:10.1056/NEJM200003093421001

Ramos-Lopez, O., Riezu-Boj, J. I., Milagro, F. I., Moreno-Aliaga, M. J., and Martinez, J. A.Project MENA (2018). Endoplasmic reticulum stress epigenetics is related to adiposity, dyslipidemia, and insulin resistance. *Adipocyte* 7, 137–142. doi:10.1080/21623945.2018.1447731

Richards, S., Aziz, N., Bale, S., Bick, D., Das, S., Gastier-Foster, J., et al. (2015). Standards and guidelines for the interpretation of sequence variants: A joint consensus recommendation of the American College of medical genetics and genomics and the association for molecular pathology. *Genet. Med.* 17, 405–424. doi:10.1038/gim.2015.30

Schröder, M., and Kaufman, R. J. (2005). ER stress and the unfolded protein response. *Mutat. Res.* 569, 29–63. doi:10.1016/j.mrfmmm.2004.06.056

Shimaoka, Y., Kosho, T., Wataya-Kaneda, M., Funakoshi, M., Suzuki, T., Hayashi, S., et al. (2010). Clinical and genetic features of 20 Japanese patients with vascular-type Ehlers–Danlos syndrome. *Br. J. Dermatol.* 163, 704–710. doi:10.1111/j.1365-2133.2010.09874.x

Smith, L. T., Schwarze, U., Goldstein, J., and Byers, P. H. (1997). Mutations in the COL3A1 gene result in the Ehlers–Danlos syndrome type IV and alterations in the size and distribution of the major collagen fibrils of the dermis. *J. . Dermatol.* 108, 241–247. doi:10.1111/1523-1747.ep12286441

Wu, J., Rutkowski, D. T., Dubois, M., Swathirajan, J., Saunders, T., Wang, J., et al. (2007). ATF6alpha optimizes long-term endoplasmic reticulum function to protect cells from chronic stress. *Dev. Cell* 13, 351–364. doi:10.1016/j.devcel.2007.07.005

frontiers | Frontiers in Genetics

TYPE Mini Review
PUBLISHED 15 March 2023
DOI 10.3389/fgene.2023.1107787

OPEN ACCESS

EDITED BY
Mahmood Rasool,
King Abdulaziz University, Saudi Arabia

REVIEWED BY
Antonella Polimeni,
Sapienza University of Rome, Italy

*CORRESPONDENCE
Emiko Okuda-Ashitaka,
emiko.ashitaka@oit.ac.jp
Ken-ichi Matsumoto,
matumoto@med.shimane-u.ac.jp

SPECIALTY SECTION
This article was submitted to Genetics of Common and Rare Diseases, a section of the journal Frontiers in Genetics

RECEIVED 25 November 2022
ACCEPTED 06 March 2023
PUBLISHED 15 March 2023

CITATION
Okuda-Ashitaka E and Matsumoto K-i (2023), Tenascin-X as a causal gene for classical-like Ehlers-Danlos syndrome. *Front. Genet.* 14:1107787. doi: 10.3389/fgene.2023.1107787

Tenascin-X as a causal gene for classical-like Ehlers-Danlos syndrome

Emiko Okuda-Ashitaka[1]* and Ken-ichi Matsumoto[2]*

[1]Department of Biomedical Engineering, Osaka Institute of Technology, Osaka, Japan, [2]Department of Biosignaling and Radioisotope Experiment, Interdisciplinary Center for Science Research, Head Office for Research and Academic Information, Shimane University, Izumo, Japan

Tenascin-X (TNX) is an extracellular matrix glycoprotein for which a deficiency results in a recessive form of classical-like Ehlers-Danlos syndrome (clEDS), a heritable connective tissue disorder with hyperextensible skin without atrophic scarring, joint hypermobility, and easy bruising. Notably, patients with clEDS also suffer from not only chronic joint pain and chronic myalgia but also neurological abnormalities such as peripheral paresthesia and axonal polyneuropathy with high frequency. By using TNX-deficient (*Tnxb*$^{-/-}$) mice, well-known as a model animal of clEDS, we recently showed that *Tnxb*$^{-/-}$ mice exhibit hypersensitivity to chemical stimuli and the development of mechanical allodynia due to the hypersensitization of myelinated A-fibers and activation of the spinal dorsal horn. Pain also occurs in other types of EDS. First, we review the underlying molecular mechanisms of pain in EDS, especially that in clEDS. In addition, the roles of TNX as a tumor suppressor protein in cancer progression have been reported. Recent *in silico* large-scale database analyses have shown that TNX is downregulated in various tumor tissues and that high expression of TNX in tumor cells has a good prognosis. We describe what is so far known about TNX as a tumor suppressor protein. Furthermore, some patients with clEDS show delayed wound healing. *Tnxb*$^{-/-}$ mice also exhibit impairment of epithelial wound healing in corneas. TNX is also involved in liver fibrosis. We address the molecular mechanism for the induction of *COL1A1* by the expression of both a peptide derived from the fibrinogen-related domain of TNX and integrin α11.

KEYWORDS

tenascin-X, Ehlers-Danlos syndromes, clEDS, pain, tumor suppressor, fibrosis

Introduction

The Ehlers-Danlos syndromes (EDS) comprise a group of rare heritable connective tissue disorders mainly characterized by a variable degree of joint hypermobility, hyperextensible skin and fragility of connective tissues. Currently, 14 EDS are classified according to typical clinical features, and 20 causal genes that are mainly responsible for collagen and extracellular matrix (ECM) synthesis and maintenance have been identified (Malfait et al., 2020). Among the 14 types of EDS, non-collagenous classical-like EDS (clEDS) is the result of tenascin-X (TNX) deficiency with homozygous or compound heterozygous mutations in its gene (*TNXB*) (Burch et al., 1997; Schalkwijk et al., 2001; Malfait et al., 2017). The major clinical features of clEDS are generalized joint hypermobility, hyperextensible velvety skin without atrophic scarring, and easy bruising (Malfait et al., 2017) (Figure 1A).

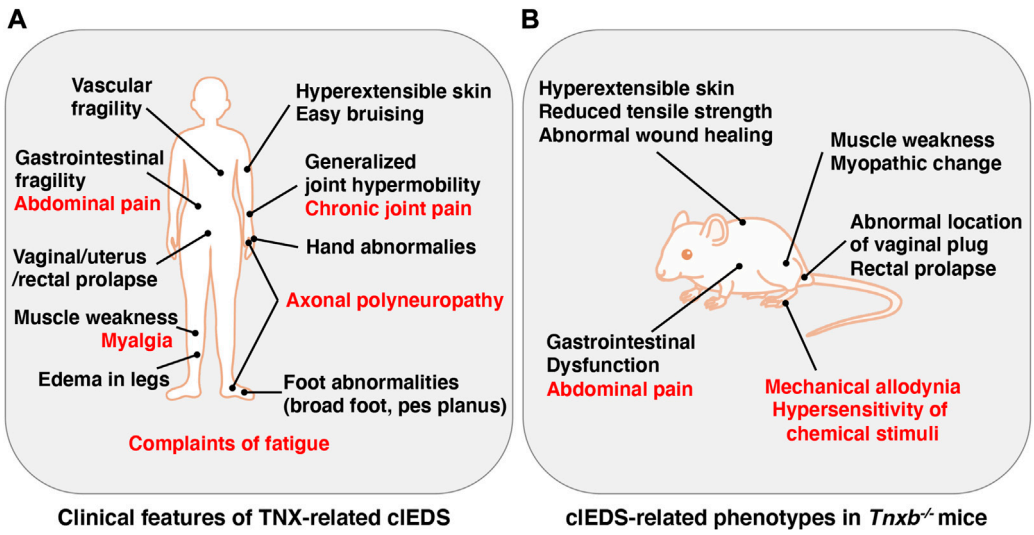

FIGURE 1
Clinical features of TNX-related clEDS **(A)** and clEDS-related phenotypes of *Tnxb*$^{-/-}$ mice **(B)**. Symptoms in many patients with TNX-related clEDS are shown in **(A)** (van Dijk et al., 2022). Major clEDS-related phenotypes exhibited in *Tnxb*$^{-/-}$ mice are shown in **(B)** (Matsumoto and Aoki, 2020). Complaints associated with pain are highlighted by red letters in **(A)** and **(B)**.

A causal gene for clEDS, *TNXB*, was identified serendipitously as an opposite strand gene (*OSG*) with its 3′ genomic overlap with the steroid 21-hydroxylase gene (*CYP21A2*) in the human major histocompatibility complex (MHC) class III region (Morel et al., 1989). Further independent analyses of the MHC class III region revealed a novel gene having the highest homology with tenascin-C (TNC) and the *OSG* is the portion of the 3' region of the gene, naming the novel gene *TNXB* (Matsumoto et al., 1992a; Matsumoto et al., 1992b; Bristow et al., 1993; Erickson, 1993). TNX is the largest glycoprotein in the tenascin family with a size of roughly 450 kDa and is composed of characteristic structural domains with a tenascin assemble region, heptad repeats, epidermal growth factor (EGF)-like repeats, fibronectin type III (FNIII)-like repeats, and a fibrinogen (FBG)-related domain (Bristow et al., 1993; Ikuta et al., 1998).

TNX is expressed prominently in a variety of tissues including the heart, skin, skeletal muscle, peripheral nerves, ligaments, tendons and the digestive tract, while there are very low expression levels in immune tissues such as the thymus, bone marrow and lymphocytes (Matsumoto et al., 1994; Geffrotin et al., 1995). Brain-derived neurotrophic factor (BDNF) has been identified as an up-regulator of TNX expression (Takeda et al., 2005) and glucocorticoids have been identified as a down-regulators of TNX expression (Sakai et al., 1996).

TNX has physiological functions in collagen deposition (Mao et al., 2002; Minamitani et al., 2004a), collagen stability (Mao and Bristow, 2001), physical property of collagen (Margaron et al., 2010) and collagen fibrillogenesis (Minamitani et al., 2004b; Egging et al., 2007). Several phenotypes tied to the function of TNX have been revealed by using *Tnxb*$^{-/-}$ mice (Matsumoto and Aoki, 2020) (Figure 1B).

In this review, we focus on the function of TNX in pain related to a characteristic of clEDS as well as in tumor suppression and fibrosis.

Clinical characteristics of TNX-related clEDS

TNX-related clEDS was identified in 56 individuals from 44 families so far (van Dijk et al., 2022). The major clinical characteristics of TNX-related clEDS are skin hyperextensibility with velvety skin texture and absence of atrophic scaring (100% of patients), generalized joint hypermobility with or without recurrent dislocations (100%), and easy or spontaneous bruising of the skin including hematomas and ecchymoses (91%), as shown in Figure 1A (Malfait et al., 2017; van Dijk et al., 2022). It has been considered that the absence of atrophic scaring is a characteristic of clEDS, distinguish it from classical EDS, but mild atrophic scarring was observed in seven clEDS patients (Chen et al., 2016; Green et al., 2020). Additional musculoskeletal presentations of TNX-related clEDS are foot abnormalities including broad/plump forefoot, brachydactyly with excessive skin, pes planus, hallux valgus, and painful soles of the feet (81%), edema in the legs in the absence of cardiac failure (25%), hand anomalies (20%), and complaints of fatigue (53%) (van Dijk et al., 2022). Cardiovascular presentations of TNX-related clEDS are vascular fragility (27%), mild valvular abnormality (16%), and cardiomyopathy (5%) (van Dijk et al., 2022). Vascular fragility has been reported to cause major medical events such as rupture of the brachial vein and aneurysmal abdominal arteries (Demirdas et al., 2017; Micale et al., 2019). Neuromuscular presentations of TNX-related clEDS are subjective muscle weakness (37%), axonal polyneuropathy (14%), and atrophy of muscles in the hands and feet (4%) (van Dijk et al., 2022). Voermans et al. (2009) reported that TNX-deficient EDS patients show muscle weakness, myalgia, easy fatigability, and limited walking distance. Physical examination revealed mild-to-moderate muscle weakness, hypotonia, reduction of vibration sense, hyporeflexia, and impairment of

mobility. Furthermore, clinical neurological studies showed axonal polyneuropathy and mild abnormal motor unit action potentials, and muscle ultrasound showed increased echo intensity and atrophy (Voermans et al., 2009). Interestingly, neuromuscular features have been observed in adults but not in children (Demirdas et al., 2017). Other presentations of TNX-related clEDS are gastrointestinal fragility including esophageal, small bowel and/or large bowel ruptures (16%), vaginal/uterus/rectal prolapse (21%), and other types of fragility including trachea rupture after intubation and defect of nasal cartilages after nose blowing (4%) (van Dijk et al., 2022).

Pain in clEDS due to TNX deficiency

Pain is a common and severe symptom in patients with various types of EDS (Chopra et al., 2017; Syx et al., 2017; Malfait et al., 2021). Pain initially occurs as acute and localized musculoskeletal nociception in different joints and limbs in relation to hypermobility, subluxations, dislocations, soft-tissue injury, myalgias, and surgery (Chopra et al., 2017). However, pain related to EDS gradually becomes chronic (lasting for longer than 3 months) and assumes a more generalized distribution (Chopra et al., 2017; Syx et al., 2017). Among the various types of EDS, chronic pain is most frequent in hypermobile EDS. Chopra et al. (2017) reported that pain in patients with hypermobile EDS occurs in various forms including generalized body pain (incidence of 90%), soft-tissue pain (90%), dislocations (78%), and joint pain including pain in the shoulders (80%), hands (75%), knees (71%), temporomandibular joints (71%), spine (67%), and elbows (43%). In addition to musculoskeletal pain, patients with hypermobile EDS suffer from chronic fatigue (95%), neuropathic pain (68%), headaches (75%), gastrointestinal pain (86%), dysmenorrhea (73%), and vulvodynia/dyspareunia (42%). Pathological chronic pain is also caused by a lesion or disease of the somatosensory nervous system, and that pain is called neuropathic pain (Jensen et al., 2011). There is a high frequency of neuropathic pain in patients with EDS who have chronic pain (Chopra et al., 2017). Neuropathic pain occurs as spontaneous pain such as shooting, and burning, or stabbing pain, an increased response to normally noxious stimuli (hyperalgesia), and pain due to normally innocuous stimuli (allodynia) (Colloca et al., 2017).

It has been reported that TNX-related clEDS patients complain of chronic pain including joint pain, myalgia, back pain, abdominal pain, and fatigue (Figure 1A) (Schalkwijk et al., 2001; Voermans et al., 2009; Demirdas et al., 2017; Green et al., 2020; van Dijk et al., 2022). We first reported pain responses in a murine TNX-deficient EDS model (Okuda-Ashitaka et al., 2020). Our studies with *Tnxb*$^{-/-}$ mice showed increased sensitivity to innocuous mechanical stimuli but not to thermal stimuli such as cold and heat, suggesting that TNX deficiency is involved in the development of mechanical allodynia, a major feature of neuropathic pain (Figure 1B) (Okuda-Ashitaka et al., 2020). Furthermore, *Tnxb*$^{-/-}$ mice also exhibited hypersensitization of myelinated Aδ- and Aβ-fibers, but not unmyelinated C fibers, by using transcutaneous sine wave stimuli (Figure 2). TNX is highly expressed in tendons, ligaments, and peripheral nerves (Geffrotin et al., 1995). TNX exists in the perineurium, endoneurium, and Schwann cells in the sciatic nerve (Matsumoto et al., 2002; Sakai et al., 2017; Okuda-Ashitaka et al., 2020). Electron microscopy analysis of the sciatic nerve showed modestly smaller inner and outer diameters of myelinated fibers and reduced collagen fibril density in the endoneurium in *Tnxb*$^{-/-}$ mice (Voermans et al., 2011), whereas there was no significant difference in the numbers of axons or thickness of the myelin sheaths in *Tnxb*$^{-/-}$ mice (Matsumoto et al., 2002). Moderate changes of myelinated fibers and hypersensitization of myelinated Aδ- and Aβ-fibers in *Tnxb*$^{-/-}$ mice may be correlated to the axonal polyneuropathy in TNX-deficient EDS (Voermans et al., 2009). Axonal polyneuropathy is thought to be one of the mechanisms of neuropathic pain in EDS (Voermans et al., 2011). Furthermore, *Tnxb*$^{-/-}$ mice showed increased levels of anatomical neuronal activation markers, phosphorylated extracellular signal-regulated kinase and neuronal nitric oxide in the spinal dorsal horn, indicating that TNX deficiency induces spinal central sensitization, namely, another mechanism of neuropathic pain (Okuda-Ashitaka et al., 2020). Similar to pain responses in *Tnxb*$^{-/-}$ mice, a murine classical EDS model, type V collagen (COL5A1) haploinsufficient (*Col5a1*$^{+/-}$) mice, showed mechanical allodynia but not thermal hyperalgesia (Syx et al., 2020). *Col5a1*$^{+/-}$ mice showed a disorganization of $Na_v1.8$-expressing fibers including above 90% C-fibers, with less fibers crossing the epidermis of footpad glabrous skin. These results indicated that pain in both TNX-related clEDS and COL5A1-related classical EDS corresponds to neuropathic pain associated with hypersensitization of myelinated Aδ- and Aβ-fibers, disorganization of $Na_v1.8$-expressing fibers, and central sensitization of the spinal cord.

Additionally, TNX influences neuronal functions in gut tissues including abdominal pain (Figure 1A). *Tnxb*$^{-/-}$ mice show hypersensitivity of colonic nociceptive afferents and increased sensory neuron sprouting in the mucosa (Aktar et al., 2018). *Tnxb*$^{-/-}$ mice also exhibited gastric dysfunction associated with accelerated gastric emptying and hypersensitivity of gastric vagal mechanoreceptors (Figure 1B) (Aktar et al., 2019), which are consistent with TNX-related clEDS patients (Schalkwijk et al., 2001; Lindor and Bristow, 2005).

TNX with tumor suppressive function

Previously, we demonstrated that *Tnxb*$^{-/-}$ mice bearing aggressive B16-BL6 melanoma cells exhibit promotion of tumor invasion and metastasis due to upregulation of matrix metalloproteinases *Mmp2* and *Mmp9* followed by enhanced activities of the MMPs (Matsumoto et al., 2001; Matsumoto et al., 2004). Conversely, overexpression of TNX in fibroblasts downregulated the expression of *Mmp2* (Matsumoto et al., 2004). In addition, silencing of long non-coding RNA (LncRNA) LINC01305 inhibited the progression of lung cancer by activating the TNX-mediated phosphatidylinositol 3-kinase (PI3K)/protein kinase B (Akt) signaling pathway (Yan et al., 2020). Moreover, it has been revealed that a functional variant in the *TNXB* promoter is associated with risk of esophageal squamous-cell carcinoma (ESCC) in the Chinese population, leading to the expression of *TNXB* being downregulated in ESCC tissues (Chang et al., 2018; Yang et al., 2020). Knockout of *TNXB* significantly increased cell proliferation of

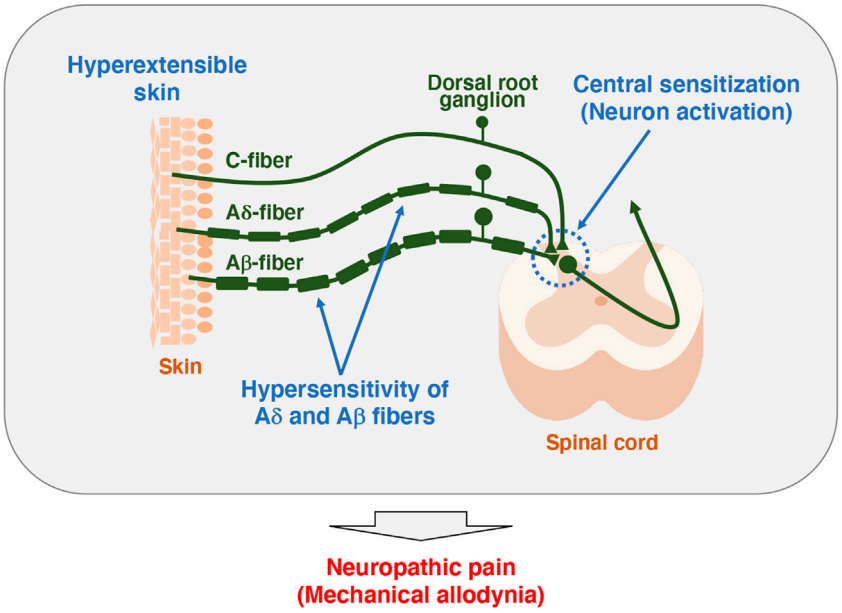

FIGURE 2
Model of pathogenesis for mechanical allodynia in *Tnxb*$^{-/-}$ mice. Somatosensory information is detected in the primary afferent fibers extending to the skin, which in turn is transmitted to the spinal cord and then to the brain. Unmyelinated C-fibers and lightly myelinated Aδ-fibers conduct noxious and thermal signals, whereas myelinated Aβ-fibers conduct innocuous signals such as touch and pressure (Moehring et al., 2018). *Tnxb*$^{-/-}$ mice exhibited increased sensitivity to innocuous mechanical stimuli but not thermal stimuli, indicating the induction of mechanical allodynia (Okuda-Ashitaka et al., 2020). Likewise, *Tnxb*$^{-/-}$ mice showed hypersensitization of myelinated Aδ- and Aβ-fibers but not C-fibers. Furthermore, levels of activated neuron markers, phosphorylation of extracellular signal-related kinase and NADPH-diaphorase activity of neuronal nitric oxide were increased in the spinal dorsal horn of *Tnxb*$^{-/-}$ mice compared to those in wild-type mice. Thus, TNX deficiency is involved in mechanical allodynia associated with hypersensitization of myelinated Aδ- and Aβ-fibers and central sensitization of the spinal cord.

ESCC cells (Yang et al., 2020). These results suggest that TNX has a tumor suppressor role. Interestingly, when carcinoma cells were transplanted into the skin of nude mice, the expression of TNX was downregulated substantially not only in the transplanted tumor cells themselves but also in the surrounding tumor stroma (Sakai et al., 1996).

In conjunction with a tumor suppressor role of TNX, the expression of TNX was shown to be downregulated in most tumor tissues such as the lung, breast, prostate, colon, stomach, liver, kidney, skin melanoma, and leiomyoma by using *in silico* large database studies of the Gene Expression Omnibus (GEO) and The Cancer Genomic Atlas (TCGA) (Liot et al., 2020), although there are some discrepancies in the expression pattern of TNX in glioma and ovarian cancer compared with those of previous published data (Hasegawa et al., 1997; Kramer et al., 2015). In another study using the TCGA database for ECM gene dysregulation in cancer, 58 out of 249 ECM genes were identified as cancer-associated ECM genes and *TNXB* was found to be the most significantly downregulated among those genes in cancers (Chakravarthy et al., 2018). Even more interesting is that *TNXB* expression is inversely correlated with tumor progression and that a high level of TNX in tumor tissues predicts a good prognosis (Liot et al., 2020).

Meanwhile, as an exception, the expression of TNX is upregulated in malignant mesothelioma (Yuan et al., 2009; Davidson, 2011; Nakayama et al., 2019). This evidence suggests that TNX is applicable as a diagnostic marker of malignant mesothelioma since most other tumors are negative for TNX expression.

Involvement of TNX in fibrosis and wound healing

Alcaraz et al. (2014) showed that a fibrinogen (FBG)-related domain of TNX (TNX-FBG) interacts with small latent TGF-β complex (SLC) and elicits the activation of its latent form into a bioactive form with integrin α11β1, leading to epithelial-to-mesenchymal transition in mammary epithelial cells. On the other hand, Liang et al. (2022) recently demonstrated that TNX-FBG interacts with mature TGF-β and impedes it from binding to its receptor, mediating flow-inducing suppression of endothelial-to-mesenchymal transition and atherosclerosis.

Previously, our group revealed that *Tnxb*$^{-/-}$ mice fed a high-fat and high-cholesterol diet with high levels of phosphorus and calcium (HFCD) exhibit less fibrotic characteristics in livers than those in wild-type mice, indicating the involvement of TNX in hepatic fibrosis (Yamaguchi et al., 2017). Fibrosis is a pathological sign of wound healing that replaces damaged tissue with collagen-rich scar tissue. We attempted to disclose the molecular mechanism by which TNX induces *in vitro* fibrosis such as the induction of type I collagen 1α (*COL1A1*) expression. Initially, we speculated that TGF-β and TNX-FBG with integrin α11β1 are involved in the induction of *COL1A1* expression since interaction of the TNX-FBG domain and TGF-β was reported previously (Alcaraz et al., 2014) and TGF-β is a well-known central mediator of fibrosis (Dewidar et al., 2019). However, contrary to our initial expectation, we found that the Yes-associated protein 1 (YAP1)

signaling pathway through integrin α11β1 plays a major role in the induction of *COL1A1* expression by expression of the TNX-FBG domain in human hepatic stellate LX-2 cells and that the minimum 15-amino acid (aa) sequence derived from the TNX-FBG domain is required for the induction of *COL1A1* expression in the LX-2 cells (Matsumoto et al., 2022). Since integrin α11β1 is known to be a receptor for type I collagen (COL1) and type II collagen (Zhang et al., 2003), it is yet to be determined whether interaction of the TNX-FBG domain with integrin α11β1 is direct or indirect for the induction of *COL1A1*expression.

According to previous reports, 41% of patients with TNX-deficient clEDS showed delayed wound healing (Demirdas et al., 2017). Notably, the corneas of *Tnxb*$^{-/-}$ mice that underwent epithelium debridement exhibited impairment of epithelial wound healing due to increased neutrophil infiltration and activation of reactive oxygen species (Sumioka et al., 2021). TNX might also be involved in the angiogenetic process during wound healing. Injury-induced corneal stromal angiogenesis in *Tnxb*$^{-/-}$ mice was impaired (Sumioka et al., 2018).

Conclusion and perspectives

In this review, we described the molecular mechanisms of pain caused by TNX deficiency as well as by mutation of collagens mimicking the characteristics of EDS, the function of TNX as a tumor suppressor, and the involvement of TNX in fibrosis.

Concerning pain associated with malfunction of the ECM, the contribution of TNX-deficient clEDS and COL5A1 haploinsufficiency-related classical EDS to the development of neuropathic pain has been revealed by using a murine EDS model. Patients with EDS take large amounts of medications such as acetaminophen, non-steroid anti-inflammatory drugs (NSAIDs), anticonvulsants, antidepressants, opioids, and lidocaine; however, current managements are inadequate (Demes et al., 2020; Whalen and Crone, 2022). Interestingly, mechanical allodynia in *Tnxb*$^{-/-}$ mice was inhibited by the anticonvulsant drug gabapentin and the mu-opioid agonist [D-Ala^2, N-MePhe^4, Gly-ol^5]-enkephalin (DAMGO) but not by the NSAID indomethacin (Okuda-Ashitaka et al., 2020). In the future, more efficacious approaches in line with the mechanisms causing pain in patients with EDS are expected.

Concerning tumor progression associated with TNX expression, the increased expression of TNX in malignant mesothelioma is very interesting, despite its expression being downregulated in most tumor tissues. Yuan et al. (2009) showed some splice variants of TNX are observed in malignant mesothelioma. The splice variants of TNX might be involved in the malignancy of mesothelioma. In the future, analyses of not only splice variants of TNX itself but also proteins that interact with their splice variants are needed to reveal the specific function of TNX in malignant mesothelioma.

Finally, we showed that *COL1A1* expression was induced by expression of both the 15-aa peptide in the TNX-FBG domain and integrin α11 in hepatic stellate LX-2 cells *in vitro* (Matsumoto et al., 2022). Further experiments are needed to determine whether expression of the 15-aa peptide from the TNX-FBG domain in liver can induce *COL1A1* expression leading to hepatic fibrosis *in vivo*.

Author contributions

EO-A and KM designed and wrote the manuscript. All authors contributed to the article and approved the submitted version.

Funding

This work was supported by the Japan Society for the Promotion of Science (JSPS) KAKENHI Grant Number JP17K09045 and Osaka Institute of Technology Research Projects Grants to EO-A and by JSPS KAKENHI Grant Number JP19K08470 and a part of Management Expenses Grants to Shimane University to KM.

Conflict of interest

The authors declare that the research was conducted in the absence of any commercial or financial relationships that could be construed as a potential conflict of interest.

Publisher's note

References

Aktar, R., Peiris, M., Fikree, A., Cibert-Goton, V., Walmsley, M., Tough, I. R., et al. (2018). The extracellular matrix glycoprotein tenascin-X regulates peripheral sensory and motor neurones. *J. Physiol.* 596 (17), 4237–4251. doi:10.1113/jp276300

Aktar, R., Peiris, M., Fikree, A., Eaton, S., Kritas, S., Kentish, S. J., et al. (2019). A novel role for the extracellular matrix glycoprotein tenascin-X in gastric function. *J. Physiol.* 597 (6), 1503–1515. doi:10.1113/jp277195

Alcaraz, L. B., Exposito, J. Y., Chuvin, N., Pommier, R. M., Cluzel, C., Martel, S., et al. (2014). Tenascin-X promotes epithelial-to-mesenchymal transition by activating latent TGF-β. *J. Cell Biol.* 205 (3), 409–428. doi:10.1083/jcb.201308031

Bristow, J., Tee, M. K., Gitelman, S. E., Mellon, S. H., and Miller, W. L. (1993). Tenascin-X: A novel extracellular matrix protein encoded by the human xb gene overlapping P450c21B. *J. Cell Biol.* 122 (1), 265–278. doi:10.1083/jcb.122.1.265

Burch, G. H., Gong, Y., Liu, W., Dettman, R. W., Curry, C. J., Smith, L., et al. (1997). Tenascin-X deficiency is associated with Ehlers-Danlos syndrome. *Nat. Genet.* 17 (1), 104–108. doi:10.1038/ng0997-104

Chakravarthy, A., Khan, L., Bensler, N. P., Bose, P., and De Carvalho, D. D. (2018). TGF-β-associated extracellular matrix genes link cancer-associated fibroblasts to immune evasion and immunotherapy failure. *Nat. Commun.* 9 (1), 4692. doi:10.1038/s41467-018-06654-8

Chang, J., Zhong, R., Tian, J., Li, J., Zhai, K., Ke, J., et al. (2018). Exome-wide analyses identify low-frequency variant in CYP26B1 and additional coding variants associated with esophageal squamous cell carcinoma. *Nat. Genet.* 50 (3), 338–343. doi:10.1038/s41588-018-0045-8

Chen, W., Perritt, A. F., Morissette, R., Dreiling, J. L., Bohn, M. F., Mallappa, A., et al. (2016). Ehlers-Danlos syndrome caused by biallelic TNXB variants in patients with congenital adrenal hyperplasia. *Hum. Mutat.* 37 (9), 893–897. doi:10.1002/humu.23028

Chopra, P., Tinkle, B., Hamonet, C., Brock, I., Gompel, A., Bulbena, A., et al. (2017). Pain management in the Ehlers-Danlos syndromes. *Am. J. Med. Genet. C Semin.Med. Genet.* 175 (1), 212–219. doi:10.1002/ajmg.c.31554

Colloca, L., Ludman, T., Bouhassira, D., Baron, R., Dickenson, A. H., Yarnitsky, D., et al. (2017). Neuropathic pain. *Nat. Rev. Dis. Prim.* 3, 17002. doi:10.1038/nrdp.2017.2

Davidson, B. (2011). The diagnostic and molecular characteristics of malignant mesothelioma and ovarian/peritoneal serous carcinoma. *Cytopathology* 22 (1), 5–21. doi:10.1111/j.1365-2303.2010.00829.x

Demes, J. S., McNair, B., and Taylor, M. R. G. (2020). Use of complementary therapies for chronic pain management in patients with reported Ehlers-Danlos syndrome or hypermobility spectrum disorders. *Am. J. Med. Genet. A* 182 (11), 2611–2623. doi:10.1002/ajmg.a.61837

Demirdas, S., Dulfer, E., Robert, L., Kempers, M., van Beek, D., Micha, D., et al. (2017). Recognizing the tenascin-X deficient type of Ehlers-Danlos syndrome: A cross-sectional study in 17 patients. *Clin. Genet.* 91 (3), 411–425. doi:10.1111/cge.12853

Dewidar, B., Meyer, C., Dooley, S., and Meindl-Beinker, A. N. (2019). TGF-β in hepatic stellate cell activation and liver fibrogenesis-updated 2019. *Cells* 8 (11), 1419. doi:10.3390/cells8111419

Egging, D., van den Berkmortel, F., Taylor, G., Bristow, J., and Schalkwijk, J. (2007). Interactions of human tenascin-X domains with dermal extracellular matrix molecules. *Arch. Dermatol. Res.* 298 (8), 389–396. doi:10.1007/s00403-006-0706-9

Erickson, H. P. (1993). Tenascin-C, tenascin-R and tenascin-X: A family of talented proteins in search of functions. *Curr. Opin. Cell Biol.* 5 (5), 869–876. doi:10.1016/0955-0674(93)90037-q

Geffrotin, C., Garrido, J. J., Tremet, L., and Vaiman, M. (1995). Distinct tissue distribution in pigs of tenascin-X and tenascin-C transcripts. *Eur. J. Biochem.* 231 (1), 83–92. doi:10.1111/j.1432-1033.1995.tb20673.x

Green, C., Ghali, N., Akilapa, R., Angwin, C., Baker, D., Bartlett, M., et al. (2020). Classical-like Ehlres-Danlos syndrome: A clinical description of 20 newly identified individuals with evidence of tissue fragility. *Genet. Med.* 22 (10), 1576–1582. doi:10.1038/s41436-020-0850-1

Hasegawa, K., Yoshida, T., Matsumoto, K., Katsuta, K., Waga, S., and Sakakura, T. (1997). Differential expression of tenascin-C and tenascin-X in human astrocytomas. *Acta Neuropathol.* 93 (5), 431–437. doi:10.1007/s004010050636

Ikuta, T., Sogawa, N., Ariga, H., Ikemura, T., and Matsumoto, K. (1998). Structural analysis of mouse tenascin-X: Evolutionary aspects of reduplication of FNIII repeats in the tenascin gene family. *Gene* 217 (1-2), 1–13. doi:10.1016/s0378-1119(98)00355-2

Jensen, T. S., Baron, R., Haanpää, M., Kalso, E., Loeser, J. D., Rice, A. S. C., et al. (2011). A new definition of neuropathic pain. *Pain* 152 (10), 2204–2205. doi:10.1016/j.pain.2011.06.017

Kramer, M., Pierredon, S., Ribaux, P., Tille, J. C., Petignat, P., and Cohen, M. (2015). Secretome identifies tenascin-X as a potent marker of ovarian cancer. *Biomed. Res. Int.* 2015, 208017. doi:10.1155/2015/208017

Liang, G., Wang, S., Shao, J., Jin, Y., Xu, L., Yan, Y., et al. (2022). Tenascin-X mediates flow-induced suppression of EndMT and atherosclerosis. *Circ. Res.* 130, 1647–1659. doi:10.1161/circresaha.121.320694

Lindor, N. M., and Bristow, J. (2005). Tenascin-X deficiency in autosomal recessive Ehlers-Danlos syndrome. *Am. J. Med. Genet. A* 135 (1), 75–80. doi:10.1002/ajmg.a.30671

Liot, S., Aubert, A., Hervieu, V., Kholti, N. E., Schalkwijk, J., Verrier, B., et al. (2020). Loss of tenascin-X expression during tumor progression: A new pan-cancer marker. *Matrix Biol. Plus* 6-7, 100021. doi:10.1016/j.mbplus.2020.100021

Malfait, F., Castori, M., Francomano, C. A., Giunta, C., Kosho, T., and Byers, P. H. (2020). The Ehlers-Danlos syndromes. *Nat. Rev. Dis. Prim.* 6 (1), 64. doi:10.1038/s41572-020-0194-9

Malfait, F., Colman, M., Vroman, R., De Wandele, I., Rombaut, L., Miller, R. E., et al. (2021). Pain in the Ehlers-Danlos syndromes: Mechanisms, models, and challenges. *Am. J. Med. Genet. C Semin. Med. Genet.* 187 (4), 429–445. doi:10.1002/ajmg.c.31950

Malfait, F., Francomano, C., Byers, P., Belmont, J., Berglund, B., Black, J., et al. (2017). The 2017 international classification of the Ehlers-Danlos syndromes. *Am. J. Med. Genet. C Semin. Med. Genet.* 175 (1), 8–26. doi:10.1002/ajmg.c.31552

Mao, J. R., and Bristow, J. (2001). The Ehlers-Danlos syndrome: On beyond collagens. *J. Clin. Invest.* 107 (9), 1063–1069. doi:10.1172/jci12881

Mao, J. R., Taylor, G., Dean, W. B., Wagner, D. R., Afzal, V., Lotz, J. C., et al. (2002). Tenascin-X deficiency mimics Ehlers-Danlos syndrome in mice through alteration of collagen deposition. *Nat. Genet.* 30 (4), 421–425. doi:10.1038/ng850

Margaron, Y., Bostan, L., Exposito, J. Y., Malbouyres, M., Trunfio-Sfarghiu, A. M., Berthier, Y., et al. (2010). Tenascin-X increases the stiffness of collagen gels without affecting fibrillogenesis. *Biophys. Chem.* 147 (1-2), 87–91. doi:10.1016/j.bpc.2009.12.011

Matsumoto, K., and Aoki, H. (2020). The roles of tenascins in cardiovascular, inflammatory, and heritable connective tissue diseases. *Front. Immunol.* 11, 609752. doi:10.3389/fimmu.2020.609752

Matsumoto, K., Arai, M., Ishihara, N., Ando, A., Inoko, H., and Ikemura, T. (1992a). Cluster of fibronectin type III repeats found in the human major histocompatibility complex class III region shows the highest homology with the repeats in an extracellular matrix protein, tenascin. *Genomics* 12 (3), 485–491. doi:10.1016/0888-7543(92)90438-x

Matsumoto, K., Ishihara, N., Ando, A., Inoko, H., and Ikemura, T. (1992b). Extracellular matrix protein tenascin-like gene found in human MHC class III region. *Immunogenetics* 36 (6), 400–403. doi:10.1007/bf00218048

Matsumoto, K., Kawakami, K., Yamada, K., and Takeshita, H. (2022). COL1A1 expression induced by overexpression of both a 15-amino acid peptide from the fibrinogen domain of tenascin-X and integrin α11 in LX-2 cells. *Mol. Med. Rep.* 26 (5), 330. doi:10.3892/mmr.2022.12846

Matsumoto, K., Minamitani, T., Orba, Y., Sato, M., Sawa, H., and Ariga, H. (2004). Induction of matrix metalloproteinase-2 by tenascin-X deficiency is mediated through the c-Jun N-terminal kinase and protein tyrosine kinase phosphorylation pathway. *Exp. Cell Res.* 297 (2), 404–414. doi:10.1016/j.yexcr.2004.03.041

Matsumoto, K., Saga, Y., Ikemura, T., Sakakura, T., and Chiquet-Ehrismann, R. (1994). The distribution of tenascin-X is distinct and often reciprocal to that of tenascin-C. *J. Cell Biol.* 125 (2), 483–493. doi:10.1083/jcb.125.2.483

Matsumoto, K., Sawa, H., Sato, M., Orba, Y., Nagashima, K., and Ariga, H. (2002). Distribution of extracellular matrix tenascin-X in sciatic nerves. *Acta. Neuropathol.* 104 (5), 448–454. doi:10.1007/s00401-002-0577-x

Matsumoto, K., Takayama, N., Ohnishi, J., Ohnishi, E., Shirayoshi, Y., Nakatsuji, N., et al. (2001). Tumour invasion and metastasis are promoted in mice deficient in tenascin-X. *Genes* 6 (12), 1101–1111. doi:10.1046/j.1365-2443.2001.00482.x

Micale, L., Guarnieri, V., Augello, B., Palumbo, O., Agolini, E., Sofia, V. M., et al. (2019). Novel TNXB variants in two Italian patients with classical-like Ehlers-Danlos syndrome. *Genes (Basel)* 10 (12), 967. doi:10.3390/genes10120967

Minamitani, T., Ariga, H., and Matsumoto, K. (2004a). Deficiency of tenascin-X causes a decrease in the level of expression of type VI collagen. *Exp. Cell Res.* 297 (1), 49–60. doi:10.1016/j.yexcr.2004.03.002

Minamitani, T., Ikuta, T., Saito, Y., Takebe, G., Sato, M., Sawa, H., et al. (2004b). Modulation of collagen fibrillogenesis by tenascin-X and type VI collagen. *Exp. Cell Res.* 298 (1), 305–315. doi:10.1016/j.yexcr.2004.04.030

Moehring, F., Halder, P., Seal, R. P., and Stucky, C. L. (2018). Uncovering the cells and circuits of touch in normal and pathological settings. *Neuron* 100 (2), 349–360. doi:10.1016/j.neuron.2018.10.019

Morel, Y., Bristow, J., Gitelman, S. E., and Miller, W. L. (1989). Transcript encoded on the opposite strand of the human steroid 21-hydroxylase/complement component C4 gene locus. *Proc. Natl. Acad. Sci. USA* 86 (17), 6582–6586. doi:10.1073/pnas.86.17.6582

Nakayama, K., Seike, M., Noro, R., Takeuchi, S., Matsuda, K., Kunugi, S., et al. (2019). Tenascin XB is a novel diagnostic marker for malignant mesothelioma. *Anticancer Res.* 39 (2), 627–633. doi:10.21873/anticanres.13156

Okuda-Ashitaka, E., Kakuchi, Y., Kakumoto, H., Yamanishi, S., Kamada, H., Yoshidu, T., et al. (2020). Mechanical allodynia in mice with tenascin-X deficiency associated with Ehlers-Danlos syndrome. *Sci. Rep.* 10 (1), 6569. doi:10.1038/s41598-020-63499-2

Sakai, H., Yokota, S., Kajitani, N., Yoneyama, T., Kawakami, K., Yasui, Y., et al. (2017). A potential contribution of tenascin-X to blood vessel formation in peripheral nerves. *Neurosci. Res.* 124, 1–7. doi:10.1016/j.neures.2017.06.003

Sakai, T., Furukawa, Y., Chiquet-Ehrismann, R., Nakamura, M., Kitagawa, S., Ikemura, T., et al. (1996). Tenascin-X expression in tumor cells and fibroblasts: Glucocorticoids as negative regulators in fibroblasts. *J. Cell Sci.* 109 (8), 2069–2077. doi:10.1242/jcs.109.8.2069

Schalkwijk, J., Zweers, M. C., Steijlen, P. M., Dean, W. B., Taylor, G., van Vlijmen, I. M., et al. (2001). A recessive form of the Ehlers-Danlos syndrome caused by tenascin-X deficiency. *N. Engl. J. Med.* 345 (16), 1167–1175. doi:10.1056/NEJMoa002939

Sumioka, T., Iwanishi, H., Okada, Y., Miyajima, M., Ichikawa, K., Reinach, P. S., et al. (2021). Impairment of corneal epithelial wound healing is association with increased neutrophil infiltration and reactive oxygen species activation in tenascin X-deficient mice. *Lab. Invest.* 101 (6), 690–700. doi:10.1038/s41374-021-00576-8

Sumioka, T., Iwanishi, H., Okada, Y., Nidegawa, Y., Miyajima, M., Matsumoto, K., et al. (2018). Loss of tenascin X gene function impairs injury-induced stromal angiogenesis in mouse corneas. *J. Cell. Mol. Med.* 22 (2), 948–956. doi:10.1111/jcmm.13397

Syx, D., De Wandele, I., Rombaut, L., and Malfait, F. (2017). Hypermobility, the Ehlers-Danlos syndromes and chronic pain. *Clin. Exp. Rheumatol.* 35 (5), 116–122.

Syx, D., Miller, R. E., Obeidat, A. M., Tran, P. B., Vroman, R., Malfait, Z., et al. (2020).Pain-related behaviors and abnormal cutaneous innervation in a murine model of classical Ehlers-Danlos syndrome. *Pain*. 2274–2283. doi:10.1097/j.pain.0000000000001935

Takeda, K., Shiba, H., Mizuno, N., Hasegawa, N., Mouri, Y., Hirachi, A., et al. (2005). Brain-derived neurotrophic factor enhances periodontal tissue regeneration. *Tissue Eng.* 11 (9-10), 1618–1629. doi:10.1089/ten.2005.11.1618

van Dijk, F. S., Ghali, N., Demirdas, S., and Baker, D. (2022). "TNXB-related classical-like Ehlers-Danlos syndrome," in *GeneReviews(®)*. M. P. Adam, D. B. Everman, G. M. Mirzaa, R. A. Pagon, S. E. Wallace, L. J. H. Bean, et al. (Seattle (WA): University of Washington, Seattle, Copyright © 1993-2022, University of Washington, Seattle. GeneReviews is a registered trademark of the University of Washington, Seattle. All rights reserved).

Voermans, N. C., van Alfen, N., Pillen, S., Lammens, M., Schalkwijk, J., Zwarts, M. J., et al. (2009). Neuromuscular involvement in various types of Ehlers-Danlos syndrome. *Ann. Neurol.* 65 (6), 687–697. doi:10.1002/ana.21643

Voermans, N. C., Verrijp, K., Eshuis, L., Balemans, M. C., Egging, D., Sterrenburg, E., et al. (2011). Mild muscular features in tenascin-X knockout mice, a model of Ehlers-danlos syndrome. *Connect. Tissue Res.* 52 (5), 422–432. doi:10.3109/03008207.2010.551616

Whalen, K. C., and Crone, W. (2022). Multidisciplinary approach to treating chronic pain in patients with Ehlers-Danlos syndrome: Critically appraised topic. *J. Pain Res.* 15, 2893–2904. doi:10.2147/jpr.S377790

Yamaguchi, S., Kawakami, K., Satoh, K., Fukunaga, N., Akama, K., and Matsumoto, K. I. (2017). Suppression of hepatic dysfunction in tenascin-X-deficient mice fed a high-fat diet. *Mol. Med. Rep.* 16 (4), 4061–4067. doi:10.3892/mmr.2017.7052

Yan, F., Liu, S. W., Li, X. Y., Li, C. C., and Wu, Y. (2020). Silencing lncRNA LINC01305 inhibits epithelial mesenchymal transition in lung cancer cells by regulating TNXB-mediated PI3K/Akt signaling pathway. *J. Biol. Regul. Homeost. Agents* 34 (2), 499–508. doi:10.23812/20-73-a-33

Yang, N., Tian, J., Wang, X., Mei, S., Zou, D., Peng, X., et al. (2020). A functional variant in TNXB promoter associates with the risk of esophageal squamous-cell carcinoma. *Mol. Carcinog.* 59 (4), 439–446. doi:10.1002/mc.23166

Yuan, Y., Nymoen, D. A., Stavnes, H. T., Rosnes, A. K., Bjørang, O., Wu, C., et al. (2009). Tenascin-X is a novel diagnostic marker of malignant mesothelioma. *Am. J. Surg. Pathol.* 33 (11), 1673–1682. doi:10.1097/PAS.0b013e3181b6bde3

Zhang, W. M., Kapyla, J., Puranen, J. S., Knight, C. G., Tiger, C. F., Pentikainen, O. T., et al. (2003). Alpha11 beta1 integrin recognizes the GFOGER sequence in interstitial collagens. *J. Biol. Chem.* 278 (9), 7270–7277. doi:10.1074/jbc.M210313200

frontiers | Frontiers in Genetics

TYPE Case Report
PUBLISHED 16 March 2023
DOI 10.3389/fgene.2023.1147607

OPEN ACCESS

EDITED BY
Tomoki Kosho,
Shinshu University, Japan

REVIEWED BY
Shujiro Hayashi,
Dokkyo Medical University, Japan
Ayca Kocaaga,
Eskisehir City Hospital, Türkiye

*CORRESPONDENCE
Fleur Stephanie van Dijk,
fleur.dijk@nhs.net

SPECIALTY SECTION
This article was submitted to Genetics of Common and Rare Diseases, a section of the journal Frontiers in Genetics

RECEIVED 18 January 2023
ACCEPTED 02 March 2023
PUBLISHED 16 March 2023

CITATION
Angwin C, Ghali N and Stephanie van Dijk F (2023), Case report and discussion: Pre-implantation genetic diagnosis with surrogacy in vascular Ehlers–Danlos syndrome.
Front. Genet. 14:1147607.
doi: 10.3389/fgene.2023.1147607

Case report and discussion: Pre-implantation genetic diagnosis with surrogacy in vascular Ehlers–Danlos syndrome

Chloe Angwin[1,2], Neeti Ghali[1,2] and Fleur Stephanie van Dijk[1,2]*

[1]London National Ehlers-Danlos Syndrome Service, North West Thames Regional Genetics Service, London North West Healthcare University NHS Trust, Harrow, United Kingdom, [2]Department of Metabolism, Digestion and Reproduction, Section of Genetics and Genomics, Imperial College London, London, United Kingdom

Introduction: Vascular Ehlers–Danlos syndrome (vEDS) is an autosomal dominant inherited connective tissue condition, characterized by generalized tissue fragility with an increased risk of arterial dissection and hollow organ rupture. In women with vEDS, pregnancy and childbirth carry significant risks of both morbidity and mortality. The Human Fertilisation and Embryology Authority has approved vEDS for pre-implantation genetic diagnosis (PGD), given the potential for life-limiting complications. PGD avoids implantation of embryos that are affected by specific disorders by carrying out genetic testing (either for a familial variant or whole gene) and selecting unaffected embryos prior to implantation.

Case: We present an essential clinical update to the only published clinical case of a woman with vEDS undergoing PGD with surrogacy, initially through stimulated in vitro fertilization (IVF) and in vitro maturation (IVM) and subsequently through natural IVF.

Discussion: In our experience, a subset of women with vEDS do wish to have biological, unaffected children through PGD despite being aware of the risks of pregnancy and delivery. Given the clinical heterogeneity in vEDS, these women could be considered on a case-by-case basis for PGD. Controlled studies with comprehensive patient monitoring evaluating the safety of PGD are essential to equitable healthcare provision.

KEYWORDS

pre-implantation genetic diagnosis, vascular, Ehlers–Danlos syndrome, *in vitro* fertilization, surrogacy

1 Introduction

Pre-implantation genetic diagnosis (PGD) is available for many inherited conditions. Vascular EDS (vEDS), an inherited tissue condition characterized by generalized tissue fragility, is an accepted indication for PGD approved by the Human Fertilisation and Embryology Authority (HFEA) (HFEA, 2010). However, there is only one documented case of PGD in a woman diagnosed with vEDS (Bergeron et al., 2014); we present her medical history with an update on important clinical update on her reproductive history. In addition, the current European Society of Cardiology (ESC) guidance on pregnancy in cardiovascular disease patients and outcomes of pregnancy in women with vEDS will be discussed.

Ehlers–Danlos syndrome (EDS) is a heterogeneous group of connective tissue disorders characterized by joint hypermobility, skin and vessel fragility, and generalized tissue friability (Malfait, 2018). VEDS is a rare inherited connective tissue disorder that, in most cases, results from heterozygous pathogenic variants in the *COL3A1* gene encoding type III collagen (Malfait et al., 2017).

Major criteria for a diagnosis of vEDS consist of i) a family history of vEDS with a documented causative variant, ii) arterial rupture at a young age, iii) spontaneous sigmoid colon perforation in the absence of known pathology, iv) uterine rupture during the third trimester in the absence of previous C-section and/or severe peripartum tears, and v) carotid-cavernous sinus fistula formation in the absence of trauma (Malfait et al., 2017).

Depending on the specific underlying *COL3A1* gene variant, there will be decreased collagen type III production; this amount can vary from 50% to 87.5% (Malfait et al., 2020). Genotype–phenotype relationships have been observed with heterozygous protein-altering variants, accounting for earlier and more severe onset of symptoms than heterozygous null variants which cause a 50% reduction of collagen type III (Frank et al., 2015; Malfait et al., 2020). Intra and interfamilial variability have been noted in families with vascular EDS with regard to the age of onset and type of clinical events (Jørgensen et al., 2015).

For women with inherited disorders who wish to become pregnant, there are a variety of options including invasive prenatal diagnosis; however, only pre-implantation genetic diagnosis allows parents to have an unaffected, biological child without the risk of termination of pregnancy when the fetus is affected (NHS England, 2014). PGD is carried out through *in vitro* fertilization (IVF) of oocytes and spermatocytes from the parents, subsequent genetic testing of early embryos for the familial pathogenic variant(s), and selection of unaffected embryos *via* genetic testing (in this case of the *COL3A1* gene) prior to transfer to the uterus (NHS England, 2014). PGD does not screen embryos for other inherited conditions, and the fetus would be at a population risk of being affected by any other disorders (NHS England, 2014).

In women with vEDS, pregnancy does not only hold the 50% risk of having an affected child but also carries risk to maternal health including arterial events, uterine rupture, and death (5% risk of death) (Pepin et al., 2000; Byers et al., 2017; Malfait et al., 2017). In women affected by vEDS, these risks can be avoided through surrogacy. However, in surrogacy, the vEDS status of the fetus can still affect the pregnancy, for example, with increased rates of premature birth for fetuses affected by vEDS (Stephens et al., 2022). Surrogacy with PGD is an additional option where unaffected embryos can be transferred to an unaffected surrogate, reducing risk to the fetus and to the surrogate. However, altruistic surrogacy often requires expenses to be paid which may exclude this option for families and still carries the population-level risks of pregnancy and childbirth for the surrogate and fetus unaffected by vEDS (UK Government, 2021).

Current ESC guidance advises that pregnancy should be avoided in all women with vEDS, given the complication risks (European Society of Cardiology, 2018). However, there are no guidelines discussing assisted reproductive techniques in these women.

2 Case report

The original report (Bergeron et al., 2014) followed a 33-year-old woman, who had been diagnosed with vEDS due to a *de novo* heterozygous pathogenic *COL3A1* variant (c.2492G>A, p. Gly831Asp). She had a desire to have children while minimizing both the risk to herself from pregnancy-related complications and of her children inheriting the pathogenic variant and being affected with vEDS. We have detailed her medical history in the following paragraphs.

She was born with a unilateral congenital hip dislocation. At the age of 9, she suffered a left anterior cruciate ligament rupture while dancing. At 27, she had a hemorrhagic rupture of a liver cyst. The following year, she developed a right peroneal arterial aneurysm, which triggered genetic testing, and was molecularly confirmed to have vEDS. At age 29, she experienced a right coronary artery dissection complicated by a right iliac artery dissection post-angiogram.

At age 30, she started pre-conception counseling for PGD with surrogacy. Standard IVF protocols were commenced at age 32; however, during the first round of hormonal stimulation, egg retrieval was delayed over the weekend, and she had a splenic artery aneurysm rupture. This was her first exposure to IVF hormonal stimulation, and she was advised to avoid further doses after concerns regarding possible hormonal effects on vasculature. She developed a left-sided deep vein thrombosis (DVT) shortly after discharge, which was managed with standard anti-coagulation protocols, and developed a liver hematoma a month later. At the age of 33, she started natural (unstimulated) IVF and underwent four cycles with successful oocyte retrieval but unsuccessful implantation. After these cycles, she began the previously reported *in vitro* maturation (IVM) cycles and underwent six cycles with successful retrieval but unsuccessful implantation (Bergeron et al., 2014).

In addition to the publication of her medical history by Bergeron et al., a different surrogate was used and the patient continued natural IVF at age 35, undergoing six cycles to create four embryos. Implantation was successful, and her son was born and confirmed with prenatal testing and postnatal testing to be negative for the familial *COL3A1* variant. She continued natural IVF and underwent 20 cycles and 19 egg retrievals (after ovulating prior to one retrieval). All egg retrievals were transvaginal under sedation and carried out by a trained gynecologist. There was no reported organ damage or significant bleeds directly associated with the transvaginal egg retrievals. During this time, she had further vEDS-related complications; at age 38, she developed a spontaneous dissection of the infrarenal aorta below the inferior mesenteric artery complicated by sigmoid volvulus which was managed endoscopically. At age 41, another implantation was successful with the same surrogate; her daughter was born and confirmed to be negative for the familial *COL3A1* variant during prenatal and postnatal genetic testing (Figure 1).

3 Discussion

The reported patient, who had experienced a number of arterial events throughout her lifetime, underwent IVF with PGD and surrogacy and, as a result, had two children unaffected by vEDS. This involved a single cycle of hormonally stimulated IVF, followed by vascular complications, then four natural (without hormonal stimulation) IVF cycles and six IVM (*in vitro* maturation, collection,

and maturation of oocytes *in vitro*) cycles without complication, and finally, 26 cycles of natural IVF with vascular complications midway through these cycles, unrelated to any procedures. As the only report in the literature of assisted conception in a woman with a molecularly confirmed diagnosis of vEDS, this report is relevant for a number of reasons. First, assisted conception and surrogacy could be considered a reproductive option for women with vEDS. Second, the sequence of serious arterial events prior to and following her single cycle of stimulated IVF questions the hypothesis that the first arterial event occurred purely due to ovarian hyperstimulation. Third, this patient underwent multiple (n = 33) transvaginal egg retrievals without complications, suggesting that this procedure may cause relatively low risks in women with vEDS. However, further investigations and formal studies are required to fully evaluate the risk of assisted conception in individuals with vEDS.

There is some evidence that hormonal treatments can exacerbate vascular fragility, alter the hemodynamic state, and precipitate cardiovascular events in susceptible patients (Iyasere and Potdar, 2022). Natural IVF involves close monitoring of natural ovulation cycles with no exogenous hormonal treatments but still requires manual egg retrieval.

General recommendations from the ESC regarding IVF in women with any cardiovascular disease include careful consideration of hormone dosages to manage or avoid prothrombotic conditions such as ovarian hyperstimulation syndrome and consideration of natural IVF (European Society of Cardiology, 2018). The ESC guidance makes no specific recommendations regarding egg retrieval risks or surrogacy in cardiovascular disease (European Society of Cardiology, 2018). General recommendations for cardiologists from the ESC advise that pregnancy is avoided in all women with a vEDS diagnosis (European Society of Cardiology, 2018). However, in reality, many female patients with vEDS continue to have pregnancies and are offered regular surveillance throughout. The lack of published data on PGD with or without surrogates in women with vEDS is important, given that there are women with vEDS who are aware of their diagnosis before they start a family and that vascular EDS is an accepted indication for PGD. Women with vEDS may potentially be discouraged from PGD as the risk from assisted reproductive techniques is unknown and pregnancy is deemed too risky. The most recent data on risks in pregnancy for women with vEDS are presented in the following paragraphs; however, it is important to note that not all individuals were diagnosed prior to pregnancy, and use of monitoring and current treatments (which are improving the life expectancy for this patient group) was not consistent (Frank et al., 2019).

Data were analyzed from 526 women with vEDS as an update to a previous cohort (Pepin et al., 2000), comparing 243 nulliparous women against a cohort of 283 women who had had at least one pregnancy (Murray et al., 2014). Women with vEDS had a pregnancy-related death rate of 4.9%. When stratified for the variant type, protein-altering variants resulted in a 5.3% death rate per delivery (30 deaths in 256 women across 565 delivered pregnancies), while there were no deaths in those women with heterozygous null variants. Importantly, Kaplan–Meier survival curve analysis showed no significant difference in survival between nulliparous and parous women with vEDS (Murray et al., 2014). In contrast, pregnancy-related mortality in the United States in 2017 was 0.02% across the entire population (Centres for Disease Control and Prevention, 2020). Within this study, a smaller cohort of 38 women with vEDS were interviewed about pregnancy-related complications; only 10.6% had a diagnosis of vEDS prior to conception, and three had null variants. Patients with null variants had a preterm delivery and third-degree and fourth-degree lacerations (Murray et al., 2014). The 35 women with protein-altering variants delivered 76 pregnancies, of which 49% (n = 35) of planned deliveries were uncomplicated. Complications included maternal death (n = 5), non-fatal vEDS-related complications (n = 5) (e.g., coronary artery dissection), and other complications (n = 46) including preterm delivery, third- or fourth-degree lacerations (only seen in vaginal deliveries), hemorrhage, and placenta previa or abruption (Murray et al., 2014).

The Registry of Pregnancy And Cardiac disease (ROPAC) has released data on pregnancy in women with thoracic aortic disease. This group contained four individuals with vEDS, one of whom had had a previous type B aortic dissection; all vEDS individuals underwent caesarean sections without complication (Campens et al., 2021).

Specific variants in *COL1A1* and *COL3A1* can result in overlapping phenotypes between classical EDS (thought to have a lower risk of vascular events) and vascular EDS. A recent study of 26 pregnancies in individuals with these variants reported no severe pregnancy-related complications (six perineal tears and one multiple miscarriage) (Colman et al., 2022). However, arterial events have been reported in this cohort during pregnancy, including a brachial artery dissection at 26 weeks in an individual with an atypical *COL3A1* variant (Ghali et al., 2019). Haploinsufficient variants in vEDS are thought to result in a milder phenotype, and a recent report of two haploinsufficient individuals did not identify any pregnancy-related complications (Kempers et al., 2022). Variation in phenotype severity may mean that pregnancy-related risk is also variable and could be assessed on a case-by-case basis (Frank et al., 2015; Jørgensen et al., 2015; Malfait et al., 2020).

Investigation of the frequency of complications related to fetal vEDS status found that premature birth was more commonly seen in affected rather than unaffected fetuses and that this was not impacted by the maternal vEDS status (Stephens et al., 2022). PGD with or without surrogacy, therefore, shows potential to reduce both maternal and fetal risks.

An alternative to PGD which ensures an unaffected child is invasive prenatal diagnosis (IPD), which would involve termination of any affected fetus (NHS England, 2014). ESC guidance discusses termination of pregnancy and recommends that for any women with high-risk cardiovascular disease, surgical termination in an experienced center is more appropriate, and medical terminations should be considered only up to 9 weeks using reduced dosages (European Society of Cardiology, 2018). However, prenatal testing can only be performed accurately after 11 weeks (Alfirevic et al., 2017). In women with vEDS, non-invasive prenatal diagnosis (NIPD) is currently not possible as the maternal variant will prevent differentiation from the fetus (Jenkins et al., 2018). Therefore, women with vEDS would have the option of a surgical termination only, which, given their generalized tissue fragility, would be considered a high-risk procedure. Additionally, the procedure of prenatal diagnosis is not without risk, particularly

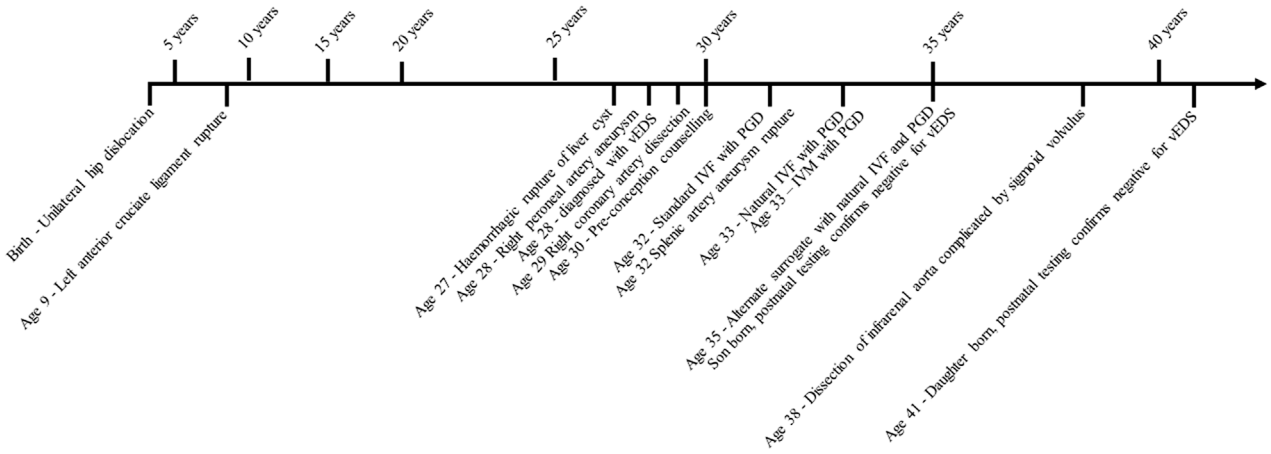

FIGURE 1
Timeline of clinical events recorded in the proband. IVF, *in vitro* fertilization; IVM, —*in vitro* maturation; vEDS, —vascular Ehlers–Danlos syndrome; PGD, —pre-implantation genetic diagnosis. Implantation and births *via* surrogate.

in the context of disorders of tissue fragility, and is also not acceptable to some individuals. Together, these concerns make prenatal diagnosis a potentially risky route and may discourage women with connective tissue disorders and vascular involvement from seeking prenatal genetic diagnosis as it would only be offered to those who would consider termination (a 50% risk for a woman with vEDS). There are no current published data on the safety of termination in women with vEDS.

In our experience, many women with vEDS remain keen to have their own biological children. Lack of communication regarding reproductive options and safety may put this group of patients at further risk as their ability to make an informed decision around reproduction is reduced and may, at worst, result in an unmonitored pregnancy. This is highlighted by the vEDS Research Collaborative members, who have recently published a research agenda which has pregnancy management as one of four important areas of focus (Sage et al., 2020).

4 Conclusion

We think that there is a place for considering each woman with vEDS for PGD with or without surrogacy on an individual basis, including medical history regarding events related to vEDS, family history, and specific underlying genetic cause. It is important to ensure that all women with vEDS who wish for biological children are counseled, informed of up-to-date risks, and have a clear understanding regarding the advantages and disadvantages of all available options including natural and hormonal IVF, PGD, and surrogacy.

We hope for a discussion regarding reproduction in women with vEDS despite the increased risk of death or complications in pregnancy in comparison to the general population. PGD offers the only route for families wishing to have unaffected biological children without the 50% risk of termination of pregnancy; if couples are well-informed of the hypothetical and potential risks, it may be that this could be offered on an individual case-by-case basis. Controlled studies with comprehensive patient monitoring evaluating the safety of PGD in these women are essential to equitable healthcare provision and patient counseling.

Data availability statement

The original contributions presented in the study are included in the article/Supplementary Material; further inquiries can be directed to the corresponding author.

Ethics statement

Written informed consent was obtained from the individual(s) for the publication of any potentially identifiable images or data included in this article.

Author contributions

CA: first authorship, data collection, and manuscript drafting; NG: patient information collection and manuscript supervision; FS: last authorship, patient information collection, and manuscript supervision.

Funding

We have open access funding for the publication of this paper (Imperial College London, PO number: 4550140).

Conflict of interest

The authors declare that the research was conducted in the absence of any commercial or financial relationships that could be construed as a potential conflict of interest.

Publisher's note

References

Alfirevic, Z., Navaratnam, K., and Mujezinovic, F. (2017). Amniocentesis and chorionic villus sampling for prenatal diagnosis. *Cochrane Database Syst. Rev.* 9 (9), CD003252. doi:10.1002/14651858.CD003252.pub2

Bergeron, M. E., Child, T., and Fatum, M. (2014). *In vitro* maturation and surrogacy in patients with vascular-type Ehlers-Danlos syndrome--a safe assisted reproductive technology approach. *Hum. Fertil. (Camb)* 17 (2), 141–144. doi:10.3109/14647273.2014.903002

Byers, P. H., Belmont, J., Black, J., De Backer, J., Frank, M., Jeunemaitre, X., et al. (2017). Diagnosis, natural history, and management in vascular Ehlers-Danlos syndrome. *Am. J. Med. Genet. C Semin. Med. Genet.* 175 (1), 40–47. doi:10.1002/ajmg.c.31553

Campens, L., Baris, L., Scott, N. S., Broberg, C. S., Bondue, A., Jondeau, G., et al. (2021). ROPAC investigators group. Pregnancy outcome in thoracic aortic disease data from the Registry of Pregnancy and Cardiac disease. *Heart* 107 (21), 1704–1709. doi:10.1136/heartjnl-2020-318183

Centres for Disease Control and Prevention (2020); Pregnancy mortality surveillance system, Available at: https://www.cdc.gov/reproductivehealth/maternal-mortality/pregnancy-mortality-surveillance-system.htm; (Accessed 20/04/2020)

Colman, M., Castori, M., Micale, L., Ritelli, M., Colombi, M., Ghali, N., et al. (2022). Atypical variants in COL1A1 and COL3A1 associated with classical and vascular ehlers-danlos syndrome overlap phenotypes: Expanding the clinical phenotype based on additional case reports. *Clin. Exp. Rheumatol.* 40 134(5):46–62. doi:10.55563/clinexprheumatol/kzkq6y

European Society of Cardiology (2019), ESC Guidelines for the management of cardiovascular diseases during pregnancy. *Rev. Esp. Cardiol. Engl. Ed.* 72(2):161. doi:10.1016/j.rec.2018.12.003

Frank, M., Adham, S., Seigle, S., Legrand, A., Mirault, T., Henneton, P., et al. (2019) Vascular ehlers-danlos syndrome: Long-term observational study, *J. Am. Coll. Cardiol.* 73. 1948–1957. doi:10.1016/j.jacc.2019.01.058

Frank, M., Albuisson, J., Ranque, B., Golmard, L., Mazzella, J. M., Bal-Theoleyre, L., et al. (2015). The type of variants at the COL3A1 gene associates with the phenotype and severity of vascular Ehlers-Danlos syndrome. *Eur. J. Hum. Genet.* 23 (12), 1657–1664. doi:10.1038/ejhg.2015.32

Ghali, N., Baker, D., Brady, A. F., Burrows, N., Cervi, E., Cilliers, D., et al. (2019). Atypical COL3A1 variants (glutamic acid to lysine) cause vascular Ehlers-Danlos syndrome with a consistent phenotype of tissue fragility and skin hyperextensibility. *Genet. Med.* 21 (9), 2081–2091. doi:10.1038/s41436-019-0470-9

Human Fertilisation and Embryology Authority (2010). HFEA licence committee meeting. Available at: https://www.hfea.gov.uk/pgt-m-conditions.

Iyasere, C., and Potdar, N. (2022). Spontaneous coronary artery dissection associated with infertility treatment. *Cureus* 14 (9), e29587. doi:10.7759/cureus.29587

Jenkins, L. A., Deans, Z. C., Lewis, C., and Allen, S. (2018). Delivering an accredited non-invasive prenatal diagnosis service for monogenic disorders and recommendations for best practice. *Prenat. Diagn* 38 (1), 44–51. doi:10.1002/pd.5197

Jørgensen, A., Fagerheim, T., Rand-Hendriksen, S., Lunde, P. I., Vorren, T. O., Pepin, M. G., et al. (2015). Vascular Ehlers-Danlos Syndrome in siblings with biallelic COL3A1 sequence variants and marked clinical variability in the extended family. *Eur. J. Hum. Genet.* 23 (6), 796–802. doi:10.1038/ejhg.2014.181

Kempers, M. J., Wessels, M., Van Berendoncks, A., van de Laar, I. M., de Leeuw, N., and Loeys, B. (2022). Phenotype of COL3A1/COL5A2 deletion patients. *Eur. J. Med. Genet.* 65 (10), 104593. doi:10.1016/j.ejmg.2022.104593

Malfait, F., Francomano, C., Byers, P., Belmont, J., Berglund, B., Black, J., et al. (2017). The 2017 international classification of the Ehlers-Danlos syndromes. *Am. J. Med. Genet. C Semin. Med. Genet. Mar.* 175 (1), 8–26. doi:10.1002/ajmg.c.31552

Malfait, F. (2018). Vascular aspects of the ehlers-danlos syndromes. *Matrix Biol.* 71-72, 380–395. doi:10.1016/j.matbio.2018.04.013

Malfait, F., Castori, M., Francomano, C. A., Giunta, C., Kosho, T., and Byers, P. H. (2020). The Ehlers-Danlos syndromes. *Nat. Rev. Dis. Prim.* 6, 64. doi:10.1038/s41572-020-0194-9

Murray, M. L., Pepin, M., Peterson, S., and Byers, P. H. (2014). Pregnancy-related deaths and complications in women with vascular Ehlers-Danlos syndrome. *Genet. Med.* 16 (12), 874–880. doi:10.1038/gim.2014.53

NHS England (2014). NHS England clinical reference group for medical genetics, clinical commissioning policy: Pre-implantation genetic diagnosis (PGD). Available at: https://www.england.nhs.uk/.

Pepin, M., Schwarze, U., Superti-Furga, A., and Byers, P. H. (2000). Clinical and genetic features of Ehlers-Danlos syndrome type IV, the vascular type. *N. Engl. J. Med.* 342 (10), 673–680. doi:10.1056/NEJM200003093421001

Sage, L., Russo, M. L., Byers, P. H., Demasi, J., Morris, S. A., Puryear, L. N., et al.Vascular Ehlers-Danlos Syndrome Research Collaborative (2020). Setting a research agenda for vascular Ehlers-Danlos syndrome using a patient and stakeholder engagement model. *J. Vasc. Surg.* 72 (4), 1436–1444.e2. doi:10.1016/j.jvs.2019.12.043

Stephens, S. B., Russo, M., Shalhub, S., Beecroft, T., Weigand, J., Milewicz, D. M., et al. (2022). Evaluating perinatal and neonatal outcomes among children with vascular Ehlers-Danlos syndrome. *Genet. Med.* 24 (10), 2134–2143. doi:10.1016/j.gim.2022.07.010

UK Government (2021). Surrogacy: Legal rights of parents and surrogates. Available at: https://www.gov.uk/legal-rights-when-using-surrogates-and-donors/maternity-leave (accessed March, 2021).

frontiers | Frontiers in Genetics

TYPE Case Report
PUBLISHED 18 April 2023
DOI 10.3389/fgene.2023.1148224

OPEN ACCESS

EDITED BY
Tomoki Kosho,
Shinshu University, Japan

REVIEWED BY
Shujiro Hayashi,
Dokkyo Medical University, Japan
Nadia Akawi,
United Arab Emirates University, United Arab Emirates
Hiromi Sanai,
Yamaguchi Grand Medical Center, Japan

*CORRESPONDENCE
Fleur Stephanie van Dijk,
fleur.dijk@nhs.net

SPECIALTY SECTION
This article was submitted to Genetics of Common and Rare Diseases, a section of the journal Frontiers in Genetics

RECEIVED 19 January 2023
ACCEPTED 23 March 2023
PUBLISHED 18 April 2023

CITATION
Angwin C, Ghali N and van Dijk FS (2023), Case report: Two individuals with *AEBP1*-related classical-like EDS: Further clinical characterisation and description of novel *AEBP1* variants.
Front. Genet. 14:1148224.
doi: 10.3389/fgene.2023.1148224

Case report: Two individuals with *AEBP1*-related classical-like EDS: Further clinical characterisation and description of novel *AEBP1* variants

Chloe Angwin[1,2], Neeti Ghali[1,2] and Fleur Stephanie van Dijk[1,2]*

[1]National Ehlers-Danlos Syndrome Service, London North West University Healthcare NHS Trust, London, United Kingdom, [2]Genetics and Genomics Division, Department of Metabolism, Digestion and Reproduction, Imperial College London, London, United Kingdom

Introduction: *AEBP1*-related classical-like EDS (clEDS type 2) is a rare type of Ehlers–Danlos syndrome (EDS) that was first reported in 2016. There are overlapping clinical features with *TNXB*-related classical-like EDS (or clEDS type 1), including skin hyperextensibility, joint hypermobility, and easy bruising. There are currently nine reported individuals with *AEBP1*-related clEDS type 2. This report confirms previous findings and provides additional clinical and molecular data on this group of individuals.

Materials and methods: Two individuals (P1 and P2), with features of a rare type of EDS, were clinically assessed in the London national EDS service and underwent genetic testing.

Results: Genetic testing in P1 revealed likely pathogenic *AEBP1* variants: c.821del: p. (Pro274Leufs*18) and c.2248T>C:p. (Trp750Arg). In P2 pathogenic *AEBP1* variants, c.1012G>T:p. (Glu338*) and c.1930C>T:p. (Arg644*) were identified.

Discussion: These two individuals increased the reported number of individuals with *AEBP1*-related clEDS to 11 (six females and five males). There are shared features with previously reported individuals, including hypermobility (11/11), skin hyperextensibility (11/11), presence of atrophic scarring (9/11), and easy bruising (10/11). In P1, a chronic right vertebral artery dissection, mild dilatation of the splenic artery, aberrant subclavian artery, and tortuous iliac arteries were observed at the age of 63 years. Cardiovascular disease has been reported, including mitral valve prolapse (4/11), peripheral arterial disease (1/11), and aortic root aneurysm requiring surgical intervention (1/11). Hair loss has been reported in 6/11 individuals (five females and one male), only one of which was documented to have a formal diagnosis of androgenetic alopecia, while other individuals were described as having thinning of hair, male pattern hair loss, or unspecified alopecia.

Conclusion: The clinical features of individuals with *AEBP1*-related EDS have not been fully elucidated yet. Hair loss is present in 6/11 individuals with *AEBP1*-related clEDS and appears to be a feature of this condition. This is the first time hair loss has been formally reported as a characteristic feature in a rare type of EDS. Cardiovascular surveillance seems warranted in this condition because 2/11 individuals have evidence of arterial aneurysm and/or dissection. Further descriptions of affected individuals are necessary to update diagnostic criteria and management guidelines.

KEYWORDS

classical-like EDS type 2, Ehlers–Danlos syndrome, hair loss, AEBP1, connective tissue disease

1 Introduction

Classical-like EDS (clEDS) is a rare type of Ehlers–Danlos syndrome (EDS), termed type 1 or 2 according to the underlying genetic cause. Recessive variants in the gene *TNXB* encoding tenascin-X result in type 1 clEDS (Malfait et al., 2017), and recessive variants in the *AEBP1* gene encoding aortic carboxypeptidase-like protein (ACLP) result in type 2 clEDS (Ritelli et al., 2019).

Major diagnostic criteria for clEDS type 1 are as published in the 2017 International Classification of the Ehlers–Danlos syndromes: (i) skin hyperextensibility without atrophic scarring, (ii) generalised joint hypermobility, and (iii) easy bruising (Malfait et al., 2017). Minor diagnostic criteria for clEDS type 1 include (i) foot deformities, (ii) lower limb oedema, (iii) mild proximal and distal muscle weakness, (iv) axonal polyneuropathy, (v) atrophy of muscles in hands and feet, (vi) acrogeric hands, brachydactyly, clinodactyly, mallet finger, and (vii) vagina/uterus/rectal prolapse (Malfait et al., 2017). The minimal suggestive diagnostic criteria included all three major criteria and a family history suggestive of autosomal recessive transmission; confirmatory molecular testing is obligatory (Malfait et al., 2017).

Recessive variants in the *AEBP1* gene were first reported and associated with clEDS in two siblings (Alazami et al., 2016). (Alazami et al., 2016) (Alazami et al., 2016; Blackburn et al., 2018; Hebebrand et al., 2019; Ritelli et al., 2019; Syx et al., 2019) (Malfait et al., 2020) *AEBP1* encodes the aortic carboxypeptidase-like protein (ACLP), which is an extracellular matrix (ECM) protein identified in dermis, periosteum, vessel walls, and lung basement membrane with fundamental roles in embryogenesis and ECM repair and maintenance (Blackburn et al., 2018; Vishwanath et al., 2020). *AEBP1* variants, as a cause of clEDS type 2, were firmly established by Blackburn et al. in their 2018 paper, who described two individuals in addition to Alazami's two individuals (Alazami et al., 2016; Blackburn et al., 2018). There are currently nine reported cases of clEDS as a result of variants in AEBP1 (Alazami et al., 2016; Blackburn et al., 2018; Hebebrand et al., 2019; Ritelli et al., 2019; Syx et al., 2019). Following these reports, distinctions have been drawn between clEDS type 1 and type 2, with type 2 including the presence of atrophic scarring and early-onset osteopenia (Malfait et al., 2020). This case summary presents two women with clEDS type 2 due to bi-allelic variants in *AEBP1*.

2 Case descriptions

2.1 Proband 1

At the time of writing, the proband (P1) was 65 years old. P1 was born at term after a normal pregnancy. At 18 months of age, bilateral dislocations of the hips were identified, requiring multiple surgeries continuing until the age of 10 years. As a child, P1 had significant joint hypermobility and required extractions for dental overcrowding. Joint dislocations after moderate trauma occurred throughout P1's lifetime, with recurrent falls due to ankle instability and ongoing, progressive joint pain in her neck, back, and shoulders requiring regular analgesia. At age 55 and 60, P1 required a left hip replacement and a left knee replacement, respectively. P1 suffers from fatigue. From a young age, the proband bruised easily and severely after mild trauma, for example, large thigh haematomas from holding a baby on the proband's lap. P1's wound healing was normal and has reported heat intolerance due to reduced sweating, although this has not been further investigated.

P1 has had two children *via* caesarean section; both deliveries required blood transfusions due to haemorrhage, and one resulted in a large haematoma post-operatively. No other family members have a similar combination of clinical features. As a young child, hair loss was observed as a single occipital patch, which progressed to complete scalp hair loss after the birth of her first child at age 20, beginning with thinning over the vertex of the scalp and progressing to include the majority of the scalp.

At the time of examination, age 62, (see Figure 1, patient's consent has been gained for the use of all clinical photographs), P1 had a high arched palate (however, with no abnormally shaped teeth and no bifid uvula), with a scoliosis of the spine convex to the left. Earlobes were notched bilaterally. Pes planus was observed bilaterally, with hammer toes and bilateral hallux valgus. The skin was observed to be hyperextensible and lax, which was thin with translucent veins particularly over the chest. Bruising and discolouration of the arms was observed. Atrophic scars were observed over the knees and at the site of the left hip surgery. Thin scars observed over the forehead and at the site of the left knee surgery. P1's Beighton score was 3/8. Hair loss was observed over the vertex and crown of the head. Body hair was also reduced including arms, legs, axillary, and pubic hair, while eyebrows and eyelashes were retained.

2.2 Investigations

A spine X-ray, at age 57, showed spondylotic changes, narrowing at C4-5 and C6-7 with severe degenerative change to the lumbar spine from L2 to L5. An echocardiogram conducted at age 54 was normal; however, at age 63, repetitive echocardiogram showed mild dilatation of the ascending aorta. A CT angiogram confirmed mild dilatation of the isthmus and ascending aorta (34 mm), as well as chronic right vertebral artery dissection, mild dilatation of the splenic artery, aberrant subclavian artery, and tortuous iliac arteries. P1 does not have cardiovascular risk factors (normotensive, BMI 22, and non-smoker).

Transmission electron microscopy of skin biopsy taken from the inner upper arm showed abundant collagen flowers (see Figure 2).

Historical diagnostic DNA analysis including MLPA for classical and arthrochalasia EDS (*COL5A1, COL5A2, COL1A1,* and *COL1A2*), classical-like EDS type 1 (*TNXB*), and vascular EDS (*COL3A1* and *COL1A1*) showed no abnormalities. Therefore, at the age of 64, P1 was included in the

10.3389/fgene.2023.1148224

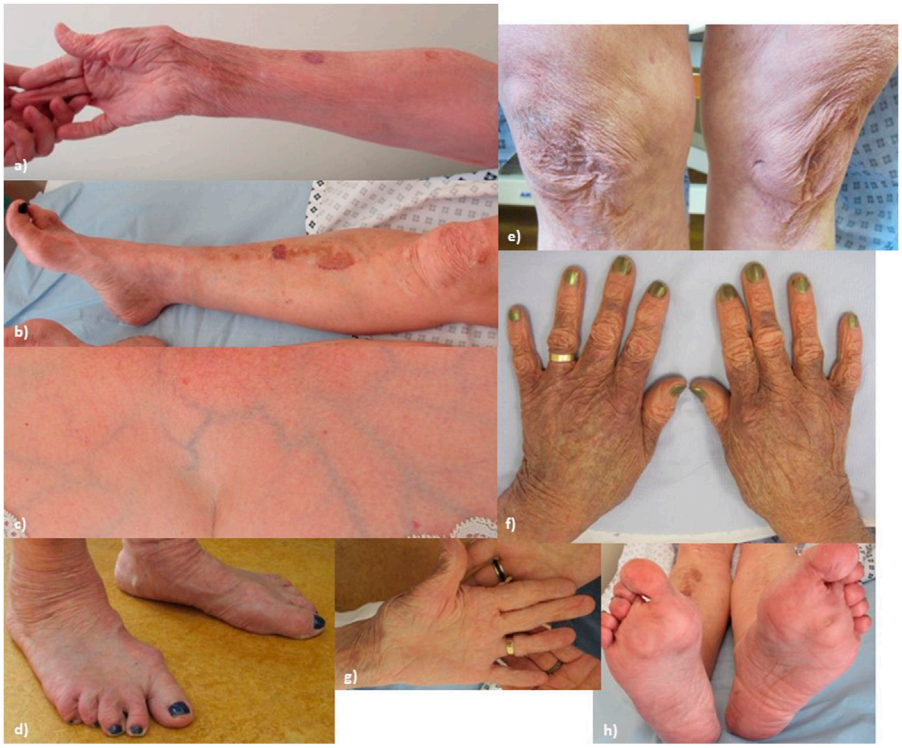

FIGURE 1
Proband 1: **(A)** increased palmar wrinkling, bruising, discolouration, and thinning of the skin over the forearms; **(B)** bruising and discolouration of shins; **(C)** skin over the chest is translucent with visible veins; **(D)** feet show pes planus with hammer toes and bilateral hallux valgus; **(E)** knees show mildly atrophic scars; **(F)** thin, discoloured skin over the dorsum of the hands; **(G)** increased palmar wrinkling and wasting of the thenar eminence; and **(H)** soles of the feet show an abnormal callus formation.

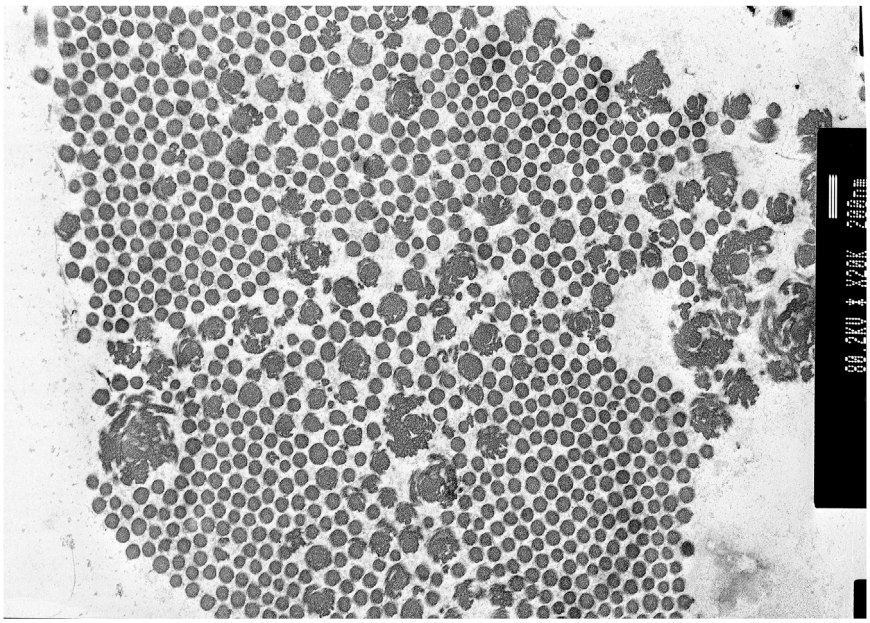

FIGURE 2
Proband 1: transmission electron microscopy (TEM) of the skin showing collagen flowers. TEM accelerating voltage at 80.2 kv and magnification ×20,000; scale bar shows 200 nm.

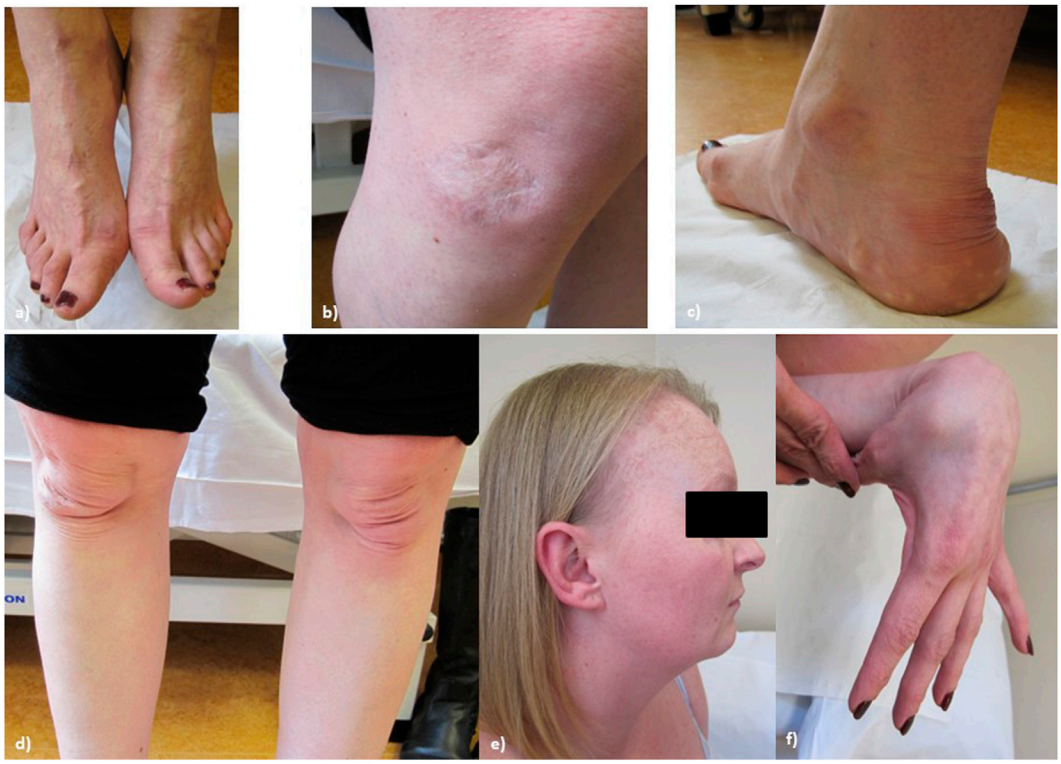

FIGURE 3
Proband 2: **(A)** bilateral hallux valgus, **(B)** atrophic scarring on the right knee, **(C)** piezogenic papules and pes planus, **(D)** bilateral patellar misalignment, **(E)** hair thinning around the frontal hairline and vertex, and **(F)** hypermobility in the hands.

United Kingdom national 100,000 Genomes Project, where likely pathogenic recessive compound heterozygous variants in *AEBP1* were identified *via* panel-based whole genome sequencing including all known genetic genes of rare EDS types, namely, c.821del; p. (Pro274fs) (PVS1, PM2, and PP4_str) and c.2248T>C p. (Trp750Arg) (PM2 and PP4_str), classified as ACMG class 4 (Richards et al., 2015; Caulfield et al., 2020).

2.3 Proband 2

At the time of writing, the proband (P2) was 41 years old. P2 was born prematurely at 35 weeks, with a low birth weight (2 kg and 25th centile) and was found to have bilateral talipes equinovarus, managed conservatively. P2 was hypermobile as a child with stretchy skin and had a left shoulder dislocation at the age of 1 year. P2 bruised easily and severely, including occasional haematomas which resolved spontaneously and required no drainage. P2's skin is not particularly fragile. P2 has had two pregnancies with vaginal deliveries, where she sustained third-degree tears (obstetric anal sphincter injury), although these healed well. In the late twenties, P2 began to develop gradually worsening lumbar and hip pain, and fatigue with poor-quality sleep. Slow growing hair and generalised thinning of the hair on the scalp were also observed in P2's 20s but were not treated. P2 has recently been diagnosed with high blood pressure, underactive thyroid, and pre-diabetes and has been prescribed clopidogrel, following a transient ischaemic attack. This was diagnosed following an episode of unilateral visual loss in the right eye, with no identified abnormalities on the echocardiogram or ultrasound of the neck. Investigative cardiac rhythm monitoring identified a short period of atrial flutter. An MRI of the head detected a small, old left temporal lacunar infarct, with no evidence of acute infarction. P2 is known to have osteopenia with reduced bone mineral density, along with some sites of osteoarthritis on further imaging of the joints.

On examination at age 34, (see Figure 3, patient's consent has been gained for the use of all clinical photographs), P2 was observed to have no skeletal abnormalities. Earlobes were notched bilaterally. P2 had bilateral pes planus, with prominent piezogenic papules over both heels. The swas hyperextensible with thinning over the chest and papyraceous scarring over the right knee. Multiple subcutaneous spheroids were observed. Follicular keratosis of the skin of the neck and axillae was also observed. On examination, P2 had a single papyraceous scar on the knee, thin skin, and hair thinning over the scalp. There was generalised hypermobility (Beighton score 9/9) plus distal hypermobility of the small joints. P2's hair was observed to be generally thin on the scalp; however, body hair was retained.

2.4 Investigations

Genetic testing at the age of 36 for *COL1A1, COL3A1, COL5A1,* and *COL5A2* including MLPA showed no abnormalities. Transmission electron microscopy of skin biopsy taken from the

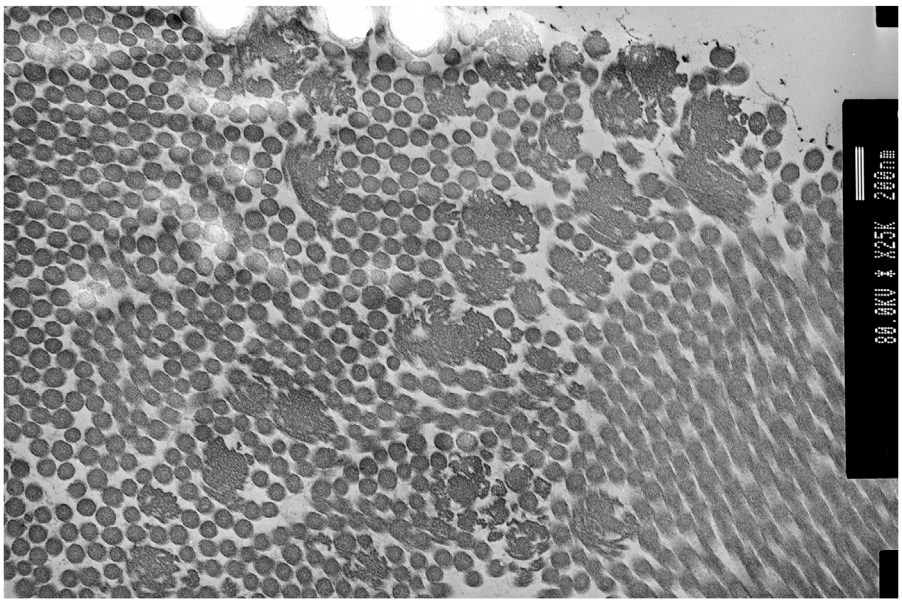

FIGURE 4
Proband 2: transmission electron microscopy (TEM) of the skin showing collagen flowers. TEM accelerating voltage at 80.2 kv and magnification ×20,000; scale bar shows 200 nm.

inner, upper arm showed clumps of collagen fibres with large collagen flowers in the papillary dermis, with normal elastic fibres (see Figure 4). At the age of 38, P2 consented to participate in the 100K project (Caulfield et al., 2020); however, sequencing from the proband's sample unfortunately failed. As such, sequencing of the United Kingdom EDS next-generation sequencing gene panel was arranged, which included *ADAMTS2, AEBP1, ALDH18A1, ATP6V0A2, ATP6V1A, ATP7A, B3GALT6, B4GALT7, BGN, C1R, C1S, CBS, CHST14, COL12A1, COL1A1, COL1A2, COL3A1, COL5A1, COL5A2, COL6A1, COL6A2, COL6A3, DSE, EFEMP2, ELN, FBLN5, FBN1, FBN2, FKBP14, GORAB, LOX, LTBP4, PLOD1, PRDM5, PYCR1, RIN2, ROBO3, SKI, SLC39A13, SMAD2, SMAD3, TGFB2, TGFB3, TGFBR1, TGFBR2, TNXB,* and *ZNF469*. Recessive variants were identified in *AEBP1* (NM_001129.4) c.1012G>T; p. (Glu338*) (PM2, PVS1, and PM3_sup) and c.1930C>T, p. (Arg644*) (PM2, PVS1, and PM3_sup), classified as ACMG class 5 (Richards et al., 2015).

3 Discussion

Recently, clEDS has been stratified into two types (1 and 2), according to the underlying genetic cause (recessive deleterious variants in *TNXB* or *AEBP1*). ClEDS type 1 was originally defined to differentiate classical EDS (cEDS), which is associated with atrophic scarring, from clEDS where scarring tends to be normal. Although there are some clinical similarities between the two clEDS types, including joint hypermobility, easy bruising, hyperextensible skin, and foot abnormalities, clEDS type 2 is reported to have additional features, including atrophic scarring and early-onset osteopenia (Malfait et al., 2020). The two individuals presented here share similar clinical features to each other, including joint hypermobility, fatigue, severe and easy bruising, hyperextensible skin with mild atrophic scarring to normal scarring, and generalised hair thinning over the scalp. Both individuals have collagen flowers on TEM, which has previously been observed in this cohort of patients (Blackburn et al., 2018).

ClEDS type 2 appears to be rare, with only nine reported individuals (Alazami et al., 2016; Blackburn et al., 2018; Hebebrand et al., 2019; Ritelli et al., 2019; Syx et al., 2019), and 11 (six females and five males), including the two cases presented here, with the mean age being 38 (range 12–65) (see table 1). There are shared features with other previously reported individuals, particularly hypermobility (11/11), skin hyperextensibility (11/11), atrophic scarring (reported in 9/11), and easy bruising (10/11) (Blackburn et al., 2018; Hebebrand et al., 2019; Ritelli et al., 2019). Cardiovascular disease has been reported as an aortic root aneurysm, requiring surgical intervention in one (1/11) person at age 36, without known cardiovascular risk factors. This individual also had a bowel rupture at a young age and suffered with significant scarring and incisional hernias (Blackburn et al., 2018). Other cardiovascular complications include mitral valve prolapse (4/11) that was discovered at ages 33, 35, 39, and 58, and peripheral arterial disease (1/11) diagnosed at age 53 (Blackburn et al., 2018; Ritelli et al., 2019). In P1, the eldest patient reported, a chronic right vertebral artery dissection, mild dilatation of the splenic artery, aberrant subclavian artery, and tortuous iliac arteries were observed at age 63 (Ritelli et al., 2019) (Hebebrand et al., 2019; Syx et al., 2019) (Blackburn et al., 2018). Osteopenia was identified in 6/11 patients including proband 2 (aged 12, 24, 33, 35, 53, and 41 years at the time of reporting) from this paper, three of whom had had fractures (Blackburn et al., 2018; Ritelli et al., 2019).

TABLE 1 Summary table of currently reported cases (Alazami et al., 2016; Blackburn et al., 2018; Hebebrand et al., 2019; Ritelli et al., 2019; Syx et al., 2019); F: female; M: male.

Paper	Alazami	Alazami	Blackburn	Blackburn	Hebebrand	Hebebrand	Ritelli	Syx	Syx	This paper	This paper
Case number	Family 1 IV:4	Family 1 IV:6	A-II:1	B-II:1	D-II:1	D-II:2	P1	P1	P2	P1	P2
Age in the report	12	24	35	33	39	38	53	58	21	65	41
Gender	F	M	M	M	F	M	F	M	F	F	F
AEBP1 variant 1	c. [1630 + 1G>A]	c. [1630 + 1G>A]	c. [1470del]	c. [1320 1326del];	c. [917dup]	c. [917dup]	c. [1925T>C]	c. [362dupA]	c. [443dupA]	c. [821del]	c.1012G>T;
	p. (Val537Leufs*31)	p. (Val537Leufs*31)	p. (Asn490_Met495delins (40))	p. (1320_1326del)	p. (Tyr306*)	p. (Tyr306*)	p. (Leu642Pro)	p. (Glu122Glyfs*16)	p. (Ala149Glyfs*57)	p. (Pro274Leufs*18)	p. (Glu338*)
AEBP1 variant 2	c. [1630 + 1G>A]	c. [1630 + 1G>A]	c. [1743C>A]	c. [1320 1326del];	c. [917dup]	c. [917dup]	c. [1925T>C];	c. [362dupA]	c. [1149 1150+2del]	c. [2248T>C]	c. [1930C>T]
	p. (Val537Leufs*31)	p. (Val537Leufs*31)	p. (Cys581*)	p. (1320_1326del)	p. (Tyr306*)	p. (Tyr306*)	p. (Leu642Pro)	p. (Glu122Glyfs*16)	p. loss of donor splice site of exon 9	p. (Trp750Arg)	p. (Arg644*)
Skin hyperextensibility	+	+	+	+	+	+	+	+	+	+	+
Scarring	Atrophic, keloid, and hyperpigmentation	Unknown	Atrophic	Atrophic and hyperpigmentation	+	+	Atrophic	Atrophic	No scarring	Atrophic	Atrophic
Easy bruising	+	Unknown	+	+	+	+	+	+	+	+	+
Joint hypermobility	+	+	+	+	+	+	+	+	+	+	+
Beighton score	8/9	Unknown	8/9	8/9	6/9	2/9	5/9	Unknown	9/9	3/9	9/9
Joint dislocations	+	Unknown	+	+	+	+	+	+	+	+	+
Osteopenia	+	+	+	+	Unknown	Unknown	+	Unknown	-	-	+
Mitral valve prolapse	-	-	+	+	+	-	-	+	-	-	-
Aortic dilatation	-	-	-	+	-	-	-	-	-	+	-
Hair thinning	Unknown	Unknown	Unknown	Unknown	Alopecia	Unknown	Alopecia	Thin, frizzled hair with partial alopecia	Thinning of hair	Hair loss on the scalp with reduced body hair	Thinning of hair
Other				Aortic root aneurysm and bowel rupture			Peripheral vascular disease			Vertebral artery dissection	

10.3389/fgene.2023.1148224

3.1 *AEBP1*

The *AEBP1* gene encodes two protein isoforms, AEBP1 and ACLP (Majdalawieh et al., 2020). AEBP1 is a transcriptional repressor of anti-inflammatory and apoptotic genes in the nucleus and can also alter cellular signalling *via* a protein–protein interaction in the cytosol (Majdalawieh et al., 2020). However, recessive *AEBP1* variants, causative of clEDS type 2, result in the disruption of ACLP (Blackburn et al., 2018; Vishwanath et al., 2020). The ACLP protein is extracellularly secreted and associated with the ECM; it is particularly expressed in the dermis, lung basement membrane, medial layer of blood vessels, and the periosteum (Blackburn et al., 2018). Post embryogenesis, ACLP has been found to be expressed during wound healing and after vessel injury (Vishwanath et al., 2020). ACLP binds with collagens in the ECM and has been found to reduce the collagen fibre diameter and increase toughness (Vishwanath et al., 2020). ACLP is also involved in intracellular signalling *via* the TGFβ pathway (Tumelty et al., 2014) and is involved in WNT/β-catenin pathway signalling through WNT3A (Teratani et al., 2018).

3.2 *AEBP1*-related classical-like EDS and hair loss

Hair loss was reported in 6/11 individuals (five females and one male), only one of which was documented to have a formal diagnosis of androgenetic alopecia (Ritelli et al., 2019), while other individuals were described as having thinning of hair, male pattern hair loss, or unspecified alopecia (Hebebrand et al., 2019; Syx et al., 2019). In other reports, hair loss is not specifically mentioned and may have been presented as a feature and not reported on. One individual reported impaired temperature sensation, but none reported reduced sweating (Blackburn et al., 2018).

Intriguingly, 6/11 individuals with *AEBP1*-related classical-like EDS experienced hair thinning and loss resembling androgenetic alopecia. So far, hair loss has not been reported in other EDS types as a typical clinical feature; however, it has been reported to be occurring inconsistently in some women with vascular EDS (Byers et al., 2017). Androgenetic alopecia, a progressive type of hair loss which affects men and women, is characterised by gradual thinning of the hair particularly over the frontal hairline, temples, and vertex, which can progress to complete hair loss over the scalp (Lolli et al., 2017). The mechanism behind these changes is not clearly understood, but there is a clear link with increased follicular sensitivity to androgens (Lolli et al., 2017). ECM changes in androgenetic alopecia have been observed but are not fully understood and include the altered deposition of elastin fibres, changes to the follicle sheath, and disruption of the basal lamina (Rushton et al., 2021). Some studies have suggested that the WNT/β-catenin pathway is the main pathway involved in the progression of androgenetic alopecia, given that androgen receptors interact with β-catenin in an androgen-dependent manner (Chesire & Isaacs, 2002; Lolli et al., 2017; Doolan et al., 2021) These findings suggest that androgens deregulate normal hair follicle differentiation *via* inhibition of the WNT pathway, which has been found to maintain the hair follicle (Kishimoto et al., 2000; Leirós et al., 2012; Lolli et al., 2017).

In individuals with pathogenic *AEBP1* variants, it is possible that WNT signalling is disrupted, resulting in this specific phenotype with androgenetic alopecia. However, given the rarity of *AEBP1*-related clEDS, there are currently no published data to support this theory.

3.3 Management recommendations

There are currently no management recommendations for type 2 clEDS published in the literature. Generalised tissue fragility, including vascular fragility, has been reported in several rare EDS types, including type 1 clEDS and vEDS, where vascular fragility is a major clinical feature (Malfait et al., 2017; van Dijk et al., 2022). Although there is a lack of natural history data on individuals with pathogenic *AEBP1* variants, there are reports of vascular complications in a high number of reported individuals and there is evidence that ACLP is a component of the arterial tunica media (Blackburn et al., 2018). This group may therefore be at risk of cardiovascular events including arterial dissections, as observed in proband 1 of this paper. We would, therefore, recommend that individuals with clEDS type 2 undergo cardiovascular investigation at diagnosis and have ongoing surveillance depending on age, symptoms, results of initial cardiovascular investigations, and considering surveillances in other rare EDS types until data on more individuals with this diagnosis become available.

As 6/11 patients had osteopenia, three of whom sustained fractures, a DEXA scan and bone markers for osteoporosis in blood and/or urine during diagnosis may be advisable in order to initiate appropriate management when necessary.

Hair loss can carry a significant psychological burden (Hunt & McHale, 2005), and patients who are experiencing distress must be referred for specialist support and consideration of management options. Both individuals reported here have been referred for evaluation by a specialist and consideration of management options.

4 Summary

This report demonstrates and expands the phenotypic spectrum of bi-allelic pathogenic *AEBP1* variants, resulting in clEDS type 2. ClEDS type 2 is an important differential in patients with joint hypermobility, skin hyperextensibility, easy bruising, hair loss, and osteopenia. Hair loss appears to be an important clinical feature in this EDS type that has not been reported in the literature as a consistent clinical feature in other types of EDS. We have made recommendations based on the current literature; however, there are currently no consensus guidelines on management.

Data availability statement

The datasets for this article are not publicly available due to concerns regarding participant/patient anonymity. Requests to access the datasets should be directed to the corresponding author.

Ethics statement

Written informed consent was obtained from the individual(s) for the publication of any potentially identifiable images or data included in this article.

Author contributions

CA: first authorship, data collection, and manuscript drafting. NG: patient information collection and manuscript supervision. FS:

last authorship, patient information collection, manuscript supervision, and research initiative.

Funding

We have open access funding for publication of this paper (Imperial College London, PO number 4550140).

Acknowledgments

The authors would like to thank the patients for taking part in this research and Professor Ferguson for the use of the transmission electron microscopy images.

Conflict of interest

The authors declare that the research was conducted in the absence of any commercial or financial relationships that could be construed as a potential conflict of interest.

Publisher's note

All claims expressed in this article are solely those of the authors and do not necessarily represent those of their affiliated organizations, or those of the publisher, the editors, and the reviewers. Any product that may be evaluated in this article, or claim that may be made by its manufacturer, is not guaranteed or endorsed by the publisher.

References

Alazami, A. M., Al-Qattan, S. M., Faqeih, E., Alhashem, A., Alshammari, M., Alzahrani, F., et al. (2016). Expanding the clinical and genetic heterogeneity of hereditary disorders of connective tissue. *Hum. Genet.* 135 (5), 525–540. doi:10.1007/s00439-016-1660-z

Blackburn, P. R., Xu, Z., Tumelty, K. E., Zhao, R. W., Monis, W. J., Harris, K. G., et al. (2018). Bi-Allelic alterations in AEBP1 lead to defective collagen assembly and connective tissue structure resulting in a variant of ehlers-danlos syndrome. *Am. J. Hum. Genet.* 102, 696–705. doi:10.1016/j.ajhg.2018.02.018

Byers, P. H., Belmont, J., Black, J., de Backer, J., Frank, M., Jeunemaitre, X., et al. (2017). Diagnosis, natural history, and management in vascular Ehlers-Danlos syndrome. *Am. J. Med. Genet. Part C Seminars Med. Genet.* 175 (1), 40–47. doi:10.1002/ajmg.c.31553

Caulfield, M., Davies, J., Dennys, M., Elbahy, L., Fowler, T., Hill, S., et al. (2020)., 1. *The national genomics research library v5*. doi:10.6084/m9.figshare.4530893.v5.1

Chesire, D. R., and Isaacs, W. B. (2002). Ligand-dependent inhibition of β-catenin/TCF signaling by androgen receptor. *Oncogene* 21 (55), 8453–8469. doi:10.1038/sj.onc.1206049

Doolan, B. J., Onoufriadis, A., Kantaputra, P., and McGrath, J. A. (2021). WNT10A, dermatology and dentistry. *Br. J. Dermatology* 185, 1105–1111. bjd. doi:10.1111/bjd.20601

Hebebrand, M., Vasileiou, G., Krumbiegel, M., Kraus, C., Uebe, S., Ekici, A. B., et al. (2019). A biallelic truncating AEBP1 variant causes connective tissue disorder in two siblings. *Am. J. Med. Genet. Part A* 179 (1), 50–56. doi:10.1002/ajmg.a.60679

Hunt, N., and McHale, S. (2005). The psychological impact of alopecia. *BMJ* 331 (7522), 951–953. doi:10.1136/bmj.331.7522.951

Kishimoto, J., Burgeson, R. E., and Morgan, B. A. (2000). Wnt signaling maintains the hair-inducing activity of the dermal papilla. *Genes and Dev.* 14 (10), 1181–1185. doi:10.1101/gad.14.10.1181

Leirós, G. J., Attorresi, A. I., and Balañá, M. E. (2012). Hair follicle stem cell differentiation is inhibited through cross-talk between Wnt/β-catenin and androgen signalling in dermal papilla cells from patients with androgenetic alopecia. *Br. J. Dermatology* 166 (5), 1035–1042. doi:10.1111/j.1365-2133.2012.10856.x

Lolli, F., Pallotti, F., Rossi, A., Fortuna, M. C., Caro, G., Lenzi, A., et al. (2017). Androgenetic alopecia: A review. *Endocrine* 57 (1), 9–17. doi:10.1007/s12020-017-1280-y

Majdalawieh, A. F., Massri, M., and Ro, H. S. (2020). AEBP1 is a novel oncogene: Mechanisms of action and signaling pathways. *J. Oncol.* 2020, 8097872–8097892. doi:10.1155/2020/8097872

Malfait, F., Castori, M., Francomano, C. A., Giunta, C., Kosho, T., and Byers, P. H. (2020). The ehlers–danlos syndromes. *Nat. Rev. Dis. Prim.* 6 (1), 64. doi:10.1038/s41572-020-0194-9

Malfait, F., Francomano, C., Byers, P., Belmont, J., Berglund, B., Black, J., et al. (2017). The 2017 international classification of the Ehlers–Danlos syndromes. *Am. J. Med. Genet. Part C Seminars Med. Genet.* 175, 8–26. doi:10.1002/ajmg.c.31552

Richards, S., Aziz, N., Bale, S., Bick, D., Das, S., Gastier-Foster, J., et al. (2015). Standards and guidelines for the interpretation of sequence variants: A joint consensus recommendation of the American College of medical genetics and genomics and the association for molecular pathology. *Genet. Med.* 17, 405–424. doi:10.1038/gim.2015.30

Ritelli, M., Cinquina, V., Venturini, M., Pezzaioli, L., Formenti, A. M., Chiarelli, N., et al. (2019). Expanding the clinical and mutational spectrum of recessive AEBP1-related classical-like Ehlers-Danlos syndrome. *Genes* 10 (2), 135. doi:10.3390/genes10020135

Rushton, D. H., Westgate, G. E., and van Neste, D. J. (2021). Following historical "tracks" of hair follicle miniaturisation in patterned hair loss: Are elastin bodies the forgotten aetiology? *Exp. Dermatol.* 31, 102–109. exd. doi:10.1111/exd.14393

Syx, D., de Wandele, I., Symoens, S., de Rycke, R., Hougrand, O., Voermans, N., et al. (2019). Bi-Allelic aebp1 mutations in two patients with ehlers-danlos syndrome. *Hum. Mol. Genet.* 28 (11), 1853–1864. doi:10.1093/hmg/ddz024

Teratani, T., Tomita, K., Suzuki, T., Furuhashi, H., Irie, R., Nishikawa, M., et al. (2018). Aortic carboxypeptidase–like protein, a WNT ligand, exacerbates nonalcoholic steatohepatitis. *J. Clin. Investigation* 128 (4), 1581–1596. doi:10.1172/JCI92863

Tumelty, K. E., Smith, B. D., Nugent, M. A., and Layne, M. D. (2014). Aortic carboxypeptidase-like protein (ACLP) enhances lung myofibroblast differentiation through transforming growth factor β receptor-dependent and -independent pathways. *J. Biol. Chem.* 289 (5), 2526–2536. doi:10.1074/jbc.M113.502617

van Dijk, F., Ghali, N., Demirdas, S., and Baker, D. (2022). *TNXB-related classical-like ehlers-danlos Syndrome*. GeneReviews® [Internet]. Seattle (WA).)

Vishwanath, N., Monis, W. J., Hoffmann, G. A., Ramachandran, B., DiGiacomo, V., Wong, J. Y., et al. (2020). Mechanisms of aortic carboxypeptidase-like protein secretion and identification of an intracellularly retained variant associated with Ehlers–Danlos syndrome. *J. Biol. Chem.* 295 (28), 9725–9735. doi:10.1074/jbc.RA120.013902

frontiers | Frontiers in Genetics

TYPE Case Report
PUBLISHED 05 May 2023
DOI 10.3389/fgene.2023.1102101

OPEN ACCESS

EDITED BY
Dimitra Kiritsi,
University of Freiburg Medical Center, Germany

REVIEWED BY
Filippo Camerota,
Sapienza University of Rome, Italy
Alexander Nyström,
University of Freiburg Medical Center, Germany
Antonella Polimeni,
Sapienza University of Rome, Italy

*CORRESPONDENCE
Tomomi Yamaguchi,
t_yamaguchi@shinshu-u.ac.jp
Tomoki Kosho,
ktomoki@shinshu-u.ac.jp

RECEIVED 18 November 2022
ACCEPTED 11 April 2023
PUBLISHED 05 May 2023

CITATION
Yamaguchi T, Hayashi S, Nagai S, Uchiyama A, Motegi S-I, Fujikawa T, Takiguchi Y and Kosho T (2023), Case report: further delineation of *AEBP1*-related Ehlers–Danlos Syndrome (classical-like EDS type 2) in an additional patient and comprehensive clinical and molecular review of the literature. *Front. Genet.* 14:1102101. doi: 10.3389/fgene.2023.1102101

Case report: further delineation of *AEBP1*-related Ehlers–Danlos Syndrome (classical-like EDS type 2) in an additional patient and comprehensive clinical and molecular review of the literature

Tomomi Yamaguchi[1,2,3]*, Shujiro Hayashi[4], So Nagai[1,5], Akihiko Uchiyama[6], Sei-Ichiro Motegi[6], Tomomi Fujikawa[3], Yuri Takiguchi[3] and Tomoki Kosho[1,2,3,7]*

[1]Center for Medical Genetics, Shinshu University Hospital, Matsumoto, Japan, [2]Department of Medical Genetics, Shinshu University School of Medicine, Matsumoto, Japan, [3]Division of Clinical Sequencing, Shinshu University School of Medicine, Matsumoto, Japan, [4]Department of Dermatology, Dokkyo Medical University, Mibu, Japan, [5]Problem-Solving Oriented Training Program for Advanced Medical Personnel: NGSD (Next-Generation Super Doctor) Project, Matsumoto, Japan, [6]Department of Dermatology, Gunma University Graduate School of Medicine, Maebashi, Japan, [7]Research Center for Supports to Advanced Science, Shinshu University, Matsumoto, Japan

The Ehlers–Danlos Syndromes (EDS), a group of hereditary connective tissue disorders, were classified into 13 subtypes in the 2017 International Classification. Recently, a new subtype of EDS called classical-like EDS type 2 (clEDS2), which is caused by biallelic variants in the adipocyte enhancer binding protein 1 (*AEBP1*) gene, was identified. We describe the 11th patient (9th family) with clEDS2, who was complicated by a critical vascular event (superior mesenteric artery aneurysm and rupture). A next-generation sequencing panel-based analysis revealed compound heterozygous variants in *AEBP1*: NM_001129.5:c.[2296G>T]; [2383dup], p.[(Glu766*)]; [(Glu795Glyfs*3)]. Light microscopic analyses showed increased interfibrillar spaces in the reticular dermis, a disorganized arrangement of collagen fibers, and decreased collagen content. An electron microscopic analysis showed the presence of collagen fibrils with irregular contours (flower-like appearance) and small collagen fibrils. A biochemical analysis showed reduced secretion of type I and type III procollagen. Clinical and molecular features of the current patient and all previously reported patients were reviewed comprehensively. Manifestations noted in most cases (>80%) included skin features (hyperextensibility, atrophic scars, easy bruising, excessive skin/skin folding, delayed wound healing, translucency, piezogenic papules), skeletal features (generalized joint hypermobility, dislocations/subluxations, pes planus), dental abnormalities, and neuromuscular abnormalities. Critical complications, each occurring in a single case, included superior mesenteric artery multiple aneurysm and rupture, aortic root dilation requiring surgery, and bowel rupture. Most *AEBP1* variants were predicted or experimentally confirmed to lead to nonsense-mediated mRNA decay, whereas one variant resulted in a protein that was retained intracellularly and not secreted. Clinical, molecular, pathological, and biochemical features of the current patient, as well as a review

of all previously reported patients, suggest the importance of the aortic carboxypeptidase-like protein encoded by *AEBP1* in collagen fibrillogenesis.

KEYWORDS

Ehlers-Danlos Syndrome, classical-like EDS type 2 (clEDS2), adipocyte enhancer binding protein 1 (*AEBP1*), aortic carboxypeptidase-like protein (ACLP), autosomal recessive, connective tissue disorders

Introduction

The Ehlers–Danlos Syndromes (EDS) are a group of hereditary connective tissue disorders (HCTDs) characterized by skin hyperextensibility, joint hypermobility, and tissue fragility. They were classified into 13 subtypes based on symptoms and causative genes in the 2017 International Classification (Malfait et al., 2017). In 2018, Blackburn et al. (2018) identified biallelic variants in the adipocyte enhancer binding protein 1 (*AEBP1*) gene in patients displaying EDS-like features that were considered to represent a new subtype of EDS and were tentatively named classical-like type 2 (clEDS2; MIM #618000) (Malfait et al., 2020). To date, 10 patients from eight families have been described (Alazami et al., 2016; Blackburn et al., 2018; Hebebrand et al., 2019; Ritelli et al., 2019; Syx et al., 2019; Maddirevula et al., 2020; Vishwanath et al., 2020; Di Giosaffatte et al., 2022).

We report here an additional patient with clEDS2 who had novel variants in *AEBP1* and was complicated by a critical vascular event.

Case description and molecular, pathological, and biochemical analysis

The patient, a 45-year-old Japanese woman, was the second child of non-consanguineous parents. No skin hyperextensibility, fragility, or joint hypermobility were noted in her mother, elder sister, or two daughters. She was a preterm and low-birth-weight (1,980 g) infant. The patient had bilateral congenital hip dislocation for which she underwent fixation with a brace, experienced repetitive episodes of skin lacerations and subcutaneous hemorrhage after minor trauma, and had marked joint laxity, with repetitive sprains caused by unstable ankle joints. In her early 20 s, she was suspected to have EDS. Intractable hair loss has been her major physical concern since around that age. She also had spinal disc herniation. At the age of 36 years, she developed massive intraabdominal hemorrhages caused by rupture of the superior mesenteric artery, which were associated with multiple aneurysms and were treated with catheter embolization. Thin translucent skin was noted (Figure 1A-a).

When the patient was referred to us at the age of 45 years, she exhibited the following characteristics: hair with a kinky texture and generalized thinning; a high palate and multiple dental caries; hyperextensible and translucent skin (Figure 1A-a, b); skin striae in the lower extremities, with atrophic scars (Figure 1A-c); soft soles; an umbilical hernia (Figure 1A-d); pes planus (Figure 1A-e); and generalized joint hypermobility (Beighton score 8/9) (Figure 1A-f). Radiological examination showed no spinal deformities. There had been no episodes of dislocations or musculoskeletal pain. No aortic root dilatation or valve abnormalities were detected on echocardiography. She had high myopia, but no hearing impairment.

Genomic DNA was extracted from peripheral blood using a QIAamp DNA Blood Mini Kit on a QIAcube (Qiagen, Valencia, CA, United States). A next-generation sequencing (NGS) panel-based analysis was performed on an Ion Torrent system (Ion Chef and Ion GeneStudio S5, Thermo Fisher Scientific, Waltham, MA, United States) using an Ion AmpliSeq custom panel for 52 genes associated with EDS and other HCTDs (Supplementary Table S1). Detected variants were annotated by SnpEff and SnpSift (https://snpeff.sourceforge.net/) using the processed vcf file of the Genome Aggregation Database (gnomAD) v2.1.1 (https://gnomad.broadinstitute.org/downloads), ToMMo 8.3KJPN Genotype Frequency Panel (v20200831) (https://jmorp.megabank.tohoku.ac.jp/202008/downloads#variant) (Tadaka et al., 2019), ClinVar (ftp://ftp.ncbi.nlm.nih.gov/pub/clinvar/vcf_GRCh37/clinvar_20220328), dbNSFP3.4c and dbscSNV1.1 (https://sites.google.com/site/jpopgen/dbNSFP). Detected variants were evaluated in accordance with the 2015 American College of Medical Genetics and Genomics/Association for Molecular Pathology (ACMG/AMP) guidelines (Richards et al., 2015) and the ClinGen Sequence Variant Interpretation Working Group recommendations (SVI recommendations). Integrative Genomics Viewer (IGV) was used to visualize read alignments (Broad Institute, Cambridge, MA, United States). The NGS panel-based analysis revealed a nonsense variant c.2296G>T,p.(Glu766*) and a frameshift variant c.2383dup,p.(Glu795Glyfs*3) in *AEBP1* (NM_001129.5), which were confirmed by Sanger sequencing (Figure 1B). The IGV revealed that the two variants were observed *in trans* (Figure 1C). The nonsense variant was registered in 8.3KJPN (1/16758, MAF = 0.0001, no homozygote) and the frameshift variant was registered in 8.3KJPN (1/16754, MAF = 0.0001, no homozygote). Both variants were classified as pathogenic (PVS1, PM2_Supporting, and PM3), in accordance with the 2015 ACMG/AMP guidelines and SVI recommendations.

Hematoxylin and eosin staining of a skin specimen obtained by a biopsy performed at the age of 36 years showed increased spaces between collagen fibers and disorganized orientations of these fibers in the lower and middle layer of the dermis (Figure 1D-b) compared with control (Figure 1D-a). Masson's trichrome staining revealed decreased collagen fibers (Figure 1D-d) compared with control (Figure 1D-c). Elastica van Gieson staining showed prominent elastic fibers due to the decreased numbers of collagen fibers (Figure 1D-f) compared with control (Figure 1D-e). An ultrastructural analysis using transmission electron microscopy of the skin specimen revealed the presence of collagen fibrils with irregular contours (flower-like appearance) and small size under the cross-sectional view (Figure 1E). Measurement of procollagen production from cultured skin fibroblasts was performed as described previously (Shimaoka et al., 2010). Briefly, dermal fibroblasts from the patient were incubated with ^{3}H-proline for 24 h. Labeled proteins secreted into the culture medium were

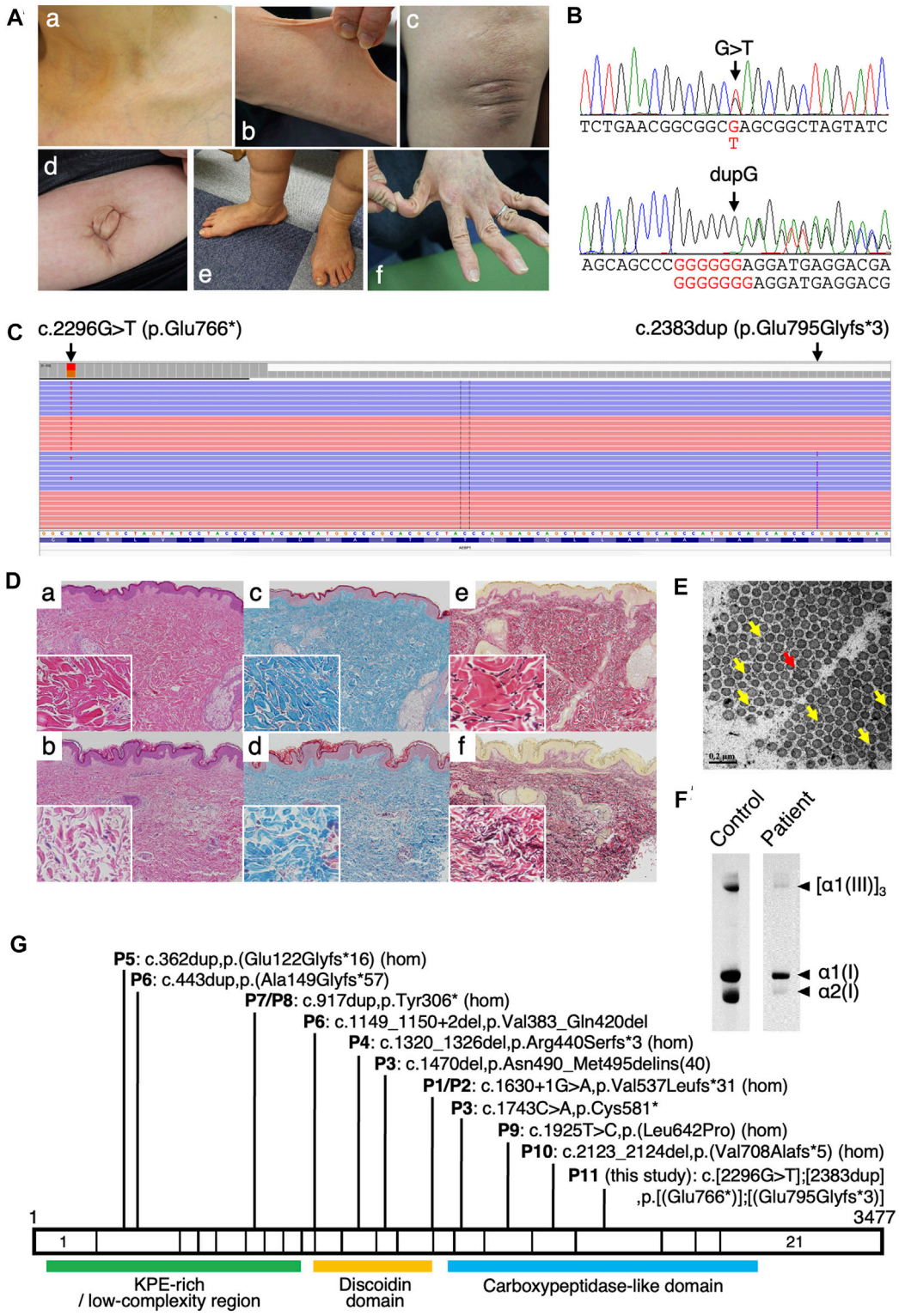

FIGURE 1
Clinical, molecular, histological, ultrastructural, and biochemical findings of the 11th patient identified with classical-like Ehlers–Danlos syndrome type 2 (clEDS2). **(A)** Clinical photographs of the current patient (Patient 11). Translucent skin on the upper chest at the age of 36 years (a). At age 45, the patient exhibited hyperextensible skin (b); a small atrophic scar (black arrow) and mild keloid formation (arrowhead) (c); an umbilical hernia (d); pes planus and edematous lower legs (e); and acrogeria-like skin on the hands, with hypermobile phalangeal joints (f). **(B)** Sanger sequencing electropherogram of variants in the adipocyte enhancer binding protein 1 gene (*AEBP1*). **(C)** Integrative Genomics Viewer visualization of the variants. The nonsense variant c.2296G>T and the frameshift variant c.2383dup are observed *in trans*. **(D)** Light microscopic images of a biopsy skin specimen (age 36) at two magnifications: low- (×20) and higher-power (×400, inset) magnifications. Hematoxylin and eosin staining showing increased spacing and disorganization of collagen fibers (b) compared with an age- and sex-matched control (a), Masson's trichrome staining showing decreased collagen
(*Continued*)

FIGURE 1 (Continued)
fibers (blue) (d) compared with control (c), and Elastica van Gieson staining showing collagen fibers (red) and elastic fibers (black) (f) compared with control (e). **(E)** Transmission electron microscopic images of the dermal collagen fibrils, showing irregular contours (flower-like appearance, red arrows) and small-sized fibrils (yellow arrows). **(F)** Type I and type III procollagen produced by cultured skin fibroblasts obtained from the patient and an age- and sex-matched control. **(G)** Schematic representation of the distribution of *AEBP1* variants in 11 patients from nine families with clEDS2 illustrated on *AEBP1* mRNA; "1" and "3477" indicate the first and the last nucleotide positions of the coding region of the mRNA, respectively. Domains of the aortic carboxypeptidase-like protein (ACLP) are shown at the corresponding exons. hom: homozygote; P1–P11: Patients 1–11; KPE-rich: lysine, proline and glutamic acid-rich.

digested with pepsin and analyzed by sodium dodecyl sulfate-polyacrylamide gel electrophoresis/fluorography. Amounts of type I and type III procollagen were both reduced compared with an age- and sex-matched individual who served as a control (Figure 1F).

Discussion

We have identified and described a 11th patient (9th family) with clEDS2, who was found to have novel compound heterozygous pathogenic variants in *AEBP1*. Detailed and comprehensive clinical and molecular features of all previously reported patients and the current patient are shown in Table 1.

Dental abnormalities, skin hyperextensibility, atrophic scars, easy bruising, and neuromuscular abnormalities were observed in all patients whose data were available. Excessive skin/skin folding (90.9%), delayed wound healing (90.9%) generalized joint hypermobility (90.9%), dislocations/(sub)luxations (90.9%), pes planus (90.9%), translucent skin (87.5%), piezogenic papules (80.0%), hernia (77.8%), osteopenia (71.4%), spine deformities (60.0%), prematurely aged appearance (57.1%), hallux valgus (54.5%), and hammertoes (54.5%) were observed in more than half of the patients whose data were available. Decreased hair described as "thinning" or "(partial) alopecia" was observed in five patients, and was a major physical concern in the current patient. The current patient developed multiple aneurysms and a rupture in the superior mesenteric artery, which was treated with catheter embolization. Cardiovascular complications reported in the previous patients included mitral valve prolapse/regurgitation, tricuspid valve regurgitation, pulmonary valve regurgitation, varicose veins, and aortic root dilation requiring surgery. A bowel rupture occurred in one patient, requiring repeated attempts to re-anastomose the bowel and colostomy. This is the first report of skin lacerations, which occurred in the current patient, whereas skin fragility was only noted in two other patients. Heterozygous individuals appear to have no relevant symptoms.

Most reported *AEBP1* variants were null variants, including nonsense, frameshift and splice site variants, predicted to lead to nonsense-mediated mRNA decay (NMD) (Table 1; Figure 1G). Some variants were experimentally confirmed to affect the gene product. In Patients 1 and 2, a homozygous splice site variant (c.1630 + 1G>A) led to activation of the cryptic 5′splice site within exon 13 and skipping of the last 22 bp of exon 13. The shift in reading frame (p.Val537Leufs*31) was predicted to lead to NMD. In Patient 3, a 1-bp deletion (c.1470del) in exon 12 in one allele led to the retention of intron 12 (p.Asn490_Met495delinsLysAlaMetArgLysTrpTrpAlaProCysProGlySerTrpLeuCysSerHisCysLeuGlyGluGlyTrpAlaLeuArgGlyAlaGlySerThrAlaLeuArgProAlaSerProGln) (Blackburn et al., 2018). Its protein was retained intracellularly and not secreted (Vishwanath et al., 2020). A non-sense variant (c.1743C>A,p.Cys581*) in the other allele in Patient 3 was predicted to lead to NMD. In Patient 4, a homozygous frameshift variant (c.1320_1326del) led to a shift in reading frame (p.Arg440Serfs*3) (Blackburn et al., 2018). No ACLP protein was detected by western blotting, suggesting NMD. In Patient 6, a 4-bp deletion (c.1149_1150+2del) in one allele led to the loss of the last 4 bp of exon 9 and skipping of exon 10, resulting in an in-frame deletion (p.Val383_Gln420del) (Syx et al., 2019). A frameshift variant (c.443dup) in the other allele in Patient 6 was predicted to lead to NMD. The mRNA expression was significantly decreased, indicating that the *AEBP1* transcript was unstable and/or prone to NMD.

In the current patient, light microscopic analyses showed increased interfibrillar spaces in the reticular dermis, a disorganized arrangement of collagen fibers and decreased collagen content, and a biochemical analysis showed reduced secretion of type I and type III procollagen. Electron microscopic analysis showed the presence of collagen fibrils with irregular contours (flower-like appearance) and small size. Blackburn et al. (2018) reported that light microscopy showed decreased collagen, while electron microscopy revealed the presence of irregular disrupted collagen fibrils. In their report, the discoidin domain, a highly conserved structural motif of ACLP, preferentially bound to collagen types I, III and V, and ACLP promoted the polymerization of type I collagen *in vitro*. Syx et al. (2019) reported electron microscopic observations that corresponded with those of Blackburn et al. (2018) and the current study, and a biochemical analysis that showed a normal electrophoretic pattern of procollagen types I, III and V. This biochemical analysis was performed on the medium of cultured skin fibroblasts to detect procollagen secreted from these fibroblasts. The discrepant results might be attributable to some functional differences between the variants reported by Syx et al. and the variants in the current patient, which could be related to the difference in the transcription status of these procollagen genes or in the secretion status of these types of procollagen. In view of all of these findings, ACLP protein is likely an important player in collagen fibrillogenesis.

In conclusion, the clinical findings and disease course in the current patient, together with the review of previously reported patients, paints a picture of the clinical similarities and variations in clEDS2. Furthermore, the biochemical and pathological findings in the current patient, in addition to the relevant findings in the previous patients, suggest the importance of ACLP in collagen fibrillogenesis. Further clinical, molecular, and pathophysiological studies are required to produce a more detailed and comprehensive delineation of this disorder.

TABLE 1 Detailed and comprehensive clinical and molecular features of all previously reported patients and the current patient.

Family no.	I		II	III	IV	V	VI		VII	VIII	IX	
Patient No.	1	2	3	4	5	6	7	8	9	10	11	
Citation(s)	Alazami et al. (2016)		Blackburn et al. (2018)		Syx et al. (2019)		Hebebrand et al. (2019)		Ritelli et al. (2019)	Di Giosaffatte et al. (2022)	This report	
	Maddirevula et al. (2020)		Vishwanath et al. (2020)									
Age at the time of report (years)	12	24	35	33	58	21	39	38	53	26	45	
Sex	Female	Male	Male	Male	Male	Female	Female	Male	Female	Male	Female	
Ethnicity	Middle Eastern	Middle Eastern	Caucasian	Caucasian	Caucasian	Caucasian	Greek	Greek	Italian	NA	Japanese	
AEBP1 variant (NM_001129.5)	c.[1630 + 1G>A]; [1630 + 1G>A]	c.[1630 + 1G>A]; [1630 + 1G>A]	c.[1470del];[1743C>A]	c.[1320_1326del]; [1320_1326del]	c.[362dup];[362dup]	c.[443dup]; [1149_1150+2del]	c.[917dup]; [917dup]	c.[917dup]; [917dup]	c.[1925T>C]; [1925T>C]	c.[2123_2124del]; [2123_2124del]	c.[2296G>T]; [2383dup]	
Protein alteration (NP_001120.3)	p.[Val537Leufs*31]; [Val537Leufs*31]	p.[Val537Leufs*31]; [Val537Leufs*31]	p.[Asn490_Met495delinsLysAlaM etArgLysTrpTrpAlaProCysP roGlySerTrpLeuCysSerHisCysLeuGlyGluGly TrpAlaLeuArgGlyAlaGlySerThrAlaLeuArgProAlaSerProGln]; [Cys581*]	p.[Arg440Serfs*3]; [Arg440Serfs*3]	p.[(Glu122Glyfs*16)]; [(Glu122Glyfs*16)]	p.[(Ala149Glyfs*57)]; [Val383_Gln420del]	p.[Tyr306*]; [Tyr306*]	p.[Tyr306*]; [Tyr306*]	p.[(Leu642Pro)]; [(Leu642Pro)]	p.[(Val708Alafs*5)]; [(Val708Alafs*5)]	p.[(Glu766*)]; [(Glu795Glyfs*3)]	
Craniofacial features	Bilateral ptosis, webbed neck, low posterior hairline, sagging cheeks, large ears, narrow/ high palate	Bilateral ptosis, webbed neck, low posterior hairline, sagging cheeks, large ears, narrow palate	–	Micrognathia	Asymmetrical face, hypertelorism, low-set and posteriorly rotated ears with attached earlobes, thin and frizzled hair, partial alopecia, webbed neck	Mild ptosis, thinning hair	Alopecia	NA	Alopecia, high palate, elongated uvula	Cleft palate, down-slanting palpebral fissures, epicanthus, deep set eyes, malar hypoplasia low set ears, micro/ retrognathia, webbed neck	Thinning and kinky hair, high palate, narrow nose	Alopecia or thinning hair 5/ 10 (50.0%)
Dental features	Abnormal dental alignment	Abnormal dental alignment	Retains a single baby tooth	NA	Bad tooth quality with severe caries	Bad tooth quality with frequent caries	NA	NA	Pyorrhea, complete dental loss at age 14	Multiple caries, periodontal disease	Multiple caries	8/8 (100%)
Cutaneous features												
Skin hyperextensibility	+	+	+	+	+	+	+	+	+	+	+	11/ 11 (100%)
Thin, translucent skin	NA	NA	NA	+	+	+	+	+	–	+	+	7/ 8 (87.5%)
Excessive skin /skin folding	+	+	+	+	+	–	+	+	+	+	+	10/ 11 (90.9%)
Delayed wound healing	+	+	+	+	+	Mild	+	+	+	–	+	10/ 11 (90.9%)
Atrophic scars	+	NA	+	+	+	+	+	+	+	+	+	10/ 10 (100%)
Easy bruising	+	NA	+	+	+	+	+	+	+	+	+	10/ 10 (100%)
Piezogenic papules	NA	NA	+	+	NA	NA	NA	NA	+	+	–	4/ 5 (80.0%)
Prematurely aged appearance	NA	NA	– (Increased acrogeria-like skin wrinkles on hands and feet)	NA	+	NA	+	+	+	–(Acrogeria-like hand appearance)	– (Acrogeria-like skin on hands)	4/ 7 (57.1%)

(Continued on following page)

10.3389/fgene.2023.1102101

TABLE 1 (*Continued*) Detailed and comprehensive clinical and molecular features of all previously reported patients and the current patient.

Family no.	I		II	III	IV	V	VI		VII	VIII	IX	
Other				Sacral dimple	Decubitus wounds on buttocks		Skin striae	Fragile skin lesions on the buttocks		Skin fragility, subcutaneous spheroids, palmar callosities	Skin lacerations after minor trauma, skin striae, velvety skin	
Skeletal features												
Generalized joint hypermobility (Beighton score)	+ (8/9)	+ (NA)	+ (8/9)	+ (8/9)	+ (NA)	+ (9/9)	+ (6/9)	− (2/9)	+ (5/9)	+ (7/9)	+ (8/9)	10/11 (90.9%)
Congenital hip dislocation	−	−	−	+	−	−	−	−	−	−	+	2/11 (18.2%)
Other dislocations	Interphalangeal/hip/knee/ankle	Hip/knee/ankle	Distal radioulnar joint	Shoulder	Elbow	−	Wrist	Clavicular/knee/ankle	Shoulder/elbow/knee/ankle	−	−	10/11 (90.9%)
Subluxations	−	−	Shoulder/hip	−	−	Temporomandibular/shoulder/elbow/thumb/hip/knee	Mandibular	−	−	+	−	
Pectus excavatum	−	NA	−	−	+	−	−	+	−	−	−	2/10 (20.0%)
Spine deformities	−	NA	−	Thoracic scoliosis with degenerative disease and facet arthrosis of spine	−	Scoliosis	Kyphoscoliosis	Kyphoscoliosis	Scoliosis (mild)	Scoliosis	−	6/10 (60.0%)
Pes planus	+	+	+	+	+	+	Mild	+	+	−	+	10/11 (90.9%)
Hallux valgus	+	+	+	+	+	−	−	−	+	−	−	6/11 (54.5%)
Hammertoes	+	+	+	+	+	−	−	−	−	+	−	6/11 (54.5%)
Osteopenia	+	+	+	+	NA	−	NA	NA	+	−	NA	5/7 (71.4%)
Other				Downsloping shoulders, severe degenerative disease requiring hip replacement	Multiple ankle distortions	Hip dysplasia, ankle sprains, drooping shoulders	Arachnodactyly, wrist and thumb signs, systemic score 8	Hindfoot deformity, arachnodactyly, wrist sign, systemic score 7	Patellar instability, gonarthrosis, rotator cuff disease, achilles tendinopathy, subacromial shoulder impingement, epitrochleitis	Short stubby fingers, hips dysmetria, absence and hypoplasia of toes	Toe/elbow joint deformity, ankle instability, sprains	
Neuromuscular features	Neonatal hypotonia	Myopathy	Delays in walking and acquisition of fine motor skills	NA	NA	Progressive decreased muscle strength, inability to walk without support	NA	NA	Neonatal severe hypotonia, delays in walking and acquisition of fine motor skills, hypotrophy of the scapular girdle	Mild perinatal hypotonia, delayed motor development, unilateral hypoplasia of right pectoralis major muscle, diastasis recti	NA	6/6 (100%)

(Continued on following page)

10.3389/fgene.2023.1102101

TABLE 1 (*Continued*) Detailed and comprehensive clinical and molecular features of all previously reported patients and the current patient.

Family no.	I		II	III	IV	V	VI		VII	VIII	IX	
Cardiovascular features	–	–	Mitral valve prolapse	Mild mitral regurgitation, bilateral stenosis of the carotids, aortic root dilation	Mild mitral valve prolapse	Vaginal hematoma after trauma, postural orthostatic tachycardia syndrome	Mitral valve prolapse, circular pericardial effusion	Varicose veins	Peripheral artery disease (intermittent claudication, peripheral cyanosis, cold skin), varicose veins	Mild regurgitation at tricuspid, pulmonary, and mitral valves, varicose veins, hematoma	Superior mesenteric artery aneurysm and rupture	
Gastrointestinal features	NA	NA	Chronic constipation	Bowel rupture	–	Gastroesophageal reflux, esophageal spasms, dysphagia, bloated feeling, abdominal cramps/ pain and episodes of constipation or diarrhea	NA	NA	–	NA	–	
Hernias	Umbilical/ventral/ inguinal hernia	NA	–	Large ventral hernia developed at surgical sites secondary to ruptured bowel	Herniation of fat in the right armpit	NA	+	–	Umbilical hernia	Inguinal hernia	Spinal disc herniation, umbilical hernia	7/ 9 (77.8%)
Urogenital features	NA	NA	Cryptorchidism	NA	NA	Urinary retention requiring catheterization, bladder cramps and urinary urgency	NA	Cryptorchidism	NA	Cryptorchidism	–	
Other features	Diabetes mellitus, cellulitis		Impaired temperature sensation, keratoconjunctivitis sicca	Elbow bursitis, hypertriglyceridemia	Spontaneous pneumothorax, myopia, tinnitus	Chronic fatigue, chronic widespread pain, mild myopia		Strabismus, astigmatism, myopia	Vocal cord nodules, subcutaneous spheroids, multiple papules with follicular prominence, chronic fatigue, myopia, astigmatism	Musculoskeletal back pain	Myopia	

AEBP1: adipocyte enhancer binding protein 1 gene; NA: not applicable; +: present; –: absent.

10.3389/fgene.2023.1102101

Data availability statement

The datasets for this article are not publicly available due to concerns regarding participant/patient anonymity. Requests to access the datasets should be directed to the corresponding authors.

Ethics statement

The studies involving human participants were reviewed and approved by the Ethics Committee of Shinshu University School of Medicine. The patients/participants provided their written informed consent to participate in this study. Written informed consent was obtained from the participant/patient(s) for the publication of this case report.

Author contributions

TY performed all molecular experiments, interpreted the data, and wrote the first draft of the manuscript. TK conceived the work, organized the data collection, interpreted the data, and wrote the clinical part of the first draft. SH conducted the histological, biochemical, and ultrastructural investigations. SN, AU, and S-IM provided clinical data. TF and YT helped to perform molecular analysis. All authors participated in revision and approval of the manuscript.

Funding

This study was supported by the following: the Grant-in-Aid for Young Scientists (19K17795) (2019–2021) (TY), from The Japan Society for the Promotion of Science, Japan; Research on Intractable Diseases (09835303, 10801776, 11948954) (2009, 2010, 2011) (TK); the Research Program on Policy of Measures for Intractable/Rare Diseases (20316866) (2020–2022) (TK); Ministry of Health, Labour and Welfare, Japan; the Program for an Integrated Database of Clinical and Genomic Information (16818213) (2016–2020) (TK); the Initiative on Rare and Undiagnosed Diseases (IRUD) (21445007) (2018–2020) (TK); and the Japan Agency for Medical Research and Development (AMED).

Acknowledgments

We are grateful to the patients and their families for their cooperation during this study. We are also thankful to Mr. Kinichi Matsuyama (Department of Pathology, Dokkyo Medical University) for their technical support on the histological, biochemical, and ultrastructural investigations. Finally, we thank Michelle Kahmeyer-Gabbe, PhD, from Edanz Group (https://en-author-services.edanzgroup.com/) for editing a draft of this manuscript.

Conflict of interest

The authors declare that the research was conducted in the absence of any commercial or financial relationships that could be construed as a potential conflict of interest.

Publisher's note

All claims expressed in this article are solely those of the authors and do not necessarily represent those of their affiliated organizations, or those of the publisher, the editors and the reviewers. Any product that may be evaluated in this article, or claim that may be made by its manufacturer, is not guaranteed or endorsed by the publisher.

Supplementary material

The Supplementary Material for this article can be found online at: https://www.frontiersin.org/articles/10.3389/fgene.2023.1102101/full#supplementary-material

References

Alazami, A. M., Al-Qattan, S. M., Faqeih, E., Alhashem, A., Alshammari, M., Alzahrani, F., et al. (2016). Expanding the clinical and genetic heterogeneity of hereditary disorders of connective tissue. *Hum. Genet.* 135, 525–540. doi:10.1007/s00439-016-1660-z

Blackburn, P. R., Xu, Z., Tumelty, K. E., Zhao, R. W., Monis, W. J., Harris, K. G., et al. (2018). Bi-allelic alterations in *AEBP1* lead to defective collagen assembly and connective tissue structure resulting in a variant of Ehlers–Danlos syndrome. *Am. J. Hum. Genet.* 102, 696–705. doi:10.1016/j.ajhg.2018.02.018

Di Giosaffatte, N., Ferraris, A., Gaudioso, F., Lodato, V., Savino, E., Celletti, C., et al. (2022). Congenital defects in a patient carrying a novel Homozygous *AEBP1* Variant: Further expansion of the phenotypic spectrum of Ehlers-Danlos syndrome classical-like type 2? *Genes (Basel)* 13, 2358. doi:10.3390/genes13122358

Hebebrand, M., Vasileiou, G., Krumbiegel, M., Kraus, C., Uebe, S., Ekici, A. B., et al. (2019). A biallelic truncating *AEBP1* variant causes connective tissue disorder in two siblings. *Am. J. Med. Genet. A* 179, 50–56. doi:10.1002/ajmg.a.60679

Maddirevula, S., Kuwahara, H., Ewida, N., Shamseldin, H. E., Patel, N., Alzahrani, F., et al. (2020). Analysis of transcript-deleterious variants in mendelian disorders: Implications for RNA-based diagnostics. *Genome Biol.* 21, 145. doi:10.1186/s13059-020-02053-9

Malfait, F., Castori, M., Francomano, C. A., Giunta, C., Kosho, T., Byers, P. H., et al. (2020). The ehlers–danlos syndromes. *Nat. Rev. Dis. Prim.* 6, 64. doi:10.1038/s41572-020-0194-9

Malfait, F., Francomano, C., Byers, P., Belmont, J., Berglund, B., Black, J., et al. (2017). The 2017 international classification of the Ehlers–Danlos syndromes. *Am. J. Med. Genet. C Semin. Med. Genet.* 175, 8–26. doi:10.1002/ajmg.c.31552

Richards, S., Aziz, N., Bale, S., Bick, D., Das, S., Gastier-Foster, J., et al. (2015). Standards and guidelines for the interpretation of sequence variants: A joint consensus recommendation of the American College of medical Genetics and Genomics and the association for molecular Pathology. *Genet. Med.* 17, 405–424. doi:10.1038/gim.2015.30

Ritelli, M., Cinquina, V., Venturini, M., Pezzaioli, L., Formenti, A. M., Maria, A., et al. (2019). Expanding the clinical and mutational spectrum of recessive *AEBP1*-related classical-like Ehlers–Danlos syndrome. *Genes (Basel)* 10, 135. doi:10.3390/genes10020135

Shimaoka, Y., Kosho, T., Wataya-Kaneda, M., Funakoshi, M., Suzuki, T., Hayashi, S., et al. (2010). Clinical and genetic features of 20 Japanese patients with vascular-type Ehlers–Danlos syndrome. *Br. J. Dermatol.* 163, 704–710. doi:10.1111/j.1365-2133.2010.09874.x

Syx, D., De Wandele, I., Symoens, S., De Rycke, R., Hougrand, O., Voermans, N., et al. (2019). Bi-allelic *AEBP1* mutations in two patients with Ehlers–Danlos syndrome. *Hum. Mol. Genet.* 28, 1853–1864. doi:10.1093/hmg/ddz024

Tadaka, S., Katsuoka, F., Ueki, M., Kojima, K., Makino, S., Saito, S., et al. (2019). 3.5KJPNv2, an allele frequency panel of 3,552 Japanese individuals including the X chromosome. *Hum. Genome Var.* 6, 28. doi:10.1038/s41439-019-0059-5

Vishwanath, N., Monis, W. J., Hoffmann, G. A., Ramachandran, B., DiGiacomo, V., Wong, J. Y., et al. (2020). Mechanisms of aortic carboxypeptidase-like protein secretion and identification of an intracellularly retained variant associated with Ehlers–Danlos syndrome. *J. Biol. Chem.* 295, 9725–9735. doi:10.1074/jbc.RA120.013902

Yamaguchi, T., Hayashi, S., Hayashi, D., Matsuyama, T., Koitabashi, N., Ogiwara, K., et al. (2022). Comprehensive genetic screening for vascular Ehlers–Danlos syndrome through an amplification-based next generation sequencing system. *Am. J. Med. Genet. A. Online ahead print* 191, 37–51. doi:10.1002/ajmg.a.62982

frontiers | Frontiers in Genetics

TYPE Original Research
PUBLISHED 31 May 2023
DOI 10.3389/fgene.2023.1136339

OPEN ACCESS

EDITED BY
Tomoki Kosho,
Shinshu University, Japan

REVIEWED BY
Anupriya Kaur,
Post Graduate Institute of Medical Education and Research (PGIMER), India
Shujiro Hayashi,
Dokkyo Medical University, Japan
Delfien Syx,
Ghent University, Belgium

*CORRESPONDENCE
G. Sobey,
glenda.sobey@nhs.net
F. S. Van Dijk,
fleur.dijk@nhs.net

RECEIVED 02 January 2023
ACCEPTED 03 April 2023
PUBLISHED 31 May 2023

CITATION
Angwin C, Zschocke J, Kammin T, Björck E, Bowen J, Brady AF, Burns H, Cummings C, Gardner R, Ghali N, Gröbner R, Harris J, Higgins M, Johnson D, Lepperdinger U, Milnes D, Pope FM, Sehra R, Kapferer-Seebacher I, Sobey G and Van Dijk FS (2023), Non-oral manifestations in adults with a clinical and molecularly confirmed diagnosis of periodontal Ehlers-Danlos syndrome. *Front. Genet.* 14:1136339. doi: 10.3389/fgene.2023.1136339

Non-oral manifestations in adults with a clinical and molecularly confirmed diagnosis of periodontal Ehlers-Danlos syndrome

C. Angwin[1,2], J. Zschocke[3], T. Kammin[4], E. Björck[5], J. Bowen[4], A. F. Brady[1,2], H. Burns[6,7], C. Cummings[1], R. Gardner[8], N. Ghali[1,2], R. Gröbner[3], J. Harris[1], M. Higgins[8], D. Johnson[4], U. Lepperdinger[9], D. Milnes[8], F. M. Pope[1,10], R. Sehra[1], I. Kapferer-Seebacher[9], G. Sobey[4]* and F. S. Van Dijk[1,2]*

[1]National EDS Service, London North West University Healthcare NHS Trust, London, United Kingdom, [2]Department of Metabolism, Digestion and Reproduction, Section of Genetics and Genomics, Imperial College London, London, United Kingdom, [3]Institute of Human Genetics, Medical University Innsbruck, Innsbruck, Austria, [4]National EDS Diagnostic Service, Sheffield Children's NHS Foundation Trust, Sheffield, United Kingdom, [5]Clinical Genetics, Karolinska University Hospital, Solna, Sweden, [6]Department Otolaryngology Head and Neck Surgery, Children's Health QLD, Brisbane, QLD, Australia, [7]School of Medicine, University of Queensland, Brisbane, QLD, Australia, [8]Clinical Genetics, Genetic Health Queensland, Brisbane, QLD, Australia, [9]Department of Operative and Restorative Dentistry, Medical University of Innsbruck, Innsbruck, Austria, [10]Department of Dermatology, Chelsea and Westminster Hospital NHS Foundation Trust, London, United Kingdom

Introduction: Periodontal Ehlers-Danlos Syndrome (pEDS) is a rare autosomal dominant type of EDS characterised by severe early-onset periodontitis, lack of attached gingiva, pretibial plaques, joint hypermobility and skin hyperextensibility as per the 2017 International EDS Classification. In 2016, deleterious pathogenic heterozygous variants were identified in *C1R* and *C1S*, which encode components of the complement system.

Materials and Methods: Individuals with a clinical suspicion of pEDS were clinically and molecularly assessed through the National EDS Service in London and Sheffield and in genetic services in Austria, Sweden and Australia. Transmission electron microscopy and fibroblast studies were performed in a small subset of patients.

Results: A total of 21 adults from 12 families were clinically and molecularly diagnosed with pEDS, with *C1R* variants in all families. The age at molecular diagnosis ranged from 21–73 years (mean 45 years), male: female ratio 5:16. Features of easy bruising (90%), pretibial plaques (81%), skin fragility (71%), joint hypermobility (24%) and vocal changes (38%) were identified as well as leukodystrophy in 89% of those imaged.

Discussion: This cohort highlights the clinical features of pEDS in adults and contributes several important additional clinical features as well as novel deleterious variants to current knowledge. Hypothetical pathogenic mechanisms which may help to progress understanding and management of pEDS are also discussed.

KEYWORDS

periodontitis, Ehlers-Danlos syndrome, complement, non-oral, genetics

Introduction

Ehlers-Danlos Syndromes (EDS) are a heterogeneous group of rare monogenic conditions that are characterized by joint hypermobility, skin and vascular fragility and generalised connective tissue friability (Malfait, 2018). Currently, there are 14 types recognized, 13 with monogenic causes by variants in 20 different genes, the majority of which encode fibrillary collagen types I, III, and V, modifying or processing enzymes (for example, collagenases and lysyl hydroxylases) or those proteins and enzymes that modify the extracellular matrix (for example, tenascin-X) (Malfait et al., 2020).

Periodontal EDS (pEDS) was first described in 1977 (Stewart et al., 1977). Currently, pEDS is diagnosed by the following major criteria: (i) severe early onset periodontitis, (ii) lack of attached gingiva, (iii) pretibial plaques, and (iv) family history of an affected first degree relative, and minor criteria: (i) easy bruising, (ii) distal joint hypermobility, (iii) skin hyperextensibility/fragility/wide or atrophic scarring, (iv) increased infection rate, (v) hernias, (vi) marfanoid facial features, (vii) acrogeria, and (viii) prominent vasculature (Malfait et al., 2017). A clinical diagnosis of pEDS can be made through a combination of criteria, the presence of major criterion (i) or major criterion (ii), plus at least two other major criteria and one minor criterion (Malfait et al., 2017).

Since the first description, pEDS has been described clinically in 165 individuals in several case reports, series and pedigree analyses (Nelson and King, 1981; Biesecker et al., 1991; Rahman et al., 2003; Reinstein et al., 2011; Reinstein et al., 2012; Reinstein et al., 2013; Kapferer-Seebacher et al., 2016; Kapferer-Seebacher et al., 2017; Cortés-Bretón Brinkmann et al., 2021; El Chehadeh et al., 2021; Stock et al., 2021; Lepperdinger et al., 2022; Nakajima et al., 2022). In 2003, linkage studies in 5 pedigrees with clinical features of pEDS identified a locus at 12p13 (Rahman et al., 2003). However, it was not until 2016 that heterozygous pathogenic variants in the genes *C1R* (MIM 613785, HGNC 1246) and *C1S* (MIM 120580, HGNC 1247) were found to be causative of pEDS (Kapferer-Seebacher et al., 2016). Unlike causative variants in other rare types, these genes do not encode proteins involved in collagen I, III, or V biosynthesis or modification of proteoglycans. Instead, they encode the protein esterases C1r and C1s, subunits of the complement 1 complex. Activation of C1r and C1s is the first step in the classical complement cascade, a major antimicrobial pathway of the innate immune system. The pathogenesis of pEDS is only partly understood; evidence suggests that oral features are linked to secretion or release of active C1r serine protease in the extracellular space. This mechanism may cause gingival hyperinflammation in response to mild biofilm accumulation, and subsequently rapidly progressing periodontal destruction leading to dental loss. (Kapferer-Seebacher et al., 2016; Kapferer-Seebacher et al., 2020). The question arises whether this hyperinflammation is also the mechanism of several non-oral features observed in pEDS (Kapferer-Seebacher et al., 2016; Kapferer-Seebacher et al., 2020).

In the current literature, 165 individuals from 34 families have been published, with 27 (likely) pathogenic variants (*C1S* = 5 variants, *C1R* = 22 variants) (Kapferer-Seebacher et al., 2016; Wu et al., 2018; Kapferer-Seebacher et al., 2019; Kapferer-Seebacher et al., 2020; Cortés-Bretón Brinkmann et al., 2021; El Chehadeh et al., 2021; Stock et al., 2021; Lepperdinger et al., 2022; Nakajima et al., 2022). Although the molecular cause for pEDS has been defined and fundamental studies are being undertaken to elucidate the pathogenic mechanism, (Kapferer-Seebacher et al., 2016), there is also a need for detailed phenotyping of molecularly confirmed adults with pEDS, to identify specific associated clinical features to improve diagnosis, understanding of pathogenesis and management. Of importance, other clinical features have recently been reported in pEDS including leukodystrophy (Kapferer-Seebacher et al., 2019) and hoarseness of voice (George et al., 2016). A recent paper reported a cohort of molecularly diagnosed individuals with pEDS and vascular abnormalities including venous insufficiency and arterial aneurysms (El Chehadeh et al., 2021). Here, we report on a spectrum of non-oral features in 21 adult individuals from 12 families with a clinically and molecularly confirmed diagnosis of pEDS with the aim of developing our understanding of clinical features and underlying pathogenic mechanisms.

Materials and methods

Patients

Patients with a suspicion of pEDS were seen in the National EDS Service in London and Sheffield and in genetic centres in Austria, Sweden and Australia. Patients with a confirmed clinical and molecular diagnosis of pEDS were included in the study. The patients were reviewed over a study period of 2019–2023. Photographs of facial features were assessed independently by three consultant geneticists, if not possible, descriptions of facial features were taken from the notes. Written consent for publication, including photographs, was obtained from all individuals. According to the Institutional Review Board (IRB) no formal research ethics approval or research and development approval was required as stipulated by the United Kingdom Policy Framework for Health and Social Care Research and the Health Research Authority decision tool.

Transmission electron microscopy and collagen electrophoresis

As part of the diagnostic process a subset of patients underwent a skin biopsy for transmission electron microscopy (TEM) (Angwin et al., 2020) and collagen electrophoresis with methodology as described by (Körkkö et al., 1998). The majority of biopsies were taken from the inner, upper forearm in order to maintain consistency of samples across the cohort.

Molecular analysis

Molecular analysis was carried out via massively-parallel sequencing (NextSeq, Illumina), and data analysis using SeqNext software and CNV Detective. Variants were analysed according to best practice guidelines for the evaluation of pathogenicity and the reporting of sequence variants in clinical molecular genetics (Richards et al., 2015). Confirmation of clinically significant sequence variants by Sanger sequencing was performed as

TABLE 1 Cohort demographics and clinical features '+' = sign is present, '-' = sign is absent, U = data unknown.

Individual	P1	P2	P3	P4	P5	P6	P7	P8	P9	P10	P11	P12	P13	P14	P15	P16	P17	P18	P19	P20	P21	Total
Gender	F	M	F	F	F	M	F	F	F	M	F	F	F	F	F	F	F	M	F	M	F	M = 5 (24%) F = 16 (76%)
Age at molecular diagnosis	33	69	73	69	60	21	40	45	59	34	41	30	39	45	24	75	28	35	33	29	26	
Gene	*C1R*	*C1R*	*C1R*	*C1R*	*C1R*	*C1R*	*C1R*	*C1R*	*C1R*	*C1R*	*C1R*	na	*C1R*	*C1R*	*C1R*	*C1R*	*C1R*	*C1R*	*C1R*	*C1R*	*C1R*	*C1R* = 20 (95%
Variant	c. (1273 + 1_1274-1) _(1348 + 1_1349-1)del	c.707T>C	c.689T>C	c.689T>C	c. (1273 + 1_1274-1) _(1348 + 1_1349-1)del	c.1073G>A	c.689T>C	c.689T>C	c.702_711 delinsT	c.702_711 delinsT	c.926G>A	na	c.869A>G	c.149_150 TC>AT	c.149_150 TC>AT	c.1339T>C	c.628T>G	c.1113C>G	c.1113C>G	c.1073G>T	c.1073G>T	
Protein	exon 10 deletion	p. (Phe236Ser)	p. (Leu230Pro)	p. (Leu230Pro)	exon 10 deletion	p. (Cys358Tyr)	p. (Leu230Pro)	p. (Leu230Pro)	p. (Lys235_ Leu237del)	p. (Lys235_ Leu237del)	p. (Cys309Tyr)	na	p. (Asp290Gly)	p. (Val50Asp)	p. (Val50Asp)	p. (Cys447Arg)	p. (Tyr210Asp)	p. (Cys371Trp)	p. (Cys371Trp)	p. (Cys358Phe)	p. (Cys358Phe)	
Dental																						
Periodonitis	+	+	+	+	+	+	+	+	U	+	U	U	+	+	+	+	+	+	+	+	+	18 (86%)
Lack of attached gingiva	+	+	+	+	+	+	+	+	U	+	U	U	+	+	+	+	+	+	+	+	+	18 (86%)
Dermatological features																						
Thin skin	+	+	+	+	+	+	-	-	U	-	+	U	+	-	-	+	-	+	+	+	+	13 (62%)
Hyperextensibiliy	-	-	-	-	-	-	-	-	+	-	-	U	-	-	-	U	-	+	-	+	+	4 (19%)
Fragility	-	+	+	+	+	+	+	+	+	+	U	U	+	-	-	+	-	+	+	+	+	15 (71%)
Easy bruising	+	+	+	+	+	+	+	+	+	+	+	U	+	+	+	+	-	+	+	+	+	19 (90%)
Long term bruising	-	+	+	+	+	+	U	+	U	+	U	U	-	-	-	U	-	+	+	+	+	11 (52%)
Pretibial discolouration	-	+	+	+	+	+	+	+	+	+	+	+	+	-	-	+	-	+	+	+	+	17 (81%)
Symmetrical discolouration	-	+	+	+	+	+	+	+ plus pigment on right calf	+	+	+	+	+ plus pigment on right calf	-	-	+	-	+	+	+	+	17 (81%)
Abnormal scarring	+ atrophic	-	+ widened	+ atrophic	-	+ atrophic	-	-	U	+ widened	-	U	+ atrophic	-	-	+ widened	-	-	+ atrophic	-	+ atrophic	9 (43%)
Thread veins	+	+	+	+	-	-	-	-	+	-	U	U	-	-	-	-	-	-	+	-	-	6 (29%)
Musculoskeletal																						
Beighton score	2/9	0/8	0/9	0/8	1/9	7/9	4/9	0/8	5/9	0/8	U	U	2/9	1/9	1/9	0/9	6/9	0/9	3/9	8/9	9/9	5 (24%)
Joint pain, age (yrs)	+	-	+	-	+	-	+	+	+	+	U	U	+	-	-	-	+	+	-	+	-	11 (52%)
	10						40	10	20	18							18	33		29		

(Continued on following page)

10.3389/fgene.2023.1136339

TABLE 1 (*Continued*) Cohort demographics and clinical features '+' = sign is present, '-' = sign is absent, U = data unknown.

Individual	P1	P2	P3	P4	P5	P6	P7	P8	P9	P10	P11	P12	P13	P14	P15	P16	P17	P18	P19	P20	P21	Total
Dislocation/ subluxations	-	+	-	-	-	-	+	-	-	U	U	U	-	-	-	+	-	+	-	-	-	4 (19%)
Spinal abnormalities	+	-	-	+	U	+	-	-	U	-	U	U	-	-	-	-	-	-	-	-	-	3 (14%)
Foot abnormality	-	-	+	+	-	U	+	-	+	+	U	U	-	-	-	+	+	-	+	-	-	8 (38%)
Ear, nose and throat																						
Voice changes (age of onset in years)	-	+55	-	-	-	+19	-	-	-	-	U	U	+20	+ U	-	+ U	-	+19	-	+14	+ U	8 (38%)
Management		tracheal resection											surgical correction	antibiotics				speech and language therapy			Surgical correction	
Complications		mid anastomotic stricture treated via laser bronchoscopy																			Surgical resection of scar tissue with local steroid injections	
Central nervous system																						
Leukodystrophy (age at scan in years)	U	U	U	+64	U	U	+41	+46	U	U	U	+30	U	U	U	U	- 30	+38	+36	+33	+30	8/ 9 (89%)
Psychological symptoms	+	-	+	-	+	+	+	+	-	+	-	-	-	-	-	-	-	+	+	+	-	10 (48%)
Tremor	-	+	-	-	-	-	+	-	-	U	-	-	-	-	-	-	-	+	-	-	-	3 (14%)
Loss of concentration	-	-	-	-	U	-	+	-	+	U	U	U	-	-	-	-	-	+	-	+	+	5 (24%)
Diplopia	-	-	-	+	-	-	-	-	-	-	U	U	-	-	-	-	-	-	-	-	-	1 (5%)
Loss of speech	-	-	-	-	-	-	-	-	-	-	U	U	-	-	-	-	-	-	-	-	-	0
Spasticity	-	-	-	-	-	-	-	-	-	-	U	U	-	-	-	-	-	-	-	-	-	0
Memory loss	-	-	-	-	-	U	-	+	+	U	U	U	+	-	-	-	-	-	-	+	-	4 (19%)
Headache	+	-	-	+	-	U	+	+	U	U	U	U	-	-	-	+	-	+	+	+	+	9 (43%)
Migraine	-	-	-	-	-	-	+	+	U	U	U	U	-	-	-	+	-	+	-	+	+	6 (29%)
Incontinence	+	-	-	-	-	-	+	-	-	U	U	U	U	-	-	U	-	-	-	-	-	2 (10%)
Back pain	+	-	-	-	+	-	+	+	+	+	U	U	U	-	-	+	-	+	-	+	-	9 (43%)

10.3389/fgene.2023.1136339

necessary. DNA changes have been described according to NM_001733.4 for *C1R* and NM_201442.3 for *C1S* and validated via Variant Validator (Freeman et al., 2018).

Results

Patients

A total of 21 adults (P1-21) from 12 families were diagnosed with pEDS, see Table 1; data on children with a confirmed molecular diagnosis of pEDS were reported previously (Kapferer-Seebacher et al., 2020). Individuals P4, P5, P9 were reported without clinical details (members of families C, E, and B, respectively) in a study by Rahman et al. demonstrating linkage to locus 12p13 (Rahman et al., 2003) and have been confirmed to have a diagnosis of pEDS in the present study. Only P13 has been clinically and molecularly reported before (George et al., 2016; Kapferer-Seebacher et al., 2016). Individuals were seen in the national EDS services in London ($n = 13$) and Sheffield ($n = 5$) and in the genetic services in Austria ($n = 2$) and Sweden ($n = 1$). The age at molecular diagnosis ranged from 21–75 years (mean 44 years). Two siblings passed away at the ages of 30 and 41, and have not been included in age of diagnosis as testing took place after death. The male: female ratio was 5:16. Ethnic backgrounds were White British, Swedish, Austrian and Latvian. Please see Supplementary Table S1 for clinical features. Four additional individuals from two families have been included in the Supplementary appendix, as they have a clinical diagnosis of pEDS but there is uncertainty about the pathogenicity of the identified variant.

Transmission electron microscopy and collagen electrophoresis

TEM was carried out in 6/21 individuals. No consistent features were observed: Irregular collagen packing (P2, $n = 1$), variability in fibril diameter (P9, P21, $n = 2$), single collagen flower (P21, $n = 1$) and protein filled rough endoplasmic reticulum in fibroblasts ($n = 2$). In 1 individual, a biopsy was taken from an area of pretibial discoloration in early adulthood, and electron microscopy showed scarring with haemosiderin deposition, inflammatory changes with mainly perivascular nodular aggregates of lymphocytes, with fragmentation leading to clumping of elastin. Fibroblast cultures with protein studies were carried out in 7 patients; of these 6 (86%) had normal type III collagen and 1 (14%) had slightly increased production of type III collagen.

Molecular analysis

All identified deleterious variants are detailed in Supplementary Table S1. Identified variants were found in *C1R* in 12/12 (100%) families. In P11 the diagnosis was made on stored DNA after death. Her sibling (P12) with a comparable phenotype was no longer alive and was not tested. Six newly described variants included in this paper are as follows: (1) *C1R* c.628T>G, p.(Tyr210Asp), (2) *C1R* c.707T>C, p.(Phe236Ser), (3) *C1R* c.926G>A, p.(Cys309Tyr), (4) *C1R* c.1273 + 1_1274-1)_(1348 + 1_1349-1)del (exon 10 deletion), (5) *C1R* c.1273 + 1_1274-1,1348 + 1_1349-1del p.(Gly425_Pro449del), and (6) *C1R* c.1339T>C, p.(Cys447Arg). All the (likely) pathogenic variants identified in this cohort are compatible with the production of stable enzymatically active C1r protein, in line with the proposed activating effect (Gröbner et al., 2019). Variants are distributed throughout the *C1R* gene, however, there appears to be a cluster of pathogenic alterations affecting the C1r interaction and catalytic domains (CUB2 and CCP1/2) (Figure 1) (Gröbner et al., 2019).

Discussion

This paper provides the first complete detailed phenotypic overview of non-oral features in a cohort of 21 adult individuals with a molecularly confirmed diagnosis of pEDS. Please see Supplementary Table S1 for detailed clinical features.

Oral manifestations

Oral manifestations of the present cohort are reported in detail elsewhere (Lepperdinger et al., 2022).

Gingival recession

Thin and fragile gingiva and periodontitis lead to gingival recession that characterizes the oral image of people affected by pEDS. In the present cohort more than 90% of dentate individuals presented with gingival recession ≥3 mm. Gingival recession provides a useful and easily assessable oral characteristic in the diagnosis of pEDS and may give initial examiners the opportunity to easily support the suspected diagnosis of pEDS.

Early and severe periodontitis

All but two dentate (with retained teeth) individuals were diagnosed with severe periodontitis at young age (≤30 years). Age of first tooth loss due to periodontal reasons was reported to be at a median of 20 years. The probability of being edentate at age 35-44 years was 28%–47%. Two individuals with excellent oral hygiene and receiving professional tooth cleaning on a regular basis had no or only mild periodontal destruction. They were clinically diagnosed with pEDS based on a lack of attached gingiva, pretibial hemosiderin depositions and an affected first degree relative.

Lack of attached gingiva

The oral feature observed in all dentate individuals who had a periodontal assessment was the generalized lack of attached gingiva ($n = 18$) (Figure 2). Unfortunately, three individuals (two deceased), did not have a complete periodontal examination. Generalized lack of attached gingiva has been reported to be pathognomonic for pEDS, and has been reported in children with pEDS in children as young as 4 years old (Kapferer-Seebacher et al., 2020).

Skin

Pretibial plaques

Pretibial plaques are strongly associated with pEDS (reported frequency of 83% in the literature) (Kapferer-Seebacher et al., 2016)

and occur in a specific pattern with hyperpigmentation, atrophy or induration and scarring of the lower limbs typically over the pretibial area, termed pretibial plaques (Kapferer-Seebacher et al., 2016; Malfait et al., 2020). Hyperpigmentation appears to develop gradually from mild, brownish hyperpigmented patches clinically in keeping with haemosiderin deposition, to indurated or atrophic plaques and can progress to cover the entire circumference of the calf. Plaques are often associated with skin fragility, whether atrophic or indurated.

In our cohort 17/21 (81%) had pretibial plaques, comparable to the literature (83%) (Figure 3). 14/17 had symmetrical pigment deposition. Plaques extended around the entire circumference of the calf in 5/17 (29%). We do not have data for age of onset, however in a recent cohort of affected children, only 2/12 (16%) reported pretibial plaques (Kapferer-Seebacher et al., 2020). Varicose veins had been diagnosed in 8/21 (38%); all these individuals also had pretibial hyperpigmentation of the lower limb, and 3 of these had extensive discolouration around the entire calf circumference. In the 4 (19%) individuals without pretibial plaques there were no common characteristics (age, underlying genetic cause, etc.) and one individual had a family member who was affected with pretibial plaques.

The mechanism for pretibial plaque development remains unclear. The discolouration may represent post-inflammatory hyperpigmentation after injury or inflammatory disorder of the skin. However, the symmetrical distribution seen in 14/17 (82%) individuals and level of hyperpigmentation is not in keeping with a purely trauma related process post-injury as is seen in other rare EDS types such as classical EDS (Bowen et al., 2017). Some individuals do not recall significant trauma to their lower limbs in the pattern of discolouration. The pretibial and calf area is a common site to be affected in disorders of metabolism or circulation, and this is, for example, seen in chronic venous disease, pretibial myxoedema in thyroid disease, necrobiosis lipoidica, pyoderma gangrenosum, and others. The proposed mechanism for this localisation is venous/lymphatic pooling of metabolites and immune complexes, resulting in increased local activity in comparison to the rest of the body (Fatourechi, 2005; Caggiati et al., 2008; Caggiati et al., 2010). A potential mechanism for the occurrence of pretibial plaques could be pooling of C1 components and related immune complexes in the lower limbs, resulting in a localised dermal inflammatory response. A recent study describing clinical features in children with pEDS who typically have no or mild cutaneous signs, including children of some of the adults included in this paper (family B, C, D, F correspond to Family 3, 5, 8, 12 respectively) (Kapferer-Seebacher et al., 2020). This could be in keeping with the hypothesis that the observed cutaneous changes are the result of chronic exposure to a higher concentration of overactivated complement components, resulting in inflammatory changes with associated hyperpigmentation and haemosiderin deposition.

It is possible that the majority of hyperpigmentary changes to the pretibial area in pEDS are a result of localized chronic inflammation, leading to melanosis, haemosiderin deposition, extracellular matrix (ECM) remodelling and angiogenesis. Further investigations are important to confirm or reject this hypothesis, for example, *in vitro* skin models, biopsy of skin and underlying tissue, and non-invasive investigations, e.g., ultrasound of microvasculature in a similar technique to (Ritelli et al., 2019).

Prolonged skin inflammation is a risk factor for development of cutaneous squamous cell carcinomas (cSCC) (Riihilä et al., 2019). Tumour derived C1r and C1s are thought to aid cSCC progression and have been suggested as an cSCC biomarker (Riihilä et al., 2020). In this cohort, P18 had an SCC excised from the area of pretibial discolouration with closure requiring skin grafting. An individual reported in the appendix has a history of multiple Basal Cell Carcinomas prior to her clinical diagnosis with pEDS (see Supplementary Appendix). Given the size of this cohort, there is no evidence of an association between increased rates of cutaneous cancers and pEDS. As with any individual, new masses on the skin in those affected by pEDS should be assessed and investigated thoroughly.

Easy bruising

Easy bruising was noted in 90% of individuals (19/21) compared to 95% in the literature. Easy bruising occurred particularly over the shins in 8/21 (38%). In 10 individuals bruising would take a prolonged period of time to fade, up to 9 months in one individual. A particular pattern of redness, swelling, pain and then prolonged bruising was observed in 2 (P8, P13) individuals after mild trauma; in P13 localised to the lower limbs and in P8 could affect any area of the body. Bruising related bleeding could contribute to haemosiderin deposition and hyperpigmentation, however one individual (P1, age 33) reported easy bruising with no evidence of pretibial changes.

Vitamin C use has been recommended as a method to possibly reduce bruising in different types of EDS. It is known to be involved and potentially increase collagen production by fibroblasts (Tajima and Pinnell, 1996; Bowen et al., 2017), however there is no current clinical evidence that it reduces bruising frequency or severity. Given that the pathophysiological mechanism of pEDS remains unclear, the role for this supplement in pEDS related bruising is unknown.

Skin hyperextensibility/fragility/wide or atrophic scarring

Hyperextensible skin was noted in 4 of 21 (19%) individuals. Fragility of the skin was found in 15/21 (71%), which was particularly concentrated over the legs and shins (n = 9). Skin graft was required for 1 individual after minor trauma to the shin. Abnormal scarring was reported in 10/21 (48%) and particularly prominent on the lower legs in 9 (although some also had abnormal scarring on arms, torso and head), described as: atrophic (n = 6), widened (n = 4) and keloid (n = 1).

Prominent vasculature and acrogeria

Thin, translucent skin was noted in 13/21 (62%) individuals within our cohort and specifically over the chest in 5 individuals. Acrogeria was not specifically noted.

Musculoskeletal

In this cohort, distal hypermobility was seen in 5/19 (26%) individuals with 2 of those having a Beighton score of 5 or over. Three additional individuals had a Beighton score of 5 or over. Dislocations were reported by 2/21 (10%) individuals following appropriate trauma (fall down stairs and road traffic accident

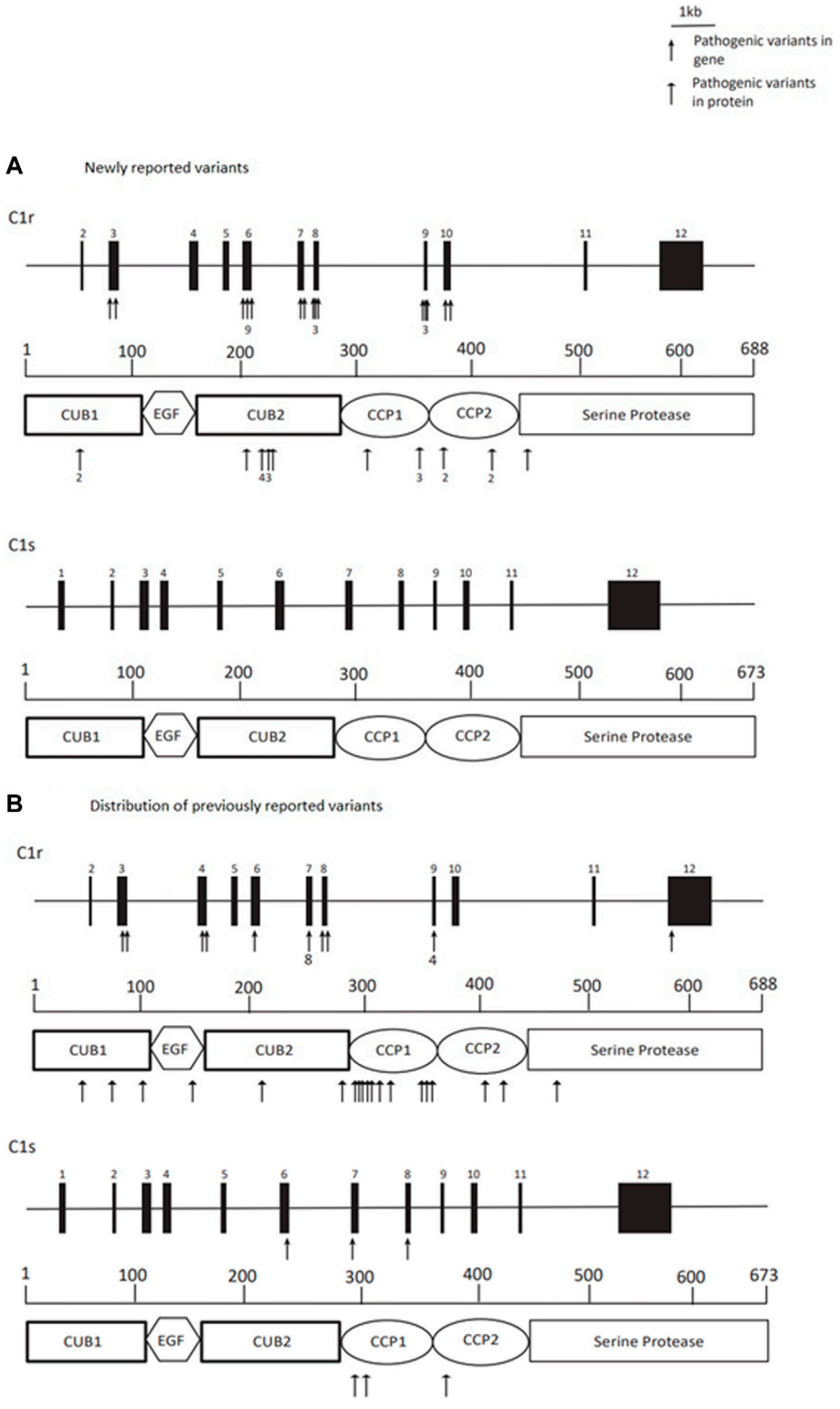

FIGURE 1
Title: Distribution of *C1R* (likely) pathogenic variants and their localisation in the C1r protein in newly reported variants from this paper, and previously reported variants in *C1R* and *C1S*. Legend. **(A)** Newly reported variants–deleterious variants are distributed throughout the *C1R* gene, however, there appears to be a cluster of alterations affecting the interaction and catalytic domains (CUB2 and CCP1/2) of the C1r protein. Arrows indicate reported variants, these are numbered where there are multiple. **(B)** Distribution of previously reported variants with clustering affecting the interaction and catalytic domains (CUB2 and CCP1/2) of both C1r and C1s proteins. Arrows indicate reported variants, these are numbered where there are multiple.

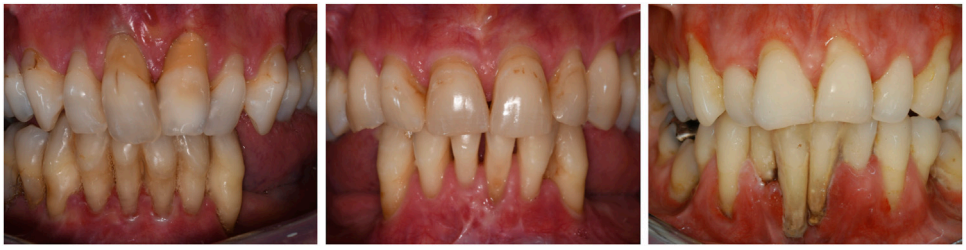

FIGURE 2
Title: Oral manifestations of pEDS. Legend: Thin and fragile gums (due to lack of attached gingiva) and periodontitis lead to gingival recession that characterizes the oral image of people affected by pEDS. Age of first tooth loss due to periodontal reasons was reported to be at a median of 20 years.

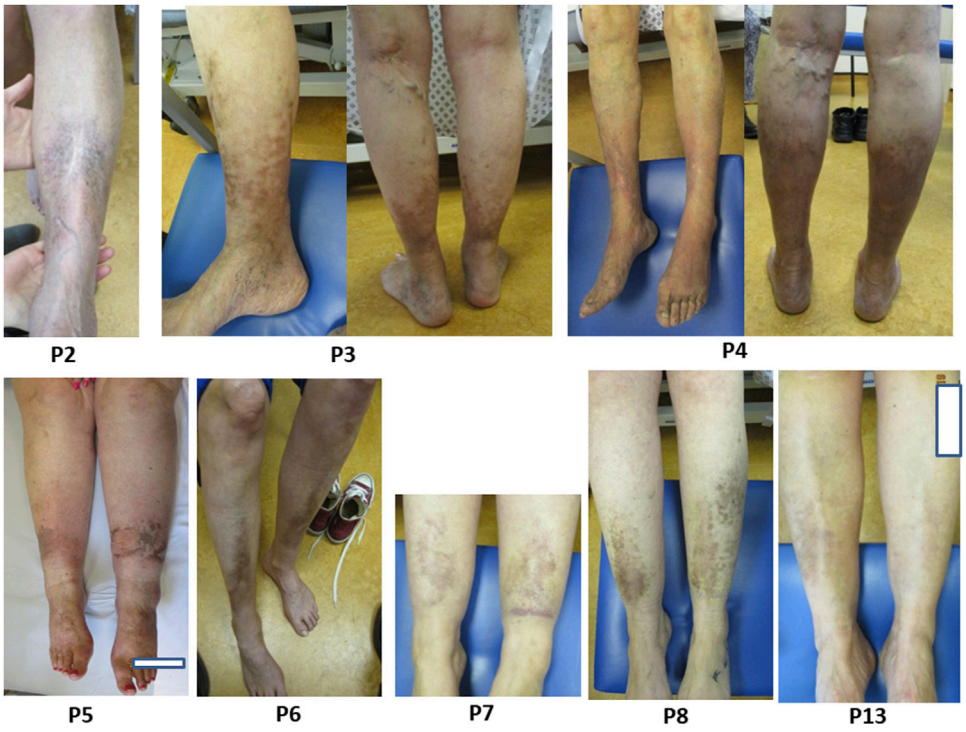

FIGURE 3
Title. Pretibial plaques in individuals with pEDS. Legend. Examples of pretibial plaques with symmetrical distribution and with some extending around the entire circumference of the calf, as observed in individuals P2, P3, P4, P5, P6, P7, P8 and P13.

both resulting in shoulder dislocations). Joint pains were reported by 11/21 (52%) individuals (generalised in 5). Joint pains typically started in early adulthood (average age 30, age range of onset 10–60 years).

Gastrointestinal

Hernia

Hernia was noted in 5/21 (23.8%) individuals: inguinal (n = 2), incisional (n = 1), umbilical (n = 1) and a combination of hiatus, inguinal and umbilical (n = 1).

Diverticular disease and bowel perforation

Diverticular disease was reported in 5/21 (24%) individuals, 1 of whom (P3) suffered a related bowel perforation. Generally, diverticulitis is considered a chronic inflammatory state, in conjunction with other lifestyle, genetic and environmental factors, at an incidence of 188/100,000 (Bharucha et al., 2015; Strate and Morris, 2019). Given its relatively high frequency in the population and the small cohort published here, no definite conclusions on association can be drawn.

Fatal spontaneous bowel perforation caused the death of individual P11 at age 41 and was also the cause of death in a sibling of P9 who passed away prior to genetic testing or assessment

but had clinical features of pEDS. Organ rupture has been previously reported in 2 patients with molecularly confirmed pEDS, although the sites of perforation are not specified (Kapferer-Seebacher et al., 2016; Kapferer-Seebacher et al., 2017). Of note, the proband of family 1 with a clinical diagnosis of pEDS (see Supplementary Appendix) had two small bowel ruptures requiring bowel resections.

Concurrent disorders

Recurrent infections

Recurrent infection has been included in the current diagnostic criteria (Malfait et al., 2017). In this cohort 7/21 (33%) individuals subjectively felt that they were more prone to recurrent infections (see Supplementary Table S1).

Inflammatory disorders

From medical history no increased infection rate was apparent. Complex Systemic Lupus Erythematosus (SLE) was reported in P10 (*C1R* (c.702_711delinsT)), with initial presentation of rash, joint aches and chest pain, developing a severe pericarditis requiring surgical intervention and a prolonged and resistant serositis. Multiple treatments for his SLE included Methotrexate, Hydroxychloroquine, Mepacrine, Rituximab and Azathioprine, however due to intolerance or minimal response he has continued to require long term steroids. P10 has recently developed three lesions on the left lower limb in keeping with a diagnosis of pyoderma gangrenosum, which have been minimally responsive to 60 mg of oral prednisolone and regular dressings. Infliximab is being considered as a management option. SLE had also been diagnosed in both siblings (did not participate in this study) of the individuals' mother (P9). P9 was not affected with SLE. Unfortunately, these family members were not available for genetic testing.

Interestingly, a study of a consanguineous family with SLE identified recessive loss of function (LOF) variants in *C1R* (with low serum levels of complement) in contrast to dominant gain of function variants seen in pEDS (Demirkaya et al., 2017). Given the United Kingdom incidence of SLE is estimated at 4.91/100,000 in the general population, (Stojan and Petri, 2018), it is currently unclear whether there is an association between pEDS and SLE; this cohort is not large enough to draw any definite conclusions.

P5 has a diagnosis of palmoplantar pustular psoriasis (PPP). This is an inflammatory disease characterized by sterile neutrophilic pustules surrounded by inflamed or reddened/discoloured skin. The mechanism of disease is unknown but which appears to be mediated by aspects of both innate and acquired immune systems (Brunasso and Massone, 2021).

P20 was diagnosed at the age of 12 with mesangiocapillary glomerulonephritis type I (now known as C3 glomerulonephritis). This condition is part of the disease entity C3 glomerulopathy caused by dysregulation of the alternative complement pathway (rather than the classical pathway which is initiated by C1) (Sethi et al., 2012; Smith et al., 2019).

In summary, in 3/21 (14%) individuals an autoimmune condition was diagnosed with one individual having a diagnosis of SLE as well as two second-degree maternal family members who also had clinical features of pEDS (not included in this study). Autoimmune condition incidence varies by disorder; however, they are largely uncommon in the general population (Wang et al., 2015). Within this group there does appear to be a propensity toward autoimmune conditions, particularly those possibly due to complement dysregulation, however the cohort is not large enough to draw any definite conclusions.

Facial features

Although Marfanoid facial features are included as minor diagnostic criteria for pEDS, none of our series showed such changes. Contrastingly we consider that 6/21 (28.5%) had features resembling those of vEDS (vascular EDS). Facial features noted in vEDS are thin vermilion of the lips, micrognathia, narrow nose, and prominent eyes (Brady et al., 2017). Typical facial features in the cohort were thin vermillion of the lips ($n = 10$) and proptosis ($n = 8$), while other observed facial features were a narrow nose ($n = 5$), narrow mouth ($n = 3$) and high palate ($n = 2$). Figure 4 and Supplementary Table S1.

Cardiovascular

Arterial events (including aneurysms/dissections of the abdominal aorta, carotid artery and cerebral artery) have been previously reported in 10/150 (6.7%) molecularly confirmed pEDS patients (Kapferer-Seebacher et al., 2016; Kapferer-Seebacher et al., 2017; El Chehadeh et al., 2021). 10/21 individuals in this cohort underwent cardiac imaging and none were found to have any structural abnormalities of the heart. In 2/6 (33%) individuals who underwent arterial imaging, aneurysms were seen: in P18 a cerebral aneurysm ($n = 1$) in the form of a small brain aneurysm projecting posteriorly from the left internal carotid artery/anterior cerebral artery junction and in P19 a right internal carotid aneurysm ($n = 1$). Both individuals had leukoencephalopathy, and the aneurysms were detected in their early 30 s. In P16, normal imaging was reported after a transient ischaemic attack age 74. Spontaneous subarachnoid haemorrhage was the cause of death in P12 at age 30, although the underlying cause of the bleed is unclear. Intracranial haemorrhages have been previously reported in the literature (Kapferer-Seebacher et al., 2021). The risk of arterial events in individuals with pEDS remains unknown. Consideration of regular arterial surveillance is advised and has been reported to be conducted with a frequency of 1.5–2 years in some services (Kapferer-Seebacher et al., 2021).

Central nervous system

White matter abnormalities have so far been detected in all patients with molecularly confirmed pEDS who have undergone cerebral imaging (10 of 10 reported patients, age range 8–68 years) (Kapferer-Seebacher et al., 2016; Kapferer-Seebacher et al., 2017; El Chehadeh et al., 2021). In this cohort, the majority of individuals ($n = 12$) did not have brain imaging at the time of reporting. In those that had imaging ($n = 9$), leukodystrophy was found in 8/9 (89%). P17, age 30, had no evidence of leukodystrophy on imaging.

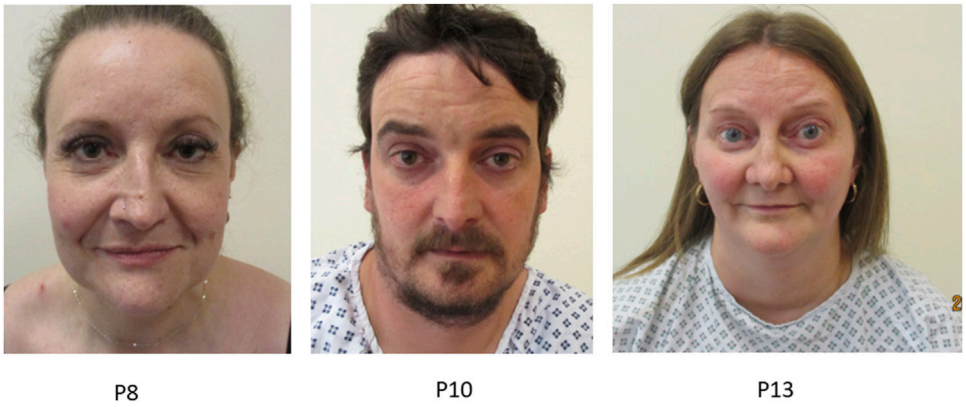

FIGURE 4
Title: Facial features in individuals with pEDS. Legend. Individuals with pEDS share facial features of that are more often seen in individuals with vascular EDS including prominent eyes, narrow nose and thin vermillion of the lips seen in individual P8, P10 and P13.

Leukodystrophy was discovered on average at age 40 (30–64 years of age), however this is dependent on age at imaging; no patients had prior imaging in childhood for comparison. The number of individuals from this cohort with these changes is likely to be underestimated as many have not undergone CNS imaging. There is currently no definite incidence data for leukodystrophy in the general adult population.

Leukodystrophies and leukoencephalopathies are a heterogenous group of disorders linked by white matter changes on imaging of the CNS which have recently been classified in 2015 (Vanderver et al., 2015). There are many distinct genetic leukoencephalopathies, and previous papers draw radiographic similarities between pEDS leukoencephalitis and genetic cerebral arteriopathies such as CADASIL (Cerebral Autosomal Dominant Arteriopathy with Subcortical Infarcts and Leukoencephalopathy) (Spranger et al., 1996; Kapferer-Seebacher et al., 2019). In contrast to these disorders and despite the radiographic similarities, neurological features are not severe, and in this cohort are mild or absent, with no evidence of cognitive decline. Neurological symptoms were reported by 11/21 (52%) individuals, including headaches (n = 8, 6 of which were migrainous), tremor (n = 3), partial bilateral palsy of fourth cranial nerve causing diplopia (n = 1), neuropathic pain (n = 2), poor memory (n = 4) and loss of concentration (n = 5). There was no evidence of lower motor neuropathology or speech disturbance. Vasculitis has previously been associated with a clinical diagnosis of pEDS (prior to available genetic testing) in an individual with periodontitis, osteolysis, cutaneous vasculitis and T cell reactivity to type 1 collagen (Hoffman et al., 1991). However, there are no currently available samples of cerebral tissue for further investigation of pathogenic mechanisms in this group.

Mental health disorder symptoms were reported in 9 individuals including alcohol dependence (n = 1), mixed anxiety and depression (n = 2), anxiety alone (n = 3) and depression alone (n = 3) associated with psychosis and a suicide attempt in 1 individual.

Currently there is no evidence that the leukodystrophy observed on imaging is linked to any specific degenerative or mental health disorder, and therefore cerebral imaging to monitor any leukodystrophy is not indicated unless the individual presents with neurological symptoms requiring imaging.

Ear, nose, and throat

Vocal changes were noted in 8/21 (38%) individuals, in 3 individuals with a *C1R* VUS reported in Supplementary Appendix and have previously been reported in two individuals in the literature (George et al., 2016; Kapferer-Seebacher et al., 2019). Vocal changes have been previously reported in pEDS, and P13 has been reported before (George et al., 2016).

Vocal changes were defined as a hoarse voice often with associated high pitch. Onset of vocal changes was reported from early teens to 55 years (average age 27 years). Various causes for the vocal changes were reported: P2 developed subglottic stenosis with osseous metaplasia of the tracheal rings with vocal cord intermission and regurgitation, requiring tracheal resection which was complicated by an anastomotic stricture and required laser ablation, P13 developed subglottic stenosis below the larynx with an associated abnormality of the cricoarytenoid joint requiring surgical correction, in P14 recurrent laryngitis was reported with as many as 5 episodes a year, in P18 vocal cord sulci responded partially to speech and language therapy, and P21 developed tracheal stenosis which was treated surgically but required recurrent resections for significant scarring and has ongoing management with local steroid injections.

Subglottic stenosis is a fibrotic narrowing of the subglottic space which can occur in different situations including trauma, infection and systemic diseases. Previous papers have investigated an autoimmune hypothesis of acquired subglottic stenosis after finding autoantibodies to type II collagen in affected children, however, further investigations have not been conclusive (Stolovitzky and Todd, 1990; Stolovitzky et al., 1997). Autoantibodies to type II, IX and XI collagen have been found in relapsing polychondritis (RP), an autoimmune disease resulting in inflammation of cartilaginous structures and other organ systems including heart valves, eyes and vasculature (Borgia et al., 2018). 50% of these individuals develop laryngotracheobronchial

involvement such as laryngomalacia and stenosis. The pathogenesis of RP is not fully understood, but animal models have shown that immune sensitization to ECM proteins can result in a clinical picture similar to RP (Loehrl and Smith, 2001).

The association between other vocal cord disorders and inflammatory and granulomatous diseases has been well documented, for example, fibro-inflammatory changes of the vocal cord commissure developing in rheumatoid arthritis (Eddaoudi et al., 2019).

Molecular diagnosis

Both we and others have reported heterozygous missense or in-frame deletion variants within the *C1R* or *C1S* genes in individuals with pEDS. The majority of variants were located in *C1R* and affected the CUB2 and CCP1 domains (Figure 1) (Kapferer-Seebacher et al., 2016) and were found to have lost the ability to interact with C1q, preventing binding but otherwise forming and being secreted normally (Gröbner et al., 2019). However, P13 was included despite being reported in previous publications (George et al., 2016; Kapferer-Seebacher et al., 2016; Gröbner et al., 2019) due to the unusual site of the pathogenic *C1R* variant c.869A>G, p.(Asp290Gly); this is the only reported pathogenic variant which is located in the C1q binding site of C1r, appearing to inhibit binding of the C1r-C1s tetramer to C1q (Gröbner et al., 2019). See Supplementary Appendix.

Conclusion

Lack of attached gingiva has been observed as early as 4 years of age and is pathognomonic for pEDS (Kapferer-Seebacher et al., 2020; Lepperdinger et al., 2022). This is the first study reporting the spectrum of extraoral clinical features assessed by specialists in inherited connective tissue disease, as observed in a series of 21 individuals with clinically and molecularly proven pEDS.

In our series, in line with previous observations, more than 80% had pretibial plaques, whilst vocal cord/laryngeal (38%) and white matter abnormalities in those that had imaging (89%) were also frequently encountered. Contrastingly, clinical features reflected in the minor criteria for a diagnosis of pEDS, namely, marfanoid facial features, acrogeria, cutaneous venous prominence and susceptibility to infection (Malfait et al., 2017) were less common and may merit revision.

Regular surveillance of the arterial tree could be considered, given the reported frequency of arterial aneurysms in this cohort (2/6, 33%) and previously reported arterial events (10/150) (El Chehadeh et al., 2021; Kapferer-Seebacher et al., 2021). Symptoms indicating concomitant autoimmune disorders or an acute abdomen should be investigated thoroughly.

Whilst there is clear clinical evidence of potentially abnormal connective tissue in pEDS as judged by features of hernias, skin and vascular fragility, other significant clinical features such as laryngeal thickening, white matter abnormalities or even the pretibial plaques are unexplained by a primary connective tissue matrix defect. Here, additional inflammatory mechanisms may be responsible and require further elucidation.

Data availability statement

The data presented in the study are deposited in the Global Variome shared LOVD database repository, please see https://databases.lovd.nl/shared/genes/C1R under the following IDs: C1R_000038, C1R_000028, C1R_000027, C1R_000030, C1R_000029, C1R_000009, C1R_000031, C1R_000032, C1R_000033, C1R_000034, C1R_000036, and C1R_000037.

Ethics statement

Written consent for publication, including photographs, was obtained from all individuals. According to the Institutional Review Board (IRB) no formal research ethics approval or research and development approval was required as stipulated by the UK Policy Framework for Health and Social Care Research and the Health Research Authority decision tool.

Author contributions

Shared first authorship: CA (first authorship: data collection and analysis and manuscript writing) and JZ (first authorship: data collection, manuscript review, patient recruitment, genetic analysis), TK data collection, patient recruitment. EB data collection, patient recruitment. JB data collection, patient recruitment. AB data collection, patient recruitment. HB data collection, patient recruitment, ENT clinical assessments. CC data collection, patient recruitment. RG data collection, genetic analysis. NG data collection, patient recruitment. JH data collection, patient recruitment. MH data collection, genetic analysis. DJ data collection, patient recruitment. UL data collection, patient recruitment, dental assessments. DM data collection, patient recruitment, genetic analysis. FP data collection, patient recruitment. RS data collection, patient recruitment. IK-S data collection, patient recruitment, genetic analysis, dental assessments. Shared last authorship: GS (last authorship: data collection, patient recruitment, supervision of manuscript) and FV (last authorship: data collection, patient recruitment, supervision of manuscript). All authors have reviewed and approved the manuscript prior to submission.

Funding

This work was supported by a grant from the Ehlers-Danlos Syndrome Society (grant number 2019.02.PRO05). Imperial College London Biomedical Research Centre provided funding for a Clinical Research Fellowship. Funding was also provided for publication in an open access journal, (Imperial College London, PO number 4550141).

Acknowledgments

We thank the participants for their kind cooperation.

Conflict of interest

The authors declare that the research was conducted in the absence of any commercial or financial relationships that could be construed as a potential conflict of interest.

Publisher's note

All claims expressed in this article are solely those of the authors and do not necessarily represent those of their affiliated organizations, or those of the publisher, the editors and the reviewers. Any product that may be evaluated in this article, or claim that may be made by its manufacturer, is not guaranteed or endorsed by the publisher.

Supplementary material

The Supplementary Material for this article can be found online at: https://www.frontiersin.org/articles/10.3389/fgene.2023.1136339/full#supplementary-material

References

Angwin, C., Ghali, N., Baker, D., Brady, A. F., Pope, F. M., Vandersteen, A., et al. (2020). Electron microscopy in the diagnosis of ehlers–danlos syndromes: Correlation with clinical and genetic investigations. *Br. J. Dermatol.* 182, 698–707. doi:10.1111/bjd.18165

Bharucha, A. E., Parthasarathy, G., Ditah, I., Fletcher, J. G., Ewelukwa, O., Pendlimari, R., et al. (2015). Temporal trends in the incidence and natural history of diverticulitis: A population-based study. *Am. J. Gastroenterol.* 110, 1589–1596. doi:10.1038/ajg.2015.302

Biesecker, L. G., Erickson, R. P., Glover, T. W., and Bonadio, J. (1991). Molecular and cytologic studies of Ehlers-Danlos syndrome type VIII. *Am. J. Med. Genet.* 41, 284–288. doi:10.1002/ajmg.1320410305

Borgia, F., Giuffrida, F., Guarneri, F., and Cannavò, S. P. (2018). Relapsing polychondritis: An updated review. *Biomedicines* 6, 84. doi:10.3390/biomedicines6030084

Bowen, J. M., Sobey, G. J., Burrows, N. P., Colombi, M., Lavallee, M. E., Malfait, F., et al. (2017). Ehlers–Danlos syndrome, classical type. *Am. J. Med. Genet. C Semin. Med. Genet.* 175, 27–39. doi:10.1002/ajmg.c.31548

Brady, A. F., Demirdas, S., Fournel-Gigleux, S., Ghali, N., Giunta, C., Kapferer-Seebacher, I., et al. (2017). The Ehlers–Danlos syndromes, rare types. *Am. J. Med. Genet. C Semin. Med. Genet.* 175, 70–115. doi:10.1002/ajmg.c.31550

Brunasso, A. M. G., and Massone, C. (2021). Recent advances in palmoplantar pustulosis. *Fac. Rev.* 10, 62. doi:10.12703/r/10-62

Caggiati, A., Rosi, C., Franceschini, M., and Innocenzi, D. (2008). The nature of skin pigmentations in chronic venous insufficiency: A preliminary report. *Eur. J. Vasc. Endovasc. Surg.* 35, 111–118. doi:10.1016/j.ejvs.2007.08.007

Caggiati, A., Rosi, C., Casini, A., Cirenza, M., Petrozza, V., Acconcia, M. C., et al. (2010). Skin iron deposition characterises lipodermatosclerosis and leg ulcer. *Eur. J. Vasc. Endovasc. Surg.* 40, 777–782. doi:10.1016/j.ejvs.2010.08.015

Cortés-Bretón Brinkmann, J., García-Gil, I., Lobato-Peña, D. M., Martínez-Mera, C., Suárez-García, M. J., Martínez-González, J. M., et al. (2021). The key role of the dental practitioner in early diagnosis of periodontal ehlers-danlos syndromes: A rare case report of siblings. *Quintessence Int.* 52, 166–174. doi:10.3290/j.qi.a45263

Demirkaya, E., Zhou, Q., Smith, C. K., Ombrello, M. J., Deuitch, N., Tsai, W. L., et al. (2017). Brief report: Deficiency of complement 1r subcomponent in early-onset systemic lupus erythematosus: The role of disease-modifying alleles in a monogenic disease. *Arthritis Rheumatol.* 69, 1832–1839. doi:10.1002/art.40158

Eddaoudi, M., Rostom, S., Amine, B., and Bahiri, R. (2019). The involvement of vocal cords in rheumatoid arthritis: A clinical case. *Pan Afr. Med. J.* 34, 102. doi:10.11604/pamj.2019.34.102.20490

El Chehadeh, S., Legrand, A., Stoetzel, C., Geoffroy, V., Billon, C., Adham, S., et al. (2021). Periodontal (formerly type VIII) Ehlers–Danlos syndrome: Description of 13 novel cases and expansion of the clinical phenotype. *Clin. Genet.* 100, 206–212. doi:10.1111/cge.13972

Fatourechi, V. (2005). Pretibial myxedema: Pathophysiology and treatment options. *Am. J. Clin. Dermatol.* 6, 295–309. doi:10.2165/00128071-200506050-00003

Freeman, P. J., Hart, R. K., Gretton, L. J., Brookes, A. J., and Dalgleish, R. (2018). VariantValidator: Accurate validation, mapping, and formatting of sequence variation descriptions. *Hum. Mutat.* 39, 61–68. doi:10.1002/humu.23348

George, S. M. C., Vandersteen, A., Nigar, E., Ferguson, D. J. P., Topham, E. J., and Pope, F. M. (2016). Two patients with Ehlers–Danlos syndrome type VIII with unexpected hoarseness. *Clin. Exp. Dermatol.* 41, 771–774. doi:10.1111/ced.12911

Gröbner, R., Kapferer-Seebacher, I., Amberger, A., Redolfi, R., Dalonneau, F., Björck, E., et al. (2019). C1R mutations trigger constitutive complement 1 activation in periodontal ehlers-danlos syndrome. *Front. Immunol.* 10, 2537. doi:10.3389/fimmu.2019.02537

Hoffman, G. S., Filie, J. D., Schumacher, H. R., Ortiz-Bravo, E., Tsokos, M. G., Marini, J. C., et al. (1991). Intractable vasculitis, resorptive osteolysis, and immunity to type I collagen in type viii ehlers-danlos syndrome. *Arthritis Rheum.* 34, 1466–1475. doi:10.1002/art.1780341119

Kapferer-Seebacher, I., Heiss-Kisielewsky, I., Pepin, M., Dorschner, M., Hale, C. J., Hanna, D., et al. (2016). Periodontal ehlers-danlos syndrome is caused by mutations in C1R and C1S, which encode subcomponents C1r and C1s of complement. *Am. J. Hum. Genet.* 99, 1005–1014. doi:10.1016/j.ajhg.2016.08.019

Kapferer-Seebacher, I., Lundberg, P., Malfait, F., and Zschocke, J. (2017). Periodontal manifestations of ehlers-danlos syndromes: A systematic review. *J. Clin. Periodontol.* 44, 1088–1100. doi:10.1111/jcpe.12807

Kapferer-Seebacher, I., Waisfisz, Q., Boesch, S., Bronk, M., van Tintelen, P., Gizewski, E. R., et al. (2019). Periodontal Ehlers–Danlos syndrome is associated with leukoencephalopathy. *Neurogenetics* 20, 1–8. doi:10.1007/s10048-018-0560-x

Kapferer-Seebacher, I., Oakley-Hannibal, E., Lepperdinger, U., Johnson, D., Ghali, N., Brady, A. F., et al. (2020). Prospective clinical investigations of children with periodontal Ehlers–Danlos syndrome identify generalized lack of attached gingiva as a pathognomonic feature. *Genet. Med.* 23, 316–322. doi:10.1038/s41436-020-00985-y

Kapferer-Seebacher, I., van Dijk, F., and Zschocke, J. (2021). "Periodontal ehlers-danlos syndrome,". [Internet] in *GeneReviews®*. Editors M. Adam, H. Ardinger, and R. Pagon (Seattle: University of Washington). Available at: https://www.ncbi.nlm.nih.gov/books/NBK572429/.

Körkkö, J., Annunen, S., Pihlajamaa, T., Prockop, D. J., and Ala-Kokko, L. (1998). Conformation sensitive gel electrophoresis for simple and accurate detection of mutations: Comparison with denaturing gradient gel electrophoresis and nucleotide sequencing. *Proc. Natl. Acad. Sci. U. S. A.* 95, 1681–1685. doi:10.1073/pnas.95.4.1681

Lepperdinger, U., Angwin, C., Milnes, D., Sobey, G., Ghali, N., Johnson, D., et al. (2022). Oral characteristics in adult individuals with periodontal Ehlers-Danlos syndrome. *J. Clin. Periodontol.* 49, 1244–1252. doi:10.1111/jcpe.13698

Loehrl, T. A., and Smith, T. L. (2001). Inflammatory and granulomatous lesions of the larynx and pharynx. *Am. J. Med.* 111, 113S–117S. doi:10.1016/s0002-9343(01)00856-7

Malfait, F., Francomano, C., Byers, P., Belmont, J., Berglund, B., Black, J., et al. (2017). The 2017 international classification of the Ehlers–Danlos syndromes. *Am. J. Med. Genet. C Semin. Med. Genet.* 175, 8–26. doi:10.1002/ajmg.c.31552

Malfait, F., Castori, M., Francomano, C. A., Giunta, C., Kosho, T., and Byers, P. H. (2020). The ehlers–danlos syndromes. *Nat. Rev. Dis. Prim.* 6, 64. doi:10.1038/s41572-020-0194-9

Malfait, F. (2018). Vascular aspects of the ehlers-danlos syndromes. *Matrix Biol.* 71-72, 380–395. doi:10.1016/j.matbio.2018.04.013

Nakajima, K., Suzuki, H., Yamamoto, M., Yamamoto, T., Kawai, T., Nakabayashi, K., et al. (2022). A familial case of periodontal Ehlers–Danlos syndrome lacking skin extensibility and joint hypermobility with a missense mutation in C1R. *J. Dermatol.* 49, 714–718. doi:10.1111/1346-8138.16372

Nelson, D., and King, R. (1981). Ehlers-Danlos syndrome type VIII. *J. Am. Acad. Dermatol.* 5, 297–303. doi:10.1016/S0190-9622(81)70095-1

Rahman, N., Dunstan, M., Teare, M. D., Hanks, S., Douglas, J., Coleman, K., et al. (2003). Ehlers-Danlos syndrome with severe early-onset periodontal disease (EDS-VIII) is a distinct, heterogeneous disorder with one predisposition gene at chromosome 12p13. *Am. J. Hum. Genet.* 73, 198–204. doi:10.1086/376416

Reinstein, E., Wang, R. Y., Zhan, L., Rimoin, D. L., and Wilcox, W. R. (2011). Ehlers-Danlos type VIII, periodontitis-type: Further delineation of the syndrome in a four-generation pedigree. *Am. J. Med. Genet. A* 155, 742–747. doi:10.1002/ajmg.a.33914

Reinstein, E., Pariani, M., Lachman, R. S., Nemec, S., and Rimoin, D. L. (2012). Early-onset osteoarthritis in Ehlers-Danlos syndrome type VIII. *Am. J. Med. Genet. A* 158, 938–941. doi:10.1002/ajmg.a.35261

Reinstein, E., Delozier, C. D., Simon, Z., Bannykh, S., Rimoin, D. L., and Curry, C. J. (2013). Ehlers-Danlos syndrome type VIII is clinically heterogeneous disorder associated primarily with periodontal disease, and variable connective tissue features. *Eur. J. Hum. Genet.* 21, 233–236. doi:10.1038/ejhg.2012.132

Richards, S., Aziz, N., Bale, S., Bick, D., Das, S., Gastier-Foster, J., et al. (2015). Standards and guidelines for the interpretation of sequence variants: A joint consensus recommendation of the American College of medical genetics and Genomics and the association for molecular pathology. *Genet. Med.* 17, 405–424. doi:10.1038/gim.2015.30

Riihilä, P., Nissinen, L., Knuutila, J., Nezhad, P. R., Viiklepp, K., and Kähäri, V. M. (2019). Complement system in cutaneous squamous cell carcinoma. *Int. J. Mol. Sci.* 20, 3550. doi:10.3390/ijms20143550

Riihilä, P., Viiklepp, K., Nissinen, L., Farshchian, M., Kallajoki, M., Kivisaari, A., et al. (2020). Tumour-cell-derived complement components C1r and C1s promote growth of cutaneous squamous cell carcinoma. *Br. J. Dermatol.* 182, 658–670. doi:10.1111/bjd.18095

Ritelli, M., Cinquina, V., Venturini, M., Pezzaioli, L., Formenti, A. M., Chiarelli, N., et al. (2019). Expanding the clinical and mutational spectrum of recessive AEBP1-related classical-like Ehlers-Danlos syndrome. *Genes (Basel)* 10, 135. doi:10.3390/genes10020135

Sethi, S., Nester, C. M., and Smith, R. J. H. (2012). Membranoproliferative glomerulonephritis and C3 glomerulopathy: Resolving the confusion. *Kidney Int.* 81, 434–441. doi:10.1038/ki.2011.399

Smith, R. J. H., Appel, G. B., Blom, A. M., Cook, H. T., D'Agati, V. D., Fakhouri, F., et al. (2019). C3 glomerulopathy — Understanding a rare complement-driven renal disease. *Nat. Rev. Nephrol.* 15, 129–143. doi:10.1038/s41581-018-0107-2

Spranger, S., Spranger, M., Kirchhof, K., and Steinmann, B. (1996). Ehlers-Danlos syndrome type VIII and leukodystrophy [3]. *Am. J. Med. Genet.* 66, 239–240. doi:10.1002/(SICI)1096-8628(19961211)66:2<239::AID-AJMG23>3.0.CO;2-T

Stewart, R. E., Hollister, D. W., and Rimoin, D. L. (1977). A new variant of ehlers-danlos syndrome: An autosomal dominant disorder of fragile skin, abnormal scarring, and generalized periodontitis. *Birth Defects Orig. Artic. Ser.* 13, 85–93.

Stock, F., Hanisch, M., Lechner, S., Biskup, S., Bohring, A., Zschocke, J., et al. (2021). Prepubertal periodontitis in a patient with combined classical and periodontal ehlers–danlos syndrome. *Biomolecules* 11, 149. doi:10.3390/biom11020149

Stojan, G., and Petri, M. (2018). Epidemiology of systemic lupus erythematosus: An update. *Curr. Opin. Rheumatol.* 30, 144–150. doi:10.1097/BOR.0000000000000480

Stolovitzky, J. P., and Todd, N. W. (1990). Autoimmune hypothesis of acquired subglottic stenosis in premature infants. *Laryngoscope* 100, 227–230. doi:10.1288/00005537-199003000-00003

Stolovitzky, J. P., Todd, N. W., Cotton, R. T., and Campbell, W. G. (1997). Autoimmune hypothesis of acquired subglottic stenosis: Lack of support at time of surgical repair in children. *Int. J. Pediatr. Otorhinolaryngol.* 38, 255–261. doi:10.1016/S0165-5876(96)01452-8

Strate, L. L., and Morris, A. M. (2019). Epidemiology, pathophysiology, and treatment of diverticulitis. *Gastroenterology* 156, 1282–1298.e1. doi:10.1053/j.gastro.2018.12.033

Tajima, S., and Pinnell, S. R. (1996). Ascorbic acid preferentially enhances type I and III collagen gene transcription in human skin fibroblasts. *J. Dermatol Sci.* 11, 250–253. doi:10.1016/0923-1811(95)00640-0

Vanderver, A., Prust, M., Tonduti, D., Mochel, F., Hussey, H. M., Helman, G., et al. (2015). Case definition and classification of leukodystrophies and leukoencephalopathies. *Mol. Genet. Metab.* 114, 494–500. doi:10.1016/j.ymgme.2015.01.006

Wang, L., Wang, F.-S., and Gershwin, M. E. (2015). Human autoimmune diseases: A comprehensive update. *J. Intern Med.* 278, 369–395. doi:10.1111/joim.12395

Wu, J., Yang, J., Zhao, J., Wu, J., Zhang, X., Leung, W. K., et al. (2018). A Chinese family with periodontal Ehlers–Danlos syndrome associated with missense mutation in the C1R gene. *J. Clin. Periodontol.* 45, 1311–1318. doi:10.1111/jcpe.12988

frontiers | Frontiers in Genetics

TYPE Original Research
PUBLISHED 16 August 2023
DOI 10.3389/fgene.2023.1238209

OPEN ACCESS

EDITED BY
Fan Jin,
Zhejiang University, China

REVIEWED BY
Ingrid Hausser,
Heidelberg University Hospital, Germany
Hiroki Yagi,
The University of Tokyo Hospital, Japan
Bart Wagner,
Royal Hallamshire Hospital,
United Kingdom

*CORRESPONDENCE
Shujiro Hayashi,
shayashi@dokkyomed.ac.jp

RECEIVED 11 June 2023
ACCEPTED 03 August 2023
PUBLISHED 16 August 2023

CITATION
Ishikawa S, Hayashi S, Sairenchi T, Miyamoto M, Yoshihara S, Kobashi G, Yamaguchi T, Kosho T and Igawa K (2023), Clinical features and morphology of collagen fibrils in patients with vascular Ehlers–Danlos based on electron microscopy.
Front. Genet. 14:1238209.
doi: 10.3389/fgene.2023.1238209

Clinical features and morphology of collagen fibrils in patients with vascular Ehlers–Danlos based on electron microscopy

Satoko Ishikawa[1], Shujiro Hayashi[1]*, Toshimi Sairenchi[2], Manabu Miyamoto[3], Shigemi Yoshihara[3], Gen Kobashi[4], Tomomi Yamaguchi[5,6,7], Tomoki Kosho[5,6,7] and Ken Igawa[1]

[1]Department of Dermatology, School of Medicine, Dokkyo Medical University, Tochigi, Japan, [2]Medical Science of Nursing, School of Nursing, Dokkyo Medical University, Tochigi, Japan, [3]Department of Pediatrics, School of Medicine, Dokkyo Medical University, Tochigi, Japan, [4]Department of Public Health, School of Medicine, Dokkyo Medical University, Tochigi, Japan, [5]Department of Medical Genetics, School of Medicine, Shinshu University, Matsumoto, Japan, [6]Center for Medical Genetics, Shinshu University Hospital, Matsumoto, Japan, [7]Division of Clinical Sequencing, School of Medicine, Shinshu University, Matsumoto, Japan

Background: Vascular-type Ehlers–Danlos syndrome (vEDS) is caused by collagen III deficit resulting from heterogeneous mutations in *COL3A1*, which occasionally causes sudden death due to arterial/visceral rupture. However, it is difficult to conduct basic research on the pathophysiology of vEDS. Moreover, the number of patients with vEDS is small, limiting the number of available samples. Furthermore, the symptoms of vEDS may vary among family members, even if they share the same mutation. Accordingly, many aspects of the pathology of vEDS remain unknown. Therefore, we investigated the structural abnormalities in collagen fibrils and endoplasmic reticulum (ER) stress in skin samples using electron microscopy as well as their relationship with clinical symptoms in 30 patients with vEDS (vEDS group) and 48 patients without vEDS (disease-negative control group).

Methods: Differences between the two groups were evaluated in terms of the sizes of collagen fibrils using coefficient of variation (COV).

Results: COV was found to be significantly higher in the vEDS group than in the disease-negative control group, indicating irregularity in the size of collagen fibrils. However, in the vEDS group, some patients had low COV and seldom experienced serious complications and ER stress.

Conclusion: ER stress might affect collagen fibril-composing proteins. Moreover, as this stress varies among people based on environmental factors and aging, it may be the underlying cause of varying vEDS symptoms.

KEYWORDS

vascular Ehlers-Danlos syndrome, COL3A1, collagen III, endoplasmic reticulum stress, unfolded protein response, collagen fibril, electron microscopy

1 Introduction

Vascular-type Ehlers–Danlos syndrome (vEDS) is an autosomal dominant inherited disorder with an incidence of 1 in 100,000–250,000 people (Byers et al., 2017). This disorder is caused by a deficit in collagen III due to heterogeneous mutations in the α1 type III collagen gene *COL3A1*. As collagen III comprises homotrimers and normal and mutant pro α1(III) chains are produced with equal frequency, approximately 90% α1(III) trimers contain ≥1 mutant α-chain (Mao and Bristow, 2001). Furthermore, reduced expression of collagen III may affect the walls of hollow organs, including the uterus, intestines, and medium- and large-sized arteries, as well as the fragility of connective tissues. Remarkably, in addition to various characteristic clinical symptoms, such as translucent skin, easy bruising, characteristic facial appearance, small joint hypermobility, and acrogeria, patients with vEDS occasionally experience fatal complications, including macrovascular rupture, intestinal perforation, and uterine rupture during pregnancy (Shimaoka et al., 2010; Malfait et al., 2017). Moreover, these patients often experience their first major complication in their early 20s, and >80% of them exhibit at least one complication by the age of 40 years, reducing their average life expectancy to 48 years (Pepin et al., 2000).

Based on the relevant literature, the pathophysiology of vEDS remains unclear. In our previous study, we found no correlation between decreased levels of collagen III produced from cultured fibroblasts, gene mutations, and clinical symptoms among Japanese patients with vEDS (Shimaoka et al., 2010; Yamaguchi et al., 2023). Notably, only nonsense mutations are known to be of mild type and are associated with a high survival rate; however, these mutations are noted in only a few cases of vEDS (Byers et al., 2017). Conversely, no correlation has been reported between other gene mutation types and clinical complications. For example, in cases of the most frequent variants of glycine (Gly) mutation in the triple helix repeat of Gly-X-Y, even if the family member(s) of the patient have the same gene mutation, the types and severity of the associated complications vary (Pepin et al., 2014). Moreover, a few patients with almost no collagen III expression have no serious complications (Shimaoka et al., 2010). In other words, collagen III levels are reduced in cases of vEDS; however, it is unclear whether this is the only cause of varying vEDS symptoms.

In a previous study, electron microscopic (EM) findings of patients with vEDS revealed that they had collagen fibrils of different sizes compared with normal controls (Smith et al., 1997). Moreover, endoplasmic reticulum (ER) dilation was observed in skin fibroblasts of patients with vEDS, indicating ER stress. Notably, ER stress is a state in which proteins with abnormal conformations and those that did not undergo normal modification (unfolded proteins) accumulate in the lumen of ER, mainly because of physiological stress, which damages cells (Rutkowski and Kaufman, 2004; Schröder and Kaufman, 2005). However, in cases of vEDS, even in the absence of physiological factors, proteins that exceed the processing capacity are accumulated in ER. This can be attributed to the fact that abnormal proteins produced by the pathogenic allele fail to maintain the triple helix structure of collagen and stick to ER. This leads to the accumulation of defective unfolded peptide chains in ER, causing ER stress (Malfait et al., 2020). Recently, we hypothesized that fibroblasts reduce the expression of other synthetic proteins in collagen fibrils, such as cartilage oligomeric matrix protein (COMP), due to ER stress, resulting in abnormally sized collagen fibrils in patients with vEDS (Ishikawa et al., 2021). This finding suggests that the varying vEDS symptoms may not be attributed to only one factor (i.e., decrease in collagen III expression). For example, in a previous study, despite the fact that collagen III was a minor component of dermal collagen fibrils, its severe reduction resulted in small or variably sized collagen fibrils and dermal thinning (Mao and Bristow, 2001). Normally, collagen III is distributed from the papillary to the reticular layer of the dermis, and the deeper the layer, the lower the distribution of collagen III and the more the increase in collagen I levels, leading to the formation of thick and strong collagen fibrils (Keene et al., 1987). We have been investigating the reticular dermis, which physiologically comprises relatively little collagen III. Accordingly, dominant collagen fibril malformation could be difficult to explain only by pathological reduction of collagen III (Ishikawa et al., 2021). In cases of vEDS, the decrease in COMP may contribute to this issue.

To the best of our knowledge, no treatment has been established for vEDS to date. In 2010, a clinical trial reported that the use of celiprolol with β2-agonist vasodilatory properties reduces the risk of arterial dissection (Ong et al., 2010). However, it remains unclear whether celiprolol exerts its beneficial effect by improving the biomechanical integrity of the aortic wall (Dubacher et al., 2020). Recently, we encountered a case in which the skin sample collected before and after celiprolol administration showed an improvement in terms of abnormalities in the fibril size of collagen and ER dilation; however, the expression level of collagen III remained the same. Moreover, we collected unique samples from patients without abnormal collagen fibril sizes despite the presence of vEDS, and in some of these patients, no serious complications occurred. Therefore, we considered that the collagen fibril size abnormality and ER stress may be associated with vEDS complications. To date, only a few comprehensive studies have reported on gene variants, EM findings, collagen III production, and clinical symptoms, with no reports on patients with vEDS. Thus, in the present study, we aimed to evaluate these factors and their relationship with ER stress in patients with vED. Moreover, here we report a case of vEDS, with data analyzed before and after celiprolol administration, along with the aforementioned unique case with mild symptoms.

2 Materials and methods

2.1 Patients and samples

For the present analysis, we collected samples from 282 patients clinically suspected with hereditary disease of the connective tissue, including vEDS, who presented at our department between 2004 and 2022 and provided their informed consent.

The exclusion criteria were as follows: patients who did not undergo genetic analysis for *COL3A1*; those aged <17 years (excluding those with asymptomatic diagnoses based on the

information of their relatives); those who did not undergo skin biopsy for sample collection from unexposed upper arms; those who did not undergo analysis for the expression level of procollagen III in cultured fibroblasts; those without full information of clinical symptoms in the medical record; and those who had reduced procollagen III levels but no *COL3A1* mutations (Supplementary Figure S1). Notably, data regarding some cases of vEDS were obtained from our previous reports (Hayashi et al., 2020; 2022; Kida et al., 2022; Yamaguchi et al., 2023).

Two or more dermatologists and one geneticist with >15 years of experience recorded the presence of clinical symptoms during diagnosis based on the clinical diagnostic criteria reported in a previous study (Beighton et al., 1998; Malfait et al., 2017). Genetic analysis was performed using the Sanger sequencing method and panel analysis with a next-generation sequencer. The variant of the detected *COL3A1* was determined by ClinVer, GenomeAD v2.1.1, and PubMed and was evaluated according to the guidelines by the American College of Medical Genetics and Genomics/Association for Molecular Pathology (2015 ACMG/AMP guidelines) (Richards et al., 2015).

Further, the samples collected for the analysis were classified into the following groups: vEDS and disease-negative control (i.e., no *COL3A1* mutation and no decrease in procollagen III levels).

2.2 Method for measuring collagen fibrils

Notably, skin samples collected from the unexposed areas of the upper arm by biopsy were incubated with 2.5% glutaraldehyde (TAAB, Laboratories Equipment Ltd., England) diluted with 0.1 M phosphate buffer for ≥2 h; subsequently, these samples were fixed with 1% osmium acid (TAAB) for 90 min. Further, the fixed tissues were dehydrated with ethanol, embedded in epoxy resin (TAAB), and observed under a JEM-1011 electron microscope (JEOL, Japan).

To measure collagen fibrils, we used the method described in a previous study (Ishikawa et al., 2021). Details of the method are included in the Supplementary Material. We found that the count of collagen fibrils and measurement of the long diameter were >400 fibrils in 10 locations and <0.25 μm^2 (magnification, ×30,000), respectively. The obtained data were then analyzed using the Statistical Package for the Social Sciences, version 18 (SPSS, Inc.), and the coefficient of variation (COV) was calculated for the measurements of the long diameter of collagen fibrils in each 0.25-μm^2. Notably, COV is used to quantify the size differences in collagen fibrils.

2.3 Methods of collagen synthesis analysis in cultured dermal fibroblasts and measurement of newly synthesized collagen

Fibroblast cultures were obtained from the skin biopsy samples using the outgrowth method described in a previous study (Hata et al., 1988). Briefly, fibroblast cultures from the skin biopsy samples were established and labeled with 2,3-[3H] proline. Further, the newly synthesized collagen was detected by electrophoresis. We numerically quantified the band intensity using a previously reported established method (Shimaoka et al., 2010). The details of these methods are described in Supplementary Material. The expression levels of type III procollagen were lower in patients with vEDS than in normal controls; conversely, the expression levels of procollagen I were almost the same between the two groups. The results of two representative patients from the above groups are shown in Supplementary Figure S2.

2.4 Real-time reverse transcription-polymerase chain reaction (PCR) assay and ATF6 and COMP immunostaining

The methods used for real-time PCR and *ATF6* and *COMP* immunostaining are presented in the Supplementary Material.

2.5 Statistical analysis

Differences between two study groups were analyzed using Student's *t*-test. Meanwhile, differences between more than three groups were analyzed using Tukey's test. p values of ≤0.05 were considered significant. Data were presented as mean ± standard error of the mean. Statistical comparisons were conducted using SPSS, version 18 (SPSS, IBM. Chicago, United States).

3 Results

3.1 High COV of collagen fibrils in vEDS

In the EM analysis of horizontal cross-section of collagen fibrils, compared with the disease-negative and normal control groups, the vEDS group presented a more noticeable variation in the size of collagen fibrils. Figure 1 shows the EM findings of representative cases of each group. We calculated the long diameter and COV for each group. Notably, COV represents the scale of variation; if it is high, the collagen fibril diameters have a high variation. Overall, 30 patients with vEDS, 48 patients without vEDS (disease-negative control), and 5 controls were analyzed in this study (Supplementary Table S1). In the vEDS group, three patients had variant of unknown significance. Remarkably, disease-negative controls were patients suspected with a hereditary connective tissue disease based on clinical information, but their diagnosis of vEDS was ruled out by genetic testing and protein analysis. In the present study, the vEDS group included 27 patients, excluding 3 patients with variant of unknown significance. Further, statistical analysis was performed for the vEDS, disease-negative control, and normal control groups (Supplementary Figure S1).

Among all participants, there was no correlation between COV and age (Supplementary Figure S3A) or sex (data not shown). In patients with vEDS, there was no correlation between COV and expression of procollagen III from cultured fibroblasts and no correlation between COV and the type of mutation (data not shown). COV was significantly higher in the vEDS group (0.184 ± 0.005) than in the disease-negative (0.142 ± 0.004) and normal (0.128 ± 0.011) control groups. However,

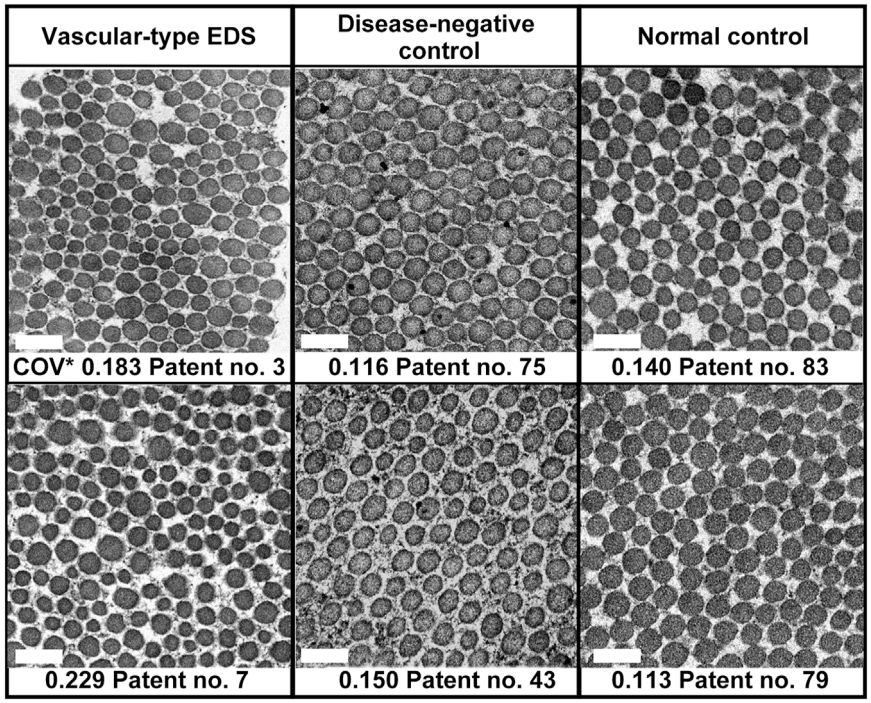

FIGURE 1
Age- and sex-matched representative electron microscopic (EM) findings of the horizontal cross-section of collagen fibrils. COV*, coefficient of variation. Magnification, ×30,000. Scale bar, 0.2 μm.

TABLE 1 Coefficient of variation of collagen fibrils and clinical symptoms of the vEDS group (n = 27).

Clinical symptoms	Positive COV ± SEM (n)[a]	Negative COV ± SEM (n)[a]	*p*-Value
Thin translucent skin	0.191 ± 0.006 (18)	0.171 ± 0.007 (9)	0.050
Arterial/intestinal/uterine fragility or rupture	0.188 ± 0.009 (16)	0.178 ± 0.005 (11)	0.353
Extensive bruising	0.185 ± 0.006 (20)	0.181 ± 0.007 (7)	0.620
Characteristic facial appearance	0.185 ± 0.009 (13)	0.183 ± 0.005 (14)	0.906
Acrogeria	0.186 ± 0.008 (9)	0.183 ± 0.006 (18)	0.791
Hypermobility of a small joint	0.186 ± 0.006 (16)	0.181 ± 0.009 (11)	0.629
Tendon and muscle rupture	0.181 ± 0.005 (6)	0.185 ± 0.006 (21)	0.621
Talipes equinovarus (clubfoot)	0.174 ± 0.009 (5)	0.186 ± 0.005 (22)	0.175
Early-onset varicose veins	(0)	(27)	-
Arteriovenous carotid-cavernous sinus fistula	0.186 ± 0.009 (7)	0.183 ± 0.005 (20)	0.860
Pneumothorax/pneumohemothorax	0.177 ± 0.006 (12)	0.190 ± 0.007 (17)	0.205
Gingival recession	0.172 ± 0.110 (2)	0.185 ± 0.005 (25)	0.426
Positive family history and sudden death of close relative(s)	0.176 ± 0.008 (7)	0.187 ± 0.006 (20)	0.318

[a]COV, coefficient of variation; SEM, standard error of the mean; (n), number of positive or negative patients.

there were no significant differences in COV between the disease-negative and normal control groups (Supplementary Figure S3B). We created a receiver-operating characteristic curve to confirm the high COV value and diagnostic reliability of vEDS (Supplementary Figure S3C). The area under the receiver-operating characteristic curve was found to be 0.861. In the vEDS and disease-negative control groups, when the cutoff value was set at 0.173 (Youden index) using SPSS version 18 (SPSS, Inc., Chicago, IL, United States), the sensitivity and specificity were 74.1% and 91.7%, respectively.

TABLE 2 Comparison between the high (>0.173) and low (<0.173) coefficient of variation subgroups.

	COV[a] > 0.173, *n* = 20	COV < 0.173, *n* = 7	*p*-Value
Age at diagnosis (Average ± SD[b])	37.0 ± 11.5	29.0 ± 7.2	0.046*
Numbers of females (F) and males (M)	F:11; M:9	F:2; M:5	
Procollagen III expression ± SEM[b]	13.0% ± 2.5%	10.7% ± 4.5%	0.657
COV ± SEM[c]	0.195 ± 0.04	0.154 ± 0.04	>0.00001*
Clinical symptoms	**Positive patients (%)**		
Thin translucent skin	15 (75%)	3 (43%)	0.187
Arterial/intestinal/uterine fragility or rupture	15 (75%)	1 (14%)	0.004*
Arterial dissection	12 (60%)	0%	>0.0001*
Extensive bruising	14 (70%)	6 (86%)	0.392
Characteristic facial appearance	11 (55%)	3 (43%)	0.612
Acrogeria	7 (35%)	2 (29%)	0.770
Hypermobility of a small joint	11 (55%)	5 (71%)	0.465
Tendon and muscle rupture	4 (20%)	2 (29%)	0.687
Talipes equinovarus (clubfoot)	3 (15%)	2 (29%)	0.519
Early-onset varicose veins	0%	0%	—
Arteriovenous, carotid-cavernous sinus fistula	6 (30%)	1 (14%)	0.392
Pneumothorax/pneumohemothorax	7 (35%)	5 (71%)	0.119
Gingival recession	1 (5%)	1 (14%)	0.588
Positive family history and sudden death of close relative(s)	5 (25%)	2 (29%)	0.371

[a]COV, coefficient of variation.
[b]SD, standard deviation.
[c]SEM, standard error of the mean.
*Significant difference, $p < 0.05$.

3.2 COV and clinical symptoms of the vEDS group

Regarding the typical clinical information of patients with vEDS, we compared COVs between the positive and negative groups for each symptom. The results are shown in Table 1. No clinical symptoms were found to be significantly correlated with COV values. In patients with thin translucent skin, the value tended to be high ($p = 0.050$), although it was not significant.

3.3 Clinical symptoms between the low and high COV subgroups in the vEDS group

In a few cases, despite the presence of vEDS, COV was not high. Further, using a cutoff value of 0.172 (Youden index), we compared patients in the high (20) and low COV subgroups (7) (Table 2). There was no significant difference in sex or procollagen III expression between the two subgroups; however, there was a significant difference in age at the time of diagnosis ($p = 0.046$). Notably, arterial/intestinal/uterine fragility or rupture and arterial dissection were predominant in the high COV subgroup ($p = 0.004$ and 0.079, respectively). No significant differences were noted in other major clinical information.

3.4 Summary of seven patients in the low COV subgroup

Here we report the cases of patients with low COV and no serious complications despite the presence of vEDS. Figure 2 shows the results of collagen expression analysis and EM findings of six patients. The expression of procollagen III was decreased in all patients, although there was no correlation between COV and procollagen III expression. Moreover, there was no common background among these patients in terms of medical histories, living histories, or environmental factors. Notably, patient 15 was the only patient in the low COV group who had organ and vessel rupture. This patient was a 42-year-old (at the time of diagnosis) woman who became pregnant with twins following fertility treatment and presented with massive uterine bleeding at 25 weeks of gestation. Being pregnant with twins is believed to have had significant effects and stress on her body.

3.5 Mild ER dilation of fibroblasts in the low COV subgroup with vEDS

We compared the characteristics of fibroblasts among the high COV, low COV, and normal control groups. In each group, we

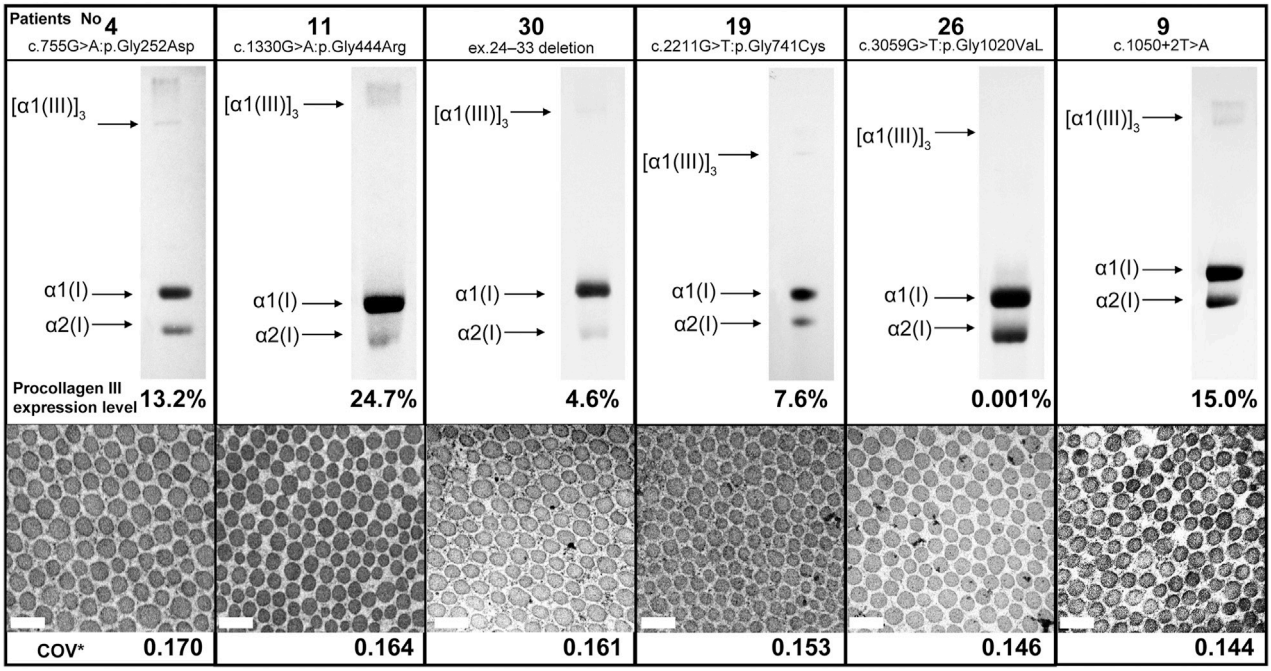

FIGURE 2
Procollagen expression analysis and collagen fibril findings of six patients from the low coefficient of variation subgroup. There was no correlation between COV and procollagen III expression. Magnification, ×30,000. Scale bar, 0.2 μm. COV*, coefficient of variation.

identified 20–30 fibroblasts from skin biopsy samples. Figure 3 shows representative EM findings (fibroblast) of each group. In the high COV subgroup, almost all cells had ER dilation (Figures 3A, B). Conversely, in the low COV subgroup, we observed mildly dilated or nondilated ER (Figures 3C, D). Normal controls exhibited no dilation of ER, except for a few cells (Figures 3E, F).

3.6 Expression of the ER stress markers ATF6 and COMP in the low COV subgroup with vEDS

To analyze the ER stress markers and *COMP*, we performed real-time PCR on mRNA obtained from cultured fibroblasts.

Notably, during ER stress, the function of inducing cell apoptosis or removing defective proteins is enhanced as a biological defense mechanism (i.e., ER stress response). Several markers are known to increase mRNA expression during ER stress. Among them, *CHOP*, *PEEK*, *IRE1*, etc. play a role in inducing cell apoptosis and avoiding ER stress as an ER stress response (Ron and Walter, 2007). However, in our study, none of these markers were significantly elevated in patients with vEDS (data not shown).

Conversely, activating transcription factor 6 (*ATF6*) is also one of the ER stress markers and is related to the elimination of defective protein; moreover, the mRNA expression of *ATF6* is increased in the ER stress condition (Wu et al., 2007). COMP is a binding partner protein for collagen fibrils, and it is known to cause ER stress and decrease the level of collagen protein in COMP-knockout mice (Schulz et al., 2016). In our previous analysis of mRNA obtained from skin fibroblast cultures of four patients with vEDS, we found that *ATF6* was significantly higher in these patients than in the normal controls, although the expression of *COMP* was significantly lower (Ishikawa et al., 2021).

In this study, we compared the mRNA expression levels of *ATF6* and *COMP* among the high and low COV subgroups, disease-negative group, and normal control group. *ATF6* was significantly higher in the high COV subgroup than in the low COV subgroup. The expression levels of *ATF6* were higher in the low COV subgroup than in the disease-negative and normal control groups, but there was no significant difference in these levels between the groups (Supplementary Figure S4A). In the high COV subgroup, the expression level of COMP was significantly lower than that in the low COV subgroup (Supplementary Figure S4B).

3.7 A case report of vEDS, with data analyzed before and after celiprolol administration

In this study, we presented an interesting case (patient 13) of vEDS with a heterozygous pathogenic variant (c.1484G>A; p. Gly495Glu) in *COL3A1* resulting in the rupture of the left lower leg artery. This patient was treated with celiprolol; the patient did not have hypertension but had an aneurysm in the iliac artery. A skin biopsy was performed before and after celiprolol administration. After 3 years of celiprolol administration, no aneurysm developed, and there was no serious adverse event. Moreover, the expression level of procollagen III did not change (Figures 4A,B), although the size differences in collagen fibrils

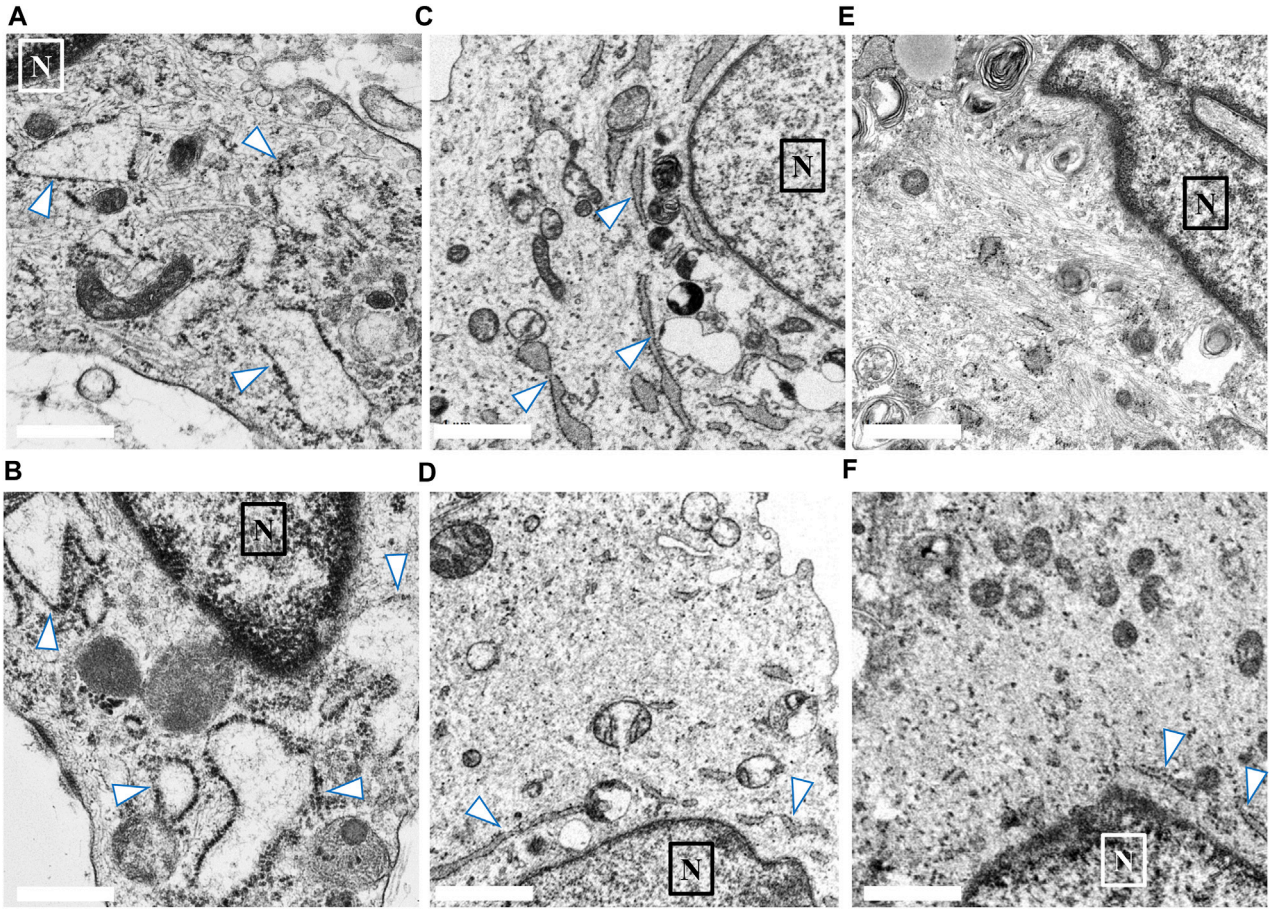

FIGURE 3
Findings of endoplasmic reticulum (ER; arrow) noted in the skin biopsy samples of the high and low coefficient of variation (COV) vascular-type Ehlers–Danlos syndrome (vEDS) subgroups and the control group. In the high COV subgroup, almost all cells showed ER dilation **(A, B)**. Conversely, in the low COV subgroup, mildly dilated or nondilated ER was observed **(C, D)**. Normal controls exhibited no dilation of ER, except for a few cells **(E, F)**. Magnification, ×50,000. Scale bar, 0.1 μm. N, nucleus.

improved (Figures 4C,D), and ER dilation was no longer noted (Figures 4E,F). Immunofluorescence staining for biopsy samples revealed strong ATF6 staining; however, COMP staining was not observed before celiprolol administration, but after administration, the expression of ATF6 decreased and COMP staining was confirmed (Figures 4G,H).

4 Discussion

In the present study, we summarized the background and conditions for skin sampling as much as possible and used COV quantification, reporting a novel finding of less serious complications of vascular events in patients with vEDS and low COV. Notably, in vEDS, symptoms vary among family members even if they share the same mutation. This is a new finding that may be related to individual variability in vEDS symptoms. Moreover, we described a case showing an improvement in abnormalities in the fibril size of collagen and ER dilation after celiprolol administration. However, although the effect of celiprolol against vEDS is important because it suggests a relationship among abnormalities in collagen fibril morphology, ER stress, and occurrence of serious complications, it remains unresolved to date.

In our previous study, we focused on the fact that skin samples from infants without vEDS show differences in collagen fibril size similar to those from patients with vEDS, suggesting that mixing of such fibrils with the newly regenerated small collagen fibrils (also observed in infants) resulted in the observed size difference (Ishikawa et al., 2021). Moreover, we found that ER-stressed fibroblasts had reduced expression levels of the constituent proteins of collagen fibrils, such as COMP, possibly leading to fragile collagen fibrils (Ishikawa et al., 2021). Among heterogeneous mutations in *COL3A1*, in the presence of splice or glycine mutations, collagen III is extremely reduced throughout life because of the dominant negative effect (Malfait et al., 2020). However, usually, patients with vEDS do not develop major symptoms by the age of 20 years (Frank et al., 2019), and even if they have the same glycine missense pathogenic variants, their symptom type and timing differ (Shimaoka et al., 2010). This suggests that other factors besides decreased collagen III also play a role in the appearance of symptoms. Notably, numerous defective peptide chains produced by the dominant negative effect accumulate

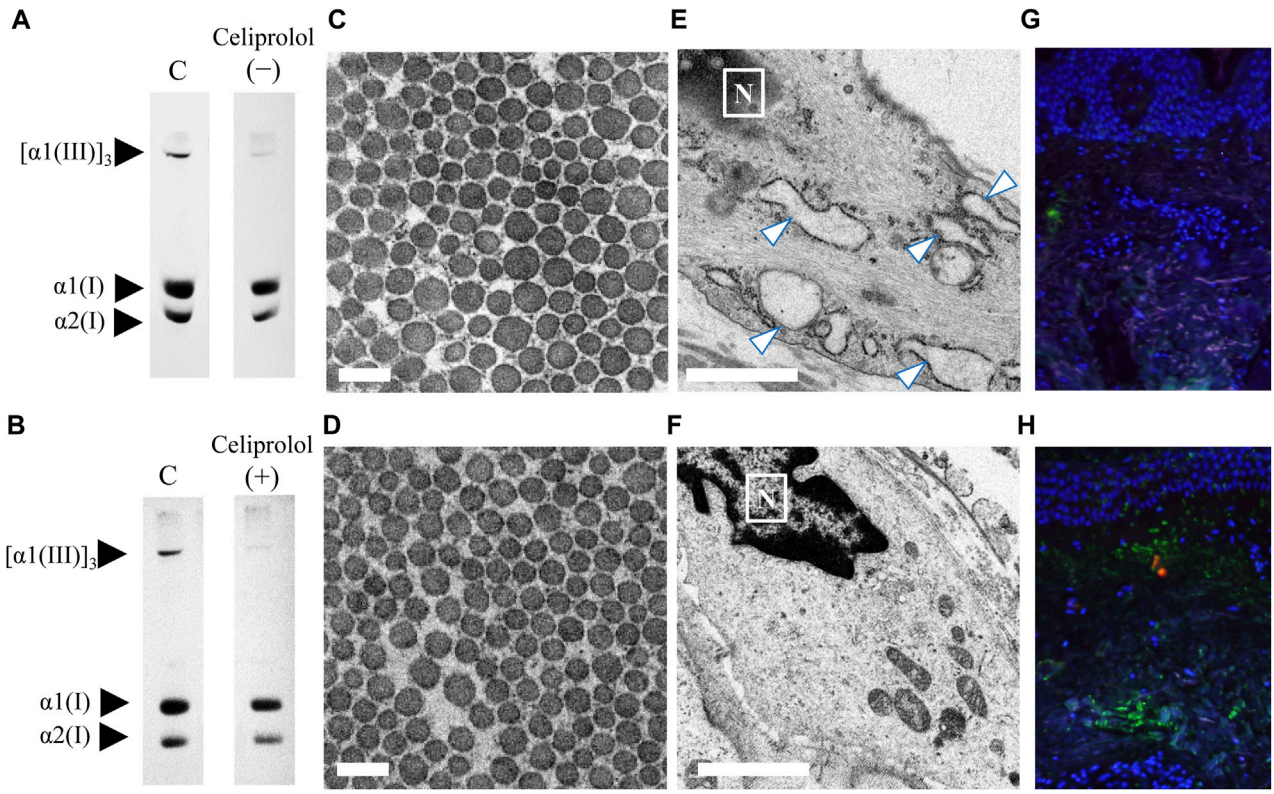

FIGURE 4
Analysis of skin biopsy samples before and after the administration of celiprolol. The expression levels of procollagen III were almost the same before **(A)** and after **(B)** celiprolol administration. There was a difference in the size of collagen fibrils before celiprolol administration **(C)**; however, the size became similar after the administration **(D)**. Magnification, ×30,000. Scale bar, 0.2 μm. Expanded endoplasmic reticulum (arrow) of fibroblasts before celiprolol administration **(E)** and normal endoplasmic reticulum after the administration **(F)**. Immunofluorescence staining of *ATF6* (red) and *COMP* (green) revealed increased ATF6 expression but decreased COMP expression before celiprolol administration **(G)**; the expression was contrary after celiprolol administration **(H)**. DAPI (blue) indicates the nucleus.

in ER, leading to ER stress. Further, owing to the influence of environmental and genetic factors, there are individual differences in ER stress response (Ramos-Lopez et al., 2018). If a patient with vEDS has high resistance to ER stress, the accumulated defective peptide chain in ER can be eliminated even if there is a decrease in collagen III expression due to genetic reasons; further, the influences of ER stress and expression of other proteins are in turn assumed to be small. This finding may explain individual differences in symptoms among patients with vEDS.

To the best of our knowledge, no targeted therapy is available for vEDS, and there is no consensus on its clinical management (Brooke, 2010). There are several reasons why evidence on the pathophysiology and treatment of vEDS has not been accumulated in the literature. First, the lack of a mouse model for effective experiments over a long time leads to a reproduced human phenotype. Second, although the recently reported transgenic mice are expected to be used in pharmacological studies for vascular events in vEDS (Dhondt et al., 2018), there are some issues such as differences in the distribution of collagen III expression between organs of mice and humans (Kuivaniemi and Tromp, 2019). Therefore, it may be difficult to use such a model in fatal complications involving other organs, such as gastrointestinal perforation. Third, it is challenging to investigate vEDS in prospective cohort studies because of the small number of patients and difficulties related to the assessment of therapy for preventing complications. Fourth, owing to legal and ethical implications, it is normally difficult to collect many samples via multiple skin biopsies from one patient. In addition, it is impossible to obtain tissue samples from organs associated with serious complications, and research is mainly conducted on skin tissue samples obtained from a single biopsy. Fifth, in fibroblasts from organs other than the skin, the effect of ER stress status and expression of proteins other than collagen III, such as COMP, cannot be assessed. Sixth, it is difficult to maintain reproducibility in experiments with fibroblasts after repeated passages. Even in fibroblasts from a group of patients with low COV who do not exhibit ER stress, repeated passage can exacerbate ER stress. Briefly, the above issues pose some obstacles in the development of basic research on vEDS.

To date, studies published in the literature have focused on the morphology of collagen fibrils and ER stress, as determined by EM, in patients with vEDS (Smith et al., 1997; Redman et al., 2021). Redman et al. (2021) suggested that treating vEDS would alleviate ER stress. These literatures show the presence of much severely expanded protein filled dermal fibroblast than those seen in our study. We are unable to offer an explanation as to how it is that despite careful search none of the fibroblasts in our samples show this so much expanded. The difference between their study

and the present study is that in the present study, more cases and detailed clinical findings were reported and comprehensive comparisons were made with observation sites and age-matched controls. However, the present study had a few additional limitations. Although various clinical findings were made in patients with vEDS, the present analysis was based on symptoms at the time of diagnosis and did not examine symptoms occurring after diagnosis. Our results suggested that serious clinical findings at this time point might be predictable using EM findings. In other words, in our study, the risk of developing serious complications was only predicted at the time of biopsy. If the patients are too young, the vEDS symptoms may not yet be manifested. Therefore, we included patients aged ≥17 years to standardize the background of the analyzed population. Nevertheless, it should be noted that the low COV subgroup had significantly younger patients. Further, it is known that ER stress is exacerbated by aging (Naidoo, 2009). In a previous study, the occurrence of ER stress, which could affect the COV of collagen fibrils, was considered in terms of genetic and environmental factors (Ramos-Lopez et al., 2018; Ishikawa et al., 2021). However, the kind of factors affecting ER stress in patients with vEDS remains unknown. Moreover, in this study, we could not find any common backgrounds between the high and low COV subgroups.

In conclusion, vEDS is a rare disease; therefore, clinical cohort studies on this disease are limited. Furthermore, to the best of our knowledge, no patient other than the present case could be analyzed before and after administration of celiprolol; therefore, the mechanism of action of celiprolol on vEDS remains unclear. Many control groups were included in the present study, and genetic testing, protein expression analysis, and EM analysis were performed for all patients to support the reliability of our results. We believe that our results provide several clues to elucidate the novel pathophysiology of vEDS. Future studies are warranted to clarify the improvement in collagen fibril formation, whether ER stress could become a new potential therapeutic target to reduce the risk of fatal complications, including vascular lesions, and whether monitoring of ER stress in skin tissue can contribute to the prediction of ER stress status in other important organs.

Data availability statement

The datasets presented in this study can be found in online repositories. The names of the repository/repositories and accession number(s) can be found in the article/Supplementary Material.

Ethics statement

The studies involving humans were approved by the institutional review board of Dokkyo Medical University (approval No. R-19-6J). The studies were conducted in accordance with the local legislation and institutional requirements. Written informed consent for participation in this study was provided by the participants' legal guardians/next of kin. Written informed consent was obtained from the individuals for the publication of any potentially identifiable images or data included in this article.

Author contributions

Conceptualization: SH; data curation: SH, TS, and GK; formal analysis: SI, TS, and GK; funding acquisition: SH, MM, and SY; investigation: SH, SI, TK, and TY; project administration: SH; supervision: TK and KI; writing–original draft preparation: SH. All authors contributed to the article and approved the submitted version.

Funding

This study was supported by a grant from Dokkyo Medical University, Project Research Grant (No. 2018-18) and a Japanese Dermatological Association Basic Medical Research grant from Shiseido (DB 2003-03). The funder was not involved in the study design, collection, analysis, interpretation of data, the writing of this article or the decision to submit it for publication.

Acknowledgments

We also thank Miki Kanno, Takashi Namatame, Kinichi Matsuyama, and Kazumi Akimoto for their technical assistance. We also would like to express our deepest gratitude to Professor Atsushi Hatamochi (died on 18 June 2018) for his great efforts in this research. Finally, we would like to thank the patients who participated in this study and all physicians nationwide who referred these patients to our department.

Conflict of interest

Part of this study was funded by NanoCarrier Co., Ltd.

The authors declare that the research was conducted in the absence of any commercial or financial relationships that could be construed as a potential conflict of interest.

Publisher's note

Supplementary material

The Supplementary Material for this article can be found online at: https://www.frontiersin.org/articles/10.3389/fgene.2023.1238209/full#supplementary-material

References

Beighton, P., De Paepe, A., Steinmann, B., Tsipouras, P., and Wenstrup, R. J. (1998). Ehlers–danlos syndromes: revised nosology, villefranche, 1997. Ehlers–Danlos national foundation (USA) and ehlers-danlos support group (UK). *Am. J. Med. Genet.* 77, 31–37. doi:10.1002/(sici)1096-8628(19980428)77:1<31::aid-ajmg8>3.0.co;2-o

Brooke, B. S. (2010). Celiprolol therapy for vascular Ehlers–Danlos syndrome. *Lancet* 376, 1443–1444. doi:10.1016/S0140-6736(10)61155-5

Byers, P. H., Belmont, J., Black, J., De Backer, J., Frank, M., Jeunemaitre, X., et al. (2017). Diagnosis, natural history, and management in vascular Ehlers–Danlos syndrome. *Am. J. Med. Genet. C Semin. Med. Genet.* 175, 40–47. doi:10.1002/ajmg.c.31553

D'hondt, S., Guillemyn, B., Syx, D., Symoens, S., De Rycke, R., Vanhoutte, L., et al. (2018). Type III collagen affects dermal and vascular collagen fibrillogenesis and tissue integrity in a mutant Col3a1 transgenic mouse model. *Matrix Biol.* 70, 72–83. doi:10.1016/j.matbio.2018.03.008

Dubacher, N., Münger, J., Gorosabel, M. C., Crabb, J., Ksiazek, A. A., Caspar, S. M., et al. (2020). Celiprolol but not losartan improves the biomechanical integrity of the aorta in a mouse model of vascular Ehlers–Danlos syndrome. *Cardiovasc. Res.* 116, 457–465. doi:10.1093/cvr/cvz095

Frank, M., Adham, S., Seigle, S., Legrand, A., Mirault, T., Henneton, P., et al. (2019). Vascular ehlers–danlos syndrome: long-term observational study. *J. Am. Coll. Cardiol.* 73, 1948–1957. doi:10.1016/j.jacc.2019.01.058

Hata, R., Kurata, S., and Shinkai, H. (1988). Existence of malfunctioning pro alpha2(I) collagen genes in a patient with a pro alpha 2(I)-chain-defective variant of Ehlers-Danlos syndrome. *Eur. J. Biochem.* 174, 231–237. doi:10.1111/j.1432-1033.1988.tb14087.x

Hayashi, S., Lin, W., Hamasaki, Y., and Igawa, K. (2020). Vascular Ehlers–Danlos syndrome patient with a novel COL3A1 gene deletion mutation without alteration in the triple sequence of (Gly-X-Y) repeat. *J. Dermatol.* 47, e390–e391. doi:10.1111/1346-8138.15558

Hayashi, S., Yamaguchi, T., Kosho, T., and Igawa, K. (2022). Case report: mild phenotype of a patient with vascular ehlers–danlos syndrome and COL3A1 duplication mutation without alteration in the [Gly-X-Y] repeat sequence. *Front. Genet.* 13, 1017446. doi:10.3389/fgene.2022.1017446

Ishikawa, S., Kosho, T., Kaminaga, T., Miyamoto, M., Hamasaki, Y., Yoshihara, S., et al. (2021). Endoplasmic reticulum stress and collagenous formation anomalies in vascular-type Ehlers–Danlos syndrome via electron microscopy. *J. Dermatol.* 48, 481–485. doi:10.1111/1346-8138.15766

Keene, D. R., Sakai, L. Y., Bächinger, H. P., and Burgeson, R. E. (1987). Type III collagen can be present on banded collagen fibrils regardless of fibril diameter. *J. Cell Biol.* 105, 2393–2402. doi:10.1083/jcb.105.5.2393

Kida, A., Hayashi, S., Ueno, Y., Kitano, H., Nakada, Y., Asakura, Y., et al. (2022). Severe clinical manifestations in an extremely low birthweight preterm baby with vascular Ehlers–Danlos syndrome. *J. Dermatol.* 49, e411–e412. doi:10.1111/1346-8138.16493

Kuivaniemi, H., and Tromp, G. (2019). Type III collagen (COL3A1): gene and protein structure, tissue distribution, and associated diseases. *Gene* 707, 151–171. doi:10.1016/j.gene.2019.05.003

Malfait, F., Castori, M., Francomano, C. A., Giunta, C., Kosho, T., and Byers, P. H. (2020). The ehlers–danlos syndromes. *Nat. Rev. Dis. Prim.* 6, 64. doi:10.1038/s41572-020-0194-9

Malfait, F., Francomano, C., Byers, P., Belmont, J., Berglund, B., Black, J., et al. (2017). The 2017 international classification of the Ehlers–Danlos syndromes. *Am. J. Med. Genet. C Semin. Med. Genet.* 175, 8–26. doi:10.1002/ajmg.c.31552

Mao, J. R., and Bristow, J. (2001). The ehlers–danlos syndrome: on beyond collagens. *J. Clin. Invest.* 107, 1063–1069. doi:10.1172/JCI12881

Naidoo, N. (2009). ER and aging-protein folding and the ER stress response. *Ageing Res. Rev.* 8, 150–159. doi:10.1016/j.arr.2009.03.001

Ong, K. T., Perdu, J., De Backer, J., Bozec, E., Collignon, P., Emmerich, J., et al. (2010). Effect of celiprolol on prevention of cardiovascular events in vascular ehlers–danlos syndrome: a prospective randomised, open, blinded-endpoints trial. *Lancet* 376, 1476–1484. doi:10.1016/S0140-6736(10)60960-9

Pepin, M. G., Schwarze, U., Rice, K. M., Liu, M., Leistritz, D., and Byers, P. H. (2014). Survival is affected by mutation type and molecular mechanism in vascular Ehlers–Danlos syndrome (EDS type IV). *Genet. Med.* 16, 881–888. doi:10.1038/gim.2014.72

Pepin, M., Schwarze, U., Superti-Furga, A., and Byers, P. H. (2000). Clinical and genetic features of Ehlers–Danlos syndrome type IV, the vascular type. *N. Engl. J. Med.* 342, 673–680. doi:10.1056/NEJM200003093421001

Ramos-Lopez, O., Riezu-Boj, J. I., Milagro, F. I., Moreno-Aliaga, M. J., and Martinez, J. A. (2018). Endoplasmic reticulum stress epigenetics is related to adiposity, dyslipidemia, and insulin resistance. *Adipocyte* 7, 137–142. doi:10.1080/21623945.2018.1447731

Redman, M. G., Wagner, B. E., Cadden, S., Baker, D., Bowen, J. M., Johnson, D., et al. (2021). Rough endoplasmic reticulum expansion: a consistent finding in a patient cohort with vascular ehlers-danlos syndrome and osteogenesis imperfecta. *Ultrastruct. Pathol.* 45, 414–420. doi:10.1080/01913123.2021.1979703

Richards, S., Aziz, N., Bale, S., Bick, D., Das, S., Gastier-Foster, J., et al. (2015). Standards and guidelines for the interpretation of sequence variants: a joint consensus recommendation of the American College of medical genetics and Genomics and the association for molecular pathology. *Genet. Med.* 17, 405–424. doi:10.1038/gim.2015.30

Ron, D., and Walter, P. (2007). Signal integration in the endoplasmic reticulum unfolded protein response. *Nat. Rev. Mol. Cell Biol.* 8, 519–529. doi:10.1038/nrm2199

Rutkowski, D. T., and Kaufman, R. J. (2004). A trip to the ER: coping with stress. *Trends Cell Biol.* 14, 20–28. doi:10.1016/j.tcb.2003.11.001

Schröder, M., and Kaufman, R. J. (2005). ER stress and the unfolded protein response. *Mutat. Res.* 569, 29–63. doi:10.1016/j.mrfmmm.2004.06.056

Schulz, J. N., Nüchel, J., Niehoff, A., Bloch, W., Schönborn, K., Hayashi, S., et al. (2016). COMP-assisted collagen secretion–a novel intracellular function required for fibrosis. *J. Cell Sci.* 129, 706–716. doi:10.1242/jcs.180216

Shimaoka, Y., Kosho, T., Wataya-Kaneda, M., Funakoshi, M., Suzuki, T., Hayashi, S., et al. (2010). Clinical and genetic features of 20 Japanese patients with vascular-type Ehlers–Danlos syndrome. *Br. J. Dermatol.* 163, 704–710. doi:10.1111/j.1365-2133.2010.09874.x

Smith, L. T., Schwarze, U., Goldstein, J., and Byers, P. H. (1997). Mutations in the COL3A1 gene result in the Ehlers–Danlos syndrome type IV and alterations in the size and distribution of the major collagen fibrils of the dermis. *J. Invest Dermatol.* 108, 241–247. doi:10.1111/1523-1747.ep12286441

Wu, J., Rutkowski, D. T., Dubois, M., Swathirajan, J., Saunders, T., Wang, J., et al. (2007). ATF6alpha optimizes long-term endoplasmic reticulum function to protect cells from chronic stress. *Dev. Cell.* 13, 351–364. doi:10.1016/j.devcel.2007.07.005

Yamaguchi, T., Hayashi, S., Hayashi, D., Matsuyama, T., Koitabashi, N., Ogiwara, K., et al. (2023). Comprehensive genetic screening for vascular Ehlers–Danlos syndrome through an amplification-based next-generation sequencing system. *Am. J. Med. Genet. A* 191, 37–51. doi:10.1002/ajmg.a.62982

frontiers | Frontiers in Genetics

TYPE Original Research
PUBLISHED 30 August 2023
DOI 10.3389/fgene.2023.1234804

OPEN ACCESS

EDITED BY
Ammar Husami,
Cincinnati Children's Hospital Medical Center, United States

REVIEWED BY
Chiara Villa,
University of Milano-Bicocca, Italy
Joshi Stephen,
Baylor College of Medicine, United States

*CORRESPONDENCE
Tomomi Yamaguchi,
t_yamaguchi@shinshu-u.ac.jp
Tomoki Kosho,
ktomoki@shinshu-u.ac.jp

RECEIVED 05 June 2023
ACCEPTED 24 July 2023
PUBLISHED 30 August 2023

CITATION
Yamaguchi T, Yamada K, Nagai S, Nishikubo T, Koitabashi N, Minami-Hori M, Matsushima M, Shibata Y, Ishiguro H, Sanai H, Fujikawa T, Takiguchi Y, Matsumoto K-I and Kosho T (2023), Clinical and molecular delineation of classical-like Ehlers–Danlos syndrome through a comprehensive next-generation sequencing-based screening system.
Front. Genet. 14:1234804.
doi: 10.3389/fgene.2023.1234804

Clinical and molecular delineation of classical-like Ehlers–Danlos syndrome through a comprehen sive next-generation sequen cing-based screening system

Tomomi Yamaguchi[1,2,3]*, Kazuo Yamada[4,5], So Nagai[1,3,6], Toshiya Nishikubo[7], Norimichi Koitabashi[8], Masako Minami-Hori[9], Masaaki Matsushima[10,11], Yuka Shibata[11], Hiroki Ishiguro[12], Hiromi Sanai[13,14], Tomomi Fujikawa[3], Yuri Takiguchi[3], Ken-Ichi Matsumoto[4] and Tomoki Kosho[1,2,3,15]*

[1]Center for Medical Genetics, Shinshu University Hospital, Matsumoto, Japan, [2]Department of Medical Genetics, Shinshu University School of Medicine, Matsumoto, Japan, [3]Division of Clinical Sequencing, Shinshu University School of Medicine, Matsumoto, Japan, [4]Department of Biosignaling and Radioisotope Experiment, Interdisciplinary Center for Science Research, Head Office for Research and Academic Information, Shimane University, Izumo, Japan, [5]Department of Legal Medicine, Faculty of Medicine, Shimane University, Izumo, Japan, [6]Problem-Solving Oriented Training Program for Advanced Medical Personnel: NGSD (Next-Generation Super Doctor) Project, Matsumoto, Japan, [7]Division of Neonatal Intensive Care, Nara Medical University, Nara, Japan, [8]Department of Cardiovascular Medicine, Gunma University Graduate School of Medicine, Maebashi, Japan, [9]Division of Dermatology, Asahikawa City Hospital, Asahikawa, Japan, [10]Department of Neurology, Faculty of Medicine and Graduate School of Medicine, Hokkaido University, Sapporo, Japan, [11]Division of Clinical Genetics, Hokkaido University Hospital, Sapporo, Japan, [12]Department of Clinical Genetics, Graduate School of Medicine, University of Yamanashi, Chuo, Japan, [13]Department of Obstetrics and Gynecology, Yamaguchi Prefectural Grand Medical Center, Yamaguchi, Japan, [14]Department of Medical Genetics, Yamaguchi Prefectural Grand Medical Center, Yamaguchi, Japan, [15]Research Center for Supports to Advanced Science, Shinshu University, Matsumoto, Japan

Classical-like Ehlers–Danlos syndrome (clEDS) is an autosomal recessive disorder caused by complete absence of tenascin-X resulting from biallelic variation in *TNXB*. Thus far, 50 patients from 43 families with biallelic *TNXB* variants have been identified. Accurate detection of *TNXB* variants is challenging because of the presence of the pseudogene *TNXA*, which can undergo non-allelic homologous recombination. Therefore, we designed a genetic screening system that is performed using similar operations to other next-generation sequencing (NGS) panel analyses and can be applied to accurately detect *TNXB* variants and the recombination of *TNXA*-derived sequences into *TNXB*. Using this system, we identified biallelic *TNXB* variants in nine unrelated clEDS patients. *TNXA*-derived variations were found in >75% of the current cohort, comparable to previous reports. The current cohort generally exhibited similar clinical features to patients in previous reports, but had a higher frequency of gastrointestinal complications (e.g., perforation, diverticulitis, gastrointestinal bleeding, intestinal obstruction, rectal/anal prolapse, and gallstones). This report is the first to apply an NGS-based screening for *TNXB* variants and represents the third largest cohort of clEDS, highlighting the importance of increasing awareness of the risk of gastrointestinal complications.

KEYWORDS

Ehlers-Danlos syndrome, classical-like, *TNXB*, tenascin-X, connective tissue disorder

Introduction

The Ehlers–Danlos syndromes (EDSs) are a group of hereditary connective tissue disorders (HCTDs) characterized by skin hyperextensibility, joint hypermobility, and tissue fragility. They are classified into 14 subtypes based on symptoms and causative genes according to the 2017 International Classification (Malfait et al., 2017) and subsequent findings (Malfait et al., 2017). The classical-like type of EDS (clEDS) is an autosomal recessive disorder caused by complete absence of tenascin-X (TNX) resulting from biallelic variation in *TNXB*. The major criteria of clEDS include: 1) skin hyperextensibility, with velvety skin texture and absence of atrophic scarring; 2) generalized joint hypermobility, with or without recurrent dislocations; and 3) easily bruisable skin/spontaneous ecchymosis. The minor criteria include: 1) foot deformities, including broad/plump forefeet, brachydactyly with excessive skin, pes planus, hallux valgus, and piezogenic papules; 2) edema in the legs in the absence of cardiac failure; 3) mild proximal and distal muscle weakness; 4) axonal polyneuropathy; 5) atrophy of muscles in the hands and feet; 6) acrogeric hands, mallet finger(s), clinodactyly, and brachydactyly; and 7) vaginal/uteral/rectal prolapse (Brady et al., 2017; Malfait et al., 2017).

Next-generation sequencing (NGS) panel-based genetic screening is a useful approach for differentiating multiple subtypes of EDS and other HCTDs with overlapping clinical manifestations (Yamaguchi et al., 2023). However, the presence of the pseudogene *TNXA*, which is >97% identical to the 3′end of *TNXB* (exons 32–44), makes it challenging to detect *TNXB* variants by conventional NGS analysis (Demirdas et al., 2017). *TNXA* is located approximately 30 kb centromere-proximal to *TNXB*. The intervening 30-kb unit is duplicated in tandem, and can undergo non-allelic homologous recombination, resulting in 30-kb deletions that include the 3′end of *TNXB* or gene conversions (Figures 1A, B) (Morissette et al., 2015; Demirdas et al., 2017). A 120-bp deletion of *TNXB* exon 35–intron 35 (c.11435_11524 + 30del) (Figure 1B) and c.12174C>G,p.(Cys4058Trp) in exon 40 (Figure 1B) are indices of *TNXA*-derived variations (Morissette et al., 2015), and have been determined to be pathogenic (Demirdas et al., 2017).

Fifty patients from 43 families with biallelic *TNXB* variants have been identified (Burch et al., 1997; Schalkwijk et al., 2001; Voermans et al., 2009; Hendriks et al., 2012; Pénisson-Besnier et al., 2013; Sakiyama et al., 2015; Chen et al., 2016; Demirdas et al., 2017; Micale et al., 2019; Rymen et al., 2019; Brisset et al., 2020; Green et al., 2020; Colman et al., 2021; Watanabe et al., 2021; Al-Harbi et al., 2022; Santoreneos et al., 2022). The largest cohort of clEDS (20 patients) was reported by Green et al. (2020), and the second largest was reported by Demirdas et al. (2017), which comprised 11 patients from seven families previously reported by the same authors (Schalkwijk et al., 2001; Voermans et al., 2009; Hendriks et al., 2012) and six new patients from four families. Genetic testing of

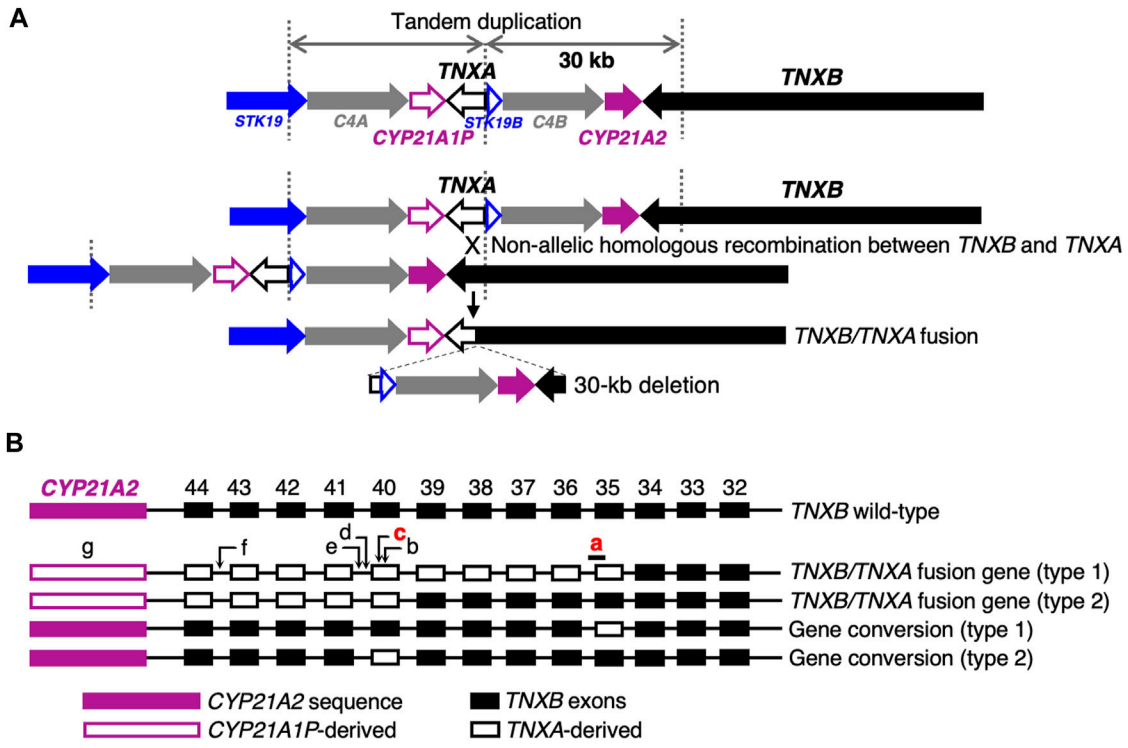

FIGURE 1
Schematic diagram of *TNXB/TNXA* fusion genes. **(A)** *TNXB/TNXA* fusion genes resulting from non-allelic homologous recombination between the *TNXA* pseudogene and *TNXB*, resulting in 30-kb deletions. **(B)** *TNXB/TNXA* fusion genes (type 1 and type 2) and gene conversions (type 1 and type 2). Seven indices of *TNXA*-derived variations are shown: **a**, 120-bp deletion (c.11435_11524 + 30del) in exon 35–intron 35; **b**, c.12150C>G,p.(Arg4050 =) in exon 40; **c**, c.12174C>G,p.(Cys4058Trp) in exon 40; **d**, c.12204 + 39dup in intron 40; **e**, c.12204 + 43T>G in intron 40; **f**, c.12628-52A>G in intron 43; **g**, *CYP21A2* deletion. Only a 120-bp deletion in exon 35–intron 35 and c.12174C>G in exon 40 shown in red have been reported to be pathogenic (Demirdas et al., 2017).

clEDS has been performed by Sanger sequencing using *TNXB*-specific primers, Sanger sequencing following long PCR using *TNXB*-specific primers for exons 32–44, and Sanger sequencing or NGS for other regions.

We describe here the development of a genetic screening system for the accurate detection of *TNXB* variants and *TNXA*-derived sequences recombined into *TNXB* that was designed to be performed similarly to other NGS panel analyses. This is also the third largest cohort and the first report of an Asian cohort of clEDS patients (eight Japanese; one Chinese), all of whom were found to have biallelic *TNXB* variation.

Materials and methods

Ethics statement

This study was approved by the Ethics Committee of Shinshu University School of Medicine (Nos. 435 and 628). Written consent was obtained from all participants before joining the study.

NGS panel

An NGS panel of 53 genes associated with various HCTDs, including *TNXB* and pseudogene *TNXA* (Supplementary Table S1), was designed by Ion AmpliSeq Designer (https://ampliseq.com/browse.action). *TNXA* was included for detection of *TNXA*-derived sequences recombined into *TNXB*.

Standard NGS panel analysis

Genomic DNA was extracted from peripheral blood using a QIAamp DNA Blood Mini Kit on a QIAcube (Qiagen, Valencia, CA, USA). Library preparation was performed using an Ion AmpliSeq Library Kit Plus (Thermo Fisher Scientific, Waltham, MA, USA). Sequencing was performed on an Ion Torrent system (Ion Chef and Ion GeneStudio S5) using an Ion 510 & 520 & 530 Kit—Chef and an Ion 520 Chip Kit (Thermo Fisher Scientific). Sequencing data were mapped using Torrent Suite software (Thermo Fisher Scientific) to human genome hg19, which masked exons 32–44 of *TNXB* and *TNXA* sequence by replacing them with "N"s. Single-nucleotide variants (SNVs) and small insertions/deletions were detected from the mapped data using the Torrent Variant Caller plug-in. Copy number variation (CNV) was analyzed using the CNV visualization method for amplification-based NGS data that was established by Nishio et al. (2018). The variants in *TNXB* were described using the NM_019105.6 transcript reference sequence, and the variant nomenclature was in accordance with the Human Genome Variation Society recommendations.

Modified NGS panel analysis using long PCR-amplified product

The method for library preparation of exons 32–44 of *TNXB* was identical to the standard NGS panel analysis, except that the template DNA was a long PCR product (diluted with water 1:200) amplified using the primer set reported by Micale et al. (2019). The forward primer, TNXB-ex31-F (5′-GTCTCTGCCCTGGGAATGA-3′; described as TNXB-LongPCR-F in Micale et al. (2019)), is a *TNXB*-specific sequence from *TNXB* exon 31, and the reverse primer, TNXB-ex44-R (5′-TGTAAACACAGTGCTGCGA-3′; described as TNXB-LongPCR-R in Micale et al. (2019)), was designed based on a common sequence of *TNXB* and *TNXA*, which is useful because it can also detect recombinant alleles. Library preparation was performed simultaneously with the standard NGS panel analysis. Libraries prepared to a concentration of 100 pM by an Ion AmpliSeq Library Kit Plus were mixed to match the number of amplicons and sequenced. The *TNXA* sequence of the human genome hg19 was masked by replacement with "N"s. However, because it was difficult to align fragments containing *TNXA*-derived 120-bp deletions to exon 35–intron 35 of *TNXB,* an exon 35/intron 35-homologous reference sequence of *TNXA* was not replaced with "N"s, and the fragments containing the *TNXA*-derived 120-bp deletions were aligned on *TNXA*. Additionally, a hotspot file to be called with or without a variant included one within exon 35 of *TNXB* and one within the exon 35-homologous sequence of *TNXA* (Supplementary Table S2). In other words, if both exon 35 of *TNXB* and the exon 35-homologous sequence of *TNXA* are called, the target is heterozygous for a *TNXA*-derived 120-bp deletion, whereas if exon 35 of *TNXB* is unable to produce a result because of lack of coverage (no call) and the exon 35-homologous sequence of *TNXA* is called, the target is homozygous for the *TNXA*-derived 120-bp deletions. A hotspot file also included c.12150C>G,p.(Arg4050 =) and c.12174C>G,p.(Cys4058Trp) in exon 40, c.12204 + 39dup and c.12204 + 43T>G in intron 40, and c.12628-52A>G in intron 43 as indices of the *TNXA*-derived variations (Figure 1B and Supplementary Table S2).

Sanger sequencing

SNVs and small deletions were confirmed by Sanger sequencing, which was performed on a 3500 Genetic Analyzer using a BigDye Direct Cycle Sequencing Kit with M13 tailed primers and a BigDye XTerminator Purification Kit (Thermo Fisher Scientific), according to the manufacturer's instructions. For SNVs and small deletions in exons 32–44 of *TNXB*, sequencing was performed using a long PCR-amplified product (diluted with water 1:50) as template DNA.

Phasing analysis

For Patient 6, long PCR was performed using primers TNXB-ex35-F (5′-AAACTCCAGGGGCTGATCC-3′), which binds specifically to normal exon 35 of *TNXB*, and TNXB-ex44-R, which binds to both *TNXB* and *TNXA*. Nested PCR of the region around exon 40 was performed using the long PCR-amplified product (diluted with water 1:50) as template DNA. For Patient 9, long PCR was performed using primers TNXB-ex26-F (5′-TGTGGGTGTGACAGGTGAGT-3′) and TNXB-ex35-R (5′-TGGTGAGGAAGCCTGTGAGA-3′), which bind specifically to normal exon 35 of *TNXB*. Nested PCR of the region around exon 27 was performed using the long PCR-amplified product (diluted with water 1:50) as template DNA. Sanger sequencing was performed as described above.

TABLE 1 Nine unrelated clEDS patients with homozygous or compound heterozygous pathogenic variants in *TNXB* (NM_019105.6).

Patient No.	Sex	Age at last observation (years)	Allele 1	Allele 2	Serum Tenascin-X
1	Female	60	Exons 2–3 deletion	Exons 2–3 deletion	N/A
2	Male	65	Gene conversion (type 1) including c.11435_11524 + 30del	Gene conversion (type 1) including c.11435_11524 + 30del	Absence
Son	Male	32	Gene conversion (type 1) including c.11435_11524 + 30del	–	N/A
3	Male	d.62	c.1650_1651del,p.(Glu552Argfs*41)	c.1650_1651del,p.(Glu552Argfs*41)	N/A
Daughter	Female	21	c.1650_1651del,p.(Glu552Argfs*41)	–	N/A
4	Female	27	c.10274C>G,p.(Ser3425*)	*TNXB/TNXA* fusion gene (type 1) including c.11435_11524 + 30del and c.12174C>G	N/A
Father	Male	N/A	c.10274C>G,p.(Ser3425*)	–	N/A
Mother	Female	N/A	–	*TNXB/TNXA* fusion gene (type 1) including c.11435_11524 + 30del and c.12174C>G	N/A
Brother	Male	N/A	–	*TNXB/TNXA* fusion gene (type 1) including c.11435_11524 + 30del and c.12174C>G	N/A
5	Female	47	c.6948del,p.(Asp2317Thrfs*53)	*TNXB/TNXA* fusion gene (type 1) including c.11435_11524 + 30del and c.12174C>G	Absence
Father	Male	77	–	*TNXB/TNXA* fusion gene (type 1) including c.11435_11524 + 30del and c.12174C>G	Reduction
Mother	Female	75	c.6948del,p.(Asp2317Thrfs*53)	–	Reduction
Sister	Female	52	–	*TNXB/TNXA* fusion gene (type 1) including c.11435_11524 + 30del and c.12174C>G	Reduction
6	Female	59	Gene conversion (type 2) including c.12174C>G	Gene conversion (type 2) including c.12174C>G	Absence
7	Male	61	Gene conversion (type 1) including c.11435_11524 + 30del	*TNXB/TNXA* fusion gene (type 2) including c.12174C>G	Absence
8	Female	8	c.8585G>A,p.(Trp2862*)	Gene conversion (type 1) including c.11435_11524 + 30del	N/A
Father	Male	48	–	Gene conversion (type 1) including c.11435_11524 + 30del	N/A
Mother	Female	48	c.8585G>A,p.(Trp2862*)	–	N/A
9	Female	69	c.9271dup,p.(Gln3091Profs*31)	*TNXB/TNXA* fusion gene (type 1) including c.11435_11524 + 30del and c.12174C>G	N/A

d, Died; N/A, not available.

Multiplex ligation-dependent probe amplification (MLPA) analysis

CNVs were confirmed by MLPA using a SALSA MLPA Kit P155-D2 (MRC-Holland, Amsterdam, Netherlands) for *TNXB* and *CYP21A2*. *CYP21A2* is a causative gene for autosomal recessive congenital adrenal hyperplasia due to 21-hydroxylase deficiency. MLPA analysis for *CYP21A2* was performed to confirm the presence of a 30-kb deletion, not to reveal the carrier status of autosomal recessive congenital adrenal hyperplasia. Electrophoresis was conducted on a 3500 Genetic Analyzer (Thermo Fisher Scientific) and the data were analyzed with Coffalyzer.Net (MRC-Holland).

Western blotting

Blood samples were centrifuged to separate serum and frozen at −80°C until use. Commercially available human sera (Lonza; BioWhittaker, Walkersville, MD, USA) were also used as a normal control. Western blotting was performed as described previously (Yamada et al., 2016).

Nano-liquid chromatography tandem mass spectrometry (nano-LC/MS/MS)

Blood samples were centrifuged to separate serum and frozen at −80°C until use. Commercially available human sera (Lonza;

TABLE 2 Detailed clinical features of the current cohort of patients with clEDS.

Patient No.	1	2	3	4	5	6	7	8	9	
Age at last observation (years)	60	65	d.62	27	47	59	61	8	69	
Sex	Female	Male	Male	Female	Female	Female	Male	Female	Female	
Ethnicity	Japanese	Japanese	Japanese	Japanese	Japanese	Chinese	Japanese	Japanese	Japanese	
Skin hyperextensibility	+	−	N/A	+	+	+	+	+	+	7/8 (87.5%)
Velvety skin texture	+	−	N/A	+	−	N/A	+	+	−	4/7 (57.1%)
Atrophic scarring	+	−	N/A	N/A	+	+	−	−	+	4/7 (57.1%)
Generalized joint hypermobility	+	− (only fingers and elbows)	N/A	+	+	+	− (only elbows and knees)	+	−	5/8 (62.5%)
Beighton score	N/A	N/A	N/A	N/A	6/9	N/A	4/9	9/9	2/9	
Recurrent dislocations	+	−	N/A	+(shoulder)	+	+(shoulder, finger, hip, toe)	+(shoulder)	+(finger)	+(shoulder, toe)	7/8 (87.5%)
Easily bruisable skin/spontaneous ecchymosis	+	+	N/A	+	+	+	+	+	+	8/8 (100%)
Eye bleeding	N/A	+(subconjunctiva)	N/A	N/A	+(conjunctiva)	N/A	N/A	+(sclera)	N/A	
Hand deformities	Acrogeric hands, mallet fingers, clinodactyly, brachydactyly	Acrogeric hands, brachydactyly	N/A	−	Acrogeric hands	N/A	N/A	Mallet fingers, brachydactyly	Acrogeric hands, clinodactyly, brachydactyly	5/6 (83.3%)
Foot deformities	Broad/plump forefoot, brachydactyly with excessive skin, pes planus, hallux valgus, piezogenic papules	Broad/plump forefoot, pes planus	N/A	−	Pes planus, hallux valgus	N/A	Pes planus	Broad/plump forefoot, pes planus, piezogenic papules	Broad/plump forefoot, brachydactyly with excessive skin, pes planus	6/7 (85.7%)
Skeletal features	NA	N/A	N/A	N/A	N/A	N/A	Pectus excavatum, scoliosis	Fractures	N/A	
Muscle weakness	+	N/A	N/A	−	+	N/A	N/A	−	+	3/5 (60.0%)

(Continued on following page)

10.3389/fgene.2023.1234804

TABLE 2 (*Continued*) Detailed clinical features of the current cohort of patients with clEDS.

Patient No.	1	2	3	4	5	6	7	8	9	
Muscle Atrophy	+	N/A	N/A	–	+	N/A	N/A	–	–	2/5 (40.0%)
Other musculoskeletal features	Distal inter-phalangeal joint pain	Muscle deficiencies	N/A	Meniscus injury, anterior cruciate ligament injury	N/A	N/A	N/A	N/A	N/A	
Cardiovascular abnormalities	N/A	Tetralogy of Fallot	N/A	–	Chronic heart failure, mitral regurgitation	Subcutaneous hematoma	Angina pectoris	Mitral regurgitation	Subcutaneous hematoma	
Hematoma	N/A	N/A	N/A	N/A	N/A	Subcutaneous, rectal	N/A	N/A	Subcutaneous	
Gastrointestinal features	Reflux esophagitis, multiple gastric polyps, low-grade tubular adenoma	Recurrent intestinal obstruction, colonic diverticulitis, rectal prolapse, gallstones, constipation	Intestinal obstruction	N/A	Small bowel diverticula and perforation, constipation, vomiting and diarrhea after eating	Anal prolapse, anal laceration, gallstones, appendicitis	Small bowl perforation, esophageal perforation, diverticulitis	Anal prolapse	Small bowl perforation, rectal prolapse, gallstones	8/8 (100%)
Urogenital features	N/A	–	N/A	N/A	N/A	N/A	Distended bladder, bladder diverticula, difficulty urinating	–	Difficulty urinating due to vaginal prolapse	
Hernia	N/A	–	N/A	N/A	N/A	N/A	Umbilical, inguinal	–	Abdominal wall incisional hernia after diaphragmatic hernia repair, hiatal hernia	
Others	Edema in the legs, axonal polyneuropathy	Translucent skin, skin striae, gingival recession, mandibular protrusion, migraine, hemopneumothrrax	N/A	N/A	Congenital cataract, generalized pain	Generalized and wandering pain, anxiety disorder, massive swelling after insect bites	Translucent skin	Stomatitis, peripheral cyanotic skin in cool environments, hyperventilation	Pulmonary embolism following gallbladder surgery, early Parkinson's disease	

d, died; N/A, not available.

10.3389/fgene.2023.1234804

BioWhittaker, Walkersville, MD, USA) were also used as a normal control. Measurement of the serum form of TNX (sTNX) concentration with AVAVSGLDPAR peptide was performed by using a quantitative nano-LC/MS/MS method as described previously (Yamada et al., 2016). The sTNX concentrations in each sample were measured three times and triplicate experiments were performed. Data are expressed as means ± standard error. The mass spectrometry proteomics data have been deposited to the ProteomeXchange Consortium via the PRIDE (Perez-Riverol et al., 2022) partner repository with the dataset identifier PXD043691.

Results

Nine unrelated patients with clEDS were found to have homozygous or compound heterozygous pathogenic variants in *TNXB* (Table 1). The variants for each allele were detected as follows: standard NGS panel analysis in Patients 1 and 3; modified NGS panel analysis using long PCR-amplified product in Patients 2, 6, and 7; and standard NGS panel analysis and modified NGS panel analysis using long PCR-amplified product in Patients 4, 5, 8, and 9. Results of modified NGS panel analysis using long PCR-amplified product were identical to those of Sanger sequencing or MLPA. Clinical and molecular features of the patient cohort are summarized in Table 2 and Figure 2, and detailed descriptions of each case are provided below.

Patient 1

Patient 1 is a 60-year-old Japanese woman who was referred to us as a suspected case of clEDS because of skin hyperextensibility, fragility, and bruisability of the skin, as well as joint hypermobility and recurrent dislocation. She had gastrointestinal complications, including reflux esophagitis, multiple gastric polyps, and colonic polyp(s), diagnosed as low-grade tubular adenomas. She presented with numbness in the hands and feet, suggestive of neuropathy.

The CNV visualization method for amplification-based NGS data (Nishio et al., 2018) revealed two copy losses spanning the start of exon 2 to the middle of exon 3 (Figure 3Aa). The start codon is in exon 2. The deletion breakpoints are unknown. MLPA also showed the two copy losses of exons 2 and 3 (Figure 3Ab).

Patient 2

Patient 2 is a 65-year-old Japanese man with tetralogy of Fallot that was surgically corrected at age 12 years. Subconjunctival hemorrhages and migraines were recurrent from age 28 years onwards. During open surgery for gallstones at age 34 years, he experienced excessive bleeding. At age 42 years, he developed bowel obstruction for which bowel resection surgery was complicated by difficulties in hemostasis and intestinal suture due to marked fragilities. Muscle defects in multiple organs were noted on histopathology. Pneumohemothorax occurred at age 44 years, which was treated with chest drainage followed by a thoracoscopic bullectomy, with no recurrence. Colonic diverticulitis occurred at age 47 years and was treated with antibiotics. He developed another bowel obstruction at age 54 years, for which bowel resection was performed. EDS was suspected on histopathology, and he was referred to our hospital for further assessment at age 56 years. His height was 162.4 cm (−1.4 standard deviation [SD]), weight was 51.3 kg (−1.1SD), and occipitofrontal circumference (OFC) was 56.2 cm (−0.9SD). He had jaw protrusion (Figure 4A), soft and wrinkled palms (Figure 4B), hypermobile and thick fingers (Figures 4C, D), skin hyperextensibility and translucency (Figure 4E), atrophic scars at surgical sutures (Figure 4F), valgus/flat feet with sole calluses (Figure 4G), skin striae, and gingival recession. His skin was thin and translucent, but not velvet-like. He was clinically suspected as having vascular EDS, and took alacepril to prevent arterial complications. His parents had no skin hyperextensibility or joint hypermobility. His son had generalized joint hypermobility in his preschool days, and a ligamental injury at the left ankle.

Modified NGS panel analysis using long PCR-amplified product detected a homozygous *TNXA*-derived 120-bp deletion in exon 35–intron 35 (c.11435_11524 + 30del). MLPA showed two copy losses of exon 35 in *TNXB* and a normal copy of *CYP21A2* (Figure 3Ba). Therefore, the patient was determined to have a type 1 gene conversion (Figure 1B). His son was found to have a one-copy loss of exon 35 in *TNXB* and a normal copy of *CYP21A2* (Figure 3Bb), confirming his carrier status for clEDS. Complete deficiency of sTNX in Patient 2 was detected through biochemical analysis using Western blotting (data not shown).

Patient 3

Patient 3 was a Japanese man who died from tongue cancer at age 62 years. He developed intestinal obstruction at age 55, which required colostomy. His daughter had abnormal scarring, soft skin, and hypermobility of the finger joints. At age 21 years, she was referred to us for evaluation regarding EDS, and was suspected to have vascular EDS. She experienced three uncomplicated pregnancies and deliveries.

Standard NGS panel analysis revealed that Patient 3 had a homozygous frameshift variant c.1650_1651del,p.(Glu552Argfs*41) in exon 3, which was confirmed by Sanger sequencing (Figure 3Ca). His daughter was found to be heterozygous for the variant (Figure 3Cb), and had no other pathogenic variants in related genes, including *COL3A1*.

Patient 4

Patient 4 is a 27-year-old Japanese woman who was referred to us at 32 weeks of gestation for suspected clEDS based on joint hypermobility (Figures 4H, I), hyperextensible, soft, and bruisable skin (Figure 4J), and recurrent dislocation. She had recurrent dislocation of the left shoulder, and underwent surgeries for meniscus injuries at ages 15 and 27 years. Cardiac ultrasonography detected no abnormalities.

Standard NGS panel analysis detected a heterozygous nonsense variant c.10274C>G,p.(Ser3425*) in exon 30, which was confirmed

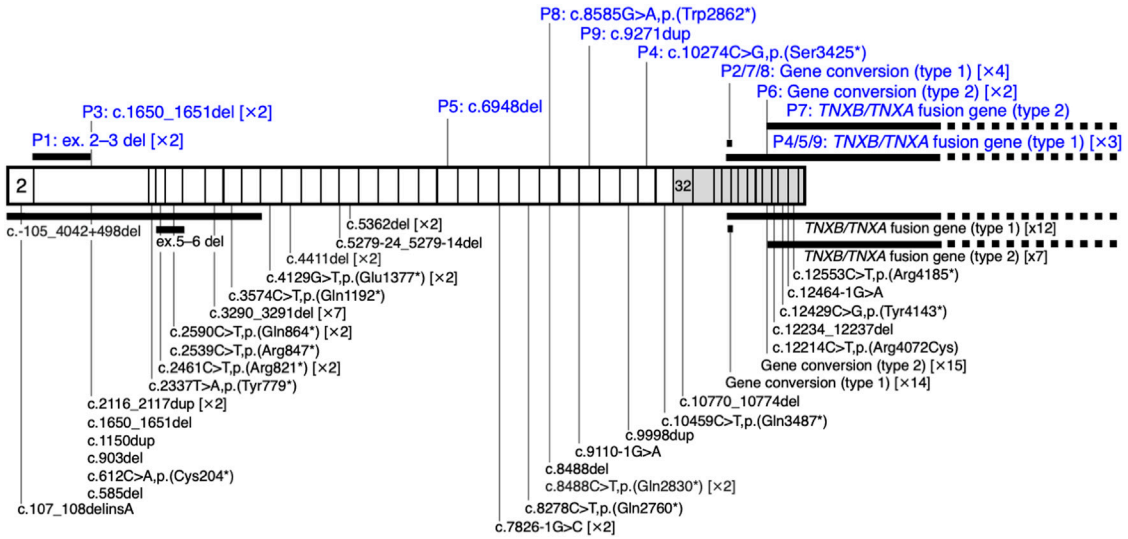

FIGURE 2
Schematic representation of the distribution of *TNXB* variants in a cohort of nine patients with clEDS. Illustration of *TNXB* variants based on NM_019105.6 of the NCBI reference sequence database (https://www.ncbi.nlm.nih.gov/RefSeq/). Exons 32–44 are highlighted with gray boxes. Variants found in the current study of patients (P)1–9 are shown in blue, above the mRNA transcript. Previously reported variants (Burch et al., 1997; Schalkwijk et al., 2001; Voermans et al., 2009; Hendriks et al., 2012; Pénisson-Besnier et al., 2013; Sakiyama et al., 2015; Chen et al., 2016; Demirdas et al., 2017; Micale et al., 2019; Rymen et al., 2019; Brisset et al., 2020; Green et al., 2020; Colman et al., 2021; Watanabe et al., 2021; Al-Harbi et al., 2022; Santoreneos et al., 2022) are shown below the mRNA transcript.

by Sanger sequencing (Figure 3D, left). Modified NGS panel analysis using long PCR-amplified product detected a heterozygous *TNXA*-derived 120-bp deletion in exon 35–intron 35 (c.11435_11524 + 30del), c.12150C>G,p.(Arg4050 =) and c.12174C>G,p.(Cys4058Trp) in exon 40, c.12204 + 39dup and c.12204 + 43T>G in intron 40, and c.12628-52A>G in intron 43. The four variants in exon 40 and intron 40 were confirmed by Sanger sequencing (data not shown). MLPA showed a one-copy loss of exon 35 in *TNXB* and a one-copy loss of *CYP21A2* (Figure 3D, right). Sanger sequencing and MLPA analysis were also performed on her parents, which revealed the heterozygous nonsense variant in her father and the single copy loss of exon 35 in *TNXB* and *CYP21A2* in her mother (Figure 3D). Therefore, it was determined that Patient 4 was compound heterozygous for the nonsense variant and a type 1 *TNXB/TNXA* fusion gene (Figure 1B). Her brother was found to have a one-copy loss of exon 35 in *TNXB* and *CYP21A2* (Figure 3D), confirming his carrier status for clEDS.

Patient 5

Patient 5 is a 47-year-old Japanese woman referred to us for a suspected diagnosis of EDS. She underwent surgery for congenital cataract. She was readily bruisable and experienced recurrent dislocation as a young child. At age 43 years, she suffered from recurrent intestinal perforation associated with multiple diverticula of the intestine. She has chronic heart failure associated with mitral valve regurgitation, generalized joint hypermobility (Beighton score 6/9) (Figures 4K, L), recurrent dislocation, skin hyperextensibility, redundancy, and bruisability (Figures 4M, N), conjunctival bruisability, generalized pain, and gastrointestinal symptoms (vomiting and diarrhea accompanied by intractable abdominal pain after eating). Her mother has bruisable skin, joint hypermobility with recurrent dislocation, pes planus, hallux valgus, and edema of the lower extremities. Her father and sister have no relevant features.

Standard NGS panel analysis detected a heterozygous frameshift variant c.6948del,p.(Asp2317Thrfs*53) in exon 20, which was confirmed by Sanger sequencing (Figures 3Ea, left). Modified NGS panel analysis using long PCR-amplified product detected a heterozygous *TNXA*-derived 120-bp deletion in exon 35–intron 35 (c.11435_11524 + 30del), c.12150C>G,p.(Arg4050 =) and c.12174C>G,p.(Cys4058Trp) in exon 40, c.12204 + 39dup and c.12204 + 43T>G in intron 40, and c.12628-52A>G in intron 43. The four variants in exon 40 and intron 40 were confirmed by Sanger sequencing (data not shown). MLPA showed the one-copy loss of exon 35 in *TNXB* and a one copy loss of *CYP21A2* (Figure 3Ea, right). Sanger sequencing and MLPA analysis were performed on her parents, which revealed the heterozygous frameshift variant in her mother and the one-copy loss of exon 35 in *TNXB* and *CYP21A2* in her father (Figure 3Ea). Therefore, it was determined that Patient 5 was compound heterozygous for the frameshift variant and a type 1 *TNXB/TNXA* fusion gene (Figure 1B). Western blot analysis and nano-LC/MS/MS detection showed complete absence of sTNX in Patient 5 (Figures 3Eb,c). The mean sTNX concentration by nano-LC/MS/MS was 25 ± 2 ng/mL (22.1% of normal) in her father, 41 ± 1 ng/mL (36.3% of normal) in her mother, and 113 ± 10 ng/mL in the normal control (Figure 3Ec). Her sister was found to have the one-copy loss of exon 35 in *TNXB* and *CYP21A2,* and a mean sTNX concentration of 33 ± 1 ng/mL (29.2% of normal) (Figure 3Ec), confirming her carrier status for clEDS.

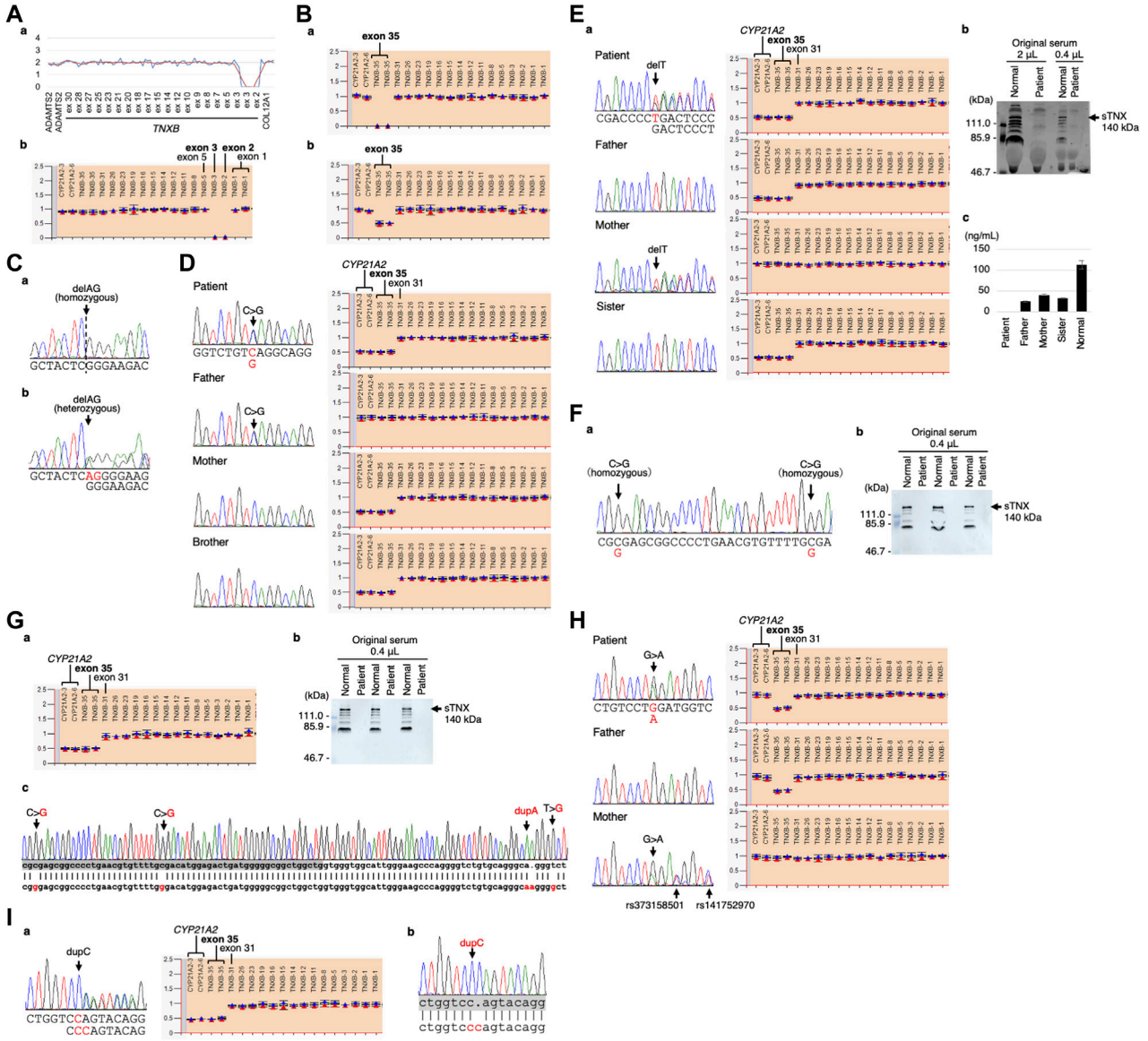

FIGURE 3
Molecular investigation of Patients 1–9. **(A)** Patient 1: homozygosity for exons 2–3 deletion detected by the CNV visualization method for an amplification-based NGS data **(a)** and validated by MLPA **(b)**. **(B)** Patient 2: homozygosity for a gene conversion characterized by *TNXA*-derived variation with validation of the exon 35 deletion by MLPA in the patient **(a)** and his son **(b)**. **(C)** Patient 3: homozygosity for a frameshift variant c.1650_1651del,p.(Glu552Argfs*41) validated by Sanger sequencing in the patient **(a)** and his daughter **(b)**. **(D)** Patient 4: compound heterozygosity for a nonsense variant c.10274C>G,p.(Ser3425*) and a *TNXB/TNXA* fusion gene characterized by *TNXA*-derived variation with validation of the nonsense variant by Sanger sequencing (left) and the *TNXB* exon 35 deletion and *CYP21A2* deletion by MLPA (right) in the patient and her family. **(E)** Patient 5: compound heterozygosity for a frameshift variant c.6948del,p.(Asp2317Thrfs*53) and a *TNXB/TNXA* fusion gene characterized by *TNXA*-derived variation with validation of the frameshift variant by Sanger sequencing (left) and the *TNXB* exon 35 deletion and *CYP21A2* deletion by MLPA (right) in the patient and her family **(a)**. Western blot analysis of sTNX in the patient **(b)** and quantification of sTNX in the patient and her family using nano-LC/MS/MS **(c)**. **(F)** Patient 6: homozygosity for a gene conversion characterized by *TNXA*-derived variation with validation by Sanger sequencing **(a)** and triplicate Western blot analysis of sTNX in the patient **(b)**. **(G)** Patient 7: compound heterozygosity for a gene conversion and a *TNXB/TNXA* fusion gene characterized by *TNXA*-derived variation with validation of the *TNXB* exon 35 deletion and *CYP21A2* deletion by MLPA **(a)**. Triplicate Western blot analysis of sTNX **(b)**. Sanger sequencing of the region around exon 40 in the normal exon 35 allele **(c)**, with the upper row showing the *TNXB* sequence and the lower row showing the *TNXA* sequence. *TNXB* exon 40 is highlighted with a gray box. **(H)** Patient 8: compound heterozygosity for a nonsense variant c.8585G>A,p.(Trp2862*) and a gene conversion characterized by *TNXA*-derived variation with validation of the nonsense variant by Sanger sequencing (left) and the *TNXB* exon 35 deletion by MLPA (right) in the patient and her parents. **(I)** Patient 9: compound heterozygosity for a frameshift variant c.9271dup,p.(Gln3091Profs*31) and a *TNXB/TNXA* fusion gene characterized by *TNXA*-derived variation with validation of the frameshift variant by Sanger sequencing (left) and the *TNXB* exon 35 deletion and *CYP21A2* deletion by MLPA (right) **(a)**. Sanger sequencing of the frameshift variant c.9271dup,p.(Gln3091Profs*31) in the normal exon 35 allele **(b)**, with the upper row showing the *TNXB* sequence and the lower row showing the *TNXA* sequence. *TNXB* exon 27 is highlighted with a gray box.

Patient 6

Patient 6 is a 59-year-old woman whose parents are Chinese and cousins. Part of her case information has been described recently (Ishiguro et al., 2022). She had shoulder dislocation at age 1 year, and was readily bruisable and experienced recurrent dislocation of the hip and finger joints, and repetitive episodes of anal prolapse, in her preschool days. She developed knee dislocation when she sat on her

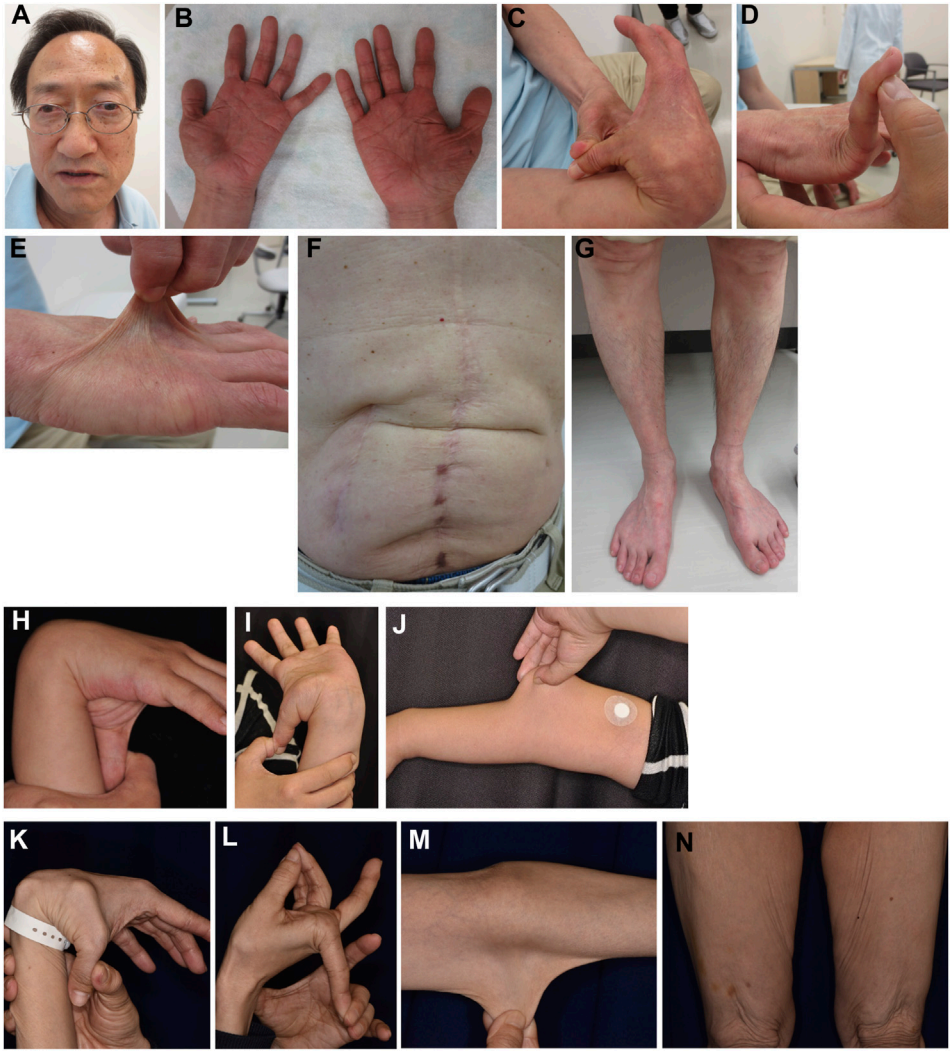

FIGURE 4
Clinical photographs of Patients 2, 4, and 5. **(A–G)** Patient 2 at age 65 years, showing jaw protrusion **(A)**, hands with thick fingers and wrinkled palms **(B)**, hypermobile finger joints **(C,D)**, hyperextensible skin **(E)**, atrophic scars at surgical sutures **(F)**, and valgus/flat feet **(G)**. **(H–J)** Patient 4 at age 27 years, showing finger joint hypermobility **(H,I)** and skin hyperextensiblity **(J)**. **(K–N)** Patient 5 at age 47 years, showing marked finger joint hypermobility **(K,L)** and skin hyperextensibility **(M)** and redundancy **(N)**.

heels in her elementary school days. At the delivery of her second child and at surgeries for appendicitis and breast cancer, she experienced massive bleeding. At age 49 years, she was referred to a genetics clinic with suspected EDS based on bruisability, skin hyperextensibility, and recurrent dislocation. While her skin hyperextensibility was mild, she had multiple bruises that included the soles of her feet, and reported massive swelling after insect bites. She had dislocation of the fingers, toes, and shoulders. Cardiac ultrasonography detected no abnormalities in the wall motion and mitral valves, and no dilatation of the aortic root. Her condition was complicated by generalized and wandering pain, sometimes unrelated to joint dislocation or other physical manifestations, and was successfully treated with duroxetine. At age 58 years, she developed anal laceration and rectal hematoma requiring emergency surgery. When seen by us at age 59 years, she had wrinkled palms (Figure 5A) and skin hyperextensibility, translucency, and bruisability (Figures 5C–G), and hypermobile finger joints (Figure 5B), mildly atrophic thighs (Figure 5G), pes planus (Figure 5H), and moderate calluses on the soles (Figure 5I).

Modified NGS panel analysis using long PCR-amplified product detected homozygous c.12150C>G,p.(Arg4050 =) and c.12174C>G,p.(Cys4058Trp) variants in exon 40, which were confirmed by Sanger sequencing (Figure 3Fa). MLPA showed a normal copy of *TNXB* and *CYP21A2* (data not shown). Therefore, this patient was determined to have a type 2 gene conversion (Figure 1B). Western blot analysis showed complete absence of sTNX (Figure 3Fb).

Patient 7

Patient 7 is a 61-year-old Japanese man whose parents were allegedly consanguineous. He was a low-birth-weight baby who was

admitted to hospital in infancy because of digestive impairment, but showed no developmental delay. From early childhood, he showed skin hyperextensibility but not fragility, and at age 3 years began suffering from recurrent shoulder dislocation. He did not participate in physical exercise in his elementary school days. At age 10 years, he developed a perforation in the intestine caused by an abdominal bruise, and was treated with emergency surgery. He worked as a carpenter, but could not carry heavy objects and became a school janitor. He got married at age 25 years. He developed a perforation in the esophagus at age 27 years and was treated with emergency surgery and subsequent mechanical ventilation for a month. During this admission, he was suspected to have EDS. He showed dilatation of the bladder resulting in difficulty with urination, and was managed with clean intermittent catheterization (CIC). He underwent a surgical reduction of the bladder that provided only tentative relief, and CIC was reintroduced. At age 42 years, he had angina pectoris. At age 57 years, he developed an inguinal hernia and diverticulitis, and was found to have bladder diverticula. When seen by us at age 61 years, his height was 167.3 cm (−0.6SD), weight was 60.0 kg (−0.3SD), OFC was 55.0 cm (−1.5SD), and arm span was 172.5 cm. He had wrinkled palms (Figure 5J), mild joint hypermobility with a Beighton score of 4/9 (Figure 5K), skin that was hyperextensible, bruisable, thin, velvety, and translucent (Figures 5L–N, R), without fragility or atrophic scars (Figure 5O). He also had, mild pectus excavatum (Figure 5N), atrophic thighs (Figure 5P), multiple varices at the knees (Figure 5Q), pes planus (Figure 5S), severe calluses on the soles (Figure 5T), mild scoliosis with a Cobb angle of 14°, a high palate with crowded teeth.

Modified NGS panel analysis using long PCR-amplified product detected a heterozygous *TNXA*-derived 120-bp deletion in exon 35–intron 35 (c.11435_11524 + 30del), c.12150C>G,p.(Arg4050 =) and c.12174C>G,p.(Cys4058Trp) in exon 40, c.12204 + 39dup and c.12204 + 43T>G in intron 40, and c.12628-52A>G in intron 43. The four variants in exon 40 and intron 40 were confirmed by Sanger sequencing (data not shown). MLPA showed the one-copy loss of exon 35 in *TNXB* and a one-copy loss of *CYP21A2* (Figure 3Ga). Western blot analysis showed complete absence of sTNX (Figure 3Gb). Long-PCR using primers TNXB-ex35-F and TNXB-ex44-R, which specifically amplify the normal allele of *TNXB* exon 35 (i.e., not the exon 35 deletion allele), and Sanger sequencing confirmed the presence of the four variants in exon 40 and intron 40 (Figure 3Gc). Therefore, it was determined that Patient 7 was compound heterozygous for a type 1 gene conversion and a type 2 *TNXB/TNXA* fusion gene (Figure 1B).

Patient 8

Patient 8 is an 8-year-old Japanese girl. Her father has skin hyperextensibility, joint hypermobility, and joint pain. Her mother, who has skin hyperextensibility and translucency, experienced fractures in the shoulder, arm, and foot. Her older brother had Perthes disease. She was born by cesarean section at 38 weeks and 4 days of gestation after a pregnancy complicated by polyhydramnios. Her birth weight was 3850 g (+2.7SD), length was 50.1 cm (+0.9SD), and OFC was 37.8 cm (+3.1SD). At age 1 month, generalized joint hypermobility was noticed, and she began receiving physical therapy from age 4 months. In infancy, she sucked poorly and had constipation requiring swab bougienage. At age 1 year, she was suspected to have autism spectrum disorder based on excessive stranger anxiety. When seen by us at age 3 years and 7 months, she was falling down easily and had generalized joint hypermobility with a Beighton score of 8/9, pes planovalgus, mild tonsil hypertrophy, a slender uvula, mild tooth irregularity, and mild reversed occlusion, but no high palate. At age 6 years and 5 months, an epiphysis of her ankle was fractured, and at age 8 years and 2 months, her weight was 24.8 kg (−0.2SD), height was 126.8 cm (+0.2SD), and OFC was 54.5 cm (+1.7SD). She frequently had stomatitis, peripheral cyanotic skin in a cool environment, and hyperventilation. Her Beighton score was 9/9. She showed limited extension of the interphalangeal joints in bilateral thumbs, and limited flexion and trigger finger of the left 4th finger, with morning stiffness. She had skin hyperextensibility and bruisability, but no episodes of skin laceration requiring surgical suture, sprains, or dislocations.

Standard NGS panel analysis detected a heterozygous nonsense variant c.8585G>A,p.(Trp2862*) in exon 25, which was confirmed by Sanger sequencing (Figure 3H, left). Modified NGS panel analysis using long PCR-amplified product detected a heterozygous *TNXA*-derived 120-bp deletion in exon 35–intron 35 (c.11435_11524 + 30del). MLPA showed the one-copy loss of exon 35 in *TNXB* and a normal copy of *CYP21A2* (type 1 gene conversion) (Figure 3H, right). Sanger sequencing and MLPA analysis were performed on her parents, revealing the heterozygous nonsense variant in her mother and the one-copy loss of exon 35 in *TNXB* in her father (Figure 3H). Therefore, it was determined that Patient 8 was compound heterozygous for the nonsense variant and a type 1 gene conversion (Figure 1B).

Patient 9

Patient 9 is a 69-year-old Japanese woman. Recurrent dislocation of the right shoulder that could be treated by self-reposition began at age 6 years and continued into adulthood. She frequently had subcutaneous hematomas, one of which led to her being suspected of having EDS in her 30s. At age 58 years, she developed a diaphragmatic hernia (hiatal hernia) that was treated by surgery, followed by an abdominal hernia. She had a pulmonary embolism after surgery for gallstones. At age 65 years, vaginal prolapse, accompanied by difficulties in defecation and urination, was noticed. She was referred to us at age 69 years for genetic evaluation in view of surgery for progressive vaginal prolapse. Brachydactyly with excessive skin (Figures 5U, W) and toe deformities (Figure 5X) were observed, but generalized joint hypermobility was not noted (Figures 5V, W). The hiatal and abdominal hernias were also found to be progressive. After this referral, she developed a small bowel perforation that healed spontaneously.

Standard NGS panel analysis detected a heterozygous frameshift variant c.9271dup,p.(Gln3091Profs*31) in exon 27, which was confirmed by Sanger sequencing (Figures 3A–I, left). Modified NGS panel analysis using long PCR-amplified product detected a heterozygous *TNXA*-derived 120-bp deletion in exon 35–intron 35 (c.11435_11524 + 30del), c.12150C>G,p.(Arg4050 =) and c.12174C>Gp.(Cys4058Trp) in exon 40, c.12204 + 39dup and c.12204 + 43T>G in intron 40, and c.12628-52A>G in intron 43. The four variants in exon 40 and intron 40 were confirmed by

10.3389/fgene.2023.1234804

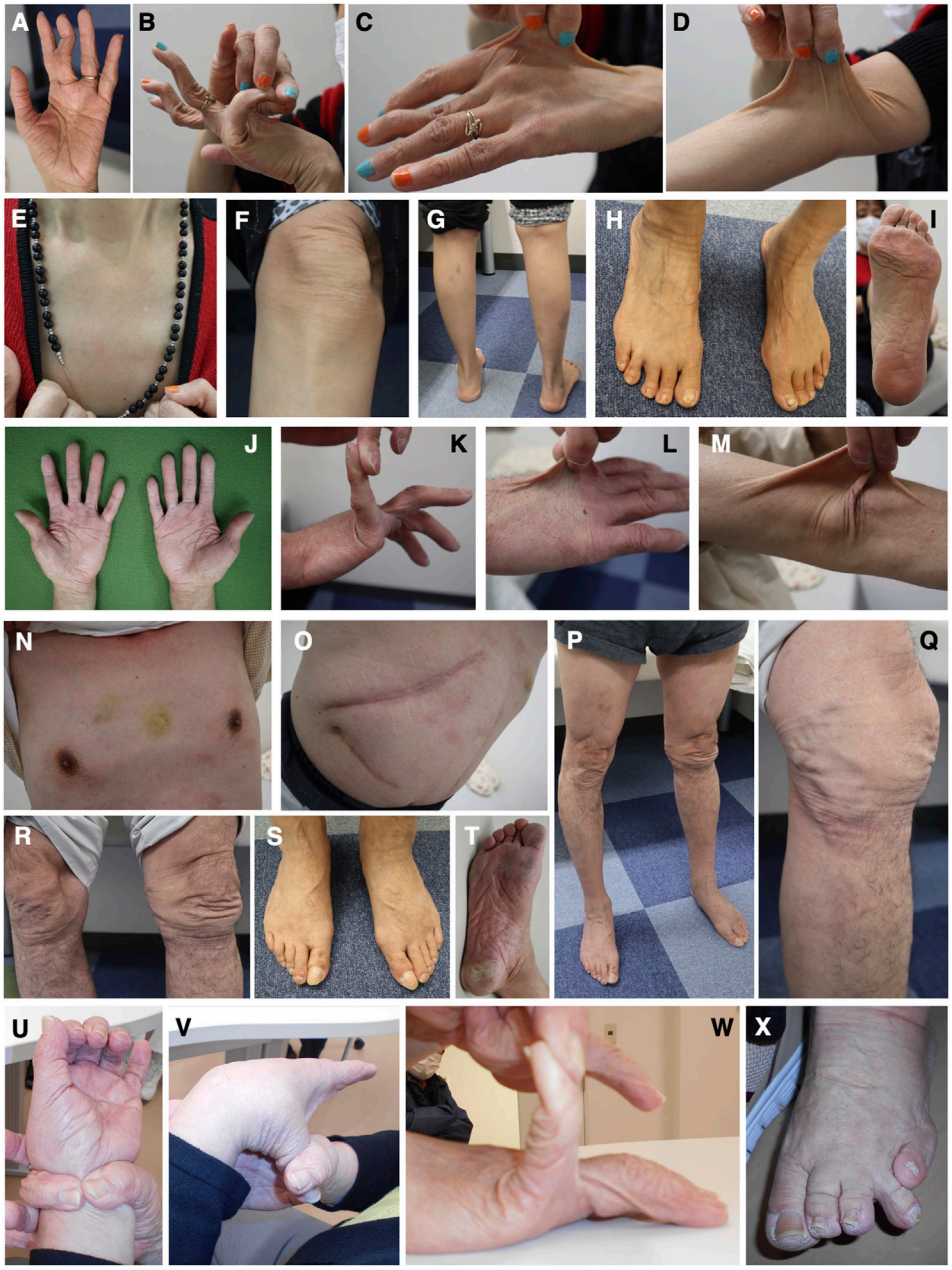

FIGURE 5
Clinical photographs of Patients 6, 7, and 9. **(A–I)** Patient 6 at age 59 years, showing wrinkled palms **(A)**, hypermobile finger joints **(B)**, skin hyperextensibility, translucency, and bruisability **(C–G)**, mildly atrophic thighs **(G)**, pes planus **(H)**, and moderate calluses on the soles **(I)**. **(J–T)** Patient 7 at age 61 years, showing wrinkled palms **(J)**, mild joint hypermobility with a Beighton score of 4/9 **(K)**, hyperextensible, bruisable, thin, velvety, and translucent skin **(L–N,R)**, without fragility or atrophic scars **(O)**, mild pectus excavatum **(N)**, atrophic thighs **(P)**, multiple varices at the knees **(Q)**, pes planus **(S)**, and severe calluses on the soles **(T)**. **(U–X)** Patient 9 at age 69 years, showing brachydactyly with excessive skin **(U,W)** and toe deformities **(X)**, but no generalized joint hypermobility **(V,W)**.

Sanger sequencing (data not shown). MLPA showed the one-copy loss of exon 35 in *TNXB* and a one-copy loss of *CYP21A2* (type 1 *TNXB/TNXA* fusion gene) (Figure 3Ia, right). Long-PCR using primers TNXB-ex26-F and TNXB-ex35-R, which specifically amplify the normal allele of *TNXB* exon 35 (i.e., not the exon 35 deletion allele) and Sanger sequencing confirmed the presence of the frameshift variant in exon 27 (Figure 3Ib). Therefore, it was determined that Patient 9 was compound heterozygous for the frameshift variant and a type 1 *TNXB/TNXA* fusion gene (Figure 1B).

Discussion

We have described detailed clinical and molecular findings of nine unrelated patients with clEDS who were found to have biallelic

TNXB variants. This is the first report to apply an NGS-based method to screen for *TNXB* variants and *TNXA*-derived sequences recombined into *TNXB*, and represents the third largest cohort of clEDS patients.

Hyperextensible skin, recurrent dislocations, easily bruisable skin, and hand and foot deformities were observed in >80% of the cases with available data. Eye bleeding, which is not included in the diagnostic criteria, was observed in three patients. Gastrointestinal complications were observed in the eight patients whose data were available, and included perforation in three patients, diverticulitis in three, gastrointestinal bleeding in two, intestinal obstruction in two, rectal or anal prolapse in four, and previously unreported gallstones in three. Clinical features of the current cohort (66.7% female; median age, 60 years) were compared with those of the largest cohort (Green et al., 2020) and the second largest cohort (Demirdas et al., 2017). Among the 20 patients reported by Green et al. (2020), 19 patients from 15 families had biallelic *TNXB* variants (68.4% female; median age, 34 years). Among the 17 patients reported by Demirdas et al. (2017), 14 patients from 11 families had biallelic *TNXB* variants (64.3% female; median age, 28 years). Eye bleeding was observed in four patients and two patients of the Green et al. and Demirdas et al. cohorts, respectively. Gastrointestinal complications, for which only rectal prolapse is included in the diagnostic criteria, were observed in six patients in Green et al. (2020), and comprised rupture in three patients, diverticulitis in three, gastrointestinal bleeding in two, and rectal prolapse in two, with no intestinal obstruction or gallstones. In the Demirdas et al. (2017) cohort, three patients had diverticulitis, one had gastrointestinal bleeding, and two had rectal prolapse, with no rupture or perforation, intestinal obstruction, or gallstones. The range of such events across all three cohorts (rupture/perforation in six patients, diverticulitis in nine, bleeding in five, obstruction in four, rectal/anal prolapse in six, and gallstones in three) highlight the importance and variability of gastrointestinal complications in patients with clEDS. The higher frequency of gastrointestinal complications in the current cohort might be a reflection of the higher median age compared to the other cohorts. This higher median age population in the current cohort could be useful in detecting age-dependent manifestations such as gastrointestinal complications, but could be less beneficial in accurately describing childhood manifestations due to recall bias.

To date, biallelic variation in *TNXB* has been documented in 50 clEDS patients from 43 families. *TNXA*-derived variations were detected in 77.8% (7/9 families) in the current cohort and in 76.7% (33/43 families) in the previous study. Most of the previously reported *TNXB* variants are null variants and include the 120-bp deletion, nonsense variants, frameshift variants, and splice site variants, which are predicted to lead to nonsense-mediated mRNA decay. In the Schalkwijk et al. (2001) study using Western blot analysis of serum samples and patient-derived fibroblast-conditioned medium, no TNX was detected in five patients with an EDS phenotype. In a type 2 *TNXB/TNXA* fusion or a type 2 gene conversion, the missense variant c.12174C>G,p.(Cys4058Trp) is considered to be pathogenic, but the effect of the altered protein is unknown. A homozygous missense variant c.12174C>G (i.e., either type 2 *TNXB/TNXA* fusion gene or type 2 gene conversion in both alleles) has been reported in multiple patients, including one patient by Hendriks et al. (2012)/Demirdas et al. (2017), one by Chen et al. (2016), and seven by Green et al. (2020). In the patient described by Hendriks et al. (2012)/Demirdas et al. (2017), there was a complete absence of serum TNX on Western blot analysis (Supplementary Table S3). In the current study, Patient 6 also showed a complete absence of serum TNX on Western blot analysis (Figure 3Fb). A compound heterozygous c.12174C>G with another variant (i.e., either type 2 *TNXB/TNXA* fusion gene or type 2 gene conversion in one allele) has also been reported in multiple patients, including one patient by Schalkwijk et al. (2001)/Demirdas et al. (2017). These studies reported a complete absence of TNX in serum and fibroblast-conditioned medium (Supplementary Table S3). In view of all these findings, the main effect of this missense variant is likely to be a disturbance in secretion or susceptibility to degradation of TNX, rather than a defect in production. In conclusion, we developed an NGS-based screening system that can accurately detect *TNXB* variants and *TNXA*-derived sequences recombined into *TNXB*. *TNXA*-derived variations were found in >75% of the current cohort, comparable to previous reports. Gastrointestinal complications (e.g., perforation, diverticulitis, gastrointestinal bleeding, intestinal obstruction, rectal/anal prolapse, and gallstones) were observed particularly frequently in the current cohort, highlighting the importance of increasing awareness of the risk of gastrointestinal complications in clEDS.

Data availability statement

Original datasets are available in a publicly accessible repository. The mass spectrometry proteomics data have been deposited to the ProteomeXchange Consortium via the PRIDE (https://proteomecentral.proteomexchange.org/cgi/GetDataset) partner repository with the dataset identifier PXD043691. The variant data have been deposited to the Global Variome shared LOVD (https://databases.lovd.nl/shared/genes/TNXB) with the individual ID 435339, 435340, 435341, 435342, 435344, 435346, 435348, 435349, 435351.

Ethics statement

The studies involving humans were approved by the Ethics Committee of Shinshu University School of Medicine. The studies were conducted in accordance with the local legislation and institutional requirements. Written informed consent for participation in this study was provided by the participants' legal guardians/next of kin. Written informed consent was obtained from the individual(s) for the publication of any potentially identifiable images or data included in this article.

Author contributions

TY performed all molecular experiments, interpreted the data, and wrote the first draft of the manuscript. TK conceived the work, organized the data collection, interpreted the data, and wrote the clinical part of the first draft. K-IM and KY conducted the Western blot analysis and nano-LC/MS/MS. SN, TN, NK, MM-H, MM, YS,

and HS provided clinical data. TF and YT helped to perform molecular analysis. All authors contributed to the article and approved the submitted version.

Funding

This study was supported by the Grant-in-Aid for Young Scientists from The Japan Society for the Promotion of Science, Japan (19K17795; 2019–2023 to TY); Research on Intractable Diseases (09835303, 10801776, 11948954; 2009–2011 to TK); the Research Program on Policy of Measures for Intractable/Rare Diseases, Ministry of Health, Labour and Welfare, Japan (20316866; 2020–2022 to TK); the Program for an Integrated Database of Clinical and Genomic Information (16818213; 2016–2020 to TK); and the Initiative on Rare and Undiagnosed Diseases, Japan Agency for Medical Research and Development (21445007; 2018–2020 to TK).

Acknowledgments

We are grateful to the patients and their families for their cooperation during this study. We also thank Michelle Kahmeyer-Gabbe, from Edanz Group (https://en-author-services.edanzgroup.com/) for editing a draft of this manuscript.

Conflict of interest

TY, TF, YT, and TK are members of the endowed chair named "Division of Clinical Sequencing, Shinshu University School of Medicine", which is sponsored by BML, Inc. and Life Technologies Japan Ltd., a subsidiary of Thermo Fisher Scientific Inc.

The remaining author declares that the research was conducted in the absence of any commercial or financial relationships that could be construed as a potential conflict of interest.

Publisher's note

Supplementary material

The Supplementary Material for this article can be found online at: https://www.frontiersin.org/articles/10.3389/fgene.2023.1234804/full#supplementary-material

References

Al-Harbi, T. M., Al-Rammah, H., Al-Zahrani, N., Liu, Y., Sleiman, P. M. A., Dridi, W., et al. (2022). Rare neurological manifestations in a Saudi Arabian patient with Ehlers–Danlos syndrome and a novel homozygous variant in the *TNXB* gene. *Am. J. Med. Genet. A* 188 (2), 618–623. doi:10.1002/ajmg.a.62539

Brady, A. F., Demirdas, S., Fournel-Gigleux, S., Ghali, N., Giunta, C., Kapferer-Seebacher, I., et al. (2017). The Ehlers–Danlos syndromes, rare types. *Am. J. Med. Genet. C Semin. Med. Genet.* 175, 70–115. doi:10.1002/ajmg.c.31550

Brisset, M., Metay, C., Carlier, R. Y., Badosa, C., Marques, C., Schalkwijk, J., et al. (2020). Biallelic mutations in Tenascin-X cause classical-like Ehlers–Danlos syndrome with slowly progressive muscular weakness. *Neuromuscul. Disord.* 30 (10), 833–838. doi:10.1016/j.nmd.2020.09.002

Burch, G. H., Gong, Y., Liu, W., Dettman, R. W., Curry, C. J., Smith, L., et al. (1997). Tenascin-X deficiency is associated with Ehlers–Danlos syndrome. *Nat. Genet.* 17, 104–108. doi:10.1038/ng0997-104

Chen, W., Perritt, A. F., Morissette, R., Dreiling, J. L., Bohn, M. F., Mallappa, A., et al. (2016). Ehlers–Danlos syndrome caused by biallelic *TNXB* variants in patients with congenital adrenal hyperplasia. *Hum. Mutat.* 37 (9), 893–897. doi:10.1002/humu.23028

Colman, M., Syx, D., Wandele, I. D., Dhooge, T., Symoens, S., and Malfait, F. (2021). Clinical and molecular characteristics of 168 probands and 65 relatives with a clinical presentation of classical Ehlers–Danlos syndrome. *Hum. Mutat.* 42 (10), 1294–1306. doi:10.1002/humu.24258

Demirdas, S., Dulfer, E., Robert, L., Kempers, M., van Beek, D., Micha, D., et al. (2017). Recognizing the tenascin-X deficient type of ehlers–danlos syndrome: A cross-sectional study in 17 patients. *Clin. Genet.* 91, 411–425. doi:10.1111/cge.12853

Green, C., Ghali, N., Akilapa, R., Angwin, C., Baker, D., Bartlett, M., et al. (2020). Classical-like ehlers–danlos syndrome: A clinical description of 20 newly identified individuals with evidence of tissue fragility. *Genet. Med.* 22 (10), 1576–1582. doi:10.1038/s41436-020-0850-1

Hendriks, A. G. M., Voermans, N. C., Schalkwijk, J., Hamel, B. C., and van Rossum, M. M. (2012). Well-defined clinical presentation of ehlers–danlos syndrome in patients with tenascin-X deficiency: A report of four cases. *Clin. Dysmorphol.* 21 (1), 15–18. doi:10.1097/MCD.0b013e32834c4bb7

Ishiguro, H., Yagasaki, H., and Horiuchi, Y. (2022). Ehlers–danlos syndrome in the field of psychiatry: A review. *Front. Psychiatry* 12, 803898. doi:10.3389/fpsyt.2021.803898

Malfait, F., Francomano, C., Byers, P., Belmont, J., Berglund, B., Black, J., et al. (2017). The 2017 international classification of the Ehlers–Danlos syndromes. *Am. J. Med. Genet. C Semin. Med. Genet.* 175, 8–26. doi:10.1002/ajmg.c.31552

Micale, L., Guarnieri, V., Augello, B., Palumbo, O., Agolini, E., Sofia, M. V., et al. (2019). Novel *TNXB* variants in two Italian patients with classical-like Ehlers–Danlos syndrome. *Genes. (Basel)* 10, 967. doi:10.3390/genes10120967

Morissette, R., Chen, W., Perritt, A. F., Dreiling, J. L., Arai, A. E., Sachdev, V., et al. (2015). Broadening the spectrum of Ehlers Danlos syndrome in patients with congenital adrenal hyperplasia. *J. Clin. Endocrinol. Metab.* 100, E1143–E1152. doi:10.1210/jc.2015-2232

Nishio, S. Y., Moteki, H., and Usami, S. I. (2018). Simple and efficient germline copy number variant visualization method for the Ion AmpliSeq™ custom panel. *Mol. Genet. Genomic Med.* 6, 678–686. doi:10.1002/mgg3.399

Pénisson-Besnier, I., Allamand, V., Beurrier, P., Martin, L., Schalkwijk, J., van Vlijmen-Willems, I., et al. (2013). Compound heterozygous mutations of the *TNXB* gene cause primary myopathy. *Neuromuscul. Disord.* 23 (8), 664–669. doi:10.1016/j.nmd.2013.04.009

Perez-Riverol, Y., Bai, J., Bandla, C., Hewapathirana, S., García-Seisdedos, D., Kamatchinathan, S., et al. (2022). The PRIDE database resources in 2022: A hub for mass spectrometry-based proteomics evidences. *Nucleic Acids Res.* 50 (1), D543–D552. doi:10.1093/nar/gkab1038

Rymen, D., Ritelli, M., Zoppi, N., Cinquina, V., Giunta, C., Rohrbach, M., et al. (2019). Clinical and molecular characterization of classical-like Ehlers–Danlos Syndrome due to a novel *TNXB* variant. *Genes. (Basel)* 10 (11), 843. doi:10.3390/genes10110843

Sakiyama, T., Kubo, A., Sasaki, T., Yamada, T., Yabe, N., Matsumoto, K. I., et al. (2015). Recurrent gastrointestinal perforation in a patient with Ehlers–Danlos syndrome due to tenascin-X deficiency. *J. Dermatol.* 42 (5), 511–514. doi:10.1111/1346-8138.12829

Santoreneos, R., Vakulin, C., Ellul, M., Rawlings, L., Hardy, T., and Poplawski, N. (2022). Recurrent pneumothorax in a case of tenascin-X deficient

Ehlers–Danlos syndrome: Broadening the phenotypic spectrum. *Am. J. Med. Genet. A* 188 (5), 1583–1588. doi:10.1002/ajmg.a.62674

Schalkwijk, J., Zweers, M. C., Steijlen, P. M., Dean, W. B., Taylor, G., van Vlijmen, I. M., et al. (2001). A recessive form of the Ehlers–Danlos syndrome caused by tenascin-X deficiency. *N. Engl. J. Med.* 345, 1167–1175. doi:10.1056/NEJMoa002939

Voermans, N. C., van Alfen, N., Pillen, S., Lammens, M., Schalkwijk, J., Zwarts, M. J., et al. (2009). Neuromuscular involvement in various types of Ehlers–Danlos syndrome. *Ann. Neurol.* 65 (6), 687–697. doi:10.1002/ana.21643

Watanabe, S., Ito, Y., Samura, O., Nakano, H., Sawamura, D., Asahina, A., et al. (2021). Novel gross deletion mutation c.-105_4042+498del in the *TNXB* gene in a Japanese woman with classical-like ehlers–danlos syndrome: A case of uneventful pregnancy and delivery. *J. Dermatol.* 48 (5), e227–e228. doi:10.1111/1346-8138.15837

Yamada, K., Watanabe, A., Takeshita, H., and Matsumoto, K. I. (2016). A method for quantification of serum tenascin-X by nano-LC/MS/MS. *Clin. Chim. Acta.* 459, 94–100. doi:10.1016/j.cca.2016.05.022

Yamaguchi, T., Hayashi, S., Hayashi, D., Matsuyama, T., Koitabashi, N., Ogiwara, K., et al. (2023). Comprehensive genetic screening for vascular Ehlers–Danlos syndrome through an amplification-based next generation sequencing system. *Am. J. Med. Genet. A* 191 (1), 37–51. doi:10.1002/ajmg.a.62982

frontiers | Frontiers in Genetics

TYPE Case Report
PUBLISHED 20 December 2023
DOI 10.3389/fgene.2023.1246712

OPEN ACCESS

EDITED BY
Tomoki Kosho,
Shinshu University, Japan

REVIEWED BY
Samira Kalayinia,
Shaheed Rajaei Cardiovascular Medical and Research Center, Iran
Tomomi Yamaguchi,
Shinshu University Hospital, Japan

*CORRESPONDENCE
Baoheng Gui,
BaohengGui@yeah.net
Cundong Mi,
md-392@126.com
Jiefeng Luo,
drljf98@163.com

†These authors have contributed equally to this work

RECEIVED 24 June 2023
ACCEPTED 04 December 2023
PUBLISHED 20 December 2023

CITATION
Wei X, Zhou X, Xie B, Shi M, Gui C, Liu B, Li C, Zhang C, Luo J, Mi C and Gui B (2023), Importance of comprehensive genetic testing for patients with suspected vascular Ehlers–Danlos syndrome: a family case report and literature review.
Front. Genet. 14:1246712.
doi: 10.3389/fgene.2023.1246712

Importance of comprehensive genetic testing for patients with suspected vascular Ehlers–Danlos syndrome: a family case report and literature review

Xianda Wei[1,2†], Xu Zhou[3†], BoBo Xie[1,2], Meizhen Shi[1,2], Chunrong Gui[1,2], Bo Liu[4], Caiyan Li[4], Chi Zhang[5], Jiefeng Luo[6]*, Cundong Mi[4]* and Baoheng Gui[1,2]*

[1]Center for Medical Genetics and Genomics, The Second Affiliated Hospital of Guangxi Medical University, Nanning, Guangxi, China, [2]The Guangxi Health Commission Key Laboratory of Medical Genetics and Genomics, The Second Affiliated Hospital of Guangxi Medical University, Nanning, Guangxi, China, [3]The Second School of Medicine, Guangxi Medical University, Nanning, Guangxi, China, [4]Department of Rheumatology and Immunology, The Second Affiliated Hospital of Guangxi Medical University, Nanning, Guangxi, China, [5]Department of Ultrasound Diagnosis, The Second Affiliated Hospital of Guangxi Medical University, Nanning, Guangxi, China, [6]Department of Neurology, The Second Affiliated Hospital of Guangxi Medical University, Nanning, Guangxi, China

Vascular Ehlers–Danlos syndrome (vEDS), the most severe type of Ehlers–Danlos syndrome, is caused by an autosomal-dominant defect in the *COL3A1* gene. In this report, we describe the clinical history, specific phenotype, and genetic diagnosis of a man who died of vEDS. The precise diagnosis of this case using whole-exome sequencing provided solid evidence for the cause of death, demonstrating the practical value of genetic counseling and analysis. Early diagnosis for the proband's son, who was also affected by vEDS, revealed initial complications of vEDS in early childhood, which have rarely been reported. We also reviewed the literature on *COL3A1* missense mutations and related phenotypes. We identified an association between digestion tract events and non-glycine missense variants, which disproves a previous hypothesis regarding the genotype–phenotype correlation of vEDS. Our results demonstrate the necessity of offering comprehensive genetic testing for every patient suspected of having vEDS.

KEYWORDS

vascular Ehlers–Danlos syndrome, vascular rupture, *COL3A1*, novel mutation, genotype–phenotype correlations

1 Introduction

Ehlers–Danlos syndrome (EDS), also known as congenital connective tissue hypoplasia syndrome, is associated with defects in collagen synthesis and metabolism. EDS represents a class of collagen disorders among the wider group of heritable connective tissue diseases. Vascular EDS (vEDS) is a specific form of EDS caused by autosomal-dominant mutations in *COL3A1*. Although vEDS is generally associated with mild skin lesions, severe cardiovascular lesions can occur in rare cases. These lesions can progress to cause aortic dissection and aneurysm, which are prone to spontaneous rupture, leading to death. As such, vEDS is the most dangerous type of EDS and has the worst prognosis.

In this report, we describe the clinical history, unique phenotype, and genetic cause of a man who died from vEDS; his son was also affected by vEDS, as confirmed by whole-exome sequencing (WES). In addition, we reviewed the literature on *COL3A1* missense mutations and related phenotypes to provide more insight into the phenotype–genotype correlation in vEDS.

2 Clinical report

The proband was a 32-year-old man. In January 2021, he presented to a local hospital because of complaints of swelling of the left forearm and bulging of the blood vessels. He subsequently repeatedly visited doctors for systemic symptoms, including severe abdominal pain, lumbago, bulging vessels, sweating, a pale face, and transient amaurosis. Symptoms improved with a small dose of glucocorticoids and symptomatic treatment. Trauma caused by a violent impact was denied. In June 2021, he developed swelling of the right forearm; pain in the right forearm, back, and abdomen; and transient black spots in his vision. Ultrasound imaging revealed arterial abnormalities. Computed tomography (CT) angiography showed bilateral internal carotid and vertebral artery aneurysms, rupture of the left ulnar artery, and pseudoaneurysm.

In July 2021, the patient visited our hospital with abdominal pain and black stools. Physical examination revealed a short height (150 cm) and low body weight (36 kg). He exhibited aging skin of the extremities, subcutaneous venous exposure, and multiple ecchymoses (non-traumatic) of the chest, right waist, and upper extremities (Figure 1A). His fingers were slender, and the joints were abnormally flexible. His right hand had excessive dorsal flexion and the little finger was pressed against the back of the hand (Figure 1B). His feet rotated inward (Figure 1C). Gastroscopy revealed no bleeding in the upper digestive tract. Vascular and abdominal CT (Figure 1D) revealed multiple aneurysms and aneurysmal dilation of the celiac trunk, proper hepatic artery, left hepatic artery, splenic artery, and both kidneys, along with arterial dissection of the celiac trunk and splenic artery. The patient experienced pain on percussion in the right renal area. Color ultrasound of the

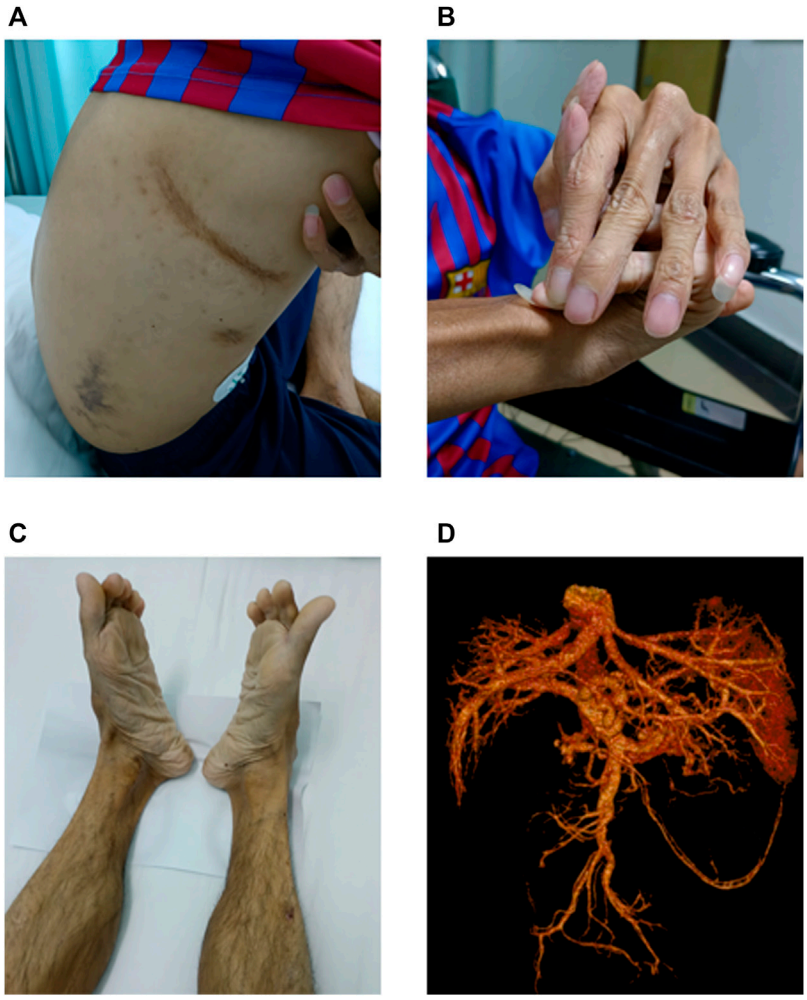

FIGURE 1
Main clinical findings of the proband. **(A)** Multiple ecchymoses (non-traumatic) in the anterior chest, right waist, and upper limbs. **(B)** Right finger with excessive dorsal flexion and the little finger pressed against the back of the hand. **(C)** Feet rotated inward. **(D)** Multiple aneurysms and aneurysmal dilation of the celiac trunk, proper hepatic artery, left hepatic artery, splenic artery, and both kidneys; arterial dissection of the celiac trunk and splenic artery is evident.

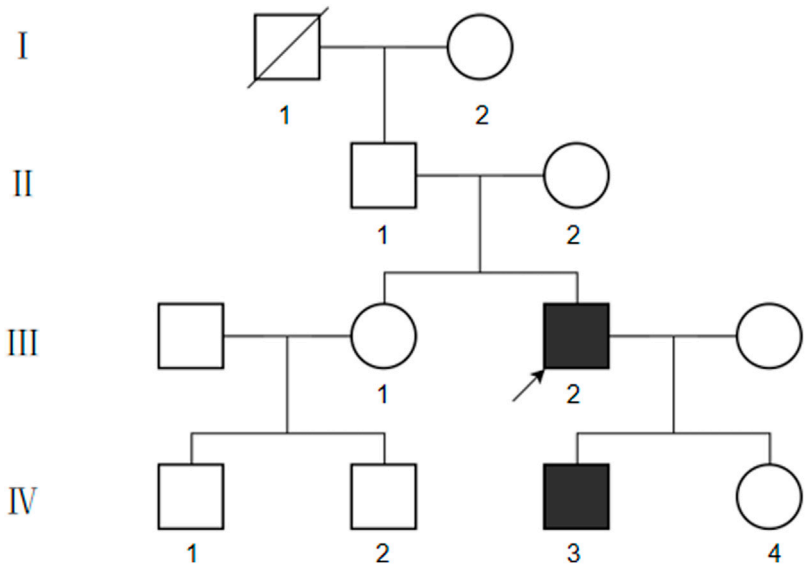

FIGURE 2
Pedigree chart of this case.

urinary system indicated mild hydrops in the right kidney, excluding the presence of urinary stones. Distal occlusion of the upper pole branch of the right renal artery, decreased perfusion of the right renal parenchyma, and a high density of fat sacs around the right kidney suggested bleeding and infarction of the right kidney. Kidney stones were further excluded by ultrasonography. Blood biochemistry tests, immunoglobulin (Ig)A/IgM/IgG, rheumatoid factors, autoantibody spectra, and cardiac color Doppler ultrasonography all exhibited negative findings. The patient died of arterial rupture and hemorrhagic shock 2 weeks after admission.

We collected basic information on the proband's family members over three generations (Figure 2). The proband's grandfather died of unknown cause, and the proband's parents, sisters, and daughters did not show any abnormalities related to vEDS. However, the proband's son, aged 3 years 4 months, had deep skin pigmentation, deep palm lines, poor wound healing of the skin, and occasional fresh blood in stools. Mosquito bites were also reported to be abnormally large at times. No surface hemangiomas were observed.

3 Genetic analysis

The rarity and complexity of the patient's clinical manifestations implied the possibility of a genetic disease. To this end, we performed trio WES of the proband and his parents after genetic counseling; genetic testing was also performed on the proband's son and proband's older sister.

Genomic DNA was extracted from blood samples using a LabAid DNA kit (Zeesan Biotech Co., Ltd., Xiamen, China); target capture for WES (Human All Exon V5 Kit, Agilent Technologies, Foster City, CA, United States) and library sequencing (NextSeq CN500 platform, Illumina, San Diego, CA, United States) were conducted following the manufacturer protocols.

Data analysis and annotation were performed using the Genome Analysis Toolkit (GATK), version 3.4.0. The variants were identified and filtered using in-house protocols. The inclusion criteria for candidate variants were as follows: 1) heterozygous variants in an established causative gene of a dominant Mendelian disorder with a likely association to the patient's phenotype; 2) variants with frequencies in the East Asian population in the gnomAD, NHLBI Exome Sequencing Project, 1000 Genomes Project, and in-house databases all <0.5%; and 3) computational evidence supports a deleterious effect of the variant. SpliceAI (Jaganathan et al., 2019), a deep-learning–based algorithm, was used to calculate the probability of splice-altering variants, providing a Δ score between 0 and 1. Candidate variants were verified by Sanger sequencing and true variants were validated following American College of Medical Genetics and Genomics/American Association of Molecular Pathology guidelines (Richards et al., 2015).

We identified a heterozygous missense variation, NM_000090.3: c.146C>T(p.Pro49Leu), in exon 2 of *COL3A1*, as the most likely genetic cause of the disease. The variant was heterozygous in the proband and his son and was absent in his parents and sister (Figure 3). The variant was classified as likely pathogenic according to the following criteria: 1) PS2: the variant was *de novo*, with both parental samples confirmed to be derived from the biological parents of the patient through single-nucleotide polymorphism analysis of trio-WES data; 2) PM2: this variant is not reported in the East Asian population database; and 3) PP2: the missense constraint Z-score of *COL3A1* in the Gnomad database was 4.09, indicating that missense variations in this gene are a common cause of disease. According to the calibration of computational tools for missense variant pathogenicity classification and ClinGen recommendations for PP3/BP4 criteria (Pejaver et al., 2022), the prediction results obtained with a single prediction software tool can be used as a basis for PP3 evidence. The single prediction tool utilized in our laboratory to determine the

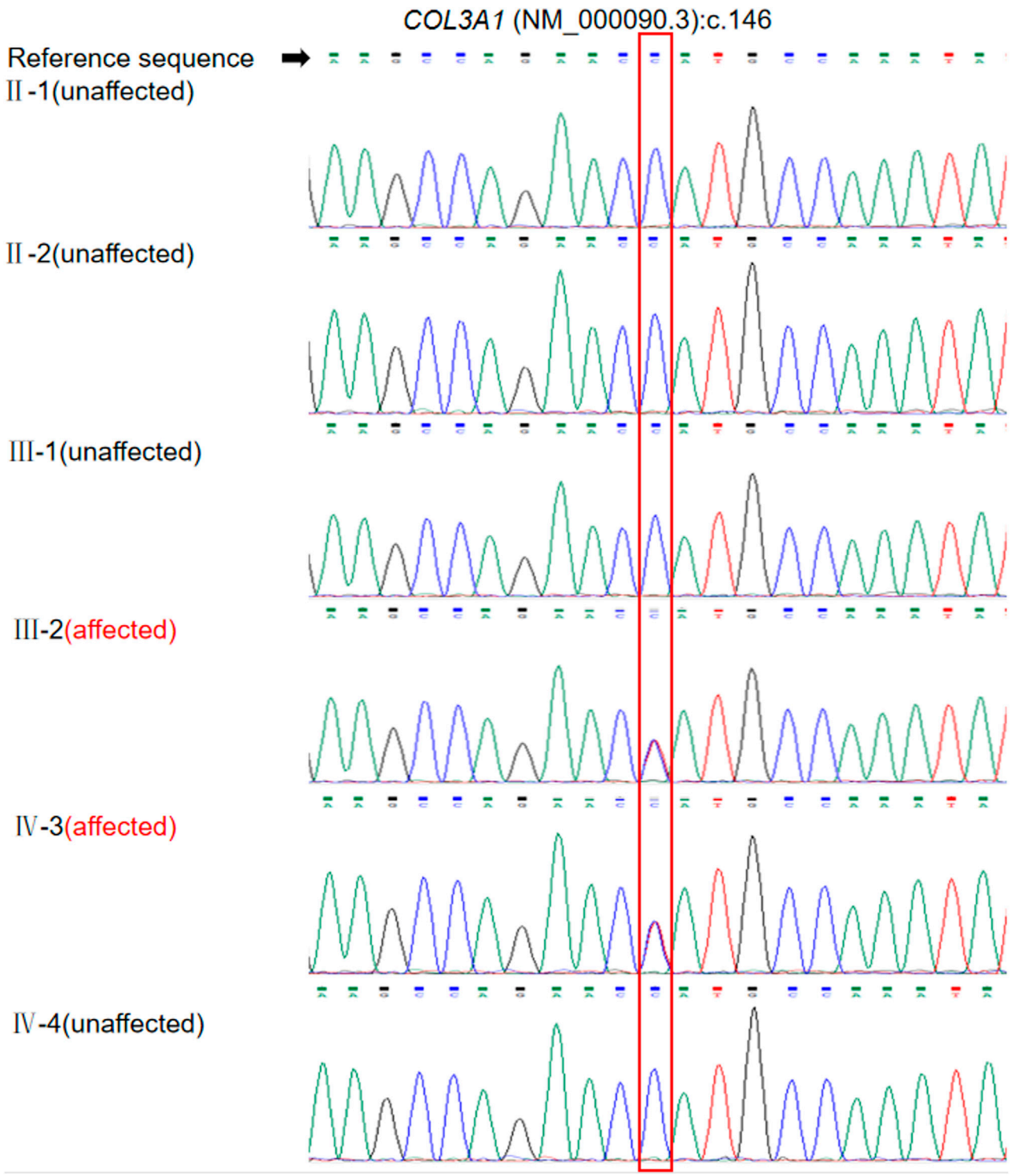

FIGURE 3
Validation of the *COL3A1* mutation c.146C>T in the patient and family members by Sanger sequencing. Annotation in the red box indicates the location of the mutation.

usage and strength of PP3 is revel. In this case, the Revel score for the *COL3A1* c.146C>T variant is only 0.586, which does not meet the criterion used for a PP3 level of supporting evidence (revel score ≥ 0.644). We also evaluated information about a previously reported variant c.145C>G p. (Pro49Ala) affecting the same residue as c.146C>T. Although homozygous c.145C>G variants have been detected in at least four patients with an autosomal recessive disorder caused by biallelic mutations in *COL3A1*, polymicrogyria with or without vascular-type EDS (OMIM 618343) (Vandervore, et al., 2017; Horn, et al., 2017), evidence

TABLE 1 Associations of vascular Ehlers–Danlos syndrome (vEDS) mutation sites with clinical phenotypes.

Mutation	Age of initial onset* or age of diagnosis# (years)	Thoracic and abdominal vascular events	Gastrointestinal events	Skin abnormalities	Distinct facial features[a]	Exercise and bone developmental abnormalities	Peripheral blood	Others	References
c.388G>T p.(Gly130Arg)	30#	+	−	−	+	+	−	+	Kroes et al. (2003)
c.721G>A p.(Glu241Lys)	0.75*	−	−	+	−	+	+	−	Ghali et al. (2019)
c.727G>A p.(Gly243Arg)	−	+	−	+	+	+	−	−	Gu et al. (2018)
c.781G>A p.(Gly261Ser)	−	+	−	−	−	−	−	+	Lee et al. (2008)
c.800G>T p.(Gly267Val)	−	+	−	−	+	−	+	+	Lipinski et al. (2009)
c.970G>A p.(Gly324Ser)	−	+	−	−	−	−	−	−	Rebelo et al. (2011)
c.1052G>T p.(Gly351Val)	−	−	+	−	−	+	+	+	Lumi et al. (2021)
c.1342G>A p.(Glu448Lys)	75	−	−	+	+	+	+	+	Colman et al. (2022)
c.1351G>A p.(Glu451Lys)	41*	−	+	+	−	−	−	+	Ghali et al. (2019)
c.1387G>A p.(Glu463Lys)	49	−	−	+	−	+	+	−	Colman et al. (2022)
c.1511G>A p.(Gly504Asp)	−	−	+	−	−	−	−	−	Nakagawa et al. (2015)
c.1862G>A p.(Gly621Glu)	−	+	−	−	−	−	+	+	Barboi et al. (2009)
c.1916G>T p.(Gly639Val)	−	+	+	−	−	−	+	−	Brightwell and Walker (2011)
c.1925G>A p.(Gly642Asp)	−	+	−	−	−	+	+	−	Ishiguro et al. (2009)
c.2044G>A p.(Glu682Lys)	UC	+	−	+	−	−	−	−	Ghali et al. (2019)
c.2194G>A p.(Gly732Arg)	9#	+	−	+	−	+	−	+	Kamalanathan et al. (2019)
c.2195G>T p.(Gly732Val)	−	+	−	+	−	−	−	−	Yang et al. (2007)

(Continued on following page)

10.3389/fgene.2023.1246712

TABLE 1 (*Continued*) Associations of vascular Ehlers–Danlos syndrome (vEDS) mutation sites with clinical phenotypes.

Mutation	Age of initial onset* or age of diagnosis# (years)	Thoracic and abdominal vascular events	Gastrointestinal events	Skin abnormalities	Distinct facial features[a]	Exercise and bone developmental abnormalities	Peripheral blood	Others	References
c.2321G>A p.(Gly774Asp)	–	+	–	–	–	–	–	+	De Sousa et al. (2020)
c.2465G>C p.(Gly822Ala)	–	–	+	–	–	–	+	–	Eder et al. (2013)
c.2512G>A p.(Gly838Ser)	4#	–	–	+	–	+	–	–	Narcisi et al. (1994)
c.2528G>A p.(Gly843Glu)	0.5*	+	–	+	–	+	–	+	Sadakata et al. (2010)
c.2644G>T p.(Gly882Cys)	–	+	–	–	–	–	–	+	Aydıner and Hançer (2020)
c.2791G>A p.(Glu931Lys)	18	–	–	+	–	–	–	–	Colman et al. (2022)
c.2791G>A p.(Glu931Lys)	16	–	+	+	–	+	–	–	Colman et al. (2022)
c.2896G>T p.(Gly966Cys)	–	+	–	+	+	+	–	–	Abrahamsen et al. (2015)
c.2932G>C p.(Gly978Arg)	–	+	–	+	–	+	–	–	Gu et al. (2018)
c.2959G>A p.(Gly987Ser)	–	–	–	+	+	+	–	+	Lan et al. (2018)
c.2996G>A p.(Gly999Asp)	37#	–	–	+	–	+	–	+	Gu et al. (2018)
c.3149G>T p.(Gly1050Val)	10*	–	–	–	–	+	–	+	Palmeri et al. (2003)
c.3175G>A p.(Gly1059Arg)	–	+	–	–	–	–	–	–	Sakai et al. (2019)
c.3440G>T p.(Gly1147Val)	UC[b]	–	–	+	–	+	–	+	Nuytinck et al. (1994)
c.3478A>G p.(Ile1160Val)	–	–	–	–	–	+	–	+	Ruscitti et al. (2021)
c.3511G>A p.(Glu1171Lys)	–	–	+	–	–	–	–	–	Ghali et al. (2019)
c.3554G>T p.(Gly1185Val)	–	–	+	–	–	–	–	+	Yang et al. (2022)

(Continued on following page)

10.3389/fgene.2023.1246712

TABLE 1 (*Continued*) Associations of vascular Ehlers–Danlos syndrome (vEDS) mutation sites with clinical phenotypes.

Mutation	Age of initial onset* or age of diagnosis# (years)	Thoracic and abdominal vascular events	Gastrointestinal events	Skin abnormalities	Distinct facial features[a]	Exercise and bone developmental abnormalities	Peripheral blood	Others	References
c.3851G>A p.(Gly1284Glu)	–	+	–	+	+	+	–	+	Jørgensen et al. (2015)

+, symptoms of the patient; –, patient does not have symptom or symptom is not reported; *, age of initial onset; #, age of diagnosis.
[a]Includes thin vermilion of the lips, micrognathia, narrow nose, and prominent eyes.
[b]UC, patient had symptoms in the neonatal period, but no specific age given.

supporting its pathogenicity in vEDS was insufficient. Thus, PM5 should not be applied to interpret c.146C>T(p.Pro49Leu) in our cases with vEDS.

Finally, we established a genetic diagnosis of vEDS for the patient and his son based on clinical and genetic findings.

4 Discussion

EDS is a heterogeneous group of connective tissue disorders that comprise a spectrum of monogenic conditions with multi-systematic and variable clinical manifestations (e.g., joint hypermotility, skin hyperextensibility, and tissue fragility) primarily affecting the skin, ligaments, joints, blood vessels, and internal organs. EDS is classified into 13 different subtypes, among which the vascular type (type IV) is the most severe and life-threatening, with arterial ruptures or dissections responsible for the majority of deaths. These events are unpredictable, and the fragility of the arterial walls often makes surgical repair difficult (Ruscitti et al., 2021).

The proband of this case had early symptoms, including peripheral vascular rupture events and skin abnormalities, which gradually evolved into thoracoabdominal vascular rupture. Although the clinical manifestations of the proband were in accordance with a diagnosis of vEDS, the rarity of this disease poses challenges for clinical diagnosis, especially for physicians in adult departments who may not have a strong awareness or sufficient knowledge of genetic disorders. We initially considered Marfan syndrome as a possible diagnosis, as the associated phenotypes overlap with those of vEDS, including aortic dissection, aortic aneurysm, and joint hypermotility. Following the advice of geneticists, we performed WES of the proband because of his multi-systematic and non-specific manifestations. The identification of a novel likely-pathogenic variation in *COL3A1*, c.146C>T, enabled a genetic diagnosis of vEDS for the patient. It should be noted that, though current evidences including the *de novo* occurrence and the absence in controls are sufficient to support the likely-pathogenicity according to the ACMG/AMP guidelines, functional evidences are still lacking. Further investigations of p.Pro49Leu mutant protein through *in vitro* or *in vivo* experiments will be vital to confirm the impact of this variant. In terms of this case, the diagnosis of vEDS with known prognosis eased the family's concerns about the cause of death. Therefore, this case demonstrates the non-negligible practical value of genetic counseling and analysis.

Approximately two-thirds of published cases of genetically diagnosed vEDS are caused by point mutations in glycine residues (Ohyama et al., 2010). A single Gly substitution destabilizes the triple helix through a local disruption in hydrogen bonding and produces a discontinuity in the register of the helix (Brodsky and Persikov,2005).In *COL1A1*, *COL2A1* and *COL7A1*, Gly substitutions have been reported to cause more severe disorders than any other single-aminoacid mutations (Marini et al., 2007; Xu et al., 2020; Gupta et al., 2023).According to a review article, all gastrointestinal events originate from glycine substitutions, splicing variants, and in-frame indels, whereas variants that cause haploinsufficiency and non-glycine missense

variants are not associated with gastrointestinal events (Frank et al., 2015). To gather the latest evidence and re-analyze the association between the *COL3A1* genotype and the vEDS phenotype, we conducted a literature review according to the following inclusion criteria: 1) reports of patients diagnosed with vEDS associated with only *COL3A1* mutation and 2) the mutation type is consistent with non-glycine missense mutations.

This search retrieved reports of 35 cases of vEDS. In contrast to the review article of Frank et al. (2015), three of our reviewed cases involved non-glycine missense variants, c.1351G>A p.(Glu451Lys), c.2791G>A p.(Glu931Lys), and c.3511G>A p. (Glu1171Lys), that were indeed associated with digestive tract symptoms (Table 1). In the present case, both the proband and his son experienced digestive tract symptoms. Thus, the present case and previous three non-glycine missense variants reported put into question the currently established relationships between the genotype of *COL3A1* and specific complications of vEDS. Accordingly, when performing genetic diagnosis for patients suspected as having vEDS, comprehensive testing of the *COL3A1* gene covering all types of variants (e.g., through next-generation sequencing) is preferred over targeted analysis of limited sites or regions (e.g., Sanger sequencing), regardless of the presence or absence of any specific symptoms.

The proband's son, who carried the same *COL3A1* mutation, developed mild symptoms, including short stature, low body weight, skin pigmentation, deep palm prints, and poor skin healing. The boy also had black stool, indicating rupture of the blood vessels in the digestive tract. These observations suggest the initial complications of vEDS in early childhood but have rarely been reported in the published literature. In earlier reports, 25% of patients with vEDS had their first symptom by the age of 20 years and >80% had at least one symptom by the age of 40 years. Based on the high complication rates, the median age at the first major vascular event and at death for patients with vEDS are reported as 24.6 and 48 years, respectively (Pepin et al., 2000).

This early genetic diagnosis of the proband's son (aged 3 years) presents an opportunity to assess the prognosis by referring to his father's case, thereby enabling early interventions for management of the disease and prevention of further serious complications. For example, patients with vEDS require daily exercise and treatment. Care should be taken to avoid trauma (e.g., collision sports, heavy lifting, and extreme weight training). Arteriography should be discouraged and used only to identify life-threatening sources of bleeding before surgical intervention because of the risk of vascular injury (Byers, 1999).

In summary, this case highlights the importance of early and accurate diagnosis, genetic counseling, and avoiding high-risk activities and procedures in patients with vEDS (Frković et al., 2022). Thus, for late-onset genetic disorders such as vEDS, active utilization of genetic testing for younger relatives could create opportunities for early diagnosis of the disease, facilitating precise counseling and prevention of fatal disease progression. Moreover, the clinical findings and genetic analysis of this case could form the basis for the design of research programs, including further functional studies or modeling investigations.

Data availability statement

The datasets for this article are not publicly available due to concerns regarding participant/patient anonymity. Requests to access the datasets should be directed to the corresponding authors.

Ethics statement

The studies involving humans were approved by the Second Affiliated Hospital of Guangxi Medical University. The studies were conducted in accordance with the local legislation and institutional requirements. Written informed consent for participation in this study was provided by the participants' legal guardians/next of kin. Written informed consent was obtained from the individual(s), and minor(s)' legal guardian/next of kin, for the publication of any potentially identifiable images or data included in this article. Written informed consent was obtained from the participant/patient(s) for the publication of this case report.

Author contributions

BG and JL organized the study. CM, BL, and CL conducted clinical evaluations. BX, MS, and CG analyzed the sequencing data. CZ conducted ultrasound testing. XW and XZ reviewed the literature and wrote this report. All authors contributed to the article and approved the submitted version.

Funding

This work was supported in part by the National Natural Science Foundation of China (82001531 and 81860272 to BG), Guangxi Major Research Program (AB22035013 to BG), Guangxi Natural Science Foundation (2023GXNSFBA026124 to CG, 2018GXNSFAA281067 to BG), Shandong Natural Science Foundation (ZR2020QH050 to XW), Initial Scientific Research Fund for Advanced Talents from The Second Affiliated Hospital of Guangxi Medical University (2019112 to BG), Special Scientific Research Fund of Guangxi Ten-Hundred-Thousand Talents Project (2021186 to BG), Science Foundation for Young Scholars of Guangxi Medical University (GXMUYSF202115 to CG), Guangxi Natural Science Foundation (2021GXNSFAA196047 to BX), and Innovation Project of Guangxi Graduate Education (YCSW2023239 to XZ).

Acknowledgments

We thank the patient and his family members for their contributions to this medical research.

Conflict of interest

The authors declare that the research was conducted in the absence of any commercial or financial relationships that could be construed as a potential conflict of interest.

Publisher's note

References

Abrahamsen, B. J. M., Kulseth, M. A. P., and Paus, B. M. P. (2015). A 19-year-old man with relapsing bilateral pneumothorax, hemoptysis, and intrapulmonary cavitary lesions diagnosed with vascular Ehlers-Danlos syndrome and a novel missense mutation in *COL3A1*. *Chest* 147, e166–e170. doi:10.1378/chest.13-3002

Aydıner, Ö., and Hançer, V. S. (2020). A novel *COL3A1* c.2644G>T; p.(Gly882Cys) variant in a Turkish family with vascular Ehlers-Danlos syndrome. *Mol. Syndromol.* 11, 110–114. doi:10.1159/000506585

Barboi, A., Dennis, C., Timins, M., Peltier, W., Klotz, C. M., and Jaradeh, S. (2009). Neuromuscular manifestations in a patient with Ehlers-Danlos syndrome type IV. *J. Clin. Neuromuscul.* 11, 81–87. doi:10.1097/CND.0b013e3181bab6e3

Brightwell, R. E., and Walker, P. J. (2011). Lower limb arterio-venous fistula as a late complication of phlebectomy in a patient with Ehlers-Danlos type IV. *Eur. J. Vasc. Endovasc. Surg.* 42, 696–698. doi:10.1016/j.ejvs.2011.06.044

Brodsky, B., and Persikov, A. V. (2005). Molecular structure of the collagen triple helix. *Adv. Protein Chem.* 70, 301–339. doi:10.1016/S0065-3233(05)70009-7

Byers, P. H. (1999). "Vascular ehlers-danlos syndrome," in *GeneReviews* (Seattle, WA: University of Washington).

Colman, M., Castori, M., Micale, L., Ritelli, M., Colombi, M., Ghali, N., et al. (2022). Atypical variants in COL1A1 and COL3A1 associated with classical and vascular Ehlers-Danlos syndrome overlap phenotypes: expanding the clinical phenotype based on additional case reports. *Clin. Exp. Rheumatol.* 40 (Suppl. 134), 46–62. doi:10.55563/clinexprheumatol/kzkq6y

De Sousa, F. D. R., Colucci, N., Dupuis, A., Toso, C., Buchs, N. C., and Abbassi, Z. (2020). Surgical management of vascular Ehlers-Danlos syndrome and its challenges: a case report. *Swiss Med. Wkly.* 150, w20379. doi:10.4414/smw.2020.20379

Eder, J., Laccone, F., Rohrbach, M., Giunta, C., Aumayr, K., Reichel, C., et al. (2013). A new *COL3A1* mutation in Ehlers–Danlos syndrome type IV. *Exp. Dermatol.* 22, 231–234. doi:10.1111/exd.12105

Frank, M., Albuisson, J., Ranque, B., Golmard, L., Mazzella, J. M., Bal-Theoleyre, L., et al. (2015). The type of variants at the *COL3A1* gene associates with the phenotype and severity of vascular Ehlers-Danlos syndrome. *Eur. J. Hum. Genet.* 23, 1657–1664. doi:10.1038/ejhg.2015.32

Frković, S. H., Marija Slišković, A., Toivonen, M., Crkvenac Gregorek, A., Šutalo, A., and Vrkić Kirhmajer, M. (2022). Vascular Ehlers-Danlos syndrome, an often unrecognized clinical entity: a case report of a novel mutation in the *COL3A1* gene. *Croat. Med. J.* 63, 394–398. doi:10.3325/cmj.2022.63.394

Ghali, N., Baker, D., Brady, A. F., Burrows, N., Cervi, E., Cilliers, D., et al. (2019). Atypical *COL3A1* variants (glutamic acid to lysine) cause vascular Ehlers–Danlos syndrome with a consistent phenotype of tissue fragility and skin hyperextensibility. *Genet. Med.* 21, 2081–2091. doi:10.1038/s41436-019-0470-9

Gu, G., Yang, H., Cui, L., Fu, Y., Li, F., Zhou, Z., et al. (2018). Vascular Ehlers-Danlos syndrome with a novel missense *COL3A1* mutation present with pulmonary complications and iliac arterial dissection. *Vasc. Endovasc. Surg.* 52, 138–142. doi:10.1177/1538574417745432

Gupta, D., Jayashankar, C., Srinivas, M., Baraka Vishwanathan, G., Reddy, K. R., Kubba, A., et al. (2023). Clinical and allelic heterogeneity in dystrophic epidermolysis bullosa-lessons from an Indian cohort. *PLoS One* 18, e0289558. doi:10.1371/journal.pone.0289558

Horn, D., Siebert, E., Seidel, U., Rost, I., Mayer, K., Abou Jamra, R., et al. (2017). Biallelic COL3A1 mutations result in a clinical spectrum of specific structural brain anomalies and connective tissue abnormalities. *Am. J. Med. Genet. A. Part A* 173, 2534–2538. doi:10.1002/ajmg.a.38345

Ishiguro, T., Takayanagi, N., Kawabata, Y., Matsushima, H., Yoshii, Y., Harasawa, K., et al. (2009). Ehlers-Danlos syndrome with recurrent spontaneous pneumothoraces and cavitary lesion on chest X-ray as the initial complications. *Intern. Med.* 48, 717–722. doi:10.2169/internalmedicine.48.1818

Jaganathan, K., Kyriazopoulou Panagiotopoulou, S., McRae, J. F., Darbandi, S. F., Knowles, D., Li, Y. I., et al. (2019). Predicting splicing from primary sequence with deep learning. *Cell* 176, 535–548. doi:10.1016/j.cell.2018.12.015

Jørgensen, A., Fagerheim, T., Rand-Hendriksen, S., Lunde, P. I., Vorren, T. O., Pepin, M. G., et al. (2015). Vascular Ehlers-Danlos syndrome in siblings with biallelic *COL3A1* sequence variants and marked clinical variability in the extended family. *Eur. J. Hum. Genet.* 23, 796–802. doi:10.1038/ejhg.2014.181

Kamalanathan, K. C., Barnacle, A. M., Holbrook, C., and Rees, C. (2019). Splenic rupture secondary to vascular Ehlers–Danlos syndrome managed by coil embolization of the splenic artery. *Eur. J. Pediatr. Surg. Rep.* 7, e83–e85. doi:10.1055/s-0039-3399555

Kroes, H. Y., Pals, G., and van Essen, A. J. (2003). Ehlers–Danlos syndrome type IV: unusual congenital anomalies in a mother and son with a *COL3A1* mutation and a normal collagen III protein profile. *Clin. Genet.* 63, 224–227. doi:10.1034/j.1399-0004.2003.00047.x

Lan, N. S. R., Fietz, M., Pachter, N., Paul, V., and Playford, D. (2018). A case of vascular Ehlers-Danlos Syndrome with a cardiomyopathy and multi-system involvement. *Cardiovasc. Pathol.* 35, 48–51. doi:10.1016/j.carpath.2018.04.006

Lee, S. T., Kim, J. A., Jang, S. Y., Kim, D. K., Kim, J. W., and Ki, C. S. (2008). A novel *COL3A1* gene mutation in patient with aortic dissected aneurysm and cervical artery dissections. *Heart Vessels* 23, 144–148. doi:10.1007/s00380-007-1027-4

Lipinski, M. J., Lipinski, S. E., Kripalani, S., Friesen, L. D., Uthlaut, B. S., and Braddock, S. R. (2009). An unusual presentation of Ehlers-Danlos syndrome vascular type with deep vein thrombosis: a case for multidisciplinary management. *Am. J. Med. Genet. A* 149A, 698–701. doi:10.1002/ajmg.a.32687

Lumi, X., Bergant, G., Lumi, A., and Mahnic, M. (2021). Outcomes of vitrectomy for retinal detachment in a patient with Ehlers–Danlos syndrome type IV: a case report. *J. Med. Case Rep.* 15, 249. doi:10.1186/s13256-021-02855-w

Marini, J. C., Forlino, A., Cabral, W. A., Barnes, A. M., San Antonio, J. D., Milgrom, S., et al. (2007). Consortium for osteogenesis imperfecta mutations in the helical domain of type I collagen: regions rich in lethal mutations align with collagen binding sites for integrins and proteoglycans. *Hum. Mutat.* 28, 209–221. doi:10.1002/humu.20429

Nakagawa, H., Wada, H., Hajiro, T., Nagao, T., Ogawa, E., Hatamochi, A., et al. (2015). Ehlers-Danlos syndrome type IV with bilateral pneumothorax. *Intern. Med.* 54, 3181–3184. doi:10.2169/internalmedicine.54.4947

Narcisi, P., Richards, A. J., Ferguson, S. D., and Pope, F. M. (1994). A family with Ehlers-Danlos syndrome type III/articular hypermobility syndrome has a glycine 637 to serine substitution in type III collagen. *Hum. Mol. Genet.* 3, 1617–1620. doi:10.1093/hmg/3.9.1617

Nuytinck, L., De Paepe, A., Renard, J. P., Adriaens, F., and Leroy, J. (1994). Single-strand conformation polymorphism (SSCP) analysis of the *COL3A1* gene detects a mutation that results in the substitution of glycine 1009 to valine and causes severe Ehlers–Danlos syndrome type IV. *Hum. Mutat.* 3, 268–274. doi:10.1002/humu.1380030315

Ohyama, Y., Iso, T., Niño, A. C. V., Obokata, M., Takahashi, R., Okumura, W., et al. (2010). Multiple spontaneous coronary artery ruptures and cardiac tamponade in vascular Ehlers-Danlos syndrome. *J. Cardiol. Cases* 3, e29–e32. doi:10.1016/j.jccase.2010.09.002

Palmeri, S., Mari, F., Meloni, I., Malandrini, A., Ariani, F., Villanova, M., et al. (2003). Neurological presentation of Ehlers-Danlos syndrome type IV in a family with parental mosaicism. *Clin. Genet.* 63, 510–515. doi:10.1034/j.1399-0004.2003.00075.x

Pejaver, V., Byrne, A. B., Feng, B. J., Pagel, K. A., Mooney, S. D., Karchin, R., et al. (2022). Calibration of computational tools for missense variant pathogenicity classification and ClinGen recommendations for PP3/BP4 criteria. *Am. J. Hum. Genet.* 109, 2163–2177. doi:10.1016/j.ajhg.2022.10.013

Pepin, M., Schwarze, U., Superti-Furga, A., and Byers, P. H. (2000). Clinical and genetic features of Ehlers–Danlos syndrome type IV, the vascular type. *N. Engl. J. Med.* 342, 673–680. doi:10.1056/NEJM200003093421001

Rebelo, M., Ramos, L., Lima, J., Vieira, J. D., Tavares, P., Teixeira, L., et al. (2011). Ehlers-Danlos syndrome type IV in association with a (c.970G>A) mutation in the *COL3A1* gene. *Acta Medica Port.* 24, 1079–1086. doi:10.20344/amp.1405

Richards, S., Aziz, N., Bale, S., Bick, D., Das, S., Gastier-Foster, J., et al. (2015). Standards and guidelines for the interpretation of sequence variants: a joint consensus recommendation of the American College of medical genetics and Genomics and the association for molecular Pathology. *Genet. Med.* 17, 405–424. doi:10.1038/gim.2015.30

Ruscitti, F., Trevisan, L., Rosti, G., Gotta, F., Cianflone, A., Geroldi, A., et al. (2021). A novel mutation in *COL3A1* associates to vascular Ehlers–Danlos syndrome with predominant musculoskeletal involvement. *Mol. Genet. Genom. Med.* 9, e1753. doi:10.1002/mgg3.1753

Sadakata, R., Hatamochi, A., Kodama, K., Kaga, A., Yamaguchi, T., Soma, T., et al. (2010). Ehlers-Danlos syndrome type IV, vascular type, which demonstrated a novel point mutation in the *COL3A1* gene. *Intern. Med.* 49, 1797–1800. doi:10.2169/internalmedicine.49.3435

Sakai, K., Toda, M., Kyoyama, H., Nishimura, H., Kojima, A., Kuwabara, Y., et al. (2019). Vascular Ehlers-Danlos syndrome with a novel missense mutation in *COL3A1*: a man in his 50s with aortic dissection after interventional treatment for hemothorax as the first manifestation. *Intern. Med.* 58, 3441–3447. doi:10.2169/internalmedicine.2983-19

Vandervore, L., Stouffs, K., Tanyalçin, I., Vanderhasselt, T., Roelens, F., Holder-Espinasse, M., et al. (2017). Bi-allelic variants in COL3A1 encoding the ligand to GPR56 are associated with cobblestone-like cortical malformation, white matter changes and cerebellar cysts. *J. Med. Genet.* 54, 432–440. doi:10.1136/jmedgenet-2016-104421

Xu, Y., Li, L., Wang, C., Yue, H., Zhang, H., Gu, J., et al. (2020). Clinical and molecular characterization and discovery of novel genetic mutations of Chinese patients with col2a1-related dysplasia. *Int. J. Biol. Sci.* 16, 859–868. doi:10.7150/ijbs.38811

Yang, F., Yang, R. J., Li, Q., Zhang, J., Meng, Y. X., Liu, X. J., et al. (2022). Whole-exome sequencing facilitates the differential diagnosis of Ehlers-Danlos syndrome (EDS). *Mol. Genet. Genom. Med.* 10, e1885. doi:10.1002/mgg3.1885

Yang, J. H., Lee, S. T., Kim, J. A., Kim, S. H., Jang, S. Y., Ki, C. S., et al. (2007). Genetic analysis of three Korean patients with clinical features of Ehlers-Danlos syndrome type IV. *J. Korean Med. Sci.* 22, 698–705. doi:10.3346/jkms.2007.22.4.698

Frontiers in Genetics

Highlights genetic and genomic inquiry relating to all domains of life

The most cited genetics and heredity journal, which advances our understanding of genes from humans to plants and other model organisms. It highlights developments in the function and variability of the genome, and the use of genomic tools.

Discover the latest Research Topics

See more →

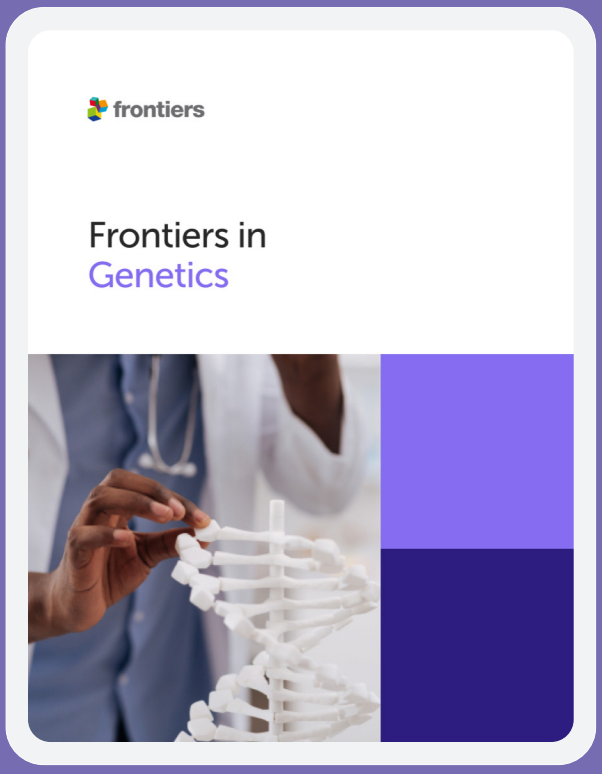

Frontiers

Avenue du Tribunal-Fédéral 34
1005 Lausanne, Switzerland
frontiersin.org

Contact us

+41 (0)21 510 17 00
frontiersin.org/about/contact